

Regulation and activities of phyto­sulfokine receptor PSKR1 in *Arabidopsis thaliana*

Dissertation

zur Erlangung des Doktorgrades der
Mathematisch-Naturwissenschaftlichen Fakultät
der Christian-Albrechts-Universität
zu Kiel

vorgelegt von

Christine Kaufmann

Kiel, Januar 2018

Referent/in: Prof. Dr. Margret Sauter

Korreferent/in: Prof. Dr. Dietrich Ober

Tag der mündlichen Prüfung: 06.04.2018

Zum Druck genehmigt: 06.04.2018

Abbreviations

Ab	antibody
ACT2	ACTIN 2
ADP	adenosine diphosphate
AHA1	Arabidopsis H ⁺ ATPase 1
AHA2	Arabidopsis H ⁺ ATPase 2
AL	activation loop
ANOVA	analysis of variance
AS	activation segment
ATP	adenosine triphosphate
BAK1	BRI1-ASSOCIATED KINASE 1
BiFC	bimolecular fluorescence complementation
BKK1	BAK1-LIKE 1
BL	brassinolide
BR	brassinosteroid
BRI1	BRASSINOSTEROID INSENSITIVE 1
BSA	bovine serum albumine
CaM	calmodulin
CaMBS	calmodulin binding site
cAMP	cyclic adenosine monophosphate
CaMV	Cauliflower mosaic virus
CDK2	CYCLIN-DEPENDENT KINASE 2
cDNA	copyDNA
cGMP	cyclic guanosine monophosphate
CID	collision-induced dissociation
CLV1	CLAVATA1
CNGC	YCLIC NUCLEOTIDE GATED CHANNEL
cNMP	cyclic nucleotide monophosphate
Col-0	ecotype Columbia-0
cpm	counts per minute
CT	C-terminus
DAMP	danger-associated molecular pattern
DEPC	diethyl pyrocarbonate
DTT	dithiothreitol
ECL	enhanced chemiluminescent
EF	calcium binding motif (E-helix-loop-F-helix)
EFR	EF-TU RECEPTOR
EF-Tu	elongation factor thermo unstable
elf18	18 amino acid fragment of EF-TU
EMS1	EXCESS MICROSPOROXYTES 1
ER	ERECTA
ERL	ERECTA-LIKE
EST	expressed sequence tag
EXP7	EXPANSIN 7
FER	FERONIA
FL	full length
FLAG	a polypeptide protein tag

flg22	22 amino acid fragment of flagellin
FLS2	FLAGELLIN-SENSITIVE 2
FRET-FLIM	Förster resonance electron transfer – fluorescence lifetime imaging microscopy
GAPC	GLYCERALDEHYDE-3-PHOSPHATE DEHYDROGENASE C
GC	guanylate cyclase
GFP	green fluorescent protein
GluC	endoprotease selective for C-terminal glutamate
GRXC2	GLUTAREDOXIN C2
GTP	guanosine tri phosphate
GUS	β-glucuronidase
HAE	HAESA
HCD	higher-energy collisional dissociation fragmentation
HEPES	4-(2-hydroxyethyl)-1-piperazineethanesulfonic acid
His ₆ or H ₆	6x-Histidine-tag
HPLC	high performance liquid chromatography
HRP	horse radish peroxidase
HSL2	HAESA-like 2
IP	immunoprecipitation
IPTG	isopropyl-β-D- thiogalactopyranoside
JKD	JACKDAW
JM	Juxtamembrane
KD	kinase domain
LB	lysogeny broth Luria/Miller liquid medium
LC-ESI-MS/MS	liquid chromatography-electrospray ionization –tandem mass spectrometry
LRR	leucine-rich repeat
MaBP	maltose binding protein
MBP	myelin basic protein
MIFE	microelectrode ion flux estimation
mRNA	messenger RNA
MYB23	MYB DOMAIN PROTEIN 23
<i>P</i>	probability
PAGE	polyacrylamide gel electrophoresis
PAMP	pathogen-associated molecular pattern
PCR	polymerase chain reaction
PD	Proteome discoverer
PDB	protein data bank
PEPR1	PEP1 RECEPTOR
PKS5	PROTEIN KINASE SOS2-LIKE 5
PP2A	PLANT PHOSPHATASE 2A
P-site	phosphorylation site
PSK	phytosulfokine
PSKR	PSK RECEPTOR
PSM	peptide-spectrum match
PSY1	PLANT PEPTIDE CONTAINING SULFATED TYROSINE 1
PSY1R	PSY1 RECEPTOR
PVDF	polyvinylidene difluoride
qPCR	quantitative PCR
q-value	the minimum false discovery rate
<i>r1r2</i>	<i>pskr1-3 pskr2-1</i>

RALF	RAPID ALKALINIZATION FACTOR
RD	arginine-aspartate
RGF1	ROOT MERISTEM GROWTH FACTOR 1
rGFP	recombinant green fluorescent protein
RLK	RECEPTOR-LIKE KINASE
RMA	robust multi-array average
RNA	ribonucleic acid
RP	reverse phase
RT	reverse transcription
RT	room temperature
SBT1.1	SUBTILASE 1.1
SCM	SCRAMBLED
SDS	sodium dodecylsulfate
SEM	standard error of the mean
Seq	sequencing
SERK	SOMATIC EMBRYOGENESIS RECEPTOR KINASE
TFA	trifluoroacetic acid
TPST	TYROSYLPROTEIN SULFOFRANSFERASE
TSTT-A	T890A/S893A/T894A/T899A
v/v	volume per volume
w/v	weight per volume
WB	Western Blot
WER	WEREWOLF
wt	wild-type

Table of contents

Abbreviations	i
Table of contents	iv
Zusammenfassung	1
Summary	3
General introduction	5
The plant hormone phytosulfokine alters growth, development and immunity	5
Processing from precursor to active PSK	6
PSK is perceived by leucine-rich repeat receptor-like kinases.....	9
PSK signaling is dependent on PSKR1 co-receptor BAK1	11
The PSK signal may be transduced by phosphorylation and cGMP	12
Objectives of this thesis	15
Chapter 1	16
Conserved phosphorylation sites in the activation loop of the Arabidopsis phytosulfokine receptor PSKR1 differentially affect kinase and receptor activity	16
Chapter 2	46
Phosphorylation of the phytosulfokine peptide receptor PSKR1 controls receptor activity	46
Chapter 3	64
Pull-down Assay to Characterize Ca ²⁺ /Calmodulin Binding to Plant Receptor Kinases.....	64
Chapter 4	74
Phytosulfokine receptor activity in the absence of its ligand PSK	74
Chapter 5	111
Phytosulfokine signaling activates proton pumps	111
Conclusive discussion and perspectives	128
PSKR1 kinase structure and intramolecular activation mechanism is conserved.....	128
Phosphorylation of the JM domain regulates PSKR1 activity.....	129
Contradictory to the dimerization model: PSKR1 is active in the absence of PSK	130
The proton pump AHA2 is a target of the PSKR1 kinase while CaM is not.....	133
References	136
Supplemental	146
Declaration of author contributions	147
Danksagung	148
Lebenslauf	149
Erklärung	150

Zusammenfassung

Der sulfatierte Peptidwachstumsfaktor Phytosulfokine (PSK) wird *in Arabidopsis thaliana* von zwei plasmamembranständigen *leucin-rich repeat* Rezeptor-ähnlichen Kinasen, PSK-Rezeptor 1 und 2 (PSKR1 und PSKR2), perzipiert. Das PSK-Signal wird vor allem durch PSKR1 vermittelt, weswegen in dieser Studie PSKR1 funktional untersucht wurde. Insbesondere wurden der Aktivierungsmechanismus, die Bindung an Calmodulin (CaM) und Substrate von PSKR1 charakterisiert. Eine Kartierung von Autophosphorylierungsstellen zeigte, dass Aminosäuren in verschiedenen Bereichen des cytoplasmatischen Rezeptorteils, wie der Juxtamembrandomäne (JM), den Kinasesubdomänen und dem C-Terminus (CT), vorkommen. Eine funktionelle Analyse über Punktmutationen der Phosphorylierungsstellen zeigte, dass Phosphorylierung des Aktivierungssegments essentiell für die Kinaseaktivität von PSKR1 ist. Aminosäuren, deren Mutation einen starken Einfluss auf die Kinaseaktivität haben, sind in PSKR1-Homologen Höherer Pflanzen stark konserviert. Ein Homologie-Modell des cytoplasmatischen Teils von PSKR1 weist eine typische zweiflügelige Kinasestruktur auf und zeigt, dass phosphorylierte Aminosäuren in katalytisch essentiellen Strukturelementen positioniert sind. Phosphorylierung der JM beeinflusst die Substratphosphorylierung *in vitro* und führt *in planta* zu einer PSK-Signalwirkung in der Wurzel jedoch nicht im Spross. Die Bindung von CaM an PSKR1 ist abhängig von Kalzium und wird durch Autophosphorylierung von PSKR1 abgeschwächt. Die Funktion der Bindung von Ca^{2+} /CaM ist unklar, liegt aber nicht in der Regulation der PSKR1-Kinaseaktivität. Eine funktionale PSKR1-Kinase ist essentiell, um Zellexpansion zu fördern. PSKR1 bindet direkt an die Protonenpumpen *Arabidopsis* H^+ -ATPase 1 und 2 (AHA1 und 2) in der Plasmamembran. Der autoinhibitorische CT von AHA2 wird *in vitro* von PSKR1 an aktivierenden Positionen phosphoryliert. *In planta* induziert PSK einen erhöhten Protonenefflux in Wurzeln von *Arabidopsis*-Keimlingen, wohingegen in der PSK-insensitiven Rezeptordoppelmutante keine Ansäuerung erfolgt. Dies lässt darauf schließen, dass AHAs ein Substrat der PSK-Rezeptoren sind. Der Verlust von PSK-Rezeptoren zusätzlich zum Verlust des ligandenaktivierenden Enzyms Tyrosylprotein-Sulfotransferase (TPST) führt zu einem gravierenderen Phänotyp hinsichtlich Wurzellänge, Seitenwurzeldichte und Wurzelhaarbildung, als der

einfache Verlust von TPST hervorruft. PSKR1-überexprimierende Keimlinge im TPST-defizitären Hintergrund weisen eine PSK-signaltypische längere Wurzel auf als TPST-Mutanten. Das Wurzelwachstum von Keimlingen mit der höchsten PSKR1-Expression kann durch PSK nicht weiter gefördert werden. Dies lässt darauf schließen, dass zum einen die Abundanz von PSKR1 limitierend für den PSK Signalweg ist und zum anderen PSKR1 ohne den Liganden PSK aktiv ist. PSKR1 heterodimerisiert mit seinem Korezeptor BAK1 und dieser ist in der Lage PSKR1 an Stellen zu phosphorylieren, an denen PSKR1 sich autophosphoryliert und somit aktiviert. Dies könnte der Mechanismus für die ligandenunabhängigen Rezeptoraktivierung sein.

Summary

In *Arabidopsis thaliana*, the sulfated peptide growth factor phytosulfokine (PSK) is perceived by two plasma membrane-bound leucine-rich repeat receptor-like kinases, termed PSK receptor 1 and 2 (PSKR1 and PSKR2). The PSK signal is mainly conveyed by PSKR1 and therefore this study focusses on the functional analysis of PSKR1. In particular, the activation mechanism, binding to calmodulin (CaM) and substrate phosphorylation were characterized. Mapping of PSKR1 auto-phosphorylation revealed that phosphosites are present in different regions of the cytoplasmic protein part including the juxtamembrane (JM) domain, all kinase subdomains and the C-terminus (CT). A functional analysis by point mutation showed that phosphorylation of amino acids in the activation segment is essential for PSKR1 activity. Amino acids, whose mutations strongly impacted kinase activity, are highly conserved in PSKR1 orthologues from higher plants. A homology model of the cytoplasmic part of PSKR1 shows a typical bilobal kinase structure and revealed that phosphorylated amino acids are positioned in catalytically essential structural elements. Phosphorylation of the JM domain impacted substrate phosphorylation *in vitro* and led *in planta* to PSK response in the root but not in the shoot. Binding of CaM to PSKR1 is dependent on calcium and reduced by autophosphorylation of PSKR1. The role of Ca²⁺/CaM binding is unclear, but is not regulation of PSKR1 kinase activity. A functional PSKR1 kinase is essential to promote cell expansion. PSKR1 binds directly to the proton pumps Arabidopsis H⁺-ATPases 1 and 2 (AHA1 and 2) in the plasma membrane. The autoinhibitory CT of AHA2 is phosphorylated by PSKR1 *in vitro* at activating positions. *In planta*, PSK induces an enhanced proton efflux in roots of Arabidopsis seedlings, whereas in the PSK-insensitive double receptor mutant no acidification takes place. This leads to the conclusion that AHAs are a substrate of PSKR1. Seedlings that lack PSK receptors in addition to the ligand activating enzyme tyrosylprotein sulfotransferase (TPST) have a more severe phenotype regarding root length, lateral root density and root hair formation compared to seedlings that only lack TPST. Furthermore, seedlings overexpressing PSKR1 in a TPST-deficient background show root elongation compared to *tpst-1* mutants similar to a PSK response. In seedlings with the highest PSKR1 expression, enhanced root growth was not further promoted by PSK. This leads to the conclusion

that on one hand the abundance of PSKR1 limits PSK signaling and on the other hand that PSKR1 is active without the ligand PSK. PSKR1 heterodimerizes with its co-receptor BAK1 which is capable to phosphorylate PSKR1 at positions that lead to active PSKR1 when autophosphorylated revealing a possible molecular mechanism of receptor activation without ligand.

General introduction

The plant hormone phytosulfokine alters growth, development and immunity

Land plants are complex organisms and communication between organs, tissues and cells is indispensable to coordinate their growth and development. Communication in plants occurs through phytohormones. Since plants are immobile not only growth and development are orchestrated by phytohormones but likewise adaptive mechanisms to abiotic stress and responses to pathogens are induced by phytohormones. Chemical compounds such as auxin, cytokinin, gibberellin, abscisic acid, brassinosteroids, jasmonic acid, salicylic acid and ethylene are known for decades and have been well studied (Santner *et al.*, 2009).

Matsubayashi and Sakagami (1996) isolated the first peptide growth factor, a disulfated pentapeptide termed phytosulfokine- α (PSK). They identified PSK as the pivotal mitogenic factor that is released to the medium by cells kept in suspension and is capable to induce proliferation of cultured cells kept at low density that would otherwise not divide. PSK was initially described as an autocrine growth factor based on its proliferative effect on cells in suspension culture. Further *in planta* studies showed that PSK signaling occurs non-cell autonomously suggesting paracrine signaling (Wheeler and Irving, 2010; Hartmann *et al.*, 2013). PSK is the first identified member of the a large class of peptide hormones (Tavormina *et al.*, 2015). It encompasses small secreted peptides that are often derived from non-functional precursors. Most members known to date are posttranslationally modified by sulfation, glycosylation, and/or hydroxylation. Peptide hormones are involved in a plethora of processes such as shoot and root apical meristem maintenance, development of specialized cells and tissues such as stomata, vasculature, root hairs and lateral roots, as well as in embryogenesis and cell death (Czyzewicz *et al.*, 2013).

In accord with its proliferative activity PSK stimulates somatic embryogenesis (Kobayashi *et al.*, 1999; Igasaki *et al.*, 2003) and promotes adventitious root formation in cucumber hypocotyls (Yamakawa *et al.*, 1998). During plant reproduction PSK promotes pollen germination (Chen *et al.*, 2000) and pollen tube elongation. PSK functions further as a short distance signal to guide the pollen tube within the funiculus to the embryo sac. Plants that lack PSK receptors produce fewer

seeds (Stührwohldt *et al.*, 2014). PSK further promotes the differentiation of mesophyll cells of *Zinnia elegans* to tracheary elements in cell cultures with low density (Matsubayashi *et al.*, 1999) by downregulating stress-response genes at the onset of the transdifferentiation process (Motosue *et al.*, 2009). A well described effect of PSK signaling is growth promotion. PSK signaling increases hypocotyl length (Stührwohldt *et al.*, 2011), leaf area (Hartmann *et al.*, 2014), primary root length (Kutschmar *et al.*, 2009) and cotton fiber cell elongation (Han *et al.*, 2014b). These effects are mainly driven by increased cell expansion rather than cell division as evident from increased leaf epidermal cell size, longer hypocotyl cells and longer cells in the root elongation zone. The molecular mechanisms that drive cell expansion in response to PSK are not well understood. Furthermore, PSK signaling differentially affects plant immunity depending on the type of the invading pathogen. The contribution of PSK signaling to plant immunity seems to be dependent on the lifestyle rather than the evolutionary origin of the pathogen (Rodiuc *et al.*, 2015). Plants lacking PSK receptors are more susceptible to necrotrophic pathogens such as *Alternaria brassicicola*, *Sclerotinia sclerotiorum* and *Ralstonia solanacearum*, whereas their resistance against (hemi-) biotrophs such as *Pseudomonas syringae* and *Hyaloperonospora arabidopsidis* is increased (Loivamäki *et al.*, 2010; Igarashi *et al.*, 2012; Mosher *et al.*, 2013; Rodiuc *et al.*, 2015). PSK signaling reduces expression of microbe-associated molecular pattern-inducible genes (Igarashi *et al.*, 2012). Expression of genes encoding for PSK precursors and PSK Receptor 1 (PSKR1) is induced by wounding, treatment with a fungal elicitor and infection with necrotrophic fungi suggesting a role for PSK in pathogen interactions, whereas infection with the hemibiotrophic bacterium *P. syringae* does not change expression (Loivamäki *et al.*, 2010).

Processing from precursor to active PSK

Both, the amino acid backbone (Bahyrycz *et al.*, 2004, 2005) and sulfation of both tyrosine residues of the pentapeptide are required for biological activity of PSK (Matsubayashi *et al.*, 1996; Matsubayashi and Sakagami, 1996; Kobayashi *et al.*, 1999; Stührwohldt *et al.*, 2011; Kwezi *et al.*, 2011; Igarashi *et al.*, 2012; Mosher *et al.*, 2013) The PSK precursor is encoded as a 75-123 amino acid preproprotein by nuclear genes (Lorbiecke and Sauter, 2002). The conserved PSK protein family

PF06404 (<http://pfam.xfam.org/family/PF06404>) consists of 352 homologous sequences found in 53 species from mono- and dicotyledonous plant species including *Arabidopsis thaliana*, *Glycine soja*, *Brassica napus*, *Zea mays* and *Oryza sativa*. The conservation throughout the plant kingdom and the presence of multiple PSK encoding genes in each specie suggests a conserved ligand-receptor interaction in higher plants. In the model organism *A. thaliana* seven loci are annotated as putative PSK precursor genes. *AtPSK1-5* are expressed with varying levels throughout all tissues and developmental stages and contain the typical PSK domain YIYTQ, resulting in a ubiquitous expression of PSK (Cheng *et al.*, 2017; Supplementary Figure 1). The pseudogene *AtPSK6* (At4g37720) encodes the PSK-related sequence YIYTH and no ESTs have been reported so far for this gene indicating that it may not be expressed. As the result of a new genome annotation, the locus *At2g22942* was annotated as another putative phytosulfokine precursor. Interestingly the encoded protein sequence contains two canonical PSK sequences. In RNA-Seqs, *AtPSK6* and *At2g22942* show only very low expression levels (Supplementary Figure 1; Cheng *et al.*, 2017) and it remains to be shown if these genes play a biological role.

PSK preproteins undergo several processing steps (Figure 1). All PSK precursors have an N-terminal signal peptide (Lorbiecke and Sauter, 2002) and are therefore targeted to the secretory pathway. Secreted proteins are often posttranslationally modified and this is also the case for proPSK after cleavage of the signal peptide. The identification of PSK was the first evidence for tyrosine-sulfation in plants (Matsubayashi and Sakagami, 1996; Moore, 2009). In animals, tyrosine sulfation was reported earlier and is catalyzed by tyrosylprotein sulfotransferases (TPSTs; EC 2.8.2.20). The *Arabidopsis* homolog TPST transfers a sulfate group each from the co-substrate adenosine 3'-phosphate 5'-phosphosulfate to the hydroxyl group of the two tyrosine residues in the PSK domain which results in tyrosine O⁴-sulfate-esters (Moore, 2003). Plant-specific TPSTs were first identified in rice, carrot, asparagus and subsequently in *A. thaliana* (Hanai *et al.*, 2000; Komori *et al.*, 2009). Aside from their catalytic activity, they do not have so much in common with their animal counterparts with low sequence homology and differences in domain structure. Human TPSTs (370 and 377 residues) are type II transmembrane proteins with a short N-terminal domain in the cytoplasm and a putative stem region between the transmembrane and catalytic domain, whereas the *Arabidopsis* TPST (500 residues) is a type I transmembrane protein with a short C-terminal domain in

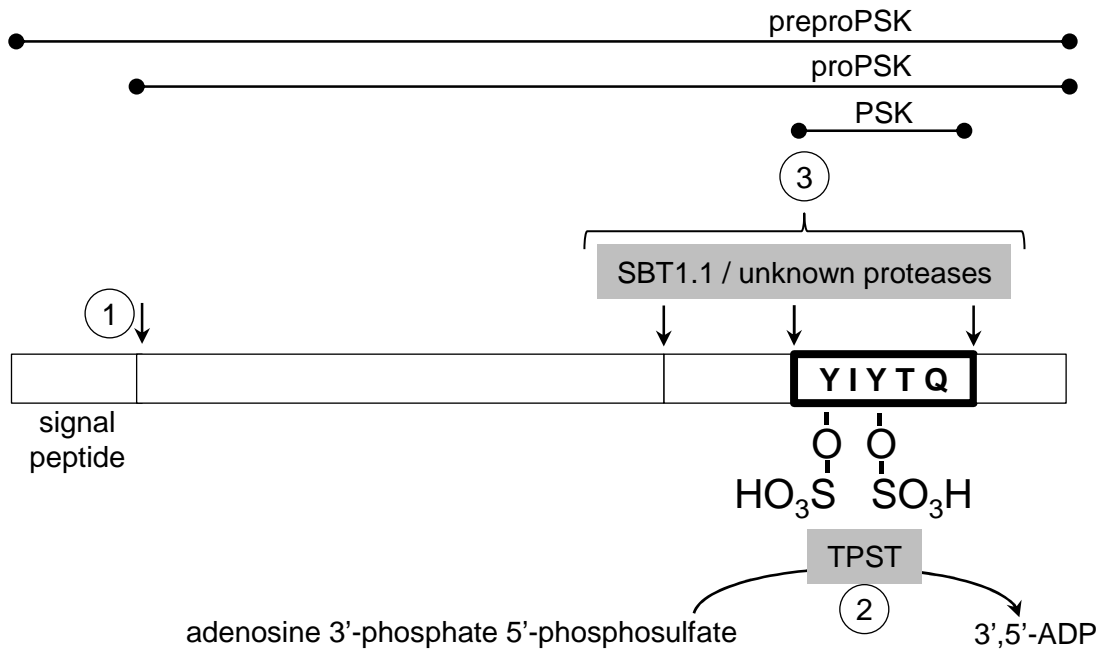


Figure 1: Processing of preproPSK to mature active PSK. 1. The signal peptide is cleaved off. 2. The tyrosine residues in the PSK domain (framed bold) are disulfated in the *cis*-Golgi by the tyrosylprotein sulfotransferase (TPST) with adenosine 3'-phosphate 5'-phosphosulfate as the sulfate group donor. 3. Unknown proteases and SUBTILASE 1.1 (SBT1.1) trim the proprotein releasing the disulfated pentapeptide as the bioactive hormone.

the cytoplasm, an N-terminal signal peptide and a heparan sulfate 6-O sulfotransferase 2 homology domain (Moore, 2009). TPST is located in the *cis*-Golgi where sulfation occurs. The gene is ubiquitously expressed with highest expression in the root apical meristem, lateral root primordia and in the vasculature (Komori *et al.*, 2009). To our current knowledge, *TPST* is a unique gene in plants and the TPST enzyme is responsible for sulfation not only of PSK but also of other sulfated peptide hormones including Plant peptide containing sulfated tyrosine 1 (PSY1) and Root meristem growth factor 1 (RGF1) (Amano *et al.*, 2007; Komori *et al.*, 2009; Matsuzaki *et al.*, 2010). TPST knockout in *A. thaliana* in *tpst-1* or *aqc1-1* causes a pleiotropic phenotype with shorter roots, reduced root apical meristem size, early senescence and a reduced number of reproductive organs (Komori *et al.*, 2009; Zhou *et al.*, 2010) caused by the collective loss of sulfated hormone peptides. Wild-type root length can be partially restored in *tpst-1* by exogenous application of a single sulfated peptide such as PSK, PSY1 and RGF1 and fully restored by applying the combination of them (Matsuzaki *et al.*, 2010).

The disulfated proPSK is secreted into the apoplast where proteolytic processing of N- and C-terminal ends must occur. In animals such proteolytic processing was reported for precursor molecules of peptide hormones and neuropeptides such as insulin and melanocyte-stimulating hormones (Seidah & Prat, 2012). Precursor processing catalyzed by prohormone convertases is essential to form the bioactive entities. The enzymes are discussed as therapeutic targets, which highlights the importance of this activating step. In plants, knowledge about proteolytic processing enzymes for secreted hormone peptides is scarce. To date, only partial cleavage of the N-terminal part from *Arabidopsis* proPSK4 was demonstrated *in vivo* by SUBTILASE 1.1, a prohormone convertase of the subtilisin-like serine protease family with the highest specificity observed *in vitro* for proPSK4 over other PSK precursors from *Arabidopsis* (Srivastava *et al.*, 2008). Further trimming by other enzymes is hypothesized since PSK derivatives with additional amino acids attached to the N- or C-terminus of the disulfated YIYDQ-sequence had a 1000-fold decreased bioactivity (Matsubayashi *et al.* 1996).

PSK is perceived by leucine-rich repeat receptor-like kinases

PSK is perceived by PSK receptors (PSKRs) at the plasma membrane, encoded by two genes in *Arabidopsis thaliana*. In carrot, the first PSK receptor, DcPSKR1, was identified by a ligand-based affinity chromatography approach (Matsubayashi *et al.*, 2002) and PSKR1 (At2g02220) and PSKR2 (At5g53890) from *Arabidopsis* were subsequently identified based on sequence homology to DcPSKR1 (Matsubayashi *et al.*, 2006; Amano *et al.*, 2007). PSKRs are leucine-rich repeat receptor-like kinases (LRR-RLKs), a protein family with 223 members in *A. thaliana* that regulate growth, development as well as defense responses against pathogens (Morillo and Tax, 2006; Gou *et al.*, 2010). LRR-RLKs are categorized based on their extracellular domain to subfamily X of receptor kinases together with other plant hormone or peptide receptors including BRASSINOSTEROID INSENSITIVE 1 (BR1), EXCESS MICROSPOROXYTES 1 (EMS1) and PSY1 RECEPTOR (PSY1R) (Diévar and Clark, 2003). PSKRs consist of an extracellular, a single α -helical plasma membrane-spanning and a cytoplasmic part (Figure 2; Matsubayashi *et al.*, 2006). The extracellular part contains 21 tandem copies of an LRR consensus sequence and is

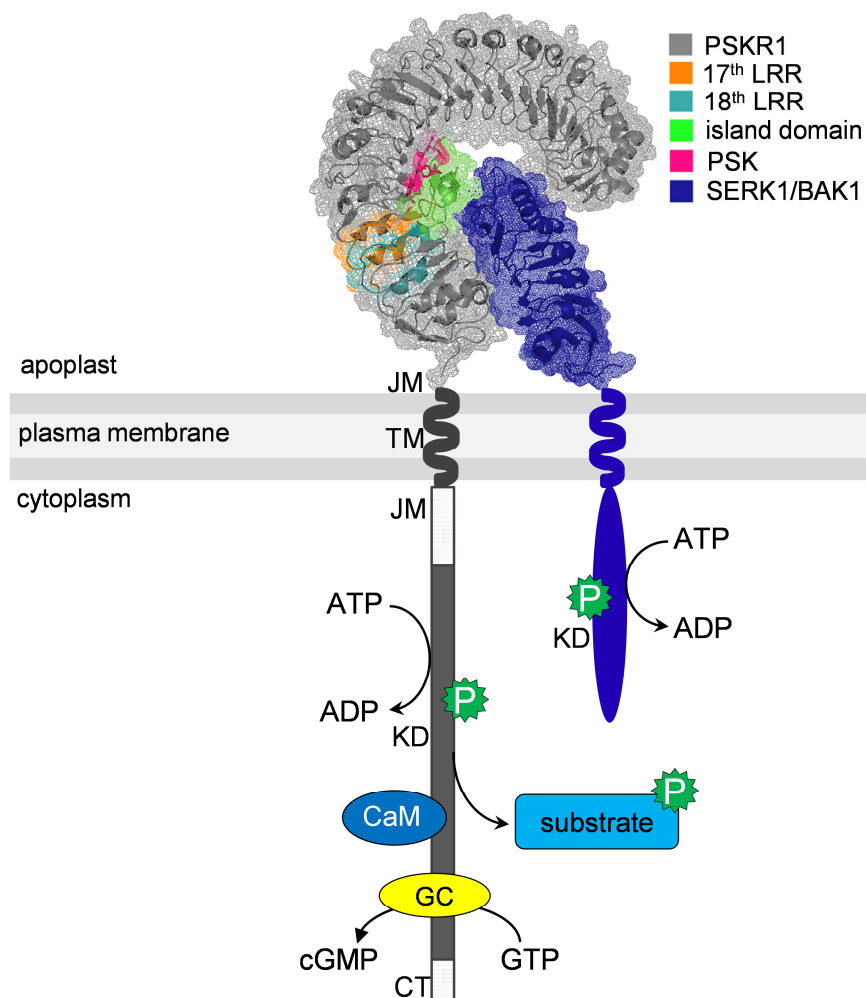


Figure 2: The PSKR1/SERK/PSK complex. PSK binds to the island domain of PSKR1 which heterodimerizes with a coreceptor of the SERK family. The cytoplasmic part of PSKR1 has an active kinase domain (KD) a guanylate cyclase center (GC) and a calmodulin (CaM) binding site. TM = helical transmembrane domain, JM = juxtamembrane domain, CT=C-terminal domain. The extracellular protein and PSK structures are shown as cartoons with the surfaces visualized by a mesh. Phosphorylation is depicted by a dark green star. (protein data bank published structure 4Z64; Wang et al. 2015).

N-glycosylated (Matsubayashi *et al.*, 2002). PSK binds to the island domain, which is embedded between the 17th and 18th LRR and is formed by ~35 hydrophilic and polar amino acids (Shinohara *et al.*, 2007). The crystal structure of the extracellular part of PSKR1 was solved by Wang *et al.* (2015) and is shaped like most plant LRR-RLKs as a flexible, twisted horseshoe or superhelix (Hohmann *et al.*, 2017). Binding of the ligand PSK to PSKR1 occurs mainly by hydrogen bond formation in which the PSK

sulfate moieties contribute to the PSK-PSKR1 interaction (Wang *et al.*, 2015). A single α -helical transmembrane domain connects the extracellular PSK-binding LRR domain with the intracellular signal-transducing domain. The intracellular receptor consists of a kinase flanked by a juxtamembrane (JM) domain next to the transmembrane helix and by a short C-terminus (CT). Within the functional kinase domain, a guanylate cyclase (GC) center and a calmodulin (CaM) binding site were identified (Kwezi *et al.*, 2011; Hartmann *et al.*, 2014). Disruption of either of these activities by point mutations renders PSKR1 inactive indicated by loss of PSK-promoted root growth (Hartmann *et al.*, 2014; Ladwig *et al.*, 2015). PSKR2 has not been examined as extensively as PSKR1 and its function is less clear. PSKR2 contributes to known PSK responses to only a minor degree or not at all. Root elongation (Hartmann *et al.*, 2013), shoot growth promotion (Stührwohldt *et al.*, 2011), and immune responses (Igarashi *et al.*, 2012) a) are conveyed predominately by PSKR1. Knockout of both PSKRs in Arabidopsis renders plants insensitive to exogenously applied PSK (Amano *et al.*, 2007; Stührwohldt *et al.*, 2014), indicating that no additional receptors convey these responses. *PSKR1* and *PSKR2* are expressed in all organs and developmental stages as shown by promoter:GUS analysis, microarray and RNA-Seq data (Supplementary Figure 1; Brady *et al.*, 2007; Wu *et al.*, 2016; Cheng *et al.*, 2017). After binding of PSK to PSKR1 the receptor is internalized by endocytosis (Rodiuc *et al.*, 2015).

PSK signaling is dependent on PSKR1 co-receptor BAK1

PSKR1 forms a nanocluster together with the co-receptor BRI1-ASSOCIATED KINASE 1 (BAK1), CYCLIC NUCLEOTIDE GATED CHANNEL 17 (CNGC17) and ARABIDOPSIS H⁺-ATPASE 1 and 2 (AHA1/2), whereby PSKR1 interacts directly with BAK1 and AHAs (Ladwig *et al.*, 2015). BAK1, also termed SERK3, is a member of the SOMATIC EMBRYOGENESIS RECEPTOR-LIKE KINASE (SERK) family and functions as a co-receptor for PSKR1 (Figure 2) and many other hormone receptors including BRI1, FLAGELLIN-SENSITIVE 2 (FLS2) and HAESA (Wang *et al.*, 2008; Schulze *et al.*, 2010; Santiago *et al.*, 2016). The SERK family, named after a *D. carota* ortholog, which is a marker for somatic embryogenesis, consists of five members in *A. thaliana* (Schmidt *et al.*, 1997; Hecht *et al.*, 2001). *AtSERK1* to 4 are widely expressed and have partially overlapping and redundant functions as co-

receptors depending on the signal pathway (reviewed in Ma *et al.*, 2016). Heterodimerization with PSKR1 was shown for SERK1, SERK2 and BAK1/SERK3 *in planta*, and dimerization with SERK1 was analyzed in detail by crystal structure analysis (Wang *et al.*, 2015). The PSKR1/BAK1 interaction is stabilized in the presence of PSK, but PSK is not located at the binding interface. This allosteric regulation by PSK is different from other LRR-RLK/SERK/ligand complexes such as FLS2/BAK1/flg22 and BRI1/BAK1/BR, in which the ligand is part of the binding interface (Santiago *et al.*, 2013; Sun *et al.*, 2013; Han *et al.*, 2014a). BAK1 belongs to subfamily II of the LRR-RLK family (Diévert and Clark, 2003). It has a small extracellular domain with only five LRRs (Chinchilla *et al.*, 2009), exhibits kinase activity, was initially described as the co-receptor of BRI1 and is therefore also involved in brassinosteroid signaling (Li *et al.*, 2002; Nam and Li, 2002). PSK signaling is dependent on brassinosteroid signaling. When biosynthesis of brassinosteroids is abolished by treatment with brassinazole or in the knockout line *det2-1*, or when perception is impaired in *bri1-9* or *bak1-3/4*, PSK-enhanced root growth and cell expansion are abolished (Hartmann *et al.*, 2013; Ladwig *et al.*, 2015).

The PSK signal may be transduced by phosphorylation and cGMP

It is not yet understood how the PSK signal is transduced intracellularly. Taking into account the established activities of PSKR1, two ways of signal transduction are conceivable, for one, by phosphorylation of target proteins and second, by cyclic guanosine monophosphate (cGMP), whereas CaM binding may have regulatory function. PSKR1 has a functional kinase, that can autophosphorylate and transphosphorylate yet unknown target proteins (Hartmann *et al.*, 2014). Transphosphorylation could initiate a cascade that may lead to gene regulation. Alternatively, or in addition PSKR1 may directly phosphorylate effector proteins involved in cell growth. PSKR1 interacts directly with the proton pumps AHA1 and AHA2 (Ladwig *et al.*, 2015), the most abundant and important of the 11 AHAs in *Arabidopsis* (Haruta *et al.*, 2010). AHA1 and AHA2 have overlapping functions and knockout of both is lethal. AHAs translocate protons driven by ATP-hydrolysis into the apoplast, thereby create an electrochemical gradient, which drives transport of solutes by secondary transporters and channels (Haruta *et al.*, 2015). Acidification of the cell wall by AHA activity drives cell expansion according to the acid-growth theory

(Hager, 2003). The activity of AHAs is regulated by phosphorylation of their autoinhibitory C-terminus (Haruta *et al.*, 2015), which was shown recently to be a target of other RLKs such as BRI1, FERONIA and PSY1R (Caesar *et al.*, 2011; Fuglsang *et al.*, 2014; Haruta *et al.*, 2014). The regulation of AHA activity is therefore an immediate response to various stimuli and could be a target of PSKR1.

CaMs are small regulatory proteins containing calcium ion binding EF-hand domains. Besides calcium-dependent protein kinases and calcineurin-B-like proteins, their function is to decode and transduce temporal changes of the cytosolic calcium concentration (Luan *et al.*, 2002; Batistič and Kudla, 2012). These calcium signatures are evoked by various processes such as biotic interactions with pathogens (Ma and Berkowitz, 2007) or symbionts (Ehrhardt *et al.*, 1996; Oldroyd and Downie, 2008), pollen tube and root hair tip growth (Hepler *et al.*, 2001), fertilization (Franklin-Tong *et al.*, 1993), abiotic stress responses (McAinsh and Pittman, 2009) and regulation of stomatal aperture by guard-cell volume (Blatt, 2000). Some of these listed processes are associated with PSK. Upon calcium binding the conformation of CaM structure changes and with this its binding behavior to target proteins, which could thereby modulate the activity of signaling pathway components (Zielinski, 1998). PSKR1 binds various CaM isoforms *in planta* (Hartmann *et al.*, 2014), but under which circumstances and this interaction occurs is not known as well as the impact on PSKR1 activities.

Besides a phosphorylation cascade, the PSK signal could be transduced through the soluble mobile cytosolic second messenger cGMP. PSK-signaling leads to increased formation of cGMP from GTP by the guanylate cyclase activity of PSKR1 (Kwezi *et al.*, 2011). cGMP is involved in protoplast expansion (Volotovski *et al.*, 1998), pathogen defense (Durner *et al.*, 1998; Hussain *et al.*, 2016) and mediation of salt and osmotic stress (Donaldson *et al.*, 2004) that have also been associated with PSK signaling. cGMP binds to CNGCs, which are voltage independent non-selective ion channels permissive to monovalent sodium and potassium ions and/or divalent calcium ions (Leng, 1999; Leng *et al.*, 2002; Balagué *et al.*, 2003; Urquhart *et al.*, 2007). CNGC17, that indirectly interacts with PSKR1 via BAK1, is one of 20 CNGC family members in Arabidopsis (Talke *et al.*, 2003). The cytoplasmic C-terminus of CNGCs encompasses partially overlapping binding sites for cNMP (cGMP or cAMP) and CaM (Köhler *et al.*, 1999). Binding of CaM to AtCNGC2 leads to inhibition of CNGC activity (Hua *et al.*, 2003). How binding of

cNMP affects CNGC activity is unclear as heterologous expressed *AtCNGC2* showed activation by cAMP (Leng *et al.*, 2002), whereas voltage independent channel activity was inhibited *in vivo* by cAMP and cGMP in root protoplasts (Maathuis and Sanders, 2001). It is not clear if and how PSK signaling affects CNGC17 activity, but a role is suggested as knockout of CNGC17 reduces the PSK-promoted protoplast expansion (Ladwig *et al.*, 2015).

Objectives of this thesis

The aim of this work is to understand the molecular mechanisms of PSK signaling with the focus on the regulation of PSK receptor activity and intracellular signal transduction. To that end, the protein structure and kinase activity of PSKR1 were functionally analyzed and interactions with CaM, BAK1 and AHA1/2 were studied to find out if these proteins are substrates of the PSKR1 kinase. The following chapters address specific questions:

Chapters 1 and 2: Which amino acids are autophosphorylated by PSKR1 and does phosphorylation change kinase activity?

Chapter 2: Is PSKR1 activity regulated by phosphorylation of the N- and C-termini of the cytosolic part of PSKR1?

Chapter 3: When does PSKR1 and CaM interaction occur and does it modulate PSKR1 kinase activity?

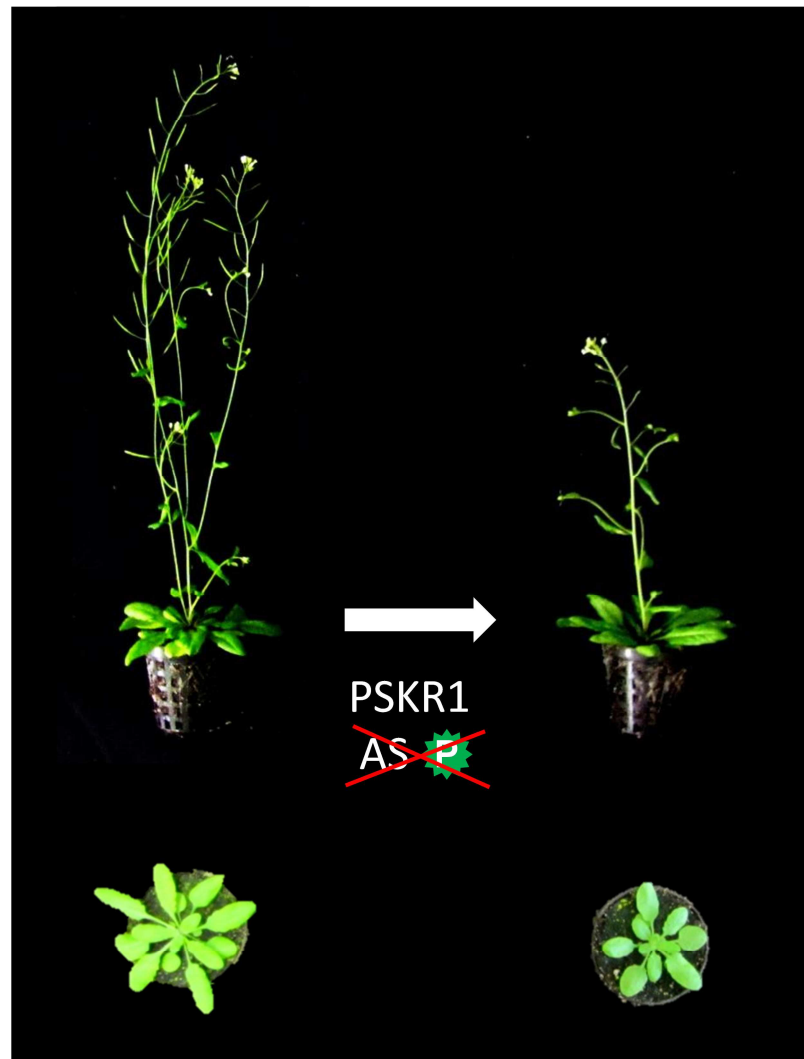
Chapter 4: Can PSKR1 signaling occur in the absence of PSK?

Chapter 5: Are the AHA proton pumps activated via phosphorylation to promote cell expansion?

Chapter 1

Conserved phosphorylation sites in the activation loop of the *Arabidopsis* phytosulfokine receptor PSKR1 differentially affect kinase and receptor activity

Hartmann, J., Linke, D., Bönniger, C., Tholey, A., & Sauter, M. (2015). *Biochemical Journal*, 472, 379–391. <https://doi.org/10.1042/BJ20150147>



Conserved phosphorylation sites in the activation loop of the *Arabidopsis* phytosulfokine receptor PSKR1 differentially affect kinase and receptor activity

Jens Hartmann*, Dennis Linke†, Christine Bönninger*, Andreas Tholey† and Margret Sauter*¹

*Entwicklungsbiologie und Physiologie der Pflanzen, Christian-Albrechts-Universität Kiel, Am Botanischen Garten 5, 24118 Kiel, Germany

†Systematische Proteomics und Bioanalytik, Christian-Albrechts-Universität Kiel, Niemannsweg 11, 24105 Kiel, Germany

PSK (phytosulfokine) is a plant peptide hormone perceived by a leucine-rich repeat receptor kinase. Phosphosite mapping of epitope-tagged PSKR1 (phytosulfokine receptor 1) from *Arabidopsis thaliana* plants identified Ser⁶⁹⁶ and Ser⁶⁹⁸ in the JM (juxtamembrane) region and probably Ser⁸⁸⁶ and/or Ser⁸⁹³ in the AL (activation loop) as *in planta* phosphorylation sites. *In vitro*-expressed kinase was autophosphorylated at Ser⁷¹⁷ in the JM, and at Ser⁷³³, Thr⁷⁵², Ser⁷⁸³, Ser⁸⁶⁴, Ser⁹¹¹, Ser⁹⁵⁸ and Thr⁹⁹⁸ in the kinase domain. The LC–ESI–MS/MS spectra provided support that up to three sites (Thr⁸⁹⁰, Ser⁸⁹³ and Thr⁸⁹⁴) in the AL were likely to be phosphorylated *in vitro*. These sites are evolutionarily highly conserved in PSK receptors, indicative of a conserved function. Site-directed mutagenesis of the four conserved residues in the activation segment, Thr⁸⁹⁰,

Ser⁸⁹³, Thr⁸⁹⁴ and Thr⁸⁹⁹, differentially altered kinase activity *in vitro* and growth-promoting activity *in planta*. The T899A and the quadruple-mutated TSTT-A (T890A/S893A/T894A/T899A) mutants were both kinase-inactive, but PSKR1(T899A) retained growth-promoting activity. The T890A and S893A/T894A substitutions diminished kinase activity and growth promotion. We hypothesize that phosphorylation within the AL activates kinase activity and receptor function in a gradual and distinctive manner that may be a means to modulate the PSK response.

Key words: activation loop, *Arabidopsis thaliana*, leucine-rich receptor receptor-like kinase, peptide signalling, phytosulfokine, PSKR1.

INTRODUCTION

The pentapeptide PSK (phytosulfokine) with the amino acid backbone YYITQ has been described as a peptide hormone that promotes plant growth through elevated cell expansion. Furthermore, its involvement in the response to pathogens has been reported [1–7]. Peptide activity depends on post-translational sulfation of the two tyrosine residues which is catalysed by the enzyme tyrosylprotein sulfotransferase in the *trans*-Golgi network [8].

Perception and transduction of the PSK signal requires a membrane-localized receptor protein. PSK is the natural ligand for the PSK receptor kinases PSKR1 and PSKR2 in *Arabidopsis thaliana*. PSKR1 and PSKR2 belong to a large monophyletic gene family of *Arabidopsis* LRR RLKs (leucine-rich repeat receptor-like kinases) [9–11]. LRR RLKs are characterized by a defined organization of functional domains: LRRs with an extracellular ligand-binding domain, a single transmembrane domain and a cytoplasmic protein portion consisting of a catalytic KD (kinase domain) flanked by two regulatory sequences, the JM (juxtamembrane) region and a CT (C-terminal) domain. PSKR1 shares this organization of functional domains. PSKR1 possesses a predicted extracellular domain with 21 LRRs. Between the 17th and 18th LRR of PSKR1 a 36-amino-acid island domain is located that was shown to bind PSK [9,12,13]. A single helical 21-amino-acid transmembrane domain spans the plasma

membrane followed by a JM region, a serine/threonine KD with its 12 conserved subdomains and a short CT domain [9,14–16] (Figure 1).

PSK perception at the cell surface probably triggers a cellular auto- and *trans*-phosphorylation cascade. It has been shown that PSKR1 kinase activity is essential for growth promotion via PSKR1 signalling, although the targets that are recognized and phosphorylated by the activated PSKR1 *in planta* are not known [16]. Ligand-induced receptor dimerization followed by autophosphorylation of the cytoplasmic domain is considered a conserved mechanism of receptor kinase action in plants and was shown for the brassinosteroid receptor BRI1 (BRASSINOSTEROID-INSENSITIVE 1) that is closely related to PSKR1 [17–19]. PSKR1, on the other hand, oligomerizes even in the absence of ligand and autophosphorylates *in vitro* [16,20]. Phosphorylation of the cytoplasmic domain of receptor kinases can occur on multiple sites in the JM region, KD and CT domain [21]. The structure of serine/threonine protein KDs is highly conserved, whereas the JM and CT regions are less conserved. The protein structure can be separated into two domains: a small N-terminal ATP-binding domain consisting of five β -sheets and one α -helix (α C) and a larger C-terminal substrate-binding domain that is predominantly helical [21,22].

A conserved activation segment with the central AL (activation loop) is located in the C-terminal lobe within the kinase subdomains VII and VIII as shown for the PSKR1 and BRI1 and

Abbreviations: AL, activation loop; BAK1, BRI1-ASSOCIATED RECEPTOR KINASE; BRI1, BRASSINOSTEROID-INSENSITIVE 1; CaMV, cauliflower mosaic virus; CID, collision-induced dissociation; CID-IT, CID in an ion trap; CV1, CLAVATA1; CT, C-terminal; HCD, higher-energy collisional dissociation fragmentation; JM, juxtamembrane; KD, kinase domain; LRR RLK, leucine-rich repeat receptor-like kinase; MBP, myelin basic protein; PSK, phytosulfokine; PSKR, phytosulfokine receptor; PSM, peptide-spectrum match; RT, reverse transcription; TFA, trifluoroacetic acid.

¹ To whom correspondence should be addressed (email msauter@bot.uni-kiel.de).

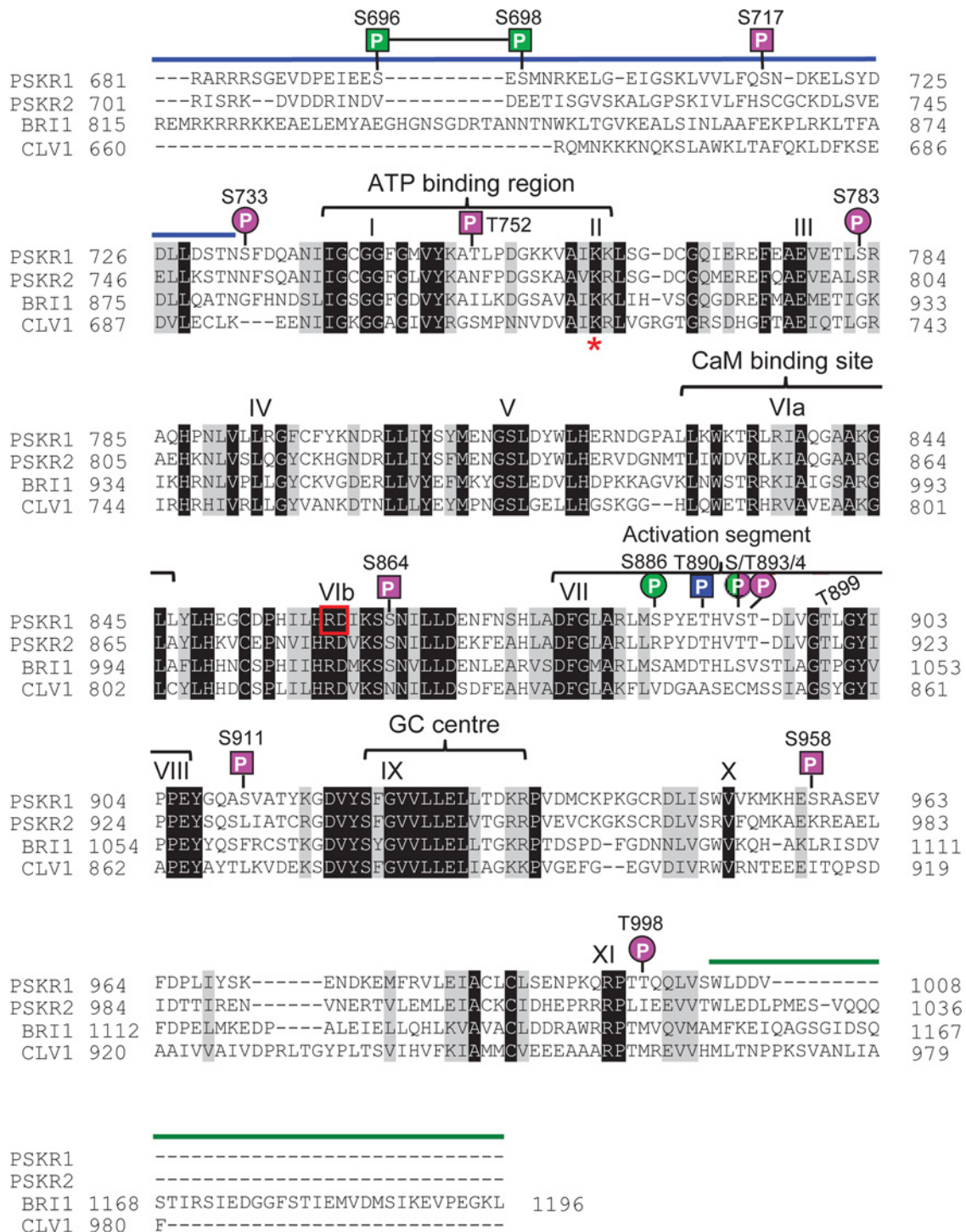


Figure 1 The cytoplasmic domain of the LRR RLK PSKR1 of *Arabidopsis* indicating conserved subdomains, guanylate cyclase centre, calmodulin-binding site and phosphorylation sites

A ClustalW multiple alignment of the cytoplasmic domains of PSKR1, PSKR2 and the related RD kinases BRI1 and CLV1 from *Arabidopsis* was carried out. The PSKRs belong to the class of RD kinases with a designated AL. The JM domain of PSKR1 from amino acids 681–732 is indicated by a blue line. The KD of PSKR1 with its 12 subdomains starts at Ser⁷³³ and ends at Ser¹⁰⁰³ (for a definition of the PSKR1 kinase subdomains, see [14,15]). An invariant lysine residue (Lys⁷⁶² in PSKR1) in the ATP-binding site located in subdomain II is indicated by a red asterisk. The invariant Arg⁸⁵⁹ and Asp⁸⁶⁰ residues in subdomain VIb are boxed in red. Indicated also are the calmodulin (CaM)-binding site, the AL and the designated guanylate cyclase (GC) centre. The C-terminal region is indicated by a green line. The short C-terminus of PSKR1 begins with amino acid 1004. Unambiguous phosphorylation sites (P) of PSKR1 are marked with squares; unconfirmed phosphorylation sites are designated by a circle. Pink indicates *in vitro* sites and green indicates *in planta* sites. Shown in blue is a site that is also phosphorylated in *E. coli*.

CLV1 (CLAVATA1) (Figure 1). PSKRs belong to the RD-type kinases. An invariant aspartate residue in subdomain VIb (Asp⁸⁶⁰ in PSKR1) is required for catalytic activity and can be found in all kinases. In RD kinases, this aspartate residue is preceded by a positively charged arginine residue (Arg⁸⁵⁹ in PSKR1) (Figure 1). Ligand-induced kinase activation of some, but not all, RD kinases necessitates phosphorylation of one to three residues in the AL [22]. In these cases, the conserved arginine residue probably interacts with phosphorylated negatively charged amino acids of the AL, resulting in charge neutralization and substrate access to the catalytic aspartate residue [23].

Compared with the KDs, the JM region and the CT domain show little sequence conservation among receptor kinases. Nonetheless, these domains were shown to regulate activity of BRI1 [24,25]. The phosphorylation state of the non-catalytic JM and CT regions of BRI1 is important not only for modulating kinase activity, but also for determining substrate specificity. It is conceivable that the JM region and CT domain of PSKR1 have similar functions in defining PSKR1 substrates and/or receptor activity. Neither the positions of phosphorylation nor their role in PSK signalling have been described to date.

To elucidate PSKR1 function, it is essential to understand early molecular events of PSKR1 signalling such as receptor modification. In the present study, we used LC-ESI-MS/MS analysis of the recombinant PSKR1 KD to show that the cytoplasmic protein portion of the receptor is autophosphorylated on specific serine and threonine residues *in vitro*. Furthermore, phosphosite mapping was performed to identify phosphorylation sites of PSKR1 *in planta*. We studied further the functional role of identified phosphorylation sites in the PSKR1 AL with respect to *in vitro* kinase activity. Additionally, the contribution of phosphorylation of specific PSKR1 AL residues to receptor function *in planta* was assessed by overexpressing site-mutated PSKR1 variants in the receptor-null background. Our data support the view that site-directed phosphoablative mutagenesis of specific PSKR1 AL residues impairs PSKR1 kinase activity *in vitro* and that phosphorylation of these serine and threonine residues is likely to be required for growth signalling through PSKR1 *in planta*.

EXPERIMENTAL

Plant material, growth conditions and transformation

All experiments were carried out with *Arabidopsis thaliana* (L.) Heynh. ecotype Columbia (Col-0). For plant growth, a 2:3 sand/humus mixture was frozen at -80°C for 2 days to avoid insect contamination. For experiments under sterile conditions, seeds were surface-sterilized for 20 min in 1 ml of 2% (w/v) sodium hypochlorite (NaClO) followed by five washing steps with autoclaved water and laid out on half-concentrated modified Murashige and Skoog medium [26] and 1.5% (w/v) sucrose, solidified with 0.38% GelriteTM (Duchefa Biochemie) and supplemented with 1 μM PSK as indicated (NeoMPS). Seeds were stratified at 4°C in the dark for 2 days and then transferred to 22°C with a 16 h light (70 μM photons $\cdot\text{m}^{-2}\cdot\text{s}^{-1}$)/8 h dark cycle.

The *pskr1-2 pskr2-1* double knockout line was described previously [3,4]. Experiments were performed with homozygous plants as tested by spraying with 200 μM glufosinate ammonium (Basta, AgrEvo). *Arabidopsis* plants were transformed with *Agrobacterium tumefaciens* (GV3101) using the floral dip method [27]. Transgenic plants were selected by spraying with 200 μM Basta. Expression of transgenes was verified by RT (reverse transcription)-PCR.

Growth measurements and statistical analysis

The software ImageJ (NIH) was used to determine root lengths from photographs. The open source program Rosette Tracker [28] was used to determine projected rosette areas from photographs. The program Minitab (<http://www.minitab.com>) was used for statistical analysis. Unless stated otherwise, statistical significance of means was tested by an ANOVA (Tukey's test) or a two-sample Student's *t* test. Constant variance and normal distribution of data were verified before statistical analysis. If one of these conditions was not achieved, the *P* value was set to <0.001 . *P* values for the Pearson product moment correlation are indicated in Figure legends. Kruskal-Wallis all-pairwise comparisons of kinase mutants were performed for autophosphorylation and for *trans*-phosphorylation activities.

Site-directed mutagenesis of the PSKR1 full-length and cytoplasmic domain coding sequence and cloning of constructs

Site-directed mutagenesis of the cytoplasmic domain of PSKR1 was performed by overlap-extension PCR [29]. Five constructs with the following substitutions were generated: T890A, T890D, T899A, S893A/T894A and TSTT-A (T890A/S893A/T894A/T899A). The encoded proteins encompassed the intracellular protein part of PSKR1 from amino acid 686 to 1008. To replace each specific serine or threonine with alanine or aspartate, primers 5'-GTCCCTACGAGGCTCATG-TAAGTAC-3' and 5'-GTACTTACATGAGCCTCGTAAGGAC-3' for T890A, primers 5'-GTCCTTACGAGGATCATGTAA-GTAC-3' and 5'-GTACTTACATGATCCTCGTAAGGAC-3' for T890D, primers 5'-CTGATTTGGTTGGAGCTTTAGGT-TAC-3' and 5'-GTAACCTAAAGCTCCAACCAAATCAG-3' for T899A, primers 5'-ACGCATGTAGCTGCTGATTTG-GTTG-3' and 5'-CAACCAAATCAGCAGCTACATGCGT-3' for S893A/T894A and primers 5'-CGAGGCTCATGTA-GCTGCTGATTTGGTTGGAGCTTTAG-3' and 5'-CTAAAG-CTCCAACCAAATCAGCAGCTACATGAGCCTCG-3' for TSTT-A were used for *in vitro* mutagenesis. PCR products were cloned into pETDuet-1 (Merck) resulting in His₆ N-terminal fusions with the five mutant PSKR1 kinases.

Point-mutated T890A, T890D, T899A, S893A/T894A and TSTT-A full-length *PSKR1* sequences were generated by overlap-extension PCR using the primers described above. The PCR fragments were cloned into the vector pB7WG2.0 downstream of the CaMV (cauliflower mosaic virus) 35S promoter using the Gateway cloning system (Life Technologies). All constructs were sequenced to verify the specific mutations and to exclude unwanted mutations. The C-terminal in-frame fusion of GFP with PSKR1 and cloning of the PSKR1-GFP construct into the vector pB7WG2.0 downstream of the CaMV 35S promoter were performed as described previously [16].

Recombinant protein expression, purification and *in vitro* kinase assay

Constructs of the five mutant PSKR1 kinases T890A, T890D, T899A, S893A/T894A and TSTT-A were transformed into *Escherichia coli* BL21(DE3) cells (Life Technologies). Protein expression was induced by adding 1 mM IPTG (Sigma-Aldrich) followed by incubation of bacterial cultures for 16 h at 20°C . Soluble proteins were purified at native conditions on a TALON column (Clontech) as described in the manufacturer's instructions and stored at 4°C .

In vitro kinase activity was assayed in 50 mM Hepes (pH 7.4), 10 mM MnCl₂, 1 mM DTT, 0.2 mM unlabelled ATP, 20 μ Ci of [γ -³²P]ATP, 0.25 μ g of affinity-purified His₆-PSKR1-KD mutant and 0.5 μ g of MBP (myelin basic protein) in a final volume of 8 μ l at 25 °C for 1 h followed by the addition of 4 \times SDS loading buffer to stop reactions. Proteins were separated by SDS/PAGE (15% gel), stained with Coomassie Blue, dried and exposed to an X-ray film. The protein bands were excised, mixed with Ultima Gold (PerkinElmer) and radioactivity was determined by liquid-scintillation counting in a Tri-Carb 2910 TR instrument (PerkinElmer). The background signal of the gel was subtracted.

Immunoprecipitation and immunoblot analysis

GFP-tagged full-length PSKR1 protein was extracted from 14-day-old 35S:PSKR1-GFP and wild-type seedlings. The plant material was ground in liquid nitrogen and the tissue was extracted in 1 ml of extraction buffer per g of plant material. The extraction buffer contained 50 mM Tris/HCl (pH 7.5), 150 mM NaCl and 1% (v/v) Igepal CA 630 (Sigma-Aldrich). After incubation of protein samples on ice for 1 h, suspensions were centrifuged at 300 g for 3 min at 4 °C. The protein concentration was determined with Roti[®]-Quant (Carl Roth). Then 10 ml (1 mg/ml) of total plant protein in extraction buffer was incubated with 100 μ l of 50% (v/v) Protein A-Sepharose CL-4B beads (GE Healthcare) in 50 mM Tris/HCl (pH 7.5) and 150 mM NaCl. The samples were centrifuged at 300 g for 3 min at 4 °C and supernatants were incubated with anti-GFP antibody (Life Technologies) as indicated for 1 h at 4 °C with gentle mixing of samples followed by the addition of 200 μ l of fresh 50% (v/v) Protein A-Sepharose CL-4B beads and overnight incubation. The Protein A-Sepharose CL-4B beads were pelleted at 300 g for 3 min and washed four times with 1 ml of washing buffer containing 50 mM Tris/HCl (pH 7.5) and 150 mM NaCl. The protein was separated on a denaturing gel, immunoblotted on to a PVDF membrane, detected with anti-GFP antibody linked to horseradish peroxidase (Life Technologies) and visualized using the ECL detection system (GE Healthcare).

In-gel digestion

To generate peptides for LC-ESI-MS/MS analysis, protein bands were excised from the SDS gels, washed with 500 μ l of water for 15 min, and destained twice in 800 μ l of 30% (v/v) acetonitrile for 30 min. Supernatants were discarded and gel slices were re-equilibrated with 500 μ l of incubation buffer (100 mM ammonium bicarbonate, pH 8) for 10 min. After removal of the supernatants, the gel slices were dried by vacuum evaporation using a SpeedVac (Eppendorf) for 30 min at room temperature. For reduction of disulfide bonds, 116 μ l of reducing solution (10 mM DTT) was added to the gel pieces and the samples were incubated at 56 °C for 30 min, followed by cooling at 4 °C for 10 min and a washing step with 150 μ l of incubation buffer for 10 min. Alkylation of cysteine thiols was performed in the dark for 20 min by addition of 100 μ l of 40 mM iodoacetamide followed by quenching with 75 μ l of reducing solution for 10 min and an additional washing step with 150 μ l of incubation buffer for 15 min. To remove reducing and alkylation contamination, the samples were washed with 150 μ l of incubation buffer for 5 min and 150 μ l of pure acetonitrile was added to initiate gel shrinking. The samples were shaken for 15 min before the supernatant was removed, and dried using a SpeedVac for 30 min at room temperature before digestion.

The protein was digested with chymotrypsin, elastase, GluC and trypsin. Enzyme/protein ratios of 1:10 were used, except for trypsin which was used at 1:20. For the *in vitro* sample, all four enzymes were used in a multi-protease approach as described previously [30]. For the *in vivo* sample with a restricted amount of starting material, only the enzymes elastase and trypsin were used. Each protease stock solution was diluted in 50 mM ammonium bicarbonate, 5% (v/v) acetonitrile and 10 μ l of the protease solution was added to the dehydrated gel slices. After incubating for 15 min, 90 μ l of digestion buffer was added and the samples were left to digest overnight at 37 °C. To extract the digested proteins, the supernatants were transferred to new tubes followed by two incubation steps with 150 μ l of extraction buffer I [60% (v/v) acetonitrile and 0.5% TFA (trifluoroacetic acid)] and with 150 μ l of pure acetonitrile for 15 min. The three extracts were combined, evaporated to dryness using a SpeedVac at room temperature, made up to 10 μ l with loading buffer A [3% (v/v) acetonitrile and 0.1% TFA] and stored at -20 °C before LC-ESI-MS/MS analysis.

Phosphopeptide enrichment

Phosphopeptides from the *in vitro* sample were enriched using TiO₂ beads (GL Sciences, MZ-Analysentechnik) similar to the method described previously [31]. First, 240 μ g of TiO₂ beads were washed twice with 20 μ l of loading buffer [80% (v/v) acetonitrile, 15% (v/v) water, 5% (v/v) TFA and 1 M glycolic acid] for 15 min with shaking. The supernatant was discarded followed by peptide dilution in 50 μ l of loading buffer. Diluted peptides were transferred and incubated with the TiO₂ beads for 15 min while shaking. Beads were pelleted and the supernatant (NB fraction) was transferred to a new tube. Then, 50 μ l of washing buffer I [80% (v/v) acetonitrile, 19% (v/v) water and 1% (v/v) TFA] was added and samples were shaken for 15 min. Beads were pelleted followed by a second washing step with washing buffer II [20% (v/v) acetonitrile, 79.8% (v/v) water and 0.2% TFA]. Combined supernatants of both washing steps were transferred to a new tube (W fraction). Before eluting the bound phosphopeptides, the beads were evaporated to dryness using a SpeedVac at room temperature for 30 min. Elution was performed twice using 50 μ l and 100 μ l of elution solution (1% NH₄OH in H₂O). Supernatants from both elution steps were combined (P fraction) and acidified with 5 μ l of pure TFA and dried using a SpeedVac. Before MS analysis, each sample (NB, W or P) was diluted in 16.5 μ l of eluent A (0.05% formic acid in water).

Mass spectrometry

Protein digests were separated and analysed by RP (reverse-phase) LC using an UltiMate 3000 nano-HPLC system (Dionex) coupled online to an LTQ Orbitrap Velos equipped with ETD support (Thermo Fisher). Solvents used for LC were: solvent A (0.05% formic acid in water) and solvent B [80% (v/v) acetonitrile and 0.04% formic acid in water]. For sample loading, a solution of 3% (v/v) acetonitrile and 0.1% TFA was used. The flow rates were 30 μ l/min for the loading and 30 nl/min for the micro-pump. Isocratic elution (5% B) was used for the first 4 min, followed by an increase to 10% B within 1 min. Then a linear gradient to 50% B within 80 min was used. Column washing was performed by a linear increase of B to 95% within 10 min and held for 5 min. Re-equilibration was set to 10 min at 5% B.

A dual top five CID (collision-induced dissociation)-HCD (higher-energy collisional dissociation fragmentation) method was written manually using XCalibur 2.1. Here, a MS full scan

was acquired at a resolution of 60000 with activated pre-scan. For fragmentation, the five most intense precursor ions were selected for fragmentation by CID (default settings) and analysis in the ion trap. Afterwards, the same five most intense precursor ions were selected for fragmentation by HCD (normalized collision energy 45%; isolation window of m/z 3; remaining settings were default). To increase the number of acquired peptide ions, dynamic exclusion was activated (repeat count of three within 20 s and an exclusion duration of 30 s; the number of entries was set to 500). For LC-ESI-MS/MS analysis, 14 μ l of the *in vivo* sample, 10 μ l of the phosphopeptide fraction and 5 μ l of the non-phosphopeptide fraction (*in vitro* sample) were injected.

Database searches and data evaluation

Proteome Discoverer 1.4 (PD) with Mascot (version 2.2.04) and SEQUEST HT (shipped with PD) were used. The complete reference proteome set of *A. thaliana* was downloaded (November 2013, taxonomy identity: *A. thaliana*, reviewed proteins only) from Uniprot. A PD workflow consisting of the following nodes was created; if not specified otherwise, the default settings were used: (0) Spectrum Files; (1) Spectrum Selector; (2) MS2 - Spectrum Processor, (3) Scan Event Filter [splitting into CID-IT (CID in an ion trap) or HCD data]; (4) Mascot or SEQUEST HT (see below); (5) phosphoRS 3.0; (6) Percolator; (8) Scan Event Filter; (11) Event Detector and (12) Precursor Ions Area Detector. In total, four (independent) database searches were performed using CID-IT or HCD MS/MS data and Mascot and SEQUEST HT respectively. The resulting four .msf files were opened together and filtered for high confidence with a validation threshold of 0.01 based on the q -value. The combination of four independent searches was required as phosphoRS 3.0 [32] is only used for the search engine node with the lowest number in the PD workflow in a multi-database search engine workflow.

For PSMs (peptide-spectrum matches), the precursor mass tolerance window was set to 10 p.p.m. Fragment ions in MS/MS spectra were matched with a tolerance window of 0.02 Da and 0.3 Da for HCD (Orbitrap) and CID (ion trap). Carbamidomethylation was set as static, and oxidation of methionine and phosphorylation of serine, threonine and tyrosine as dynamic modification respectively. No-enzyme specificity was set as at least two (elastase and trypsin) and four (chymotrypsin, elastase, GluC and trypsin) different proteases were used respectively.

For data evaluation, GAMBAS (version 3) scripts were written in house. These scripts were used to group peptide identification features of the phosphopeptides identified. The .txt files of the PSMs were loaded and phosphorylated peptide identifications were grouped together on the basis of their sequence, retention time difference (<20 min) and $[M + H]^+$ m/z values. Using these data, the start and end position of the peptide within the protein of interest was extracted. Furthermore, it was determined (Boolean value) whether this peptide was identified by Mascot or SEQUEST with CID and HCD respectively. Additionally, the number of hits for each of the four combinations was counted. The average peptide $[M + H]^+$ mass, its average retention time and precursor mass (obtained from the Precursor Ions Area Detector) were calculated.

To allow for improved data handling of the high complex peptide composition with up to four enzymes that release peptides with nearly identical, but overlapping, sequences, the phosphorylation site mapping was performed by (i) using the results from the search engines, and (ii) the phosphoRS score. For the search-engine-based approach, (i), the number of phosphorylation site localizations was counted and the maximal

value reported and set as 'most likely'. In addition, the number of hits for this modification was set in relation to the overall number of peptide hits within the peptide under investigation. PhosphoRS report percentages were calculated by dividing the phosphoRS score by the accumulated value. Finally, the results were normalized to an accumulated value of 100%. The percentage values for each modification within a peptide under investigation were summed and divided by the number of hits. This value is reported and used as 'normalized' phosphoRS probability value.

RESULTS AND DISCUSSION

Identification of PSKR1 autophosphorylation sites

To understand phosphorylation-dependent signalling mechanisms of PSKR1, one aim of the present study was to identify phosphorylation sites in the cytoplasmic domain of the receptor using MS analysis. PSKR1s belong to the large family of RD-type LRR RLKs, many of which are activated by phosphorylation of one or more residues in the AL (Figure 1). Regulation of receptor activity may also occur through phosphorylation of other subdomains. To identify phosphorylated amino acid residues in PSKR1, ectopically expressed His₆-tagged soluble PSKR1 KD (His₆-PSKR1-KD) protein was autophosphorylated *in vitro* as shown previously [16]. The protein was separated on an SDS gel and subjected to an in-gel multi-protease digestion procedure [30], using two relatively low-specific (chymotrypsin and elastase) and two high-specific (GluC and trypsin) proteases. Phosphopeptides were enriched using TiO₂ and then analysed by LC-ESI-MS/MS. Two different MS/MS approaches, namely CID-IT and HCD in an Orbitrap mass analyser, were used, as the acquisition of a dual fragmentation method can increase the accuracy of phosphorylation site mapping utilizing computational proteomics tools [33].

On the basis of phosphopeptide grouping applied to estimate the correctness of the automated phosphorylation site mapping (see the Experimental section for further information), various phosphorylated peptides could be identified and their phosphorylation sites localized. Manual MS/MS spectra interpretation was done to verify the identifications.

Site mapping was significantly facilitated by using the four proteases and both the phosphoRS score [32] and the search engine results, e.g. for four peptides MSPYETHV, MSPYETHVSTDLVGTL, RLMSPYETHVSTDLVGTL and LMSPYETHVSTDLVGLGYPPEYQASVATYK, covering the phosphorylation site Thr⁸⁹⁰ (Supplementary Figures S1A-S1D respectively). The use of four different proteases generated peptides ranging from 8 to 33 amino acids ($[M + H]^+$: 1043.4-3667.7) with different physicochemical properties (e.g. change of fragmentation pattern by C-terminal residues). This enabled us to localize the phosphorylation site with high confidence. Overall, using this multi-protease strategy, a sequence coverage of 99% was achieved for the His₆-PSKR1-KD protein.

On the basis of the dataset and on the number of PSM and phosphoRS scores, eight phosphorylation sites were identified: Ser⁷¹⁷ in the JM domain, Ser⁷³³, Thr⁷⁵², Ser⁷⁸³, Ser⁸⁶⁴, Ser⁹¹¹, Ser⁹⁵⁸ and Thr⁹⁹⁸ (Figure 1 and Table 1). Moreover, on the basis of automated and manual inspection of the data, at least one and possibly two sites (Thr⁸⁹⁰, Ser⁸⁹³ or Thr⁸⁹⁴) in the AL of PSKR1 spanning residues 886-894 is likely to be phosphorylated (Figures 1 and 2A, and Table 1). Here, Thr⁸⁹⁰ represented the most likely phosphorylation site on the basis of the automated phosphorylation site mapping approaches (phosphoRS score and database search engines). In addition, peptides covering this

potential phosphorylation site show a high diversity of sequence length (between 8 and 33 amino acids) and starting positions (883–886). This resulted in 29 unique peptide sequences encompassing different modification forms of a peptide with the same sequence that, as a group, can be used for phosphorylation site localization. Together with these singly phosphorylated peptide species, a second, doubly phosphorylated, form was also detected, probably a combination of Thr⁸⁹⁰ and Ser⁸⁹³ or Thr⁸⁹⁰ and Thr⁸⁹⁴. However, owing to the close proximity of Ser⁸⁹³ and Thr⁸⁹⁴, an unambiguous localization of the second site was not possible. At present, we cannot exclude that both forms exist in parallel.

To verify that the identified amino acids were indeed targets of autophosphorylation by PSKR1 rather than targets of *E. coli* kinases we expressed and affinity-purified kinase-inactive His₆-PSKR1(K762E)-KD protein [16]. In this mutant protein, an invariant lysine residue in subdomain II that is conserved in all kinases and that is essential for kinase activity was replaced by glutamate [34]. Kinase-inactive His₆-PSKR1(K762E)-KD protein was subjected to a phosphorylation assay and phosphopeptide analysis by LC-ESI-MS/MS. The sequence coverage of His₆-PSKR1(K762E)-KD was comparable with that obtained for His₆-PSKR1-KD. For this mutant protein, one phosphorylation site (Thr⁸⁹⁰) was determined *in vitro* (median phosphoRS score >99%; Supplementary Table S1) suggestive of *trans*-phosphorylation of this residue by *E. coli*.

To compare the precursor ion signal areas and the PSM respectively, as a quantitative measure of the extent of phosphorylation, the corresponding values (i.e. precursor area or PSM) of the sample were divided by the sum of sample and control. In total, 11 peptide species (including forms with different modifications) were identified for the phosphorylation site Thr⁸⁹⁰ (Supplementary Table S2). To normalize the data, the median of all 11 peptide species was calculated. For the precursor area, median values of 94.5% (His₆-PSKR1-KD) and 5.5% [His₆-PSKR1(K762E)-KD] was obtained. Similar values were calculated for the PSM [89.7% for His₆-PSKR1-KD and 10.3% for His₆-PSKR1(K762E)-KD]. To evaluate the extent of phosphorylation between His₆-PSKR1-KD and His₆-PSKR1(K762E)-KD, the same approach as described before was performed. Comparing the peptide sequences, the percentage distribution [His₆-PSKR1-KD/(His₆-PSKR1-KD + His₆-PSKR1(K762E)-KD)] was 94% and 90% for the label-free and SPC (spectral counting) approach respectively (Supplementary Table S2), indicating that the extent of phosphorylation in His₆-PSKR1(K762E)-KD was much lower. Nonetheless, the kinase-inactive His₆-PSKR1(K762E)-KD protein is a suitable substrate for an as yet unknown bacterial kinase. Probably, phosphorylation takes place during ectopic expression of the mutant protein in *E. coli*. It is unlikely that the phosphorylation event originates from any kinase activity of the mutant His₆-PSKR1(K762E)-KD protein, since a replacement of the invariant lysine residue in subdomain II by glutamate results in a loss of kinase-mediated phosphotransfer [34]. Consistent with this, His₆-PSKR1(K762E)-KD kinase activity was essentially abolished (Figure 2). Phosphorylations at the JM domain, the KD and close to the CT domain result from activity of the wild-type His₆-PSKR1-KD protein and reveal a pattern that is common for receptor kinases [21,23].

Identification of *in planta* PSKR1 phosphorylation sites

To identify *in planta* PSKR1 phosphorylation sites, a C-terminally GFP-tagged full-length PSKR1 sequence was generated, placed

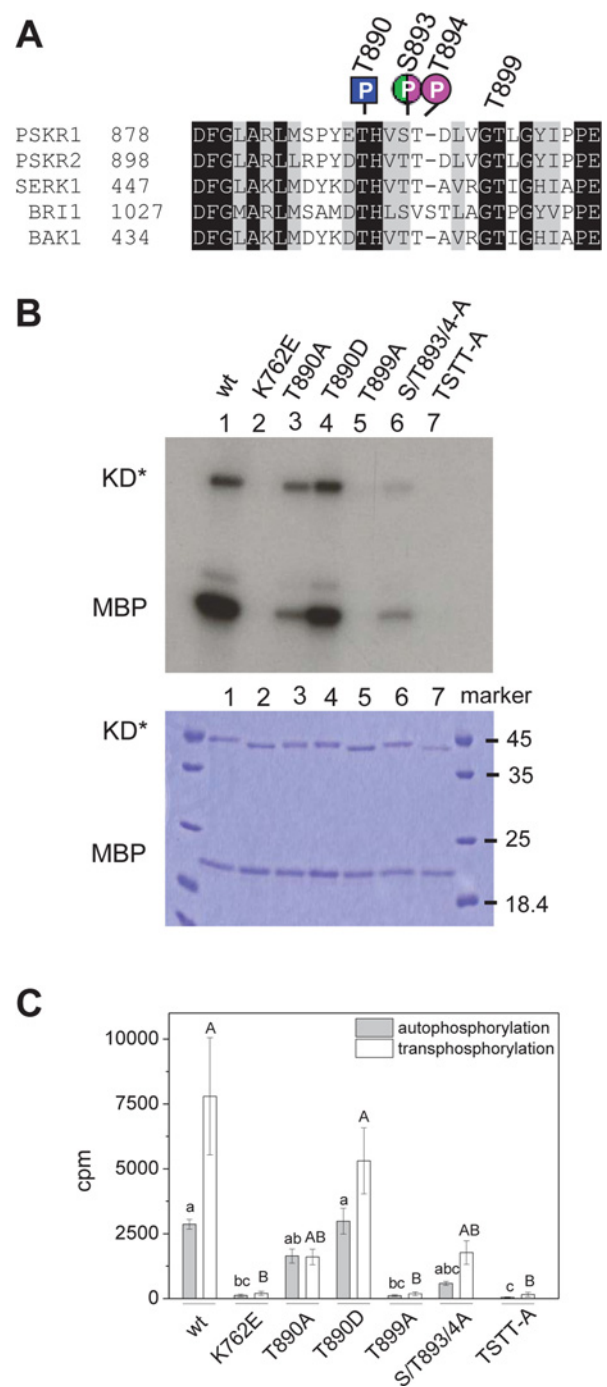


Figure 2 Site-directed mutagenesis of PSKR1 activation segment or KD residues impairs kinase activity *in vitro*

(A) Alignment of the activation segments encompassing the AL (Ser⁸⁸⁶–Thr⁸⁹⁴ in PSKR1) of PSKR1, PSKR2, SERK1, BRI1 and BAK1. The phosphorylation sites of PSKR1 that were identified *in vitro* (magenta), *in planta* (green) or in the kinase-inactive variant in *E. coli* (blue) are indicated. (B) Top: autoradiograph of recombinant PSKR1-KD variants (KD*) showing autophosphorylation of KD* and *trans*-phosphorylation of MBP: wild-type (lane 1), the kinase-inactive His₆-PSKR1(K762E)-KD (lane 2), His₆-PSKR1(T890A) (lane 3), His₆-PSKR1(T890D) (lane 4), His₆-PSKR1(T899A) (lane 5), His₆-PSKR1(S893A/T894A) (lane 6), and His₆-PSKR1(TSTT-A) (lane 7). Bottom: Coomassie Blue-stained gel as a control for protein loading. (C) Mean ± S.E.M. radioactivity ($n = 6$ from three independent experiments) of *trans*-phosphorylated [³²P]MBP and autophosphorylated [³²P]KD* is given as c.p.m. Kruskal–Wallis all-pairwise comparisons were performed for autophosphorylation (lower-case letters) and for *trans*-phosphorylation (capital letters) activities. TSTT-A, T890A/S893A/T894A/T899A; wt, wild-type.

Table 1 Identification of *in vitro* phosphorylation sites of His₆-PSKR1-KD protein by LC-ESI-MS/MS

Residue	Median phosphoRS score	Average phosphoRS score	Standard error	Number of unique* peptides	Number of accumulative PSMs†
Ser ⁷¹⁷	100.00	88.69	7.47	9	134
Ser ⁷³³	48.30	48.30	–	1	28
Thr ⁷⁵²	100.00	100.00	–	1	2
Ser ⁷⁸³	58.40	58.40	–	1	11
Ser ⁸⁶⁴	98.20	98.20	–	1	5
Thr ⁸⁹⁰	95.95	86.99	2.44	48	1306
Thr ⁸⁹⁰ and Ser ⁸⁹³ /Thr ⁸⁹⁴	Ambiguous	Ambiguous	Ambiguous	9	142
Ser ⁹¹¹	100.00	100.00	–	1	9
Ser ⁹⁵⁸	89.80	79.95	5.97	11	99
Thr ⁹⁹⁸	61.15	61.15	11.15	2	3

*Unique peptides are identified peptide sequences which can be used for unambiguous peptide and protein identification. For the multi-protease approach applied in the present study, this also includes overlapping peptide sequences.

†PSMs are MS/MS spectra to which a peptide sequence was mapped by a database search algorithm and validated further by false discovery rate analysis (1%). Here, the total number of PSMs was summed for each individual phosphorylation site.

under control of the CaMV 35S promoter and stably expressed in wild-type plants. PSKR1-GFP fluorescence was observed in mesophyll protoplasts derived from 4-week-old *35S:PSKR1-GFP* plants where it was localized to the plasma membrane as expected (Figure 3C). Roots of 5-day-old *35S:PSKR1-GFP* seedlings were significantly longer than wild-type roots indicating that receptor overexpression caused a specific growth response (Figures 3A and 3B) and that the GFP fusion did not impair *in planta* receptor function. Total protein was extracted from 14-day-old *35S:PSKR1-GFP* and from wild-type seedlings followed by immunoprecipitation with anti-GFP antibody. A band with a size of approximately 175 kDa was detected in protein samples of the transgenic line, but not in the sample from wild-type seedlings (Figure 3D). GFP has a molecular mass of ~27 kDa and the *Arabidopsis* PSKR1 protein has a calculated mass of 112353 Da. However, the PSKR from *Daucus carota* was shown to be glycosylated *in planta*, increasing its molecular mass by ~10 kDa. The ~175 kDa protein band was detected in Western blot analysis with anti-GFP antibody, suggesting that it corresponded to the PSKR1-GFP fusion protein. This was subsequently verified by LC-ESI-MS/MS. The amount of immunoprecipitated PSKR1-GFP protein correlated with the anti-GFP antibody concentration that was used for immunoprecipitation.

To identify *in planta* PSKR1 phosphorylation sites, the PSKR1-GFP band was excised, in-gel digested with trypsin or elastase and subjected to LC-ESI-MS/MS analysis. The phosphorylated peptides identified are listed in Supplementary Table S3 and representative MS/MS spectra are shown in Supplementary Figures S2A–S2C. Combining the peptides generated by elastase and tryptic digestion, 74.70% of the protein sequence was covered. Three possible phosphorylation sites were identified. Ser⁶⁹⁸ (median phosphoRS score >93%; Figure 1A and Supplementary Table S3), which is located in the JM region represents a true *in planta* phosphorylation site. A double-phosphorylated peptide probably at Ser⁶⁹⁶ and Ser⁶⁹⁸ was also detected. A third site was located at Ser⁸⁸⁶ or Ser⁸⁹³ (Figures 1A and 2A, and Supplementary Table S3). Unfortunately, an unambiguous localization of this phosphorylated residue was not possible. More residues may be phosphorylated *in planta* that may be identified using the native promoter or an optimized extraction procedure. Nonetheless, the data indicate that at least one site (Ser⁸⁸⁶ or Ser⁸⁹³) in the AL of PSKR1 is phosphorylated *in planta*.

Taken together, the LC-ESI-MS/MS analyses identified only phosphorylation of serine/threonine residues consistent with the fact that PSKR1 displays a predicted serine/threonine kinase catalytic domain based on the 12 subdomains that are characteristic of this class of kinases [9,14,15]. A preference for serine over threonine residues was observed which has also been shown for the LRR RLKs BRI1 and CLV1 [35–37]. A recent study found that BRI1, BAK1 (BRI1-ASSOCIATED RECEPTOR KINASE) and BKK1 (BAK1-LIKE 1) are also autophosphorylated at tyrosine residues, indicating that these are dual-specificity kinases [38]. Bojar et al. [39] report conservation of the conformation of the AL and of core phosphorylation sites among different plant RLKs [40–44]. It is hence conceivable that PSKR1 could also exhibit dual specificity, although phosphorylation of tyrosine residues was not detected in the present study.

Conservation of serine/threonine residues in positions aligning with phosphosites in PSKR1

To identify conserved positions of phosphorylatable amino acids in PSKR1 throughout the plant kingdom, we identified PSKR1 as well as PSKR2 orthologues from the genomes of 35 higher plants and of two mosses using the Phytozome database [45]. The intracellular kinase sequences were aligned (Supplementary Figures S4 and S5). The conservation of phosphorylatable amino acids at each site of PSKR1 and PSKR2 orthologues is summarized in Figure 4. Three of the positions that are phosphorylated in the AL of PSKR1, Thr⁸⁹⁰, Ser⁸⁹³ and Thr⁸⁹⁴, were conserved in all PSKR1 and PSKR2 orthologues including those from mosses. The ambiguous phosphorylation site at Ser⁸⁸⁶ was conserved in PSKR1 homologues from Brassicaceae only. A serine residue aligns with Ser⁸⁶⁴ in subdomain V1b N-terminal to the activation segment in all plant PSKR1 and PSKR2 homologues, indicative of a conserved function in PSKR1.

In the JM region, the position of at least one of the two residues Ser⁶⁹⁶ and Ser⁶⁹⁸ was conserved in 83.3% of higher plant PSKR1 orthologues, but not in PSKR2 orthologues. In PSKR1, Ser⁷¹⁷ was exclusive to *A. thaliana*, whereas Ser⁷¹⁷ was present in ~22% of higher plant PSKR2 orthologues, mostly from the Brassicaceae lineage.

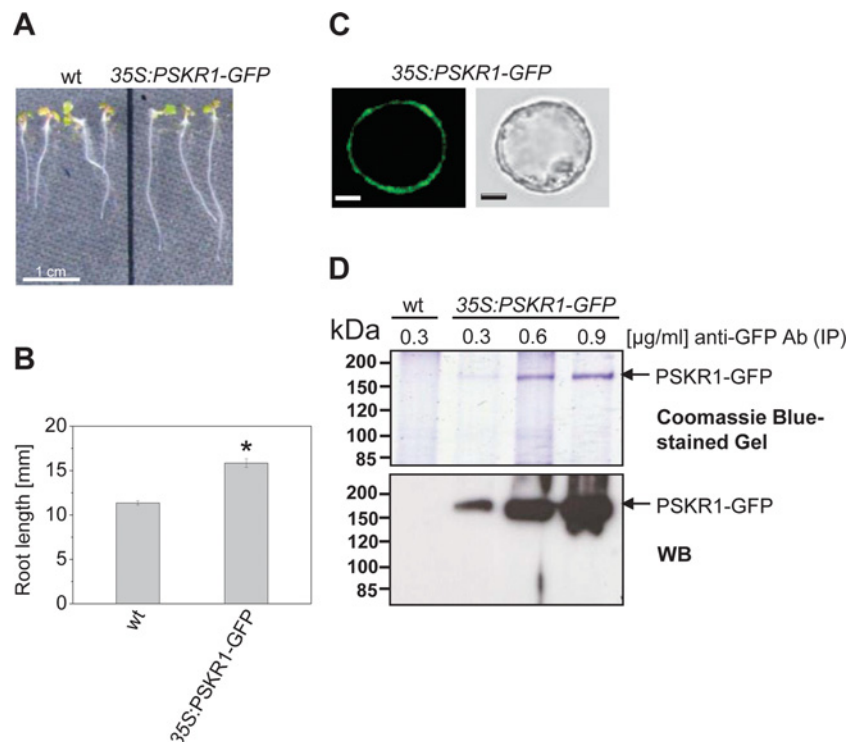


Figure 3 Functional analysis, localization and purification of PSKR1-GFP

(A) Phenotypes of 5-day-old seedlings from wild-type and *35S:PSKR1-GFP* expressed in the wild-type background. (B) Mean \pm S.E.M. root lengths were determined in two independent experiments with at least 46 seedlings analysed per genotype. The asterisk indicates significantly different values between wild-type and *35S:PSKR1-GFP* ($P < 0.05$, two-sample Student's *t* test). (C) PSKR1-GFP localization was analysed by confocal laser-scanning microscopy in mesophyll protoplasts of 4-week-old soil-grown *35S:PSKR1-GFP* plants. The receptor protein is expressed and localized at the plasma membrane. Scale bars, $5 \mu\text{m}$. (D) Immunoprecipitation of PSKR1-GFP from total protein extracts obtained from seedlings expressing PSKR1-GFP with anti-GFP antibody added at the concentrations indicated. As a control, extract from wild-type seedlings was analysed. The proteins immunoprecipitated from wild-type and PSKR1-GFP extracts were separated by SDS/PAGE (10% gel) and fusion protein was detected with an anti-GFP antibody. Molecular masses of marker proteins are indicated in kDa. Ab, antibody; IP, immunoprecipitation; WB, Western blot; wt, wild-type.

Subdomain X is overall little conserved and Ser⁹⁵⁸ that was phosphorylated in PSKR1 was present at this position only in that receptor. By contrast, Thr⁹⁹⁸ was conserved in 83.3% of PSKR1 orthologues, but in only one PSKR2 protein. The positions of the phosphorylated serine residues in the JM region of PSKR1 are not conserved in the two moss homologues, whereas, in most higher plant orthologues, at least one of the two positions is occupied by a phosphorylatable amino acid. Taken together, the positions of phosphorylatable amino acids in the AL are strictly conserved in PSKR1, suggesting a conserved mode of receptor regulation. By contrast, positions of PSKR1 phosphosites in the JM region are not retained in PSKR2 orthologues and are altogether absent from PSKR orthologues from mosses. Possibly, regulation via phosphorylation of the JM region has evolved early during higher plant evolution, possibly arising from a need for more complex receptor regulation in cormophytes. The differences in phosphosites between PSKR1 and PSKR2 orthologues suggest that regulation at these sites has evolved faster and is less subject to selection pressure than the regulation of the AL.

To date, regulation of only a few of the 610 RLKs encoded in the *Arabidopsis* genome [46] has been analysed and therefore our knowledge on conserved and unique modes of plant receptor regulation at the level of phosphorylation is limited [24,37,47–49]. The detailed analysis provided in the present study not only helps to further our understanding of PSK signalling, but also provides comparative data for the study of related RLKs.

Phosphoablative mutagenesis suggests that phosphorylation within the AL activates PSKR1

The activation segment starts at the highly conserved DFG motif in kinase subdomain VII and most often terminates with the sequence APE in subdomain VIII [14,15,22] (Figures 1 and 2A). It consists of the Mg²⁺-binding loop, the β -9 sequence, the AL (Ser⁸⁸⁶-Thr⁸⁹⁴ in PSKR1) and the p + 1 loop with Thr⁸⁹⁹ in PSKR1 [50]. Phosphorylation of one to three residues in the AL results in a conformational change accompanied by kinase activation. In some cases, it also affects binding of kinase substrates [22,23]. To resolve the ambiguities concerning specific *in vitro* phosphorylation sites in the AL of PSKR1 and to test for a functional role of these phosphorylation sites with respect to kinase activity, site-directed mutagenesis was performed on the soluble KD of PSKR1 (PSKR1-KD). The serine and threonine residues were mutated to alanine which prevents phosphorylation and, in the case of Thr⁸⁹⁰, to aspartate which acts as a phosphomimic [23,36]. PSKR1-KD proteins with T890A, T890D, T899A and S893A/T894A mutations, or the quadruple mutation T890A/S893A/T894A/T899A (denoted TSTT-A), were ectopically expressed as fusion proteins with an N-terminal His₆ tag. Auto- and *trans*-phosphorylation of the common substrate MBP were analysed *in vitro* using radiolabelled [γ -³²P]ATP. As controls, the wild-type His₆-PSKR1-KD and the His₆-PSKR1(K762E)-KD variant were analysed [16]. Even though Thr⁸⁹⁰ was a target of *trans*-phosphorylation by *E. coli*, it cannot be ruled out that it is also a target of autophosphorylation.

	JM					Activation loop						CT		
	S696	S698	S717	S733	T752	S783	S864	S886	T890	S893	T894	S911	S958	T998
Embryophyte														
— <i>Physcomitrella patens</i>	--	--	--	--	--	--	++	++	+	++	++	--	--	--
Tracheophyte														
— <i>Selaginella moellendorffii</i>	--	--	--	--	--	--	++	--	++	••	++	++	--	--
Angiosperm														
— <i>Amborella trichopoda</i>	--	--	--	--	+•	++	++	--	++	••	++	+•	--	--
Grass														
— <i>Brachypodium distachyon</i>	--	•-	--	--	+•	++	++	--	++	••	++	+•	--	•-
— <i>Oryza sativa</i>	--	•-	--	--	+•	++	++	--	++	••	++	+•	--	+•
— <i>Panicum virgatum</i>	--	--	--	--	+•	++	++	--	++	••	++	--	--	•-
— <i>Setaria italica</i>	•-	•-	--	--	+•	++	++	--	++	••	++	+•	--	+•
— <i>Sorghum bicolor</i>	--	•-	--	--	+•	++	++	--	++	••	++	+•	--	+•
— <i>Zea mays</i>	--	•-	--	--	+•	++	++	--	++	••	++	+•	--	+•
Eudicot														
— <i>Aquilegia coerulea</i>	--	+•	--	--	+•	++	++	--	++	+•	++	+•	--	+•
Pentapetales														
— <i>Mimulus guttatus</i>	+•	•-	--	--	--	++	++	--	++	+•	++	+•	--	--
— <i>Solanum lycopersicum</i>	--	+•	--	--	--	++	++	--	++	••	++	+•	--	••
— <i>Solanum tuberosum</i>	--	+•	--	--	--	++	++	--	++	••	++	+•	--	••
— <i>Vitis vinifera</i>	+•	--	--	--	--	++	++	--	++	••	++	--	--	--
Rosid														
Malvidae														
— <i>Eucalyptus grandis</i>	--	--	--	--	+•	++	++	--	++	••	++	+•	--	+•
— <i>Populus trichocarpa</i>	--	•-	--	--	+•	++	++	--	++	••	++	--	--	+•
— <i>Linum usitatissimum</i>	+•	--	--	--	•-	++	++	--	++	••	++	--	--	--
— <i>Manihot esculenta</i>	--	•-	--	--	+•	++	++	--	++	••	++	+•	--	+•
— <i>Ricinus communis</i>	--	•-	--	--	+•	++	++	--	++	••	++	+•	--	+•
Brassicales-Malvales														
— <i>Carica papaya</i>	--	--	--	--	++	++	++	--	++	••	++	++	--	++
— <i>Gossypium raimondii</i>	--	•-	-+	--	+•	++	++	--	++	••	++	+•	--	+•
— <i>Theobroma cacao</i>	--	•-	-+	--	•-	++	++	--	++	••	++	+•	--	+•
Brassicaceae														
— <i>Arabidopsis lyrata</i>	+•	+•	-+	+•	+•	++	++	+•	++	+•	++	+•	--	+•
— <i>Arabidopsis thaliana</i>	+•	+•	++	+•	+•	++	++	+•	++	+•	++	+•	+•	+•
— <i>Boechera stricta</i>	+•	+•	-+	+•	+•	++	++	+•	++	+•	++	+•	--	+•
— <i>Brassica rapa</i>	--	+•	-+	--	--	++	++	+•	++	+•	++	+•	--	+•
— <i>Capsella grandiflora</i>	+•	+•	-+	+•	+•	++	++	+•	++	+•	++	+•	--	+•
— <i>Capsella rubella</i>	+•	+•	-+	+•	+•	++	++	+•	++	+•	++	+•	--	+•
— <i>Eutrema salsugineum</i>	--	+•	-+	-+	+•	++	++	+•	++	+•	++	+•	--	+•
Citrus														
— <i>Citrus sinensis</i>	--	•-	--	--	++	++	++	--	++	••	++	+•	--	+•
— <i>Citrus clementina</i>	--	•-	--	--	++	++	++	--	++	••	++	+•	--	+•
Fabidae														
— <i>Cucumis sativus</i>	+•	--	--	--	+•	++	++	--	++	••	++	+•	--	+•
— <i>Glycine max</i>	--	--	--	--	••	++	++	--	++	••	++	--	--	--
— <i>Malus domestica</i>	--	•-	--	--	•-	++	++	--	++	••	++	+•	--	+•
— <i>Medicago truncatula</i>	+•	--	--	--	••	++	++	++	++	••	++	--	--	--
— <i>Phaseolus vulgaris</i>	--	--	--	--	••	++	++	--	++	••	++	--	--	--
— <i>Prunus persica</i>	•-	+•	--	--	+•	++	++	--	++	••	++	+•	--	+•

Figure 4 Conservation of serine and threonine residues of PSKR1 orthologues (left symbol) and PSKR2 orthologues (right symbol) in positions aligning with PSKR1 phosphorylation sites

A dot indicates a conserved substitution of the respective residue by serine, threonine or tyrosine; – indicates no conservation, and + indicates a conserved P site. The species tree used in the present study was constructed by modifying the Phytozome version 10 plant tree of life.

On the basis of this reasoning, we included analysis of this residue. The T890A mutation resulted in overall reduced kinase activity compared with the wild-type, whereas the T890D mutant displayed wild-type activity (Figures 2B and 2C). The auto-, but not *trans*-, phosphorylation activity of the S893A/T894A mutant was lower than that of the T890A mutant.

Several studies described an important role for AL phosphorylation in the kinase activity of BRI1 and BAK1 [24,25,41,44]. Mutations of BRI1 AL residues corresponding to PSKR1 Thr⁸⁹⁰ and Ser⁸⁹³ likewise had a moderate effect on BRI1 kinase activity, indicating that the kinase activities of soluble PSKR1-KD and BRI1-KD are regulated in a similar manner by this residue. BAK1-KD is also autophosphorylated at two residues equivalent to Thr⁸⁹⁰ and Ser⁸⁹³. However, single mutations of BAK1 AL residues corresponding to PSKR1 Thr⁸⁹⁰, Ser⁸⁹³ and Thr⁸⁹⁴ had little effect on BAK1 kinase activity, revealing a distinct difference between this co-receptor and the receptors BRI1 and PSKR1. Replacement of all three threonine residues by alanine in the AL of BAK1 abolished its activity.

Interestingly, BRI1 and SERK1 AL residues corresponding to PSKR1 Thr⁸⁹⁰ and Ser⁸⁹³ affect substrate phosphorylation more than autophosphorylation *in vitro* [24,25]. On the basis of the crystal structure of the BRI1 KD, the BRI1 AL residues corresponding to PSKR1 Thr⁸⁹⁰ and Ser⁸⁹³ were found to be phosphorylated and were surface-oriented, probably contributing to the stabilization of the conformation of the AL by interaction with a third residue equivalent to PSKR1 His⁸⁹¹ [41]. In the dephosphorylated state, the AL impairs ATP binding and/or lowers the rate of phosphotransfer to the substrate [21,22]. Dependent on its phosphorylation state, the AL is characterized by defined conformational changes [23,37]. Our data suggest that differential phosphorylation of the AL may result in partial receptor activation.

Thr⁸⁹⁹ was not identified as a site of phosphorylation. Nonetheless, it is conserved in all PSKR1 and PSKR2 orthologues from higher and lower plants (Figure 4, and Supplementary Figures S4 and S5) and the equivalent residue in BRI1 was shown to be a likely candidate for phosphorylation [24]. Thr⁸⁹⁹ was therefore included in this mutational analysis. The T899A mutant was inactive, strongly arguing for a crucial role of the invariant Thr⁸⁹⁹ in kinase activity. Similarly, the quadruple TSTT-A mutation resulted in loss of kinase activity.

Phosphoablative mutagenesis within the AL differentially alters PSKR1 activity *in planta*

The high conservation of potential phosphosites in the AL of PSKR orthologues and the differential effect of individual phosphosites on PSKR1 kinase activity prompted us to analyse the impact of AL phosphorylation and of the adjacent Thr⁸⁹⁹ on growth regulation by PSKR1 *in planta*. To that end, we generated T890A, T890D, T899A, S893A/T894A and TSTT-A point-mutated full-length *PSKR1* sequences that were expressed under the control of the CaMV 35S promoter in the receptor-null background. Expression of the transgenes was analysed in 5-day-old seedlings in the independent lines 35S:*PSKR1(T890A)*-1,2,3,4; 35S:*PSKR1(T899A)*-1,2,3,4,5, 35S:*PSKR1(S893A/T894A)*-1,2,3,4,5, 35S:*PSKR1(TSTT-A)*-1,2,3 and 35S:*PSKR1(T890D)*-1,2,3,4,5 by RT-PCR (Supplementary Figures S3A and S3B). In the null background line *pskr1-3 pskr2-1* (denoted *r1r2*), no *PSKR1* mRNA was detected, indicating that growth promotion was driven exclusively by the respective receptor variant.

Transgenic lines expressing the various receptor mutants were analysed for their ability to rescue the short-root phenotype of the PSKR-null mutant *r1r2*. Root lengths of 5-day-old wild-type, *r1r2*, *r1r2 35S:PSKR1-GFP-1*, *r1r2 35S:PSKR1(T890A)*, *r1r2 35S:PSKR1(T890D)*, *r1r2 35S:PSKR1(T899A)*, *r1r2 35S:PSKR1(S893A/T894A)* and *r1r2 35S:PSKR1(TSTT-A)* seedlings as well as their responsiveness to exogenously supplied PSK were measured (Figures 5A and 5B). *r1r2* roots were significantly shorter than wild-type roots. Expression of wild-type PSKR1 in *r1r2 35S:PSKR1-GFP-1* seedlings rescued the short-root phenotype of *r1r2* and resulted in root lengths similar to that of wild-type.

The phosphoablative mutations in the AL and of the adjacent Thr⁸⁹⁹ impaired root elongation in different ways. The T890A mutant did not, or only weakly, rescue the short-root phenotype of *r1r2* in accord with the reduced kinase activity of this mutant (Figures 2B and 5A). However, *r1r2 35S:PSKR1(T890A)*-1,2,3,4 seedlings were still responsive to PSK, indicating that activation of the receptor by ligand binding is not fully dependent on Thr⁸⁹⁰. Replacing Thr⁸⁹⁰ by a phosphomimic aspartate residue resulted in wild-type root lengths in five independent lines (Figure 5B). At least two of the *r1r2 35S:PSKR1(T890D)* lines (4 and 5) had an overexpression phenotype [4], indicative of an active receptor. None of the lines displayed enhanced root elongation when treated with PSK, possibly because the response was saturated. The PSKR1(S893A/T894A) receptor had weak root-growth-promoting activity in accord with the weak *in vitro* kinase activity (Figures 2B and 5A). Root lengths were intermediate between those of the receptor-null mutant and the wild-type (Figure 5A). Unlike the PSKR1(T890A) receptor, which was activated by PSK, ablation of the phosphosites Ser⁸⁹³/Thr⁸⁹⁴ abolished responsiveness to PSK in four of the five PSKR1(S893A/T894A) lines and diminished it considerably in the fifth line.

An intriguing difference between *in vitro* kinase activity and *in planta* receptor function was unveiled for the PSKR1(T899A) mutant. Even though this residue was not identified as being phosphorylated, it is a conserved residue in all PSKRs, and the BRI1 AL residue corresponding to PSKR1 Thr⁸⁹⁹ is a likely phosphosite *in planta* [24]. Mutation of the conserved AL residue in BRI1 and BAK1 that corresponds to Thr⁸⁹⁹ in PSKR1 abolished the kinase activities of both receptors. Whereas the T899A mutation in PSKR1-KD similarly abolished kinase activity *in vitro* (Figures 2B and 2C), it did not impair basal PSKR1 receptor activity *in planta* (Figure 5A). This suggests that folding of the KD in an active receptor *in planta* may depend on other factors. It is conceivable that the PSKR1(T899A) receptor is complemented by heterodimerization with another kinase *in planta* that aids in signal transduction as demonstrated recently for BAK1 [20]. The PSKR1(T899A) seedlings were, however, unresponsive to PSK, indicating some impairment in signal regulation.

Mutating all three serine and threonine residues in the AL and Thr⁸⁹⁹ to alanine not only abolished kinase activity, but also, upon *in planta* expression, resulted in roots that were as short as or shorter than the roots of *r1r2* seedlings, indicating that this receptor was inactive *in planta* (Figure 5A). The importance of these AL residues to receptor activity *in planta* is supported by the fact that all sites are under high selection pressure in PSKR1 and PSKR2 orthologues.

Analysis of soil-grown plants revealed that the phosphoablative mutations had a similar effect on plant shoot growth as it had on seedling root growth and hence confirmed the differential effect of specific phosphosites on receptor activity (Figure 6). The rosette sizes of 4-week-old *r1r2 35S:PSKR1(T890A)* and of *r1r2 35S:PSKR1(S893A/T894A)* plants as well as the flower

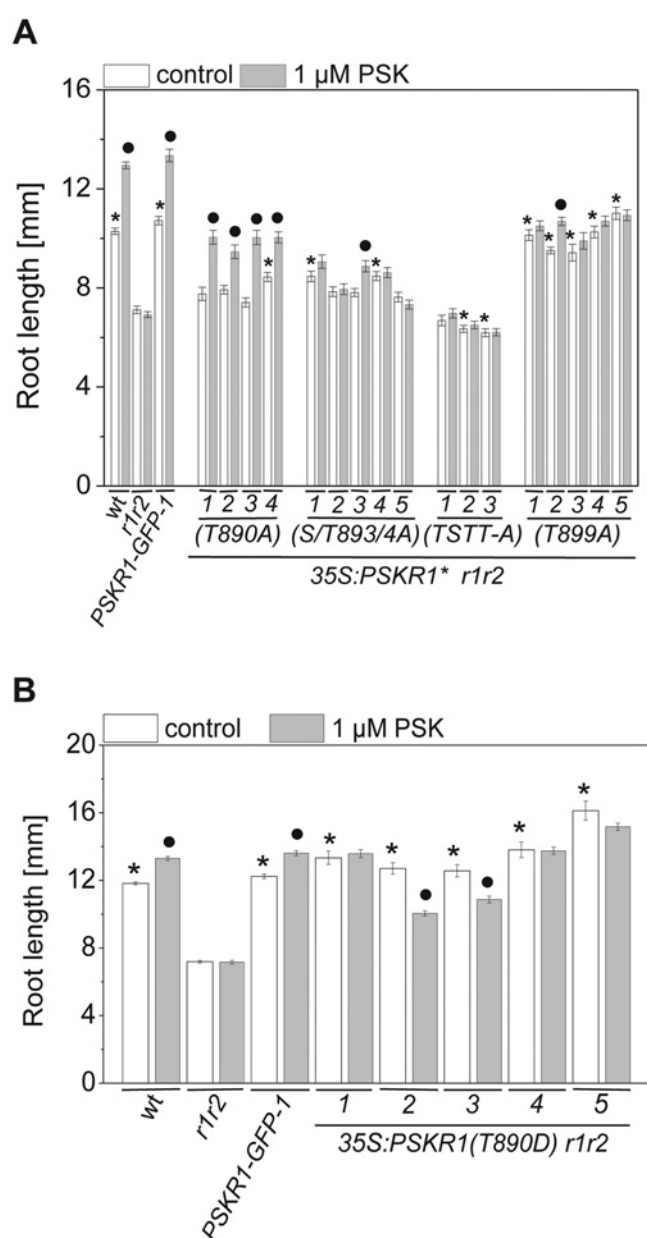


Figure 5 Inhibition of phosphorylation of specific activation segment residues through site-directed mutagenesis differentially impairs growth signalling by PSKR1 in seedling roots

(A) Seedlings of up to five independent transgenic lines of the PSKR1(T890A), PSKR1(S893A/T894A), PSKR1(T899A), and PSKR1(TSTT-A) mutants in the receptor-null *r1r2* background were grown with or without $1 \mu\text{M}$ PSK for 5 days. Mean \pm S.E.M. root lengths were determined in three independent experiments with at least 48 seedlings analysed per genotype. Asterisks indicate significantly different values between *r1r2* and the lines expressing different receptor variants ($P < 0.001$, two-sample Student's *t* test). Circles indicate significantly different values between treatments for each genotype ($n \geq 32$; $P < 0.001$). (B) Mean \pm S.E.M. root lengths were determined in five independent lines of the phosphomimic receptor variant PSKR1(T890D) expressed in the receptor-null *r1r2* background. At least 57 seedlings were analysed per genotype in three independent experiments in the absence or presence of $1 \mu\text{M}$ PSK. Asterisks indicate significantly different values between *r1r2* and the PSKR1(T890D) lines ($P < 0.001$, two-sample Student's *t* test). Circles indicate significantly different values between treatments for each PSKR1(T890D) line ($n \geq 50$; $P < 0.001$). S/T893/4A, S894A/T894A; wt, wild-type.

stalks of 6-week-old plants were intermediate between *r1r2* and wild-type plants (Figure 6A and 6B). The rosette sizes of *r1r2* *35S:PSKR1(T899A)* plants had wild-type size as was observed for

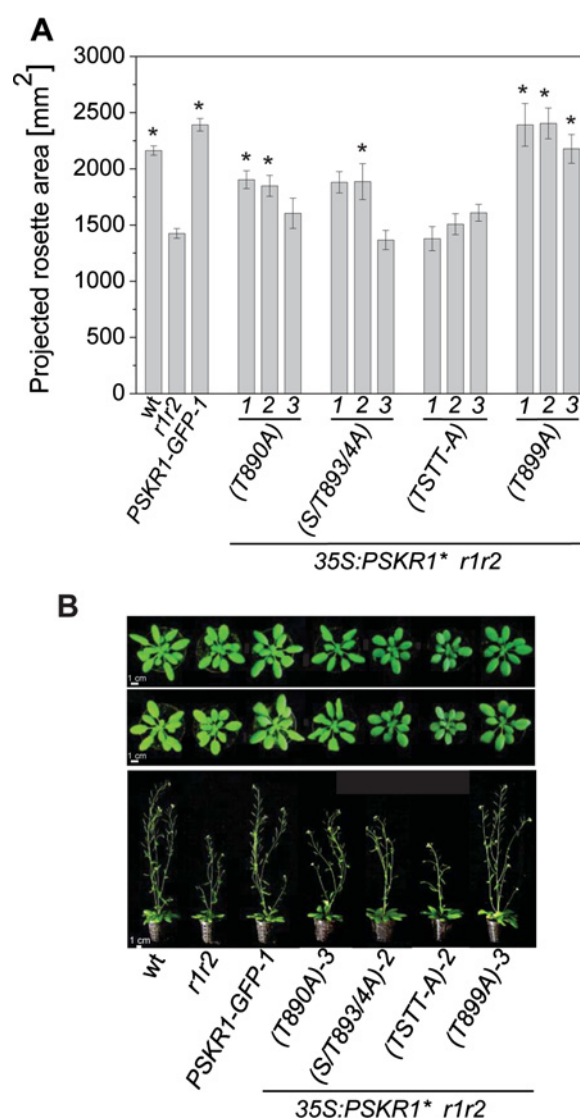


Figure 6 Preventing phosphorylation of specific activation segment residues impairs shoot growth

(A) The mean \pm S.E.M. projected rosette area from PSKR1(T890A), PSKR1(S893A/T894A), PSKR1(T899A) and PSKR1(TSTT-A) plants ($n = 8-9$) was calculated using the program Rosette Tracker [28]. Wild-type plants and plants complemented with a GFP-tagged wild-type receptor in the receptor-null background were included as controls. Asterisks indicate significantly different values between *r1r2* and the receptor variants ($P < 0.05$, two-sample Student's *t* test). (B) Representative phenotypes of 4-week-old (upper row) and of 6-week-old (lower row) soil-grown plants from wild-type, *r1r2*, *35S:PSKR1-GFP-1*, *35S:PSKR1(T890A)-3*, *35S:PSKR1(S893A/T894A)-2*, *35S:PSKR1(TSTT-A)-2* and *35S:PSKR1(T899A)-3*. Scale bars, 1 cm. S/T893/4A, S894A/T894A; wt, wild-type.

seedling roots (Figures 5A and 6A). And as with seedling roots, the rosettes and flower stalks of *r1r2* *35S:PSKR1(TSTT-A)-1,2,3* plants were no bigger than those of *r1r2*. Hence the concerted phosphoablative mutations in the activation segment of PSKR1 resulted in the inability of the PSKR1(TSTT-A) receptor to rescue the short-root and small-shoot phenotype of receptor-null plants.

In summary, our results showed that PSKR1 belongs to the RD-type kinases that require phosphorylation within the AL for their full activation. Phosphoablative mutations of one or two AL phosphosites partially reduced kinase activity and receptor function, but did not abolish it. We hypothesize that differential phosphorylation of AL residues of PSKR1 can modulate receptor activity.

AUTHOR CONTRIBUTION

Jens Hartmann, Dennis Linke, Andreas Tholey and Margret Sauter designed experiments. Jens Hartmann, Dennis Linke and Christine Bönniger performed the research. All authors analysed the data. Margret Sauter wrote the paper.

ACKNOWLEDGEMENT

We thank Hashim Abdirashid for his input in Phytozome analyses.

FUNDING

Financial support by the Deutsche Forschungsgemeinschaft (DFG) [grant number SA 495/13-1 (to M.S.)] and the DFG Cluster of Excellence 'Inflammation at Interfaces' (to A.T.) is gratefully acknowledged.

REFERENCES

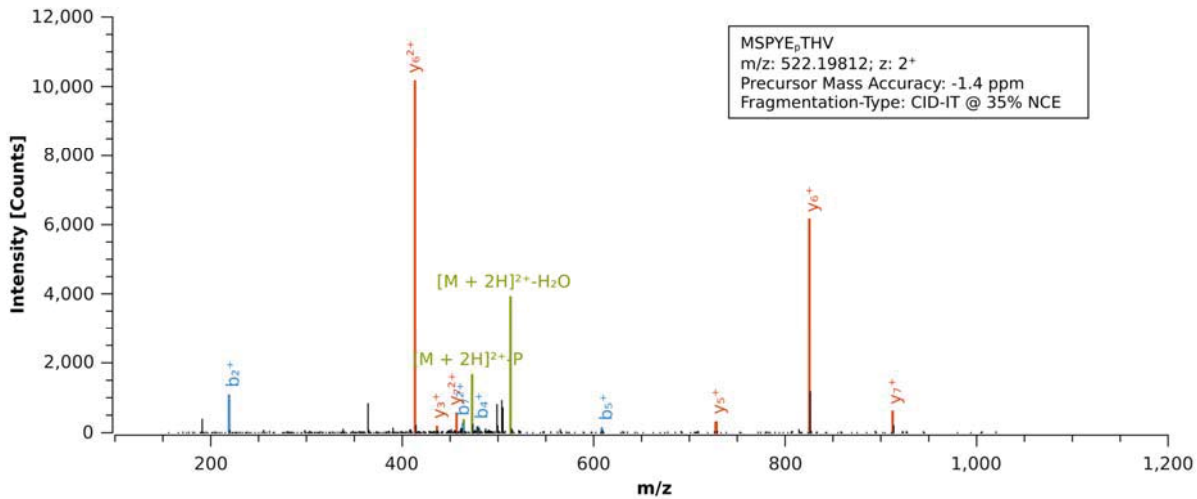
- Matsubayashi, Y. and Sakagami, Y. (1996) Phytosulfokine, sulfated peptides that induce the proliferation of single mesophyll cells of *Asparagus officinalis* L. *Proc. Natl. Acad. Sci. U.S.A.* **93**, 7623–7627 [CrossRef PubMed](#)
- Amano, Y., Tsubouchi, H., Shinohara, H., Ogawa, M. and Matsubayashi, Y. (2007) Tyrosine-sulfated glycopeptide involved in cellular proliferation and expansion in *Arabidopsis*. *Proc. Natl. Acad. Sci. U.S.A.* **104**, 18333–18338 [CrossRef PubMed](#)
- Stührwoldt, N., Dahlke, R.I., Steffens, B., Johnson, A. and Sauter, M. (2011) Phytosulfokine- α controls hypocotyl length and cell expansion in *Arabidopsis thaliana* through phytosulfokine receptor 1. *PLoS One* **6**, e21054 [CrossRef PubMed](#)
- Hartmann, J., Stührwoldt, N., Dahlke, R.I. and Sauter, M. (2013) Phytosulfokine control of growth occurs in the epidermis, is likely to be non-cell autonomous and is dependent on brassinosteroids. *Plant J.* **73**, 579–590 [CrossRef PubMed](#)
- Loivamäki, M., Stührwoldt, N., Deeken, R., Steffens, B., Roitsch, T., Hedrich, R. and Sauter, M. (2010) A role for PSK signaling in wounding and microbial interactions in *Arabidopsis*. *Physiol. Plant.* **139**, 348–357 [PubMed](#)
- Mosher, S., Seybold, H., Rodriguez, P., Stahl, M., Davies, K.A., Dayaratne, S., Morillo, S.A., Wierzbza, M., Favery, B., Keller, H. et al. (2013) The tyrosine-sulfated peptide receptors PSKR1 and PSY1R modify the immunity of *Arabidopsis* to biotrophic and necrotrophic pathogens in an antagonistic manner. *Plant J.* **73**, 469–482 [CrossRef PubMed](#)
- Shen, Y. and Diener, A.C. (2013) *Arabidopsis thaliana* RESISTANCE TO FUSARIUM OXYSPORIUM 2 implicates tyrosine-sulfated peptide signaling in susceptibility and resistance to root infection. *PLoS Genet.* **9**, e1003525 [CrossRef PubMed](#)
- Komori, R., Amano, Y., Ogawa-Ohnishi, M. and Matsubayashi, Y. (2009) Identification of tyrosylprotein sulfotransferase in *Arabidopsis*. *Proc. Natl. Acad. Sci. U.S.A.* **106**, 15067–15072 [CrossRef PubMed](#)
- Matsubayashi, Y., Ogawa, M., Morita, M. and Sakagami, Y. (2002) An LRR receptor kinase involved in perception of a peptide plant hormone, phytosulfokine. *Science* **296**, 1470–1472 [CrossRef PubMed](#)
- Shiu, S.H., Karlowski, W.M., Pan, R., Tzeng, Y.H., Mayer, K.F. and Li, W.H. (2004) Comparative analysis of the receptor-like kinase family in *Arabidopsis* and rice. *Plant Cell* **16**, 1220–1234 [CrossRef PubMed](#)
- Gish, L.A. and Clark, S.E. (2011) The RLK/Pelle family of kinases. *Plant J.* **66**, 117–127 [CrossRef PubMed](#)
- Matsubayashi, Y., Ogawa, M., Kihara, H., Niwa, M. and Sakagami, Y. (2006) Disruption and overexpression of *Arabidopsis* phytosulfokine receptor gene affects cellular longevity and potential for growth. *Plant Physiol.* **142**, 45–53 [CrossRef PubMed](#)
- Shinohara, H., Ogawa, M., Sakagami, Y. and Matsubayashi, Y. (2007) Identification of ligand binding site of phytosulfokine receptor by on-column photoaffinity labeling. *J. Biol. Chem.* **282**, 124–131 [CrossRef PubMed](#)
- Hanks, S.K., Quinn, A.M. and Hunter, T. (1988) The protein kinase family: conserved features and deduced phylogeny of the catalytic domains. *Science* **241**, 42–52 [CrossRef PubMed](#)
- Lindberg, R.A., Quinn, A.M. and Hunter, T. (1992) Dual-specificity protein kinases: will any hydroxyl do? *Trends Biochem. Sci.* **17**, 114–119 [CrossRef PubMed](#)
- Hartmann, J., Fischer, C., Dietrich, P. and Sauter, M. (2014) Kinase activity and calmodulin binding are essential for growth signaling by the phytosulfokine receptor PSKR1. *Plant J.* **78**, 192–202 [CrossRef PubMed](#)
- Kim, T.W. and Wang, Z.Y. (2010) Brassinosteroid signal transduction from receptor kinases to transcription factors. *Annu. Rev. Plant Biol.* **61**, 681–704 [CrossRef PubMed](#)
- Clouse, S.D. (2011) Brassinosteroid signal transduction: from receptor kinase activation to transcriptional networks regulating plant development. *Plant Cell* **23**, 1219–1230 [CrossRef PubMed](#)
- Wang, Z.Y., Bai, M.Y., Oh, E. and Zhu, J.Y. (2012) Brassinosteroid signaling network and regulation of photomorphogenesis. *Annu. Rev. Genet.* **46**, 701–724 [CrossRef PubMed](#)
- Ladwig, F., Dahlke, R.I., Stührwoldt, N., Hartmann, J., Harter, K. and Sauter, M. (2015) Phytosulfokine regulates growth in *Arabidopsis* through a response module at the plasma membrane that includes CYCLIC NUCLEOTIDE-GATED CHANNEL 17, H⁺-ATPase and BAK1. *Plant Cell* **27**, 1–12 [CrossRef PubMed](#)
- Huse, M. and Kuriyan, J. (2002) The conformational plasticity of protein kinases. *Cell* **109**, 275–282 [CrossRef PubMed](#)
- Adams, J.A. (2003) Activation loop phosphorylation and catalysis in protein kinases: is there functional evidence for the autoinhibitor model? *Biochemistry* **42**, 601–607 [CrossRef PubMed](#)
- Johnson, L.N., Noble, M.E. and Owen, D.J. (1996) Active and inactive protein kinases: structural basis for regulation. *Cell* **85**, 149–158 [CrossRef PubMed](#)
- Wang, X., Goshe, M.B., Soderblom, E.J., Phinney, B.S., Kuchar, J.A., Li, J., Asami, T., Yoshida, S., Huber, S.C. and Clouse, S.D. (2005) Identification and functional analysis of *in vivo* phosphorylation sites of the *Arabidopsis* BRASSINOSTEROID-INSENSITIVE1 receptor kinase. *Plant Cell* **17**, 1685–1703 [CrossRef PubMed](#)
- Wang, X., Kota, U., He, K., Blackburn, K., Li, J., Goshe, M.B., Huber, S.C. and Clouse, S.D. (2008) Sequential transphosphorylation of the BRI1/BAK1 receptor kinase complex impacts early events in brassinosteroid signaling. *Dev. Cell* **15**, 220–235 [CrossRef PubMed](#)
- Murashige, T. and Skoog, F. (1962) A revised medium for rapid growth and bioassays with tobacco cultures. *Plant Physiol.* **15**, 473–497 [CrossRef](#)
- Clough, S.J. and Bent, A.F. (1998) Floral dip: a simplified method for *Agrobacterium*-mediated transformation of *Arabidopsis thaliana*. *Plant J.* **16**, 735–743 [CrossRef PubMed](#)
- De Vylder, J., Vandenbussche, F., Hu, Y., Philips, W. and Van Der Straeten, D. (2012) Rosette Tracker: an open source image analysis tool for automatic quantification of genotype effects. *Plant Physiol.* **160**, 1149–1159 [CrossRef PubMed](#)
- Horton, R.M., Hunt, H.D., Ho, S.N., Pullen, J.K. and Pease, L.R. (1989) Engineering hybrid genes without the use of restriction enzymes: gene splicing by overlap extension. *Gene* **77**, 61–68 [CrossRef PubMed](#)
- Schlosser, A., Vanselow, J.T. and Kramer, A. (2005) Mapping of phosphorylation sites by a multi-protease approach with specific phosphopeptide enrichment and NanoLC-MS/MS analysis. *Anal. Chem.* **77**, 5243–5250 [CrossRef PubMed](#)
- Zarei, M., Sprenger, A., Gretzmeier, C. and Dengjel, J. (2013) Rapid combinatorial ERLIC-SCX solid-phase extraction for in-depth phosphoproteome analysis. *J. Proteome Res.* **12**, 5989–5995 [CrossRef PubMed](#)
- Taus, T., Köcher, T., Pichler, P., Paschke, C., Schmidt, A., Henrich, C. and Mechtler, K. (2011) Universal and confident phosphorylation site localization using phosphoRS. *J. Proteome Res.* **10**, 5354–5362 [CrossRef PubMed](#)
- Linke, D., Hung, C.W., Cassidy, L. and Tholey, A. (2013) Optimized fragmentation conditions for iTRAQ-labeled phosphopeptides. *J. Proteome Res.* **12**, 2755–2763 [CrossRef PubMed](#)
- Kamps, M.P. and Sefton, B.M. (1986) Neither arginine nor histidine can carry out the function of lysine-295 in the ATP-binding site of p60src. *Mol. Cell. Biol.* **6**, 751–757 [CrossRef PubMed](#)
- Williams, R., Wilson, J. and Meyerowitz, E. (1997) A possible role for kinase-associated protein phosphatase in the *Arabidopsis* CLAVATA1 signaling pathway. *Proc. Natl. Acad. Sci. U.S.A.* **94**, 10467–10472 [CrossRef PubMed](#)
- Stone, J.M., Trotochaud, A.E., Walker, J.C. and Clark, S.E. (1998) Control of meristem development by CLAVATA1 receptor kinase and kinase-associated protein phosphatase interactions. *Plant Physiol.* **117**, 1217–1225 [CrossRef PubMed](#)
- Oh, M.H., Ray, W.K., Huber, S.C., Asara, J.M., Gage, D.A. and Clouse, S.D. (2000) Recombinant brassinosteroid insensitive 1 receptor-like kinase autophosphorylates on serine and threonine residues and phosphorylates a conserved peptide motif *in vitro*. *Plant Physiol.* **124**, 751–766 [CrossRef PubMed](#)
- Oh, M.H., Wang, X., Kota, U., Goshe, M.B., Clouse, S.D. and Huber, S.C. (2009) Tyrosine phosphorylation of the BRI1 receptor kinase emerges as a component of brassinosteroid signaling in *Arabidopsis*. *Proc. Natl. Acad. Sci. U.S.A.* **106**, 658–663 [CrossRef PubMed](#)
- Bojar, D., Martinez, J., Santiago, J., Rybin, V., Bayliss, R. and Hothorn, M. (2014) Crystal structures of the phosphorylated BRI1 kinase domain and implications for brassinosteroid signal initiation. *Plant J.* **78**, 31–43 [CrossRef PubMed](#)
- Klaus-Heisen, D., Nurisso, A., Pietraszewska-Bogiel, A., Mbengue, M., Camut, S., Timmers, T., Pichereaux, C., Rossignol, M., Gadella, T.W., Imberly, A. et al. (2011) Structure–function similarities between a plant receptor-like kinase and the human interleukin-1 receptor-associated kinase-4. *J. Biol. Chem.* **286**, 11202–11210 [CrossRef PubMed](#)

- 41 Oh, M.H., Wang, X., Wu, X., Zhao, Y., Clouse, S.D. and Huber, S.C. (2010) Autophosphorylation of Tyr-610 in the receptor kinase BAK1 plays a role in brassinosteroid signaling and basal defense gene expression. *Proc. Natl. Acad. Sci. U.S.A.* **107**, 17827–17832 [CrossRef PubMed](#)
- 42 Yan, L., Ma, Y., Liu, D., Wei, X., Sun, Y., Chen, X., Zhao, H., Zhou, J., Wang, Z., Shui, W. and Lou, Z. (2012) Structural basis for the impact of phosphorylation on the activation of plant receptor-like kinase BAK1. *Cell Res.* **22**, 1304–1308 [CrossRef PubMed](#)
- 43 Yun, H.S., Bae, Y.H., Lee, Y.J., Chang, S.C., Kim, S.K., Li, J. and Nam, K.H. (2009) Analysis of phosphorylation of the BRI1/BAK1 complex in arabidopsis reveals amino acid residues critical for receptor formation and activation of BR signaling. *Mol. Cell* **27**, 183–190 [CrossRef](#)
- 44 Shah, K., Vervoort, J. and de Vries, S.C. (2001) Role of threonines in the *Arabidopsis thaliana* somatic embryogenesis receptor kinase 1 activation loop in phosphorylation. *J. Biol. Chem.* **276**, 41263–41269 [CrossRef PubMed](#)
- 45 Goodstein, D.M., Shu, S., Howson, R., Neupane, R., Hayes, R.D., Fazo, J., Mitros, T., Dirks, W., Hellsten, U., Putnam, N. and Rokhsar, D.S. (2012) Phytozome: a comparative platform for green plant genomics. *Nucleic Acids Res.* **40**, 1178–1186 [CrossRef](#)
- 46 Shiu, S.H. and Bleecker, A.B. (2001) Receptor-like kinases from *Arabidopsis* form a monophyletic gene family related to animal receptor kinases. *Proc. Natl. Acad. Sci. U.S.A.* **98**, 10763–10768 [CrossRef PubMed](#)
- 47 Wang, X., Li, X., Meisenhelder, J., Hunter, T., Yoshida, S., Asami, T. and Chory, J. (2005) Autoregulation and homodimerization are involved in the activation of the plant steroid receptor BRI1. *Dev. Cell* **8**, 855–865 [CrossRef PubMed](#)
- 48 Meyer, M.R., Lichti, C.F., Townsend, R.R. and Rao, A.G. (2011) Identification of *in vitro* autophosphorylation sites and effects of phosphorylation on the *Arabidopsis* CRINKLY4 (ACR4) receptor-like kinase intracellular domain: insights into conformation, oligomerization, and activity. *Biochemistry* **50**, 2170–2186 [CrossRef PubMed](#)
- 49 Bajwa, V.S., Wang, X., Blackburn, R.K., Goshe, M.B., Mitra, S.K., Williams, E.L., Bishop, G.J., Krasnyanski, S., Allen, G., Huber, S.C. and Clouse, S.D. (2013) Identification and functional analysis of tomato BRI1 and BAK1 receptor kinase phosphorylation sites. *Plant Physiol.* **163**, 30–42 [CrossRef PubMed](#)
- 50 Nolen, B., Taylor, S. and Ghosh, G. (2004) Regulation of protein kinases: controlling activity through activation segment conformation. *Mol. Cell* **1**, 661–675 [CrossRef](#)

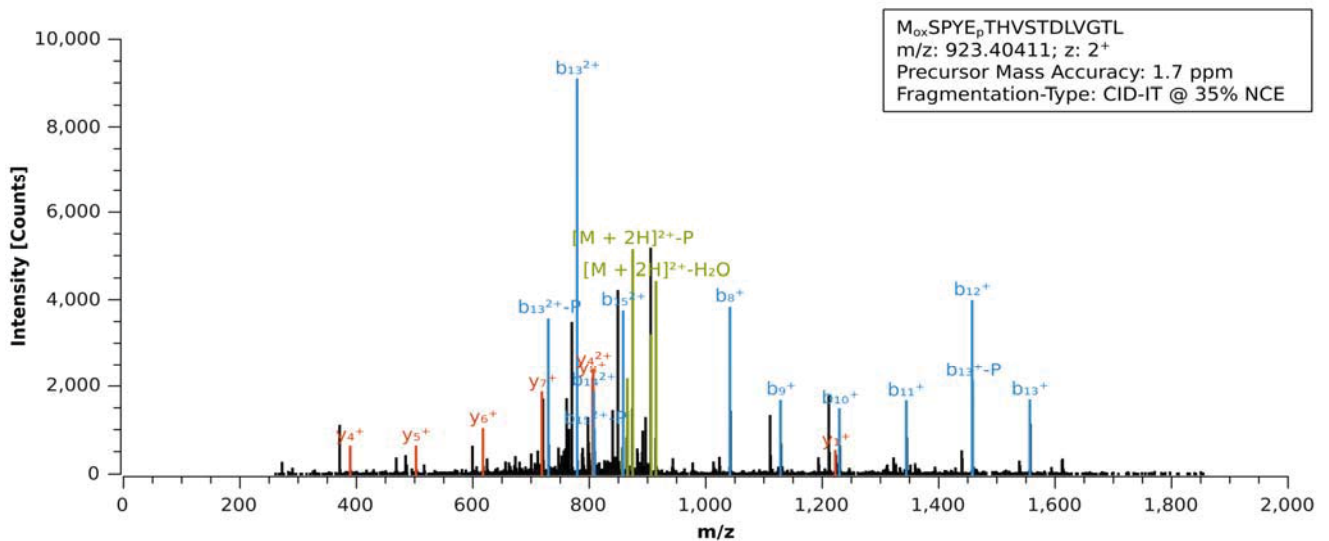
Received 3 February 2015/8 October 2015; accepted 15 October 2015
Accepted Manuscript online 15 October 2015, doi:10.1042/BJ20150147

Supplemental Figure S1A, B

A



B



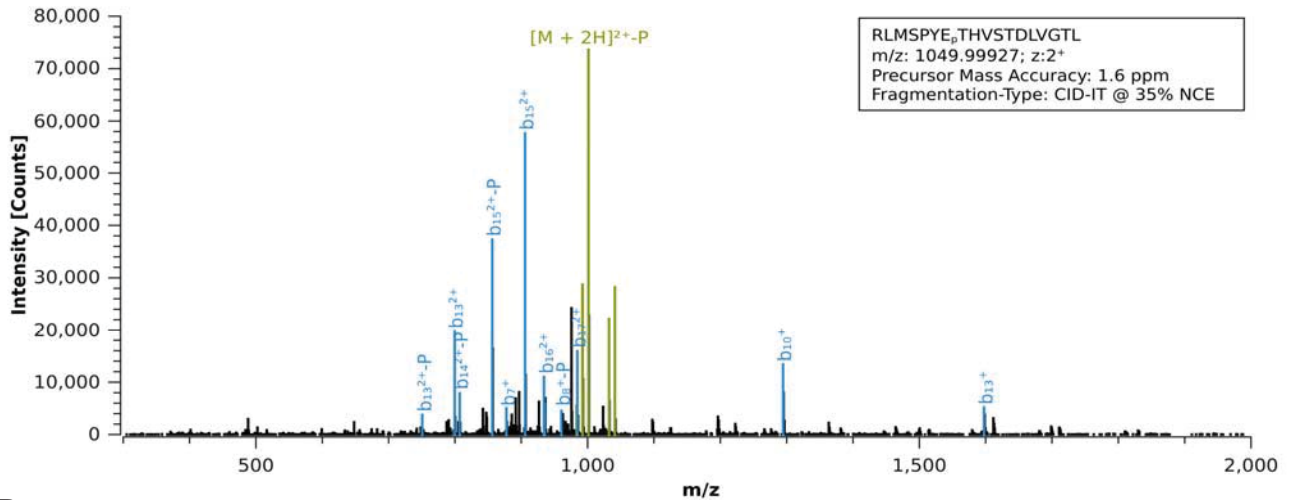
Supplemental Figure S1. LC-ESI MS/MS spectra identifying PSKR1 *in vitro* phosphorylation sites.

(A) LC-ESI MS/MS of the phosphopeptide MSPYEpTHV with a measured m/z value of 522.20; a precursor charge state of 2⁺. Calculated mass deviation was -1.4 ppm. The precursor ion was fragmented by Collision Induced Dissociation (CID) and analysed in the ion trap mass analyser (IT). The normalized collision energy was set to 35%. Peptide ions, which were passing the filter settings were annotated in red (y-ions) and blue (b-ions). Precursor related ions were labeled in green.

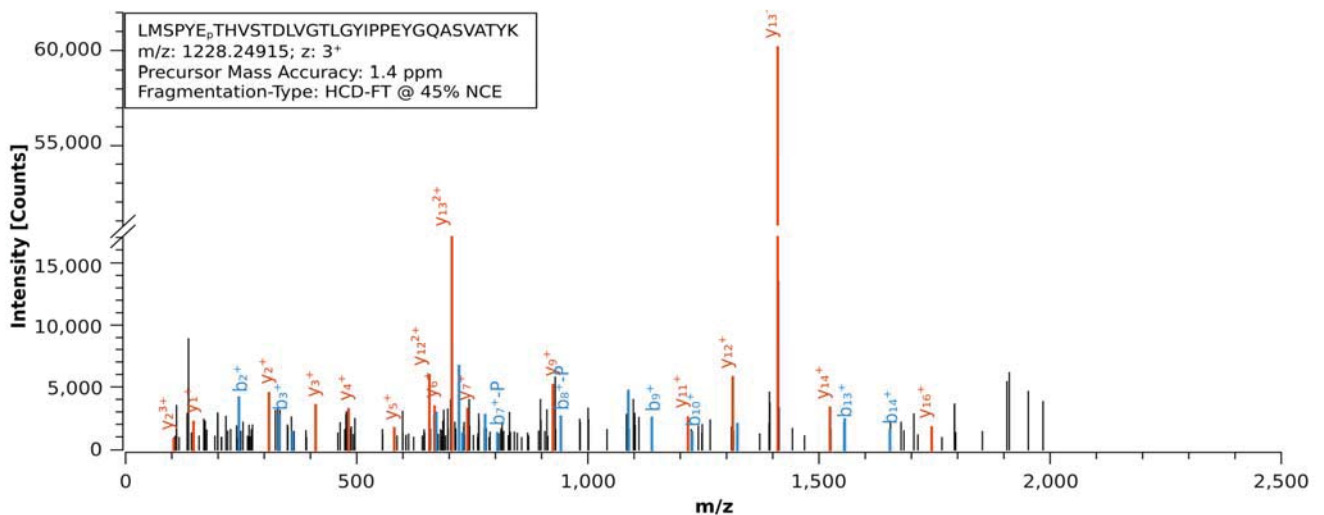
(B) LC-ESI MS/MS of the phosphopeptide MoxSPYEpTHVSTDLVGTL with a measured m/z value of 923.40; a precursor charge state of 2⁺. The mass deviation was calculated to be 1.7 ppm. Precursor ion fragmentation and analysis were carried out as described for (A).

Supplemental Figure S1C, D

C



D



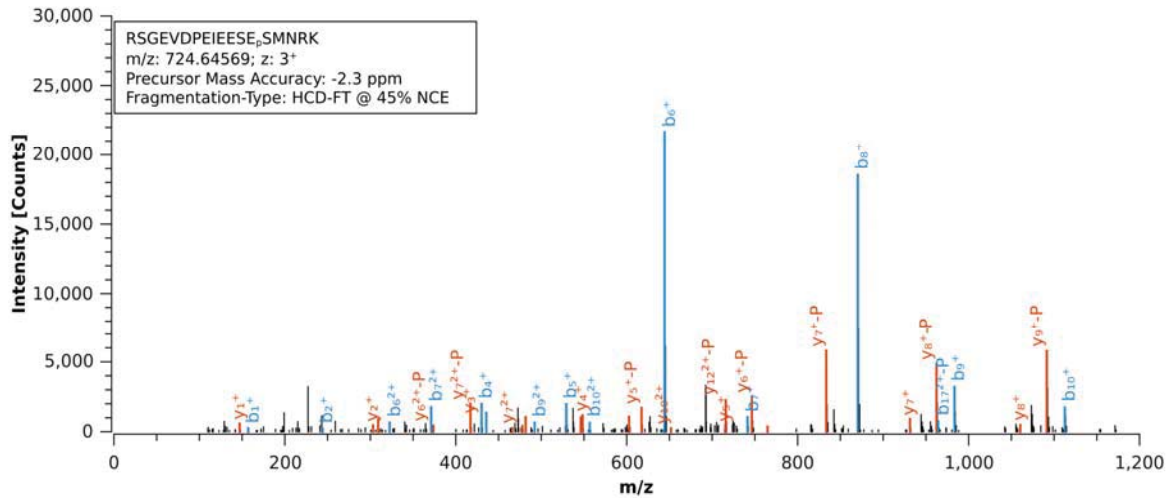
Supplemental Figure S1. LC-ESI MS/MS spectra identifying PSKR1 *in vitro* phosphorylation sites.

(C) LC-ESI MS/MS of the phosphopeptide RLMSPYE_PTHVSTDLVGTL with a measured *m/z* value of 1050.00; a precursor charge state of 2+. The mass deviation was calculated to be 1.6 ppm. Precursor ion fragmentation and analysis were carried out as described for (A).

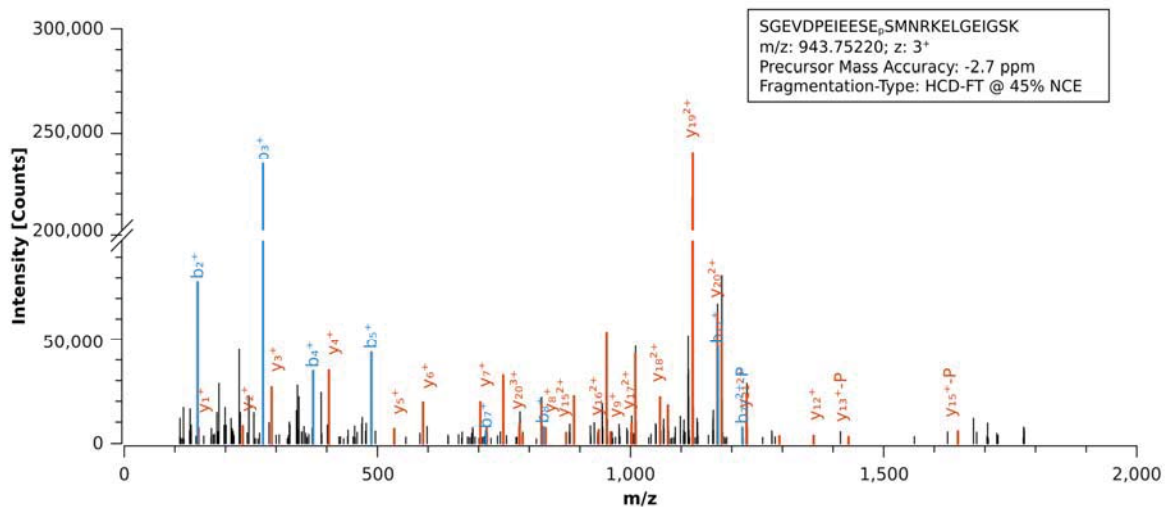
(D) LC-ESI MS/MS of the phosphopeptide LMSPYE_PTHVSTDLVGLGYPPEYQASVATYK with a measured *m/z* value of 1228.24; a precursor charge state of 3+. The mass deviation was calculated to be 1.4 ppm. The precursor ion was fragmented by Higher Energy Collision Dissociation (HCD) and analysed in the Orbitrap mass analyser (FT). The normalized collision energy was set to 45%.

Supplemental Figure S2A, B

A



B



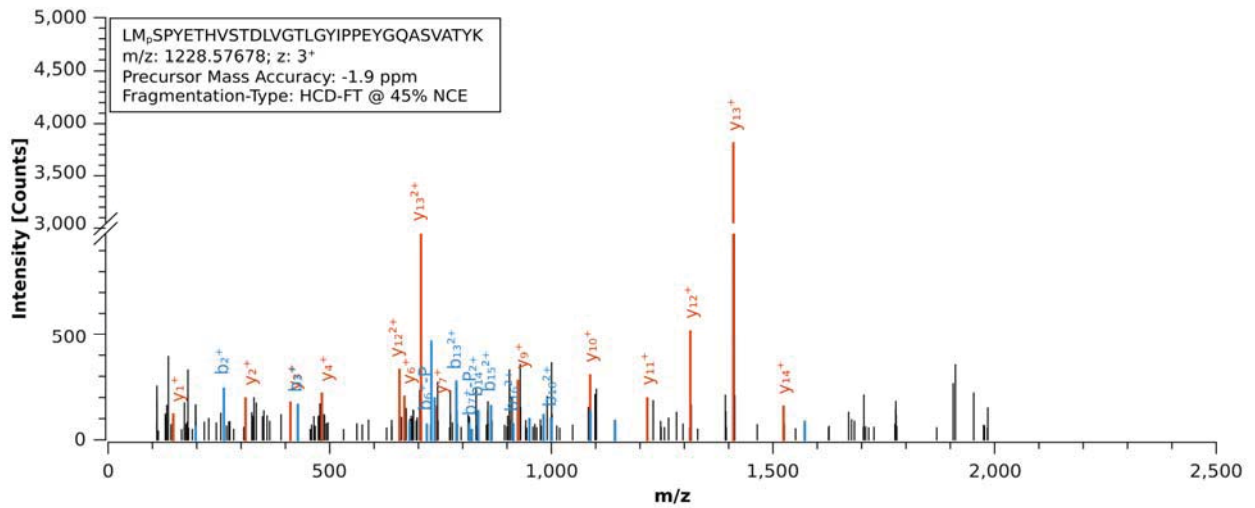
Supplemental Figure S2. LC-ESI MS/MS spectra identifying PSKR1 *in planta* phosphorylation sites.

(A) LC-ESI MS/MS measurement in Orbitrap of the phosphopeptide RSGEVDPEIEESEpSMNRK with a measured m/z value of 724.64, a precursor charge state of 3⁺. The mass deviation was calculated to be -2.3 ppm. The precursor ion was fragmented by Higher Energy Collision activated dissociation (HCD) and analyzed in the Orbitrap mass analyzer (FT). The normalized collision energy was set to 45%. Peptide ions, which were passing the filter settings were annotated in red (y-ions) and blue (b-ions).

(B) LC-ESI MS/MS measurement in Orbitrap of the phosphopeptide SGEVDPEIEESEpSMNRKELGEIGSK with a measured m/z value of 943.75, a precursor charge state of 3⁺. The mass deviation was calculated to be -2.7 ppm. Precursor ion fragmentation and analysis were carried out as described for (A).

Supplemental Figure S2C

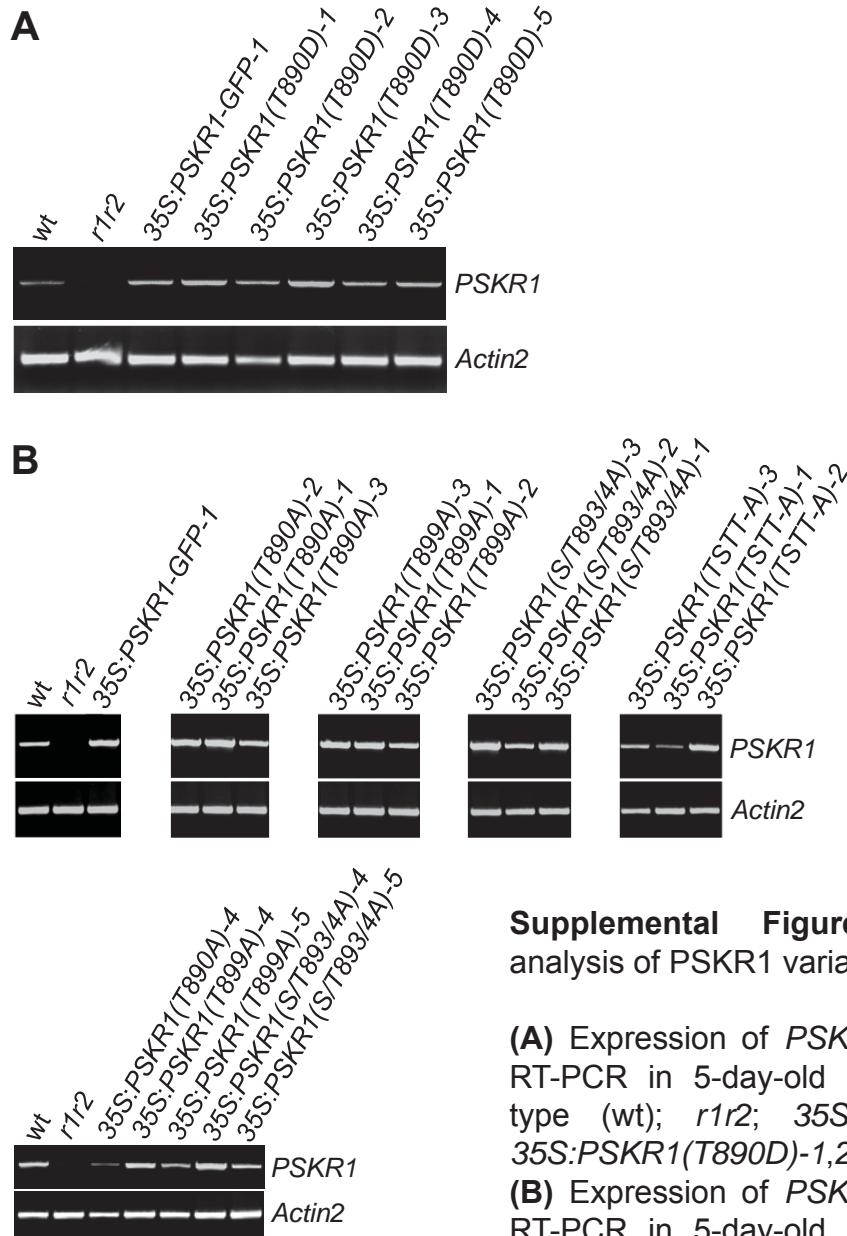
C



Supplemental Figure S2. LC-ESI MS/MS spectra identifying PSKR1 *in planta* phosphorylation sites.

(C) LC-ESI MS/MS measurement in Orbitrap of the phosphopeptide LM_pSPYETHVSTDLVGLGYIPPEYGQASVATYK with a measured m/z value of 1228.57, a precursor charge state of 3⁺. The mass deviation was calculated to be -1.9 ppm. Precursor ion fragmentation and analysis were carried out as described for (A).

Supplemental Figure S3



Supplemental Figure S3. Expression analysis of *PSKR1* variants.

(A) Expression of *PSKR1* was analyzed by RT-PCR in 5-day-old seedlings from wild-type (wt); *r1r2*; 35S:*PSKR1*-GFP-1 and 35S:*PSKR1*(T890D)-1,2,3,4,5 lines.

(B) Expression of *PSKR1* was analyzed by RT-PCR in 5-day-old seedlings from wild-type (wt), *r1r2*, 35S:*PSKR1*-GFP-1; 35S:*PSKR1*(T890A)-1,2,3,4; 35S:*PSKR1*(T899A)-1,2,3,4,5; 35S:*PSKR1*(S/T893/4A)-1,2,3,4,5 and 35S:*PSKR1*(TSTT-A)-1,2,3 each in the *r1r2* background. *Actin2* cDNA was amplified as a control for RNA input.

Supplemental Figure S4

Species	Position	Sequence	Position
<i>Arabidopsis thaliana</i>	681	RARRRSGEVDPEIEESESMMNR-KELGEIGSKLVVLFQSN	729
<i>Physcomitrella patens</i>	1008	RWRLKQEAIAKTKDLERMKLTVMMEAGACMVIPKSKEPLSINVAMFEQPLLRLTLADILL	1068
<i>Selaginella moellendorffii</i>	719	MLSFSSRAGHRQDIAGRNFKEMSVQMMDLTVMFGQRYR	768
<i>Amborella trichopoda</i>	710	RRHRKRKCGDGVCRTAGGIR--RSSEFGSRMVLFPQDQK	758
<i>Brachypodium distachyon</i>	718	MKRSFRRQDHTVKAVADTDG--ALELAPASLVLLFQNKDDD	766
<i>Oryza sativa</i>	717	LKSSFRQDYIVKAVADYITE---ALELAPASLVLLFQNKDDG	765
<i>Panicum virgatum</i>	706	RIVHSRMQEPNPKAVANAE---DSESSNSCLVLLFQNN	750
<i>Setaria italica</i>	717	LKSRFRQDHTVKAVADYITNR---ALELAPASLVLLFQNKDD	764
<i>Sorghum bicolor</i>	715	LKSSFNKQDHTVKAVKDTNQ---ALELAPASLVLLFQNKAD	762
<i>Zea mays</i>	717	LKSNFRQDHTVKAVADYITDR---ALELAPASLVLLFQNKAD	764
<i>Aquilegia coerulea</i>	684	TRTDSHKQDHTKVDNFDSSD--NVLYPSGSRVLLFEDEDN	733
<i>Mimulus guttatus</i>	685	VCSRRRQDPEMEYERTSSKTDYFETS SVVILCQNKDKD-INISSTSKKEIFLDDLLK	744
<i>Solanum lycopersicum</i>	631	VRASSRKVVDQEKELDASNRE--LEDLGSLLVIFPHNKE	679
<i>Solanum tuberosum</i>	677	IRASSRKVVDQEKELDASNRE--LEDLGSLLVIFPHNKE	725
<i>Vitis vinifera</i>	465	IPVVGDFIVDLDEEIEE-RPHR-LS-EVLGSSKLVLFQNSGC	512
<i>Eucalyptus grandis</i>	679	MRAHRRGEVDPEKEVVGRKE--RDIEDLESRLVLMFQNKDR	728
<i>Populus trichocarpa</i>	693	LRAHNRGEVDPEKVDADITND--KDEEFGSRLVLLQNKES	742
<i>Linum usitatissimum</i>	719	RRARGDLINSLDEEAEE-ESQR-SS-QALMTSKLVLFQNSDC	766
<i>Manihot esculenta</i>	693	RAHSRGEVDAEKEGVEITND--KDLEELGSRVLLFQNKEN	742
<i>Ricinus communis</i>	678	LRAHSRGEVDPEKEEANTND--KDLEELGSKLVVLFQNKEN	727
<i>Carica papaya</i>	582	LRAHSRGEVDPER-DFDGN--KDLEELGSRVLLFQNKED	630
<i>Gossypium raimondii</i>	678	LRTHKRNEVDPEKEEPTND--KNLEELSSRLVLLFQNWES	727
<i>Theobroma cacao</i>	680	LRAHNRGEVDPEKEEPTND--KDLEELSSRLVLLFQNRRT	729
<i>Arabidopsis lyrata</i>	681	RARRRSGEVDPEIEESESMMNR-KELGEIGSKLVVLFQNN	729
<i>Arabidopsis thaliana</i>	681	RARRRSGEVDPEIEESESMMNR-KELGEIGSKLVVLFQSN	729
<i>Boechera stricta</i>	691	RARRRSGEVDPEIEESESMMNR-KELGEIGSKLVVLFQNN	739
<i>Brassica rapa</i>	689	HARRRSGEVDPEIEESESMMNR-KDLEEGSKLVVLFQSD	736
<i>Capsella grandiflora</i>	675	RARRRSGEVDPEIEESESMMNR-KELGEIGSKLVVLFQNN	723
<i>Capsella rubella</i>	689	RARRRSGEVDPEIEESESMMNR-KELGEIGSKLVVLFQNN	737
<i>Eutrema salsugineum</i>	690	RARRRSGEVDPEIEESESMMNR-KEVEEIGSKLVVLFQNN	737
<i>Citrus sinensis</i>	692	LRAHSRGEVDPEKEEANTND--KDLEELGSKLVVLFPHNKE	739
<i>Citrus clementina</i>	692	LRAHSRGEVDPEKEEANTND--KDLEELGSKLVVLFPHNKE	739
<i>Cucumis sativus</i>	366	LRPPRGRVGDPEVEEENIDN--KDLEEVKTGLVLLFQNN	414
<i>Glycine max</i>	724	KRDDDKPMDFDELNGRPRR-LS-EALASSKLVLFQNSDC	772
<i>Malus domestica</i>	688	VRAHSRREVDPEREDHDTNG--KDLEELGSKLVVLFQNKDA	737
<i>Medicago truncatula</i>	720	KREEDKPIDSDPEEMGRPRR-LSSEGFVASKLVLFQNSDC	769
<i>Phaseolus vulgaris</i>	720	RRDDDKPIDNDEELNGRPRR-LS-EALVSSKLVLFQNSDC	711
<i>Prunus persica</i>	689	LRAHSRREVDPEKEEYDSNG--KDLEELGSKVLLFQNKDT	738

ATP binding region

Species	Position	Sequence	Position
<i>A. thaliana</i>	730	STNSFDQANI ICGGFGMVKYKALLPDGKVAIKKLSGD--CGQIEREFQAEVETLSRAQHPNLVLLRGFCFYKN-DRLLIYSYMEGSLDYWLHERND	824
<i>P. patens</i>	1069	ATNNFCKTNI IGDGGFGTVYKAVLPDTRKVAIKKLSGD--RSQGNREFLAEMETLGKVKHRLVPLLGYSFCGE-EKLLVYEMVNGSLDYLRLNRAD	1164
<i>S. moellendorffii</i>	769	ATNNFDATNI ICGGFGLVKALPDGRKVAIKKLSGD--CGQIEREFQAEVETLSRAQHPNLVLLRGFCFYKN-DRLLIYSYMEGSLDYWLHERSD	866
<i>A. trichopoda</i>	759	ATDNFDQANI ICGGFGLVYKALLPDGRKVAIKKLSGD--CGQIEREFQAEVETLSRAQHPNLVLLRGFCFYKN-DRLLIYSYMEGSLDYWLHERLD	853
<i>B. distachyon</i>	767	STNNFDQANI ICGGFGLVYKALLPDGATIAIKKLSGD--FGQMEREFQAEVETLSRAQHPNLVLLRGFCFYKN-DRLLIYSYMEGSLDYWLHEKPD	861
<i>O. sativa</i>	766	STNNFDQANI ICGGFGLVYKALLPDGATIAIKKLSGD--FGQMEREFQAEVETLSRAQHPNLVLLRGFCFYKN-DRLLIYSYMEGSLDYWLHEKPD	860
<i>P. virgatum</i>	751	STNNFDQAY IVCGGFGLVYKALPDGRVAIKKLSGD--YSQIEREFQAEVETLSRAQHPNLVLLRGFCFYKN-DRLLIYSYMEGSLDYWLHERAD	845
<i>S. italica</i>	765	STNNFDQANI ICGGFGLVYKALLPDGATIAIKKLSGD--FGQMEREFQAEVETLSRAQHPNLVLLRGFCFYKN-DRLLIYSYMEGSLDYWLHENPN	859
<i>S. bicolor</i>	763	STNNFDQANI ICGGFGLVYKALPDGAAIAIKKLSGD--FGQMEREFQAEVETLSRAQHPNLVLLRGFCFYKN-DRLLIYSYMEGSLDYWLHEKPD	857
<i>Z. mays</i>	765	STNNFDQANI ICGGFGVYKALPDGAAIAIKKLSGD--FGQMEREFQAEVETLSRAQHPNLVLLRGFCFYKN-DRLLIYSYMEGSLDYWLHESPD	859
<i>A. coerulea</i>	734	STNNFDQANI ICGGFGLVYKALPDGRKVAIKKLSGD--CGQIEREFQAEVETLSRAQHPNLVLLRGFCFYKN-DRLLIYSYMEGSLDYWLHEKLD	828
<i>M. guttatus</i>	745	ATNNFDQANI ICGGFGLVYKALPDGAAIAIKKLSGD--FGQMEREFQAEVETLSRAQHPNLVLLRGFCFYKN-DRLLIYSYMEGSLDYWLHEKVD	839
<i>S. lycopersicum</i>	680	CTDNFDQSN IVCGGFGLVYKALLRDGRKVAIKKLSGD--YQMEREFQAEVETLSRAQHPNLVLLRGFCFYKN-DRLLIYSYMEGSLDYWLHEKVD	774
<i>S. tuberosum</i>	726	CTDNFDQSN IVCGGFGLVYKALLRDGRKVAIKKLSGD--YQMEREFQAEVETLSRAQHPNLVLLRGFCFYKN-DRLLIYSYMEGSLDYWLHEKVD	820
<i>V. vinifera</i>	513	STNNFDQANI ICGGFGLVYKALPDGTRAAIKKLSGD--CGQIEREFQAEVETLSRAQHPNLVLLRGFCFYKN-DRLLIYSYMEGSLDYWLHEKVD	607
<i>E. grandis</i>	729	ATNNFDQANI ICGGFGMVKYKALFPDGTKLAIKKLSGD--CGQIEREFQAEVETLSRAQHPNLVLLRGFCFYKN-DRLLIYSYMEGSLDYWLHEKPD	823
<i>P. trichocarpa</i>	743	FTNNFDQANI ICGGFGLVYKALLPDGRKVAIKKLSGD--SGQMDREFQAEVETLSRAQHPNLVLLRGFCFYKN-DRLLIYSYMEGSLDYWLHEKLD	837
<i>L. usitatissimum</i>	767	ATNNFDQANI ICGGFGLVYKALSPNGKAAIKKLSGD--CGQIEREFQAEVETLSRAQHPNLVLLRGFCFYKN-DRLLIYSYMEGSLDYWLHEKVD	861
<i>M. esculenta</i>	743	STNNFDQANI ICGGFGLVYKALLPDGRKVAIKKLSGD--CGQIEREFQAEVETLSRAQHPNLVLLRGFCFYKN-DRLLIYSYMEGSLDYWLHEKID	837
<i>R. communis</i>	728	STNNFDQANI ICGGFGLVYKALLPDGRKVAIKKLSGD--CGQIEREFQAEVETLSRAQHPNLVLLRGFCFYKN-DRLLIYSYMEGSLDYWLHEKID	822
<i>C. papaya</i>	631	STNNFDQANI ICGGFGLVYKALLPDSRVAIKKLSGD--CGQMDREFQAEVETLSRAQHPNLVLLRGFCFYKN-DRLLIYSYMEGSLDYWLHEKID	725
<i>G. raimondii</i>	728	STNNFDQANI ICGGFGLVYKALLPDGRKVAIKKLSGD--CGQMDREFQAEVETLSRAQHPNLVLLRGFCFYKN-DRLLIYSYMEGSLDYWLHEKVD	822
<i>T. cacao</i>	730	STNNFDQANI ICGGFG-----GLMDREFQAEVETLSRAQHPNLVLLRGFCFYKN-DRLLIYSYMEGSLDYWLHEKVD	801
<i>A. lyrata</i>	730	STNSFDQANI ICGGFGMVKYKALLPDGKVAIKKLSGD--CGQIEREFQAEVETLSRAQHPNLVLLRGFCFYKN-DRLLIYSYMEGSLDYWLHERND	824
<i>A. thaliana</i>	730	STNSFDQANI ICGGFGMVKYKALLPDGKVAIKKLSGD--CGQIEREFQAEVETLSRAQHPNLVLLRGFCFYKN-DRLLIYSYMEGSLDYWLHERND	824
<i>B. stricta</i>	740	STNSFDQANI ICGGFGMVKYKALLPDGKVAIKKLSGD--CGQIEREFQAEVETLSRAQHPNLVLLRGFCFYKN-DRLLIYSYMEGSLDYWLHERND	834
<i>B. rapa</i>	737	STNNFDQANI ICGGFGLVYKALPDGRKVAIKKLSGD--CGQIEREFQAEVETLSRAQHPNLVLLRGFCFYKN-DRLLIYSYMEGSLDYWLHERND	831
<i>C. grandiflora</i>	724	STNSFDQANI ICGGFGMVKYKALLPDGKVAIKKLSGD--CGQIEREFQAEVETLSRAQHPNLVLLRGFCFYKN-DRLLIYSYMEGSLDYWLHERND	818
<i>C. rubella</i>	738	STNSFDQANI ICGGFGMVKYKALLPDGKVAIKKLSGD--CGQIEREFQAEVETLSRAQHPNLVLLRGFCFYKN-DRLLIYSYMEGSLDYWLHERND	832
<i>E. salsugineum</i>	738	STNNFDQANI ICGGFGLVYKALPDGRKVAIKKLSGD--CGQIEREFQAEVETLSRAQHPNLVLLRGFCFYKN-DRLLIYSYMEGSLDYWLHERND	832
<i>C. sinensis</i>	740	STNNFDQANI ICGGFGLVYKALPDGRNVAIKKLSGD--CGQIEREFQAEVETLSRAQHPNLVLLRGFCFYKN-DRLLIYSYMEGSLDYWLHEKLD	834
<i>C. clementina</i>	740	STNNFDQANI ICGGFGLVYKALPDGRNVAIKKLSGD--CGQIEREFQAEVETLSRAQHPNLVLLRGFCFYKN-DRLLIYSYMEGSLDYWLHEKLD	834
<i>C. sativus</i>	415	STNNFDQANI ICGGFGLVYKALPDGRKVAIKKLSGD--CGQMDREFQAEVETLSRAQHPNLVLLRGFCFYKN-DRLLIYSYMEGSLDYWLHEKPD	509
<i>G. max</i>	773	STNNFDQANI ICGGFGLVYKALPNGKAAIKKLSGD--CGQIEREFQAEVETLSRAQHPNLVLLRGFCFYKN-DRLLIYSYMEGSLDYWLHEKVD	867
<i>M. domestica</i>	738	STNNFDQANI ICGGFGLVYKALPDGKVAIKKLSGD--CGQMDREFQAEVETLSRAQHPNLVLLRGFCFYKN-DRLLIYSYMEGSLDYWLHEKID	832
<i>M. truncatula</i>	770	ATSNFDQANI IVCGGFGLVYKALPNGKAAIKKLSGD--CGQMDREFQAEVETLSRAQHPNLVLLRGFCFYKN-DRLLIYSYMEGSLDYWLHEKVD	864
<i>P. vulgaris</i>	769	STNNFDQANI ICGGFGLVYKALPNGTAAIKKLSGD--CGQIEREFQAEVETLSRAQHPNLVLLRGFCFYKN-DRLLIYSYMEGSLDYWLHEKVD	863
<i>P. persica</i>	739	STNNFDQANI ICGGFGLVYKALLPDGKVAIKKLSGD--CGQMDREFQAEVETLSRAQHPNLVLLRGFCFYKN-DRLLIYSYMEGSLDYWLHEKID	833

		CaM binding site		Activation segment						
		P		P P P P		P				
<i>A. thaliana</i>	825	GPALLKWKTRLR	IAQGAAGLLYLHEGCDPHILHRDIKS	SNILLDENFN	SHLADFGLARLMS	-PYE	THVSTDLVGT	LGYPPEYQA	SVATYKGDVY	920
<i>P. patens</i>	1165	AVEHLDWAKRFK	IAMGSARGLNFLHHGFIPHIHRDIKA	SNVLLDADFE	PRVADFGLARLI	S-AYE	THVSTDLVGT	LGYPPEYQ	SWRSTTRGDVY	1260
<i>S. moellendorffii</i>	867	GGSRLLWRHRLA	ILRETARGLVYLRHCNPVIVHRDIKS	SNILLDGLDR	AHVADFGLARLML	-PSD	THVSTDLVGT	LGYPPEYA	QSEASLRGDVY	962
<i>A. trichopoda</i>	854	GGSMLDWASRL	MAQGAAGHGLAYLHQTCENPILHRDIKS	SNILLDEEFA	HADFGLARLIL	-PYD	THVSTDLVGT	LGYPPEYQA	SVATFKGDVY	949
<i>B. distachyon</i>	862	GPPKLSWQRR	LQIAKGAARGLAYLHLSQCPHILHRDIKS	SNILLDENFE	AQADFGLARLIC	-PYD	THVSTDLVGT	LGYPPEYQS	SVATFKGDVY	957
<i>O. sativa</i>	861	GPSRLSWQTR	LQIAKGAARGLAYLHLSQCPHILHRDIKS	SNILLDEEFA	HADFGLARLIC	-PYD	THVSTDLVGT	LGYPPEYQS	SVANFKGDVY	956
<i>P. virgatum</i>	846	GAYALDWETRL	RIAQGAARGLAYLHMSCDPHILHRDIKS	SNILLDENFE	AHADFGLARLIC	-AYE	THVSTDLVGT	LGYPPEYQS	SPVATYKGDY	941
<i>S. italica</i>	860	GPSRLIWIPI	RQIAKGAARGLAYLHLSQCPHILHRDIKS	SNILLDENFE	AHADFGLARLIC	-PYA	THVSTDLVGT	LGYPPEYQS	SVATFKGDVY	955
<i>S. bicolor</i>	858	GPSRLIWPRL	QIAKGAARGLAYLHLSQCPHILHRDVKS	SNILLDENFE	AHADFGLARLIC	-PYA	THVSTDLVGT	LGYPPEYQS	SVATFKGDVY	953
<i>Z. mays</i>	860	GPSRLIWPRL	QIAKGAARGLAYLHLSQCPHILHRDIKS	SNILLDENFE	AHADFGLARLIC	-PYA	THVSTDLVGT	LGYPPEYQS	SVATFKGDVY	955
<i>A. coerulea</i>	829	GAYALDWETRL	RIAQGAARGLAYLHQSEPHILHRDVKS	SNILLDENFE	AHADFGLARLIL	-PYD	THVSTDLVGT	LGYPPEYQA	SVATFKGDVY	924
<i>M. guttatus</i>	840	GPTSLDWETRL	NIKAAGARGLAYLHQSEPHILHRDIKS	SNILLNEKE	FAHADFGLARLIL	-PYD	THVSTDLVGT	LGYPPEYQA	SVATYKGDVY	935
<i>S. lycopersicum</i>	775	GPALLDWDLR	LQIAQGAARGLAYLHLACEPHILHRDIKS	SNILLDENFE	AHADFGLARLI	IR-PYD	THVSTDLVGT	LGYPPEYQA	SVATYKGDVY	870
<i>S. tuberosum</i>	821	GPALLDWDLR	LQIAQGAARGLAYLHLACDPHILHRDIKS	SNILLDENFE	AHADFGLARLI	IR-PYD	THVSTDLVGT	LGYPPEYQA	SVATYKGDVY	916
<i>V. vinifera</i>	608	GSFLTWDTRV	KIAQGAARGLAYLHQSEPHILHRDIKS	SNILLDETF	EAHADFGLARLIL	-PYD	THVSTDLVGT	LGYPPEYQS	TLTATFKGDVY	703
<i>E. grandis</i>	824	GPCLLDWCKRL	RIAQGAARGLAYLHQSEPHIVHRDVKS	SNILLDGNF	EAHADFGLARLIR	-AYD	THVSTDLVGT	LGYPPEYGM	AVATCKGDVY	919
<i>P. trichocarpa</i>	838	GPSLSDWTR	LQIAQGAARGLAYLHQSEPHIVHRDIKS	SNILLDENF	VAHADFGLARLIL	-PYD	THVSTDLVGT	LGYPPEYQA	AVATYMGDVY	933
<i>L. usitatissimum</i>	862	GPSVLQWEAR	LKIAKGAAGLAYLHKVCEPHIVHRDVKS	SNILLDDKF	EAHADFGLSRLLR	-PYD	THVSTDLVGT	LGYPPEYS	QALATATCRGDVY	957
<i>M. esculenta</i>	838	GPSLDDWTR	LKIAQGAARGLAYLHQSEPHILHRDIKS	SNILLDENFE	AHADFGLARLIL	-PSD	THVSTDLVGT	LGYPPEYQA	SVATYKGDVY	933
<i>R. communis</i>	823	GPTLLDWVTR	LQIAQGAARGLAYLHQSEPHILHRDIKS	SNILLNENF	EAHADFGLARLIL	-PYD	THVSTDLVGT	LGYPPEYQA	SVATYKGDVY	918
<i>C. papaya</i>	726	GLSSLDWNTR	IQIAIGAARGLAYLHQSEPHILHRDIKS	SNILLDENFE	AHADFGLARLIL	-PYD	THVSTDLVGT	LGYPPEYQA	SVATYKGDVY	821
<i>G. raimondii</i>	823	GPSLLSWETR	LKIAQGAARGLAYLHQSEPHILHRDIKS	SNILLDENF	KAHADFGLARLIL	-PYD	THVSTDLVGT	LGYPPEYQA	SVATYKGDVY	918
<i>T. cacao</i>	802	GPSLDDWTR	LQIAQGAARGLAYLHQSEPHILHRDIKS	SNILLDENF	VAHADFGLARLIL	-PYD	THVSTDLVGT	LGYPPEYQA	SVATYKGDVY	897
<i>A. lyrata</i>	825	GPALLKWRTR	LRRIAQGAAGLLYLHEGCDPHILHRDIKS	SNILLDENFN	SHLADFGLARLMS	-PYE	THVSTDLVGT	LGYPPEYQA	SVATYKGDVY	920
<i>A. thaliana</i>	825	GPALLKWKTR	LRRIAQGAAGLLYLHEGCDPHILHRDIKS	SNILLDENFN	SHLADFGLARLMS	-PYE	THVSTDLVGT	LGYPPEYQA	SVATYKGDVY	920
<i>B. stricta</i>	835	GPALLKWKTR	LRRIAQGAAGLLYLHEACDPHILHRDIKS	SNILLDENF	DSHLADFGLARLMS	-PYE	THVSTDLVGT	LGYPPEYQA	SVATYKGDY	930
<i>B. rapa</i>	832	GPALLDWRTR	LRRIAQGAARGLYLYHACDPHILHRDIKS	SNILLDENF	DSHLADFGLARLMS	-PYE	THVSTDLVGT	LGYPPEYQA	SVATFKGDVY	927
<i>C. grandiflora</i>	819	GPALLNWRTR	LRRIAQGAAGLLYLHEACDPHILHRDIKS	SNILLDENF	TSHLADFGLARLMS	-PYE	THVSTDLVGT	LGYPPEYQA	SVATYKGDY	914
<i>C. rubella</i>	833	GPALLNWRTR	LRRIAQGAAGLLYLHEACDPHILHRDIKS	SNILLDENF	TSHLADFGLARLMS	-PYE	THVSTDLVGT	LGYPPEYQA	SVATYKGDY	928
<i>E. salusigneum</i>	833	GPALLDWRTR	LRRIAQGAARGLYLYHACDPHILHRDIKS	SNILLDENF	DSHLADFGLARLMS	-PYE	THVSTDLVGT	LGYPPEYQA	SVATYKGDVY	928
<i>C. sinensis</i>	835	GPSLDDWTR	LHIAQGAARGLAYLHQSEPHILHRDIKS	SNILLDGNF	GAHADFGLARLIL	SPYD	THVSTDLVGT	LGYPPEYQA	SVATYKGDVY	931
<i>C. clementina</i>	835	GPSLDDWTR	LHIAQGAARGLAYLHQSEPHILHRDIKS	SNILLDGNF	GAHADFGLARLIL	SPYD	THVSTDLVGT	LGYPPEYQA	SVATYKGDVY	931
<i>C. sativus</i>	510	GSSCLDWTR	LQIARGAAGLAYLHQSEPHILHRDIKS	SNILLDKNF	KAHADFGLARLIL	-PYD	THVSTDLVGT	LGYPPEYQS	LIATYRGDVY	605
<i>G. max</i>	868	ENSALKWDSR	LKVAQGAARGLAYLHKCEPPIVHRDVKS	SNILLDDNF	EAHADFGLSRLLQ	-PYD	THVSTDLVGT	LGYPPEYS	QTLTATFRGDVY	963
<i>M. domestica</i>	833	GPTSLDWNTR	LKIAQGAARGLAYLHQSEPHILHRDIKS	SNILLDENF	KAHADFGLARLIH	-PYA	THVSTDLVGT	LGYPPEYQA	SVATYKGDVY	928
<i>M. truncatula</i>	865	GNSALKWDR	LKIAQGAARGLAYLHKCEPPIVHRDIKS	SNILLNDKF	EAHADFGLSRLLS	-PYD	THVSTDLVGT	LGYPPEYS	QTLTATFRGDVY	960
<i>P. vulgaris</i>	864	ESALKWDAR	LKIAQGAARGLAYLHKCEPPIVHRDVKS	SNILLDDKF	EAHADFGLSRLLQ	-PYD	THVSTDLVGT	LGYPPEYS	QTLTATFRGDVY	959
<i>P. persica</i>	834	GPSLDDWNTR	LQIAQGAARGLAYLHQSEPHILHRDIKS	SNILLDENF	KAHADFGLARLIL	-PYD	THVSTDLVGT	LGYPPEYQA	SVATYKGDVY	929

		GC centre		P		P							
<i>A. thaliana</i>	921	SFGVLLLELLT	DKRPP--VDMCKPKGCRDLISWVVKMKHE	FRASEVFDPLI	YSKENDK----	EMFRVLEIACL	CLSENPKQRPT	QQLVSWLDDV	1008				
<i>P. patens</i>	1261	SYGVILLELLT	GKEPTGSDVKDYHEGGNVLQWARQMIKAGNA	ADVLDPIVSDG	PWKC----	KMLKVLHIAN	MCMAEDP	VKRPMSLQVVKLLKDV	1350				
<i>S. moellendorffii</i>	963	SFGVLLVLEVL	SRRRP--VDACRRGGIRDLPVVEGMQATGR	GIEIVDPLLLQ	NYSEVDALEEMLR	VLVDVAC	YCVDSQRR	PIEGIEVVAWLDAV	1054				
<i>A. trichopoda</i>	950	SFGVLLLELLT	GKRPP--VDVCKPKGCRDLISWVILQKSE	GRESEVDFPFY	YKQNDK----	QMLQMLEVAC	CLSNACKAR	PFICQVVSWLDSI	1037				
<i>B. distachyon</i>	958	SFGVLLLELLT	GKRPP--VDMCKPKGARELISWVIMHMK	GENREADVLD	RAMYKKEKYEI----	QMMKMI	DIACL	CISSEPKLRPL	HELVLWIDTI	1045			
<i>O. sativa</i>	957	SFGVLLLELLT	GKRPP--VDMCKPKGARELISWVLMHMK	KEKCEAEVLD	RAMYDKKFEM----	QMVQMI	DIACL	CISSEPKLRPL	HELVLWLDNI	1044			
<i>P. virgatum</i>	942	SFGVLLLELLT	TGRRP--VDMCRPKGTRDVSWVLMQKE	EGRETEV	FHPISHHKENES----	QLIRVLE	IAICL	CVTAAPKSRPT	SQLVAVLDDI	1029			
<i>S. italica</i>	956	SFGVLLLELLT	GKRPP--VDMCKPKGARELISWVTHMK	KENRETVDL	RAMYDKKFEM----	EMMQMI	DIACL	CVSDSPKLRPL	HQLVLWLDNI	1043			
<i>S. bicolor</i>	954	SFGVLLLELLT	GKRPP--VDMCKPKGARELISWVTHMK	KENREADVLD	RAMYDKKFET----	QMIQMI	DIACL	CVSDSPKLRPL	HQLVLWLDNI	1041			
<i>Z. mays</i>	956	SFGVLLLELLT	GKRPP--IDMCKPKGARELISWVLMK	KENREADVLD	RAMYDKKFET----	QMRQVI	DIACL	CVSDSPKLRPL	HQLVMWLDNI	1043			
<i>A. coerulea</i>	925	SFGVLLLELLT	GKRPP--MDMCKPKDRRLISWVFMK	KEKREAEV	IDPFIYDKQ	QHKD----	EILRALE	IAICL	CLSESPKVRPS	QQIVSWLNI	1012		
<i>M. guttatus</i>	936	SFGVLLLELLT	GKRPP--MDMCKPKGCRDLISWVVKMK	HEENRASEV	DFPIYDKQ	NDK----	EMLR	WK-----	992				
<i>S. lycopersicum</i>	871	SFGVLLLELLT	TCKRPP--MDPCKPRASDLISWVIMQ	MKQKRETEV	FDPLIYDKQ	QHKH----	EMLLVLE	IAICL	CLHSEPKIRPS	SQLVTWLDNI	958		
<i>S. tuberosum</i>	917	SFGVLLLELLT	TCKRPP--MDPCKPRASDLISWVIMQ	MKQKRETEV	FDPLIYDKQ	QHKH----	EMLLVLE	IAICL	CLHSEPKIRPS	SQLVTWLDNI	1004		
<i>V. vinifera</i>	704	SFGVLLLELLT	TGRRP--VEVCKGKNCRDLSWVFMK	SEKKEEQIM	DSVVDK	DREK----	QFLEV	LGIA	CRCIDQDP	QRPSIDQVVSWLDAV	791		
<i>E. grandis</i>	920	SFGVLLLELLT	GKRPP--MDMCKPKGSRDLISWVIR	MKENRESEV	DFPIYDKQ	NDK----	EILR	VLEI	ACL	CLSNACKAR	PFICQVVSWLDDG	1006	
<i>P. trichocarpa</i>	934	SFGVLLLELLT	GKRPP--MDMCKPKGSRDLISWVIM	QKKNRESEV	DFPIYDKQ	NDK----	ELQR	VLEI	ARL	CLSEYPKLRPS	SQLVSWLDNI	1021	
<i>L. usitatissimum</i>	958	SFGVLLLELLT	TCRPP--VEVCKGKSCRDLSWVFMK	FEKRVSEI	IDASV	WDKDQEK----	QLVEM	LEI	ACR	CLDHEPRR	PFIEEVVSCLDGI	1045	
<i>M. esculenta</i>	934	SFGVLLLELLT	GKRPP--MDMCKPKGSRDLISWVIM	QKKNRESEV	DFPFIYDKQ	QHKD----	QLLQV	FDI	ACL	CLSESPKVRPS	ITQLVSWLENT	1021	
<i>R. communis</i>	919	SFGVLLLELLT	GKRPP--MDMCKPKGSRDLISWVIM	QKKNRESEV	DFPFIYDKQ	NDK----	QLLQV	LDI	ACL	CLSESPKVRPS	ITQLVSWLDGI	1006	
<i>C. papaya</i>	822	SFGVLLLELLT	GKRPP--MDMCKPKGSRDLISWAI	QKKNRENEV	DFPFIYDKQ	QHKD----	EMCL	VLI	ACI	CLSECPKVRPT	SQLVSWLDNI	909	
<i>G. raimondii</i>	919	SFGVLLLELLT	GKRPP--MDMCKPKGTRDLISWVIR	MKENRESEV	DFPFIYDKQ	QHKD----	EMLR	VLEI	ACL	CLSESPKIRPT	SQLVYWLDDV	1006	
<i>T. cacao</i>	898	SFGVLLLELLT	GKRPP--MDMCKPKGSRDLISWVIR	MKENRESEV	DFPFIYDKQ	QHKD----	EMLR	VLEI	ACL	CLSESPKVRPT	SQLVSWLDDV	985	
<i>A. lyrata</i>	921	SFGVLLLELLT	DKRPP--VDMCKPKGCRDLISWVVKMK	HEENRASEV	DFPFIYDKQ	NDK----	EMFR	VLEI	IT	ACL	CLSENPKQRPT	QQLVSWLDDV	1008
<i>A. thaliana</i>	921	SFGVLLLELLT	DKRPP--VDMCKPKGCRDLISWVVKMK	HEENRASEV	DFPFIYDKQ	NDK----	EMFR	VLEI	IA	ACL	CLSENPKQRPT	QQLVSWLDDV	1008
<i>B. stricta</i>	931	SFGVLLLELLT	DKRPP--VDMCKPKGCRDLISWVVKMK	NENRASEV	DFPFIYDKQ	NDK----	EMFR	VLEI	IA	ACL	CLNENPKQRPT	QQLVSWLHDV	1018
<i>B. rapa</i>	928	SFGVLLLELLT	DKRPP--VDMCKPKGRELISWVVMK	SEGRASEV	DFPFIH	IGKVNEE----	EMFR	VLEI	EA	ACL	CLSHNPKLRPT	SQLVSWLDDV	1015
<i>C. grandiflora</i>	915	SFGVLLLELLT	GKRPP--VDMCKPKGSRDLISWVIM	KENRASEV	DFPFIYDKQ	NDK----	EMLR	VLEI	IA	ACL	CLSESPKVRPT	SQLVSWLDDV	1002
<i>C. rubella</i>	929	SFGVLLLELLT	DKRPP--VDMCKPKGSRDLISWVVMK	YENRASEV	DFPFIYR	KENEK----	EMLR	VLEI	IA	ACL	CLSENPKQRPT	SQLVSWLDDV	1016
<i>E. salusigneum</i>	929	SFGVLLLELLT	DKRPP--VDMCKPKGSRDLISWVVMK	NENRASEV	DFPFIH	IGKENEK----	EMLR	VLEI	EA	ACL	CLSENPKQRPT	SQLVSWLDDV	1016
<i>C. sinensis</i>	932	SFGVLLLELLT	GKRPP--MDMCKPKGSRDLISWVIR	MKENRESEV	DFPFIYDKQ	QHKD----	EMLR	VLDI	ACL	CLSESPKVRPT	SQLVSWLDSI	1019	
<i>C. clementina</i>	932	SFGVLLLELLT	GKRPP--MDMCKPKGSRDLISWVIR	MKENRESEV	DFPFIYDKQ	QHKD----	EMLR	VLDI	ACL	CLSESPKVRPT	SQLVSWLDSI	1019	
<i>C. sativus</i>	606	SFGVLLLELLT	GKRPP--IDMCRPKGLRDLISWVFM	QRKDKKVEV	DFPFIYDKQ	KNEM----	AMVE	VLDI	ACL	CLCKVPKERS	SQLVTWLDKC	693	
<i>G. max</i>	964	SFGVLLLELLT	TGRRP--VEVIKGNCRNLVSWVYQ	MSENKEQEIF	DPFIYDKQ	HEK----	QLLE	VLA	IA	ACK	CLNQDP	QRPSIEIVVSWLDSV	1051
<i>M. domestica</i>	929	SFGVLLLELLT	GKRPP--MDMCKPKCRDLISWAFQ	MKREKKESEV	DFPFIYDKQ	QHKD----	ELLC	VF	EA	ACL	CLSGSPKVRPS	SQLVTWLDNI	1016
<i>M. truncatula</i>	961	SFGVLLLELLT	TARRP--VEVIKGNCRNLVSWVYQ	MSENKEQEIF	DPFIYDKQ	HEK----	QLLE	VLSI	ACK	CLNQDP	QRPSIEIVVSWLDSV	1048	
<i>P. vulgaris</i>	960	SFGVLLLELLT	TGRRP--VEVIKGNCRNLVSWVYQ	MSENKEQEIF	DPFIYDKQ	HEK----	QLLE	MLA	IA	ACK	CLNQDP	QRPSIEIVVSWLDCV	1047

<i>A.thaliana</i>		-----	
<i>P.patens</i>	1351	EMSSQLSTHDDAQ-----	1363
<i>S.moellendorffii</i>	1055	GSSRLKVGLGKP-----	1066
<i>A.trichopoda</i>	1038	GADSQQT-----	1045
<i>B.distachyon</i>	1046	DTSGEAIN-----	1053
<i>O.sativa</i>	1045	GGSTEATK-----	1052
<i>P.virgatum</i>	1030	AEDSVLEQPEVSGGFNLLA-----	1048
<i>S.italica</i>	1044	GVSSDAPK-----	1051
<i>S.bicolor</i>	1042	GVTSDAPK-----	1049
<i>Z.mays</i>	1044	GVTSEPK-----	1051
<i>A.coerulea</i>	1013	DTYGP-----	1017
<i>M.guttatus</i>		-----	
<i>S.lycopersicum</i>	959	NTPPDVHVF-----	967
<i>S.tuberosum</i>	1005	NTPPDVHVF-----	1013
<i>V.vinifera</i>	792	GKEGVLPLFIAFEISSFSFFLS-----	813
<i>E.grandis</i>		-----	
<i>P.trichocarpa</i>	1022	DTNT-----	1025
<i>L.usitatissimum</i>	1046	GDT-----	1048
<i>M.esculenta</i>	1022	DISTA-----	1026
<i>R.communis</i>	1007	DNT-----	1010
<i>C.papaya</i>	910	ETTSSILIM-----	918
<i>G.raimondii</i>	1007	TSLSSV-----	1012
<i>T.cacao</i>	986	DISI-----	989
<i>A.lyrata</i>		-----	
<i>A.thaliana</i>		-----	
<i>B.stricta</i>		-----	
<i>B.rapa</i>		-----	
<i>C.grandiflora</i>		-----	
<i>C.rubella</i>		-----	
<i>E.salsugineum</i>		-----	
<i>C.sinensis</i>	1020	I-----	
<i>C.clementina</i>	1020	I-----	
<i>C.sativus</i>	694	TFYNQPYTPHNKFFVSLVYISTFFSSLN	721
<i>G.max</i>	1052	RFDGSQQ-----	1058
<i>M.domestica</i>	1017	NTKKV-----	1021
<i>M.truncatula</i>	1049	KVDGFQQ-----	1055
<i>P.vulgaris</i>	1048	RFDGSQQ-----	1054
<i>P.persica</i>	1018	STKN-----	1021

Supplemental Figure S4. Alignment of PSKR1 orthologs from higher plants and mosses. The intracellular sequences from 37 LRR-RLKs with highest similarity to Arabidopsis PSKR1 were identified from the Phytozome database. The positions of the phosphorylation sites identified in *Arabidopsis thaliana* PSKR1 are indicated. Green denotes sites identified in PSKR1 *in planta* and magenta those identified *in vitro*. Indicated in blue is the T890 that is also transphosphorylated by *E. coli*. Squares indicate unambiguous residues whereas circles indicate phosphorylation sites whose position was not confirmed. Red indicates a conserved residue at the respective position in PSKR1 orthologs and yellow a functionally conserved S/T or Y residue in PSKR1 orthologs.

Supplemental Figure S5

Species	Gene	Position	Sequence	Position
<i>Arabidopsis thaliana</i>	PSKR1	681	RARRRSGEVDPEI---EES ES SM-----NRKELGEIGSKLVVLFQ S ---NDKELSYDDLDD	729
<i>Physcomitrella patens</i>		817	EVEAKDLEKAKLNMNMTLDPCS----LSLDKMKEPLSINVAMFEQ--PLLRLTLADVLR	869
<i>Selaginella moellendorffii</i>		721	SFSRRAR-AGHRQD----IAGRN----FKEMSVQMMDLTVMFQ--RYRRITVGDLLK	768
<i>Amborella trichopoda</i>		650	HMSRKE--ERYQNGEVVSDR----SHRPSESGSKLVLLFQ N -PEGMELTINDLLK	700
<i>Brachypodium distachyon</i>		690	NISKGE--ASAI S D---EDAEG----DCHDPYYSKPVLF F EN-S-AKELTVSDLLK	736
<i>Oryza sativa</i>		711	NISKRE--VSIID D ---EEING----SCHDSYD-YWKPVLFFQ D -S-AKELTVSDLLK	756
<i>Panicum virgatum</i>		586	NMSKRE--VSAIDY---EDTEG----SCHELYDSYLKPVLF F Q N -SAVKELTVSDLV R	633
<i>Setaria italica</i>		695	NMSKRE--VSAIDY---EETEG----SCHELYDSYKPVLF F Q N -SAVKELTVSDLV R	742
<i>Sorghum bicolor</i>		703	NMSKRE--VTAIDY---EDTEG----SSHELYDTYKPVLF F Q N -STVKELTVSDLV R	750
<i>Zea mays</i>		696	NMSKRE--VSAIE H E---EDTEG----SCHELYGSYKPVLF F Q N -SAVKELTVSDLV R	744
<i>Aquilegia coerulea</i>		713	KISRKD-VRY P MD---DVEENF-CRSNRFS-EALGSSKLVILF Q N-SESKELTIGD L LK	764
<i>Mimulus guttatus</i>		702	RVSRKD-NRAP V E---DLDEEED-----SRTTGQPK-MVIF K N-ADFKDLTVSD L LK	747
<i>Solanum lycopersicum</i>		685	RVSRRD-AG H QIG---DFEEDFSR--PPRSSDTF V PSK-LVLF Q N-SDCKELTVAD L LK	735
<i>Solanum tuberosum</i>		712	RVSRRD-AG H QIG---DFEEDFSR--PPRSSDTF V PSK-LVLF Q N-SDCKELTVAD L LK	762
<i>Vitis vinifera</i>		462	EVI P Y-VGD P IV---DLDEEED-----SRPHRLS-EVLGSSK-LVLF Q N-SGCKDLSVAD L LK	512
<i>Eucalyptus grandis</i>		715	KILRRD-VND H ID---DLHEEL-GRPHRLS-GTLE S SK-LVLF Q N-SDCKDLTVAD L LK	765
<i>Populus trichocarpa</i>		715	KMSRRN-VGD P IG---DLDEEG-SLPHRLS-EALRSSK-LVLF Q N-SDCKELSVAD L LK	765
<i>Linum usitatissimum</i>		716	MMSRRA-RG D LIN---NLDEE E ---SESQRSS-QALMT S K-LVLF Q N-SDCKDLTV D L L K	766
<i>Manihot esculenta</i>		716	KMSKRD-VGD P IE---DLDEE V -SWPHRLS-EGLGSSK-LVLF Q N-SECKDLTVAD L LK	766
<i>Ricinus communis</i>		714	KISRDRYVGD P FD---DLDEE V -SRPHRLS-EALGSSK-LVLF Q N-SDCKDLTVAD L LK	765
<i>Carica papaya</i>		583	RAHSR-GE V DPER---DFD E -----NEKDLEELGSR L VVLFQ N KE D NK D LS F DD L LK	630
<i>Gossypium raimondii</i>		716	RMSKRD-VG S TVD---NLDEE L -SRSHRLS-EALGSSK-LVLF Q S- S NCKELTV D L L K	766
<i>Theobroma cacao</i>		716	RMSRRD-VGD P ID---DLDEE L -SRSHRLS-EALGSSK-LVLF Q S- S NCKELTV D L L K	766
<i>Arabidopsis lyrata</i>		701	RISRKD-S D DRIN---DVDEE T ---ISGVPKALG P SK-IVLF H S-CGCKDLSV E EL L K	749
<i>Arabidopsis thaliana</i>		701	RISRKD-V D DRIN---DVDEE T ---ISGVS K ALG P SK-IVLF H S-CGCKDLSV E EL L K	749
<i>Boechera stricta</i>		701	RISRKD- A DDRIN---DVDEE T ---ISGVPKALG P SK-IVLF H S-CGCKDLSV E EL L K	749
<i>Brassica rapa</i>		674	RLSRKE-G D DRVN---DADEE-----V P KAPL S SK-IVLF H S-CGCKDLTVAD L LK	718
<i>Capsella grandiflora</i>		701	RISRKD- A DDRIN---DVDEE T ---VSGVPKALG P SK-IVLF H S-CGCKDLSV E EL L K	749
<i>Capsella rubella</i>		701	RISRKD- A DDRIN---DVDEE T ---ISGVPKALG P SK-IVLF H S-CGCKDLSV E EL L K	749
<i>Eutrema salusigneum</i>		682	RLSRKD- A DRVN---D I DEEM---ISDV P KAP G T S K-IVLF H S-CGCKDLSVAD L LK	730
<i>Citrus sinensis</i>		714	KMSRRD-SG C PID---DLDE D M-GR P Q R LS-EALASSK-LVLF Q N-SDCKDLTVSD L LK	764
<i>Citrus clementina</i>		718	KMSRRD-SG C PID---DLDE D M-GR P Q R LS-EALASSK-LVLF Q N-SDCKDLTVSD L LK	768
<i>Cucumis sativus</i>		724	KISRKD-VG D RRNR F DE E FD R ---ADRLSGALG S SK-LVLF Q N-SECKDLTV A EL L K	775
<i>Glycine max</i>		721	KMSKRD-DD K PM D ---NFDEELNGR P RL S -EALASSK-LVLF Q N-SDCKDLTVAD L LK	772
<i>Malus domestica</i>		718	KMSRRG-A K D I D---DFD E -----SRPHR I S-GALASSK-LVLF Q N-SDCKD F TVSD L LK	767
<i>Medicago truncatula</i>		717	RMSKRE-ED K PID---SFDEEMSGR P RL S SE G F V ASK-LVLF Q N-SDCKDLTVSD L LK	769
<i>Phaseolus vulgaris</i>		717	RT S RRD-DD K PID---NYDEELNGR P RL S -EALV S SK-LVLF Q N-SDCKDLTVAD L LK	768
<i>Prunus persica</i>		716	KMSRRG-V K D Q ND---DFD D DL-SRPHRLS-GALASSK-LVLF Q N-SDCKELTV D L L K	766

ATP binding region

Species	Gene	Position	Sequence	Position
<i>A. thaliana</i>	PSKR1	730	ST N S F D Q ANIIGCGGF G LVYKA L LPDG T KAAV K RLSGD C G--QIEREF F AE V ET L S R AQ H PN L V L LR G FC F Y K N-DRLLI S Y M EN G SL D Y W L H ER N D	824
<i>P. patens</i>		870	ATNGFSK T NIIGDGG F GVYKA L PDGR I V A IK L KL H GL S --QGN R E F LA E ME T LG K V K HR H LV P LL G Y C S F GE-EK L L V D Y DM K NG S LD L W L R N RA D	964
<i>S. moellendorffii</i>		769	ATNNFDAT N IIGCGGF L VYKA N LPD G N V VAIK R L T SE D GG P Q M ER E FD A EL T SL G NI T HP N LV S LE G Y C RL G MR D RL V Y S Y M EN G SL D Y W L H ER S D	866
<i>A. trichopoda</i>		701	STNNFDQ A NIIGCGGF L VYKA L LPD N T K AAIK R LSG D CG--Q M ER E F R AE V EAL S RA Q H K N L V S LR G Y C RH G N-DRLLI S Y M EN G SL D Y W L H ER L D	853
<i>B. distachyon</i>		737	STNNFDE A NIIGCGGF G LVYKA L LPD G T K AAV K RLSG D SG--Q M ER E F H AE V EAL S RA Q A H K N L V SL R G Y CR Y R D -DRLLI Y T M EN N S L D Y W L HER E D	831
<i>O. sativa</i>		757	STNNFDQ A NIIGCGGF L VYKA L LPD G T K AAV K RLSG D CG--Q M ER E F R AE V EAL S RA Q A H K N L V SL R G Y CR Y R G N-DRLLI S Y M EN N S L D Y W L HER S D	851
<i>P. virgatum</i>		634	STNNFDQ A NIIGCGGF L VYKA L LPD G T K AAV K RLSG D Y G --Q M ER E F R AE V EAL S RA Q A H K N L V TL R G Y CR Y R G N-DRLLI S Y M EN G SL D Y W L H ER S D	728
<i>S. italica</i>		743	STNNFDQ A NIIGCGGF L VYKA L LPD G T K AAV K RLSG D CG--Q M ER E F R AE V EAL S RA Q A H K N L V TL R G Y CR Y R G N-DRLLI S Y M EN G SL D Y W L H ER S D	837
<i>S. bicolor</i>		751	STNNFDQ A NIIGCGGF L VYKA L LPD G T K AAV K RLSG D CG--Q M ER E F R AE V EAL S RA Q A H K N L V TL K G Y CR Y R G N-DRLLI S Y M EN G SL D Y W L H ER S D	845
<i>Z. mays</i>		745	STNNFDQ A NIIGCGGF L VYKA L LPD G T K AAV K RLSG D CG--Q M ER E F R AE V EAL S RA Q A H K N L V TL K G Y CR Y R G N-DRLLI S Y M EN G SL D Y W L H ER S D	839
<i>A. coerulea</i>		765	STNNFDQ A NIIGCGGF L VYKA N LP N GS K AAIK R LSG D CG--Q M ER E F R AE V EAL S RA Q A H K N L V PL Q Y C RH G N-DRLLI S Y M EN G SL D Y W L H ER V D	859
<i>M. guttatus</i>		748	STNNF S Q S NI V CGCG F L V Y R AD F PN G AA A IK R LSG D CG--Q M ER E F R AE V EAL S RA Q A H K N L V SL Q Y C I Y R N -DRLLI S Y M EN G SL D Y W L H E Q I E	842
<i>S. lycopersicum</i>		736	STNNF N Q S NI V CGCG F L V Y K AEL P NG I KT A IK R LSG D CG--Q M ER E F R AE V EAL S RA Q H K N L V S L Q Y C Q H G S -DRLLI S Y M EN G SL D Y W L H ER V D	830
<i>S. tuberosum</i>		763	STNNF N Q S NI V CGCG F L V Y K AEL P NG I KT A IK R LSG D CG--Q M ER E F R AE V EAL S RA Q H K N L V S L Q Y C Q H G S -DRLLI S Y M EN G SL D Y W L H ER V D	857
<i>V. vinifera</i>		513	STNNF N Q A NIIGCGGF L VYKA N LPD G T R AAIK R LSG D CG--Q M ER E F R AE V EAL S RA Q H K N L V S L Q Y C RH G N-DRLLI S Y M EN G SL D Y W L H ER V D	607
<i>E. grandis</i>		766	STSN F SQ A NIIGCGGF L VYKA N LP N G M AAIK R LSG D CG--Q V ER E F H AE V EAL S RA Q H K N L V S L Q Y C RH G N-DRLLI S Y M EN G SL D Y W L H ER V D	860
<i>P. trichocarpa</i>		766	STNNF N Q A NIIGCGGF L VYKA N FP D T K AAIK R LSG D CG--Q M ER E F R AE V EAL S RA Q H K N L V S L Q Y C RH G N-DRLLI S Y M EN G SL D Y W L H ES V D	860
<i>L. usitatissimum</i>		767	ATNNF S Q A NIIGCGGF L VYKA N LP N G K AAIK L SG D CG--Q I ER E F R AE V EAL S RA Q H K N L V S L Q Y C K H G S -DRLLV S Y M EN G SL D Y W L H EC V D	861
<i>M. esculenta</i>		767	STNNF N Q A NIIGCGGF L VYKA N LP N G T AAIK R LSG D CG--Q M ER E F R AE V EAL S RA Q H K N L V S L Q Y C RH G N-DRLLI S Y M EN G SL D Y W L H EC V D	861
<i>R. communis</i>		766	ATNNF N Q A NIIGCGGF L VYKA L SL N PG A AAIK R LSG D CG--Q M ER E F R AE V EAL S RA Q H K N L V S L Q Y C RH G N-DRLLI S Y M EN G SL D Y W L H EC A D	860
<i>C. papaya</i>		631	STNNFDQ A NIIGCGGF L VYKA L LP D SR K V A IK R LSG D CG--Q M D R E F R A E V EAL S RA Q H P N L V L L Q Y C M H K N -DRLLI S Y M EN G SL D Y W L H E K I D	725
<i>G. raimondii</i>		767	STNNF N Q A NIIGCGGF L VYKA L LPD G T N AAV K RLSG D CG--Q M ER E F R AE V EAL S RA Q H K N L V S L Q Y C K H G N -DRLLI S Y M EN G SL D Y W L H ES V D	861
<i>T. cacao</i>		767	STNNF N Q A NIIGCGGF L VYKA L LPD G T K AAV K RLSG D CG--Q M ER E F R AE V EAL S RA Q H K N L V S L Q Y C K H G N -DRLLI S Y M EN G SL D Y W L H ES V D	861
<i>A. lyrata</i>		750	STNNF S Q A NIIGCGGF L VYKA N FP D GS K AAV K RLSG D CG--Q M ER E F R AE V EAL S RA E H K N L V S L Q Y C K H G N -DRLLI S Y S F M EN G SL D Y W L H ER V D	844
<i>A. thaliana</i>		750	STNNF S Q A NIIGCGGF L VYKA N LP N G M AAIK R LSG D CG--Q V ER E F R AE V EAL S RA E H K N L V S L Q Y C K H G N -DRLLI S Y M EN G SL D Y W L H ER V D	844
<i>B. stricta</i>		750	STNNF S Q A NIIGCGGF L VYKA N FP D GS K AAV K RLSG D CG--Q M ER E F R AE V EAL S RA E H K N L V S L Q Y C K H G N -DRLLI S Y S F M EN G SL D Y W L H ER V D	844
<i>B. rapa</i>		719	STNG F SQ A NIIGCGGF L VYKA N LPD G S K AAV K RLSG D CG--Q M ER E F R AE V EAL S RA E H E N L V S L Q Y C K H G D -DRLLI S Y S F M EN G SL D Y W L H ER V D	813
<i>C. grandiflora</i>		750	STNNF S Q A NIIGCGGF L VYKA N FPD G S K AAV K RLSG D CG--Q M ER E F R AE V EAL S RA E H K N L V S L Q Y C K H G N -DRLLI S Y S F M EN G SL D Y W L H ER V D	844
<i>C. rubella</i>		750	STNNF S Q A NIIGCGGF L VYKA N FPD G S K AAV K RLSG D CG--Q M ER E F R AE V EAL S RA E H K N L V S L Q Y C K H G N -DRLLI S Y S F M EN G SL D Y W L H ER V D	844
<i>E. salusigneum</i>		731	ST N F SQ A NIIGCGGF L VYKA N LPD G S K AAV K RLSG D CG--Q M ER E F R AE V EAL S RA E H K N L V S L Q Y C K H G N -DRLLI S Y S F M EN G SL D Y W L H ER V D	825
<i>S. sinensis</i>		765	STNNF N Q A NIIGCGGF L VYKA L LT N G T KAAV K RLSG D CG--Q M ER E F R AE V EAL S RA Q H K N L V S L Q Y C RH G N-DRLLI S Y M EN G SL D Y W L H ES V D	859
<i>C. clementina</i>		769	STNNF N Q A NIIGCGGF L VYKA L LT N G T KAAV K RLSG D CG--Q M ER E F R AE V EAL S RA Q H K N L V S L Q Y C RH G N-DRLLI S Y M EN G SL D Y W L H ES V D	863
<i>C. sativus</i>		776	ATCN F Q A NIIGCGGF L VYKA L SL N PG M AAV K RL T GD C G--Q M ER E F R AE V EAL S RA Q H K N L V S L Q Y C K H G N -DRLLI S Y M EN G SL D Y W L H EV D	870
<i>G. max</i>		773	STNNF N Q A NIIGCGGF L VYKA L LP N G A AAV K RLSG D CG--Q M ER E F R AE V EAL S RA Q H K N L V S L K G Y CR H G N -DRLLI S Y S LE N G S L D Y W L H EC V D	867
<i>M. domestica</i>		768	STNNF N Q A NIIGCGGF L VYKA N LP N G M AAIK R LSG D CG--Q M ER E F R AE V EAL S RA Q H K N L V S L Q Y C RH G N-DRLLI S Y M EN G SL D Y W L H ES V D	862
<i>M. truncatula</i>		770	ATSN F Q A NIIGCGGF L VYKA L LP N G M AAIK R LSG D CG--Q M ER E F R AE V EAL S RA Q H K N L V S L K G Y CR H G N -DRLLI S Y M EN G SL D Y W L H EC V D	864
<i>P. vulgaris</i>		769	STNNF N Q A NIIGCGGF L VYKA L LP N G T KAAIK R LSG D CG--Q M ER E F R AE V EAL S RA Q H K</	

		CaM binding site				Activation segment			
<i>A. thaliana</i>	PSKR1	825	GPALLKWKTRLRIAQGAAGLLYLHEGCDPHILHRDIKSN	P	SNILLDENFN	SHVSD	LDVGLTGYIPPEYQAS	VATYKGDVY	920
<i>P. patens</i>		965	ALEHLDPKFRFRIALGSARGLCFLHHGFIPHIHRDIKSN	P	SNILLDANFEP	RVADFLGLARLI	SAYDSHVS	TDIAGTFGYIPPEYQSWRSTTRGDVY	1060
<i>S. moellendorffii</i>		867	GGSRLLTWRHRLAILETARGLEYLHRGNPHIVHRDIKSN	P	SNILLDGDRLAHVADFLGLARMLPSDTHVTT	DELVGLTGYIPPEYQAS	SEASLRGDVY	962	
<i>A. trichopoda</i>		854	EGLMLDWGTRLKIAQGSARGLAYLHRVCDPNIHRDVKSN	P	SNILLNDKFEAHLADFLGLSRLLRPYDTHVTT	DLVGLTGYIPPEYQTLTATPKGDVY		949	
<i>B. distachyon</i>		832	GGYMLKWDSSLKIAQGSARGLAYLHKVCEPNIHRDVKSN	P	SNILLNENFEAHLADFLGLARLMQPYDTHVTT	DLVGLTGYIPPEYSQSLIATPKGDVY		927	
<i>O. sativa</i>		852	GGYMLKWE SRLKIAQGSARGLAYLHKVCEPNIHRDVKSN	P	SNILLNENFEAHLADFLGLARLIQPYDTHVTT	DLVGLTGYIPPEYSQSVIATPKGDVY		947	
<i>P. virgatum</i>		729	GGYMLKWE SRLKIAQGSARGLAYLHKVCEPNIHRDVKSN	P	SNILLNENFEAHLADFLGLARLIQPYDTHVTT	DLVGLTGYIPPEYSQSVIATPKGDVY		824	
<i>S. italica</i>		838	GGYMLKWE SRLKIAQGSARGLAYLHKVCEPNIHRDVKSN	P	SNILLNENFEAHLADFLGLARLIQPYDTHVTT	DLVGLTGYIPPEYSQSVIATPKGDVY		933	
<i>S. bicolor</i>		846	GGYMLKWE SRLKIAQGSARGLAYLHKVCEPNIHRDVKSN	P	SNILLNENFEAHLADFLGLARLIQPYDTHVTT	DLVGLTGYIPPEYSQAVIATPKGDVY		941	
<i>Z. mays</i>		840	GGYVLTWE SRLKIAQGSARGLAYLHKVCEPNIHRDVKSN	P	SNILLNENFEAHLADFLGLARLIQPYDTHVTT	DLVGLTGYIPPEYSQAVIATPKGDVY		935	
<i>A. coerulea</i>		860	GGSVLKWDVRLKIAQGAAGKGLAYLHKVCEPNIHRDVKSN	P	SNILLDENFDAHLADFLGLARLLCPYDTHVTT	DLVGLTGYIPPEYSQTLTATPKGDVY		955	
<i>M. guttatus</i>		843	DGSFLDWEKRLKIAARGAACGLAYLHN--EPNIHRDIKSN	P	SNILLNEKFDAHLADFLGLSRLLRPHYDTHVTT	DLVGLTGYIPPEYSQSLAATFRGDVY		936	
<i>S. lycopersicum</i>		831	-GSSLTWDMRLKIAQGAARGLAYLHK--EPNIHRDIKSN	P	SNILLNERFEAHLADFLGLSRLLRPHYDTHVTT	DLVGLTGYIPPEYSQTLTATFRGDVY		923	
<i>S. tuberosum</i>		858	-GSSLTWDIRLKIAQGAAGHGLAYLHK--EPNIHRDIKSN	P	SNILLNERFEAHLADFLGLSRLLRPHYDTHVTT	DLVGLTGYIPPEYSQTLTATFRGDVY		950	
<i>V. vinifera</i>		608	GGSFLLTWDTRVKIAQGAARGLAYLHKVCEPNIHRDVKSN	P	SNILLDENFDAHLADFLGLARLLCPYDTHVTT	DLVGLTGYIPPEYSQTLTATPKGDVY		703	
<i>E. grandis</i>		861	GGSVLAWDVRKIAQGAARGLAYLHKVCEPNIHRDVKSN	P	SNILLDEKFEAHLADFLGLSRLLRPHYDTHVTT	DLVGLTGYIPPEYSQTLTATFRGDVY		956	
<i>P. trichocarpa</i>		861	GTSVLKWEVRLKIAQGAACGLAYLHKVCEPNIHRDVKSN	P	SNILLDENFEAHLADFLGLSRLLRPHYDTHVTT	DLVGLTGYIPPEYSQTLMATCRGDVY		956	
<i>L. usitatissimum</i>		862	GPSVLQWEARLKIAGAAGKGLAYLHKICEPNIHRDVKSN	P	SNILLDEKFEAHLADFLGLSRLLRPHYDTHVTT	DLVGLTGYIPPEYSQALATATCRGDVY		957	
<i>M. esculenta</i>		862	GASFLKWDVRLKVAQGAASGLAYLHKVCEPNIHRDVKSN	P	SNILLDEKFEAHLADFLGLSRLLRPHYDTHVTT	DLVGLTGYIPPEYSQTLTATCRGDVY		957	
<i>R. communis</i>		861	GASFLKWEVRLKIAQGAASGLAYLHKVCEPNIHRDVKSN	P	SNILLDEKFEAHLADFLGLSRLLRPHYDTHVTT	DLVGLTGYIPPEYSQTLTATCRGDVY		918	
<i>C. papaya</i>		726	GLSSLDWNTRIQAIGAARGLAYLHQSEPHILHRDIKSN	P	SNILLDENFEAHLADFLGLARLLPYDTHVTT	DLVGLTGYIPPEYQAS	VATYKGDVY	821	
<i>G. raimondii</i>		862	GSSVLKWDVRLKIAQGAARGLAYLHKVCEPNIHRDVKSN	P	SNILLDEKFEAHLADFLGLSRLLRPHYDTHVTT	DLVGLTGYIPPEYSQTLTATCRGDVY		957	
<i>T. cacao</i>		862	GSSILKWDVRLKIAQGAARGLAYLHKVCEPNIHRDVKSN	P	SNILLDENFDAHLADFLGLARLLCPYDTHVTT	DLVGLTGYIPPEYSQTLTATCRGDVY		957	
<i>A. lyrata</i>		845	GNMTLKWVRLKIAQGAARGLAYLHKVCEPNIHRDVKSN	P	SNILLDEKFEAHLADFLGLARLLRPHYDTHVTT	DLVGLTGYIPPEYSQSLIATCRGDVY		940	
<i>A. thaliana</i>		845	GNMTLKWVRLKIAQGAARGLAYLHKVCEPNIHRDVKSN	P	SNILLDEKFEAHLADFLGLARLLRPHYDTHVTT	DLVGLTGYIPPEYSQSLIATCRGDVY		940	
<i>B. stricta</i>		845	GNMTLKWVRLKIAQGAARGLAYLHKVCEPNIHRDVKSN	P	SNILLDEKFEAHLADFLGLARLLRPHYDTHVTT	DLVGLTGYIPPEYSQSLIATCRGDVY		940	
<i>B. rapa</i>		814	GSTTLKWDVRLKIAQGAARGLAYLHKVCEPNIHRDVKSN	P	SNILLDEKFEAHLADFLGLARLLRPHYDTHVTT	DLVGLTGYIPPEYSQALATCRGDVY		909	
<i>C. grandiflora</i>		845	GNMTLKWVRLKIAQGAARGLAYLHKVCEPNIHRDVKSN	P	SNILLDEKFEAHLADFLGLARLLRPHYDTHVTT	DLVGLTGYIPPEYSQSLIATCRGDVY		940	
<i>C. rubella</i>		845	GNMTLKWVRLKIAQGAARGLAYLHKVCEPNIHRDVKSN	P	SNILLDEKFEAHLADFLGLARLLRPHYDTHVTT	DLVGLTGYIPPEYSQSLIATCRGDVY		940	
<i>E. salsugineum</i>		826	GNMTLKWVRLKIAQGAARGLAYLHKVCEPNIHRDVKSN	P	SNILLDEKFEAHLADFLGLARLLRPHYDTHVTT	DLVGLTGYIPPEYSQSLIATCRGDVY		921	
<i>C. sinensis</i>		860	KDSVLKWDVRLKIAQGAARGLAYLHKVCEPNIHRDVKSN	P	SNILLDEKFEAHLADFLGLSRLLRPHYDTHVTT	DLVGLTGYIPPEYSQTLTATCRGDVY		955	
<i>C. clementina</i>		864	KDSVLKWDVRLKIAQGAARGLAYLHKVCEPNIHRDVKSN	P	SNILLDEKFEAHLADFLGLSRLLRPHYDTHVTT	DLVGLTGYIPPEYSQTLTATCRGDVY		959	
<i>C. sativus</i>		871	NDSILKWETRLKIAQGAAGHGLAYLHKCEPNIHRDVKSN	P	SNILLDDRFEAHLADFLGLSRLLRPHYDTHVTT	DLVGLTGYIPPEYSQTLTATCRGDVY		966	
<i>G. max</i>		868	ENSALKWDSRLKVAQGAARGLAYLHKCEPNIHRDVKSN	P	SNILLDDNFEAHLADFLGLSRLLRPHYDTHVTT	DLVGLTGYIPPEYSQTLTATCRGDVY		963	
<i>M. domestica</i>		863	GSVLLKWDVRLKIAQGAARGLAYLHKVCEPNIHRDVKSN	P	SNILLDEKFEAHLADFLGLSRLLRPHYDTHVTT	DLVGLTGYIPPEYSQTLTATCRGDVY		958	
<i>M. truncatula</i>		865	GNALKWVRLKIAQGAAGHGLAYLHKCEPNIHRDVKSN	P	SNILLNDKFEAHLADFLGLSRLLRPHYDTHVTT	DLVGLTGYIPPEYSQTLTATCRGDVY		960	
<i>P. vulgaris</i>		864	ESALKWDARLKIAQGAARGLAYLHKCEPNIHRDVKSN	P	SNILLDDKFEAHLADFLGLSRLLRPHYDTHVTT	DLVGLTGYIPPEYSQTLTATCRGDVY		959	
<i>P. persica</i>		862	GVSLKWDVRLKIAQGAARGLAYLHKCEPNIHRDIKSN	P	SNILLDEKFEAHLADFLGLSRLLRPHYDTHVTT	DLVGLTGYIPPEYSQTLTATCRGDVY		957	

		GC centre							
<i>A. thaliana</i>	PSKR1	921	SFGVLLLELLTGRRP-VDMCKPKGCRDLISWVVKMKHES	P	RSRASEVFDPL-IYSKEND---	KEMFRVLEIACLCLSENPKQRPT	QQLVSWLDDV		1008
<i>P. patens</i>		1061	SYGVILLEMLTGKEPTRDDFKDIEGNNLVGWVRQVIRKGDAPKALDSEVSKGPKWN---		TMLKVLHIANLCTAEDP	IRRPMTLQVVKFLKDI		1149	
<i>S. moellendorffii</i>		963	SFGVLLVLELTSRRP-VDACRRGGIRDLPWVEGMQATGRGIE		IVDPDLLQNYSEVDALEEMLRVLDVACVCDSCPQR	RGIEEVAWLDV		1054	
<i>A. trichopoda</i>		950	SFGVLLLELLTGRRP-VDVCKSKGKCRDLVSWVFMKSEKKEE		IFVFP-LWSKAHE--	KQLLVLEIACRCIERDPRRPS	IQQVSWLDSV	1037	
<i>B. distachyon</i>		928	SFGVLLLELLTGRRP-VGVLIVK--WDLVSWTLQMQSENKEE		QIFDKL-IWSKEHE--	KQLLAVLEAACRCINADPRQRPPIEQVVAWLDGI		1013	
<i>O. sativa</i>		948	SFGVLLLELLTGRRP-MDVSKAKGSRDLVSVLQMKSEKKEE		QIFDFTL-IWSKTHE--	KQLFVLEAACRCISTDPRQRPPIEQVVAWLDV		1035	
<i>P. virgatum</i>		825	SFGVLLLELLTGRRP-VDVSKSKGSRDLISWVLQMKSEKKEE		QIFDRL-IWSKAHE--	KQLLSVLEITCKCISADPRQRPPIEQVVSCLDKV		912	
<i>S. italica</i>		934	SFGVLLLELLTGRRP-VDVSKSKGSRDLISWVLQMKSEKKEE		QIFDRL-IWSKAHE--	KQLLSVLEITCKCISADPRQRPPIEQVVSCLDNV		1021	
<i>S. bicolor</i>		942	SFGVLLLELLTGRRP-VDVSKFKGSRDLISWVLQMKSEKKEE		QIFDRL-IWSKTHE--	KQLLSVLEITACKCISTDPRQRPPIEQVVSCLDNV		1029	
<i>Z. mays</i>		936	SFGVLLLELLTGRRP-VDVSRKSGSRDLISWVLQMKSEKKEE		QIFDRL-IWSKAHE--	KQLLSVLEITACKCISADPRQRPPIEQVVSCLDNV		1023	
<i>A. coerulea</i>		956	SFGVLLLELLTSRRP-VDVCKAKGTRDLVSWVLQLENKEE		QIFDPS-IWSKSLE--	KQFIEVLGVACKCIDQDPRRPSIEQVVSCLDSI		1043	
<i>M. guttatus</i>		937	SFGVLLLELLTGRRP-VEVCKGKNCRDLSWVFMKSEKKEE		IFDPS-IWSKSLE--	KQFIEVLGVACKCIDQDPRRPSIEQVVSCLDSI		1025	
<i>S. lycopersicum</i>		924	SFGVLLLELLTGRRP-VEVCRGKNCRDLSWVFMKSEKKEE		IFDFT-IWDTSYE--	KQLEVLVSIACQCIVQDPRQRPPIEQVVSCLDSI		1011	
<i>S. tuberosum</i>		951	SFGVLLLELLTGRRP-VEVCRGKNCRDLSWVFMKSEKKEE		IFDFT-IWDTSYE--	RQLEVLVSIACQCIVQDPRQRPPIEQVVSCLDSI		1038	
<i>V. vinifera</i>		704	SFGVLLLELLTGRRP-VEVCKGKNCRDLSWVFMKSEKKEE		IQMDS-VWDKRE--	KQFLEVLGIACRCIDQDPRRPSIEQVVSCLDSV		791	
<i>E. grandis</i>		957	SFGVLLLELLTGRRP-VEVCKGKNCRDLSWVFMKSEKKEE		IFDPS-IWVKHE--	RQVLEVLVSIACRCIERDPRRPSIEQVVSCLDSV		1044	
<i>P. trichocarpa</i>		957	SFGVLLLELLTGRRP-VEVCKGKNCRDLSWVFMKSEKREAE		IDPA-IWVDKHQ--	KQFEMLEIACRCIDQDPRRPSIEQVVSCLDSV		1044	
<i>L. usitatissimum</i>		958	SFGVLLLELLTGRRP-VEVCKGKNCRDLSWVFMKFEKRVSE		IDTS-IWVDKRE--	KQVEMLEIACRCIDQDPRRPSIEQVVSCLDSI		1045	
<i>M. esculenta</i>		958	SFGVLLLELLTGRRP-VEVCKGKNCRDLSWVFMKSEKREAE		IFDPS-MWDDIE--	KQFEMLEIACRCIDQDPRRPSIEQVVSCLDSI		1045	
<i>R. communis</i>		919	SFGVLLLELLTGRRP-VEVCKGKNCRDLSWVFMKSEKREAE		IFDPS-IWVDKRE--	KQVEMLEIACRCIDQDPRRPSIEQVVSCLDSI		1044	
<i>C. papaya</i>		822	SFGVLLLELLTGRRP-MDMCKPKGSRDLISWVFMKSEKREAE		IFDPS-IYDKQHD--	KEMCLVLIACICLSECPKVRPT	QQLVSWLDNI	909	
<i>G. raimondii</i>		958	SFGVLLLELLTGRRP-VEVCKGKNCRDLSWVFMKFEKRESE		IDSS-IWVDKRE--	KQLLEMLEIACRCIDQDPRRPSIEQVVSCLDSI		1045	
<i>T. cacao</i>		958	SFGVLLLELLTGRRP-VEVCKGKNCRDLSWVFMKSEKREAE		IDPS-IWVDKRE--	KQLEMLEIACRCIDQDPRRPSIEQVVSCLDSI		1045	
<i>A. lyrata</i>		941	SFGVLLLELLTGRRP-VEVCKGKNCRDLSWVFMKSEKREAE		IFDIT-IRENVNE--	KTVLEMLEIACRCIDQDPRRPSIEQVVSCLDSI		1028	
<i>A. thaliana</i>		941	SFGVLLLELLTGRRP-VEVCKGKNCRDLSWVFMKSEKREAE		IFDIT-IRENVNE--	RTVLEMLEIACRCIDQDPRRPSIEQVVSCLDSI		1028	
<i>B. stricta</i>		941	SFGVLLLELLTGRRP-VEVCKGKNCRDLSWVFMKSEKREAE		IFDIT-IRENVNE--	KTVLEMLEIACRCIDQDPRRPSIEQVVSCLDSI		1028	
<i>B. rapa</i>		910	SFGVLLLELLTGRRP-VEVCKGKNCRDLSWVFMKSEKREAE		IFDIT-MREVDVE--	KEVLEMLEIACRCIDQDPRRPSIEQVVSCLDSI		997	
<i>C. grandiflora</i>		941	SFGVLLLELLTGRRP-VEVCKGKNCRDLSWVFMKSEKREAE		IFDIT-IRENVNE--	KTVLEMLEIACRCIDQDPRRPSIEQVVSCLDSI		1028	
<i>C. rubella</i>		941	SFGVLLLELLTGRRP-VEVCKGKNCRDLSWVFMKSEKREAE		IFDIT-IRENVNE--	KTVLEMLEIACRCIDQDPRRPSIEQVVSCLDSI		1028	
<i>E. salsugineum</i>		922	SFGVLLLELLTGRRP-VEVCKGKNCRDLSWVFMKSEKREAE		IFDIT-IHDNLNE--	KAVLEMLEIACRCIDQDPRRPSIEQVVSCLDSI		1009	
<i>C. sinensis</i>		956	SFGVLLLELLTGRRP-VEVCKGKNCRDLSWVFMKSEKREAE		IFDIT-IWVKRE--	KQLEMLEIACRCIDQDPRRPSIEQVVSCLDSI		1043	
<i>C. clementina</i>		960	SFGVLLLELLTGRRP-VEVCKGKNCRDLSWVFMKSEKREAE		IFDIT-IWVKRE--	KQLEMLEIACRCIDQDPRRPSIEQVVSCLDSI		1047	
<i>C. sativus</i>		967	SFGVLLLELLTGRRP-VEVCKGKNCRDLSWVFMKSEKREAE		IFDIT-IWNTNSK--	KQILEVLGITCKCIEQDPRRPSIEQVVSCLDSV		1054	
<i>G. max</i>		964	SFGVLLLELLTGRRP-VEVCKGKNCRDLSWVFMKSEKREAE		IFDIT-IWVKDHE--	KQLEMLEIACRCIDQDPRRPSIEQVVSCLDSV		1051	

<i>M. domestica</i>	959	SFGVVLELLTGRRP-VEVCRGKNCRDLVSWMFQMRFEKRDEEIIDSS-IWNKNHE---KQLLDVLGVACKCLDPNPRQRPFIIEVVVSCLDGI	1046
<i>M. truncatula</i>	961	SFGVVLELLTARRP-VEVIKGNCRNLVSWVYQMKYENKQEIFDQT-IWEKERE---KQLLEVLSIACKCLDQDPRQRPSEIMVVSWLDSV	1048
<i>P. vulgaris</i>	960	SFGVVLELLTGRRP-VEVIKGNCRNLVFWVFMKSENKEQDIFDPA-IWHKDRE---KQLLEMLAIACKCLDQDPRQRPPIEVVVSWLDCV	1047
<i>P. persica</i>	958	SFGVVLELLTGRRP-VEVCRGKNCRDLVSWMFQMKSEKREEEIIDSS-IWNKDHE---KQLLEVLTGTCKCLDPNPRQRPSEIEVVVSWLDGI	1045

<i>A. thaliana</i>	PSKR1	-----	
<i>P. patens</i>	1150	EDQDHV-----	1155
<i>S. moellendorffii</i>	1055	GSSRLKVGLGKP-----	1066
<i>A. trichopoda</i>	1038	GDAEPVR-----	1044
<i>B. distachyon</i>	1014	SP-----	1015
<i>O. sativa</i>		-----	
<i>P. virgatum</i>		-----	
<i>S. italica</i>		-----	
<i>S. bicolor</i>		-----	
<i>Z. mays</i>	1024	V-----	
<i>A. coerulea</i>	1044	PVDEA-----	1048
<i>M. guttatus</i>	1026	EMEKA-----	1030
<i>S. lycopersicum</i>	1012	ASVKER-----	1017
<i>S. tuberosum</i>	1039	GSVKER-----	1044
<i>V. vinifera</i>	792	GKEGVLPLFIAFEISSFSFFLS-----	813
<i>E. grandis</i>	1045	GIEGSPGS-----	1052
<i>P. trichocarpa</i>	1045	SKVLNNEL-----	1052
<i>L. usitatissimum</i>	1046	GDT-----	1048
<i>M. esculenta</i>	1046	GIQGA-----	1050
<i>R. communis</i>	1045	GIQGAQ-----	1050
<i>C. papaya</i>	910	ETTSSILIM-----	918
<i>G. raimondii</i>	1046	GNEVVVRQ-----	1052
<i>T. cacao</i>	1046	EHEVVQQ-----	1052
<i>A. lyrata</i>	1029	PMESVQQQ-----	1036
<i>A. thaliana</i>	1029	PMESVQQQ-----	1036
<i>B. stricta</i>	1029	PMESVQ-----	1034
<i>B. rapa</i>	998	PNQ-----	1000
<i>C. grandiflora</i>	1029	PMESVQQQ-----	1036
<i>C. rubella</i>	1029	PMESVQQQ-----	1036
<i>E. salsugineum</i>	1010	PVESVQQQ-----	1017
<i>C. sinensis</i>	1044	GIDAA-----	1048
<i>C. clementina</i>	1048	GIDAA-----	1052
<i>C. sativus</i>	1055	TSIHTQ-----	1060
<i>G. max</i>	1052	RFDGSQQ-----	1058
<i>M. domestica</i>	1047	GFESGKQ-----	1053
<i>M. truncatula</i>	1049	KVDGFQQ-----	1055
<i>P. vulgaris</i>	1048	RFDGSQQ-----	1054
<i>P. persica</i>	1046	GFESGTQ-----	1052

Supplemental Figure S5. Alignment of PSKR2 orthologs from higher plants and mosses. The intracellular sequences from 37 LRR-RLKs with highest similarity to Arabidopsis PSKR2 were identified from the Phytozome database. The positions of the phosphorylation sites identified in *Arabidopsis thaliana* PSKR1 are indicated. Green denotes sites identified in PSKR1 *in planta* and magenta those identified *in vitro*. Indicated in blue is the T890 that is also transphosphorylated by *E. coli*. Squares indicate unambiguous residues whereas circles indicate phosphorylation sites whose position was not confirmed. Red indicates a conserved residue at the respective position in PSKR2 orthologs and yellow a functionally conserved S/T or Y residue in PSKR2 orthologs.

Supplemental Table 1

Supplemental Table 1. Identification of a single phosphorylation at T890 of H₆-PSKR1-K762E protein by LC-ESI MS.

Peptide Properties

Sequence	Start	End	Phospho-Site Equalling	Search Engine Score [%]	phosphoRS Score [%]	Phospho-Site Position	MH+ [Da]	RT [min]	Precursor Area
HVSTDLVGTL	891	900	no	100,0	50	-	1121,52	63,45	1,40E+006
MSPYETHVST	885	894	yes	100,0	95,9	890	1231,47	42,65	2,19E+005
MSPYETHVSTDLV	885	897	yes	100,0	100	890	1574,64	56,63	1,55E+007
MSPYETHVSTDLVGTL	885	900	yes	100,0	99,4	890	1845,80	67,08	3,97E+007
MSPYETHVSTDLVGTL	885	900	yes	100,0	87,9	890	1829,80	69,51	2,21E+006
RLMSPYETHVST	883	894	yes	100,0	100	890	1516,65	45,45	3,41E+006
RLMSPYETHVST	883	894	yes	100,0	86,3	890	1500,65	50,14	9,14E+005
RLMSPYETHVSTDLV	883	897	yes	100,0	85	890	1843,83	58,46	7,63E+006
RLMSPYETHVSTDLV	883	897	yes	100,0	99,9	890	1827,84	63,04	1,28E+006
RLMSPYETHVSTDLVGTL	883	900	yes	95,7	99,5	890	2114,98	66,42	5,53E+006
RLMSPYETHVSTDLVGTL	883	900	yes	100,0	100	890	2098,99	62,68	3,19E+007

Supplemental Table 2

Supplemental Table 2. Verification of the extent of phosphorylation between H₆-PSKR1-KD and H₆-PSKR1-K762E. A semi-quantitative label-free (precursor area) and spectral counting approach (SPC) was performed.

Peptide Properties													
Origin	Sequence	Start	End	Phospho-Site Equalling	Search Engine Score [%]	phosphoRS Score [%]	Phospho-Site Position	MH+ [Da]	RT [min]	Precursor Area	Ratio Sample vs Control	PSMs	Ratio Sample vs Control
Sample	HVSTDLVGTL	891	900	yes	68,4	59,9	894	1.121,52	61,88	2,52E+007	94,8	19	90,5
Control	HVSTDLVGTL	891	900	no	100,0	50	-	1121,52	63,45	1,40E+006	5,2	2	9,5
Sample	MSPYETHVST	885	894	yes	100,0	76,1	890	1.231,47	40,89	1,74E+007	98,8	25	96,2
Control	MSPYETHVST	885	894	yes	100,0	95,9	890	1231,47	42,65	2,19E+005	1,2	1	3,8
Sample	MSPYETHVSTDV	885	897	yes	88,6	84,1	890	1.574,64	55,56	2,16E+008	93,3	44	84,6
Control	MSPYETHVSTDV	885	897	yes	100,0	100	890	1574,64	56,63	1,55E+007	6,7	8	15,4
Sample	MSPYETHVSTDVVGTL	885	900	yes	96,5	86,9	890	1.845,80	67,1	2,64E+008	86,9	115	87,1
Control	MSPYETHVSTDVVGTL	885	900	yes	100,0	99,4	890	1845,80	67,08	3,97E+007	13,1	17	12,9
Sample	MSPYETHVSTDVVGTL	885	900	yes	100,0	98,9	890	1.829,80	66,17	2,01E+008	98,9	34	87,2
Control	MSPYETHVSTDVVGTL	885	900	yes	100,0	87,9	890	1829,80	69,51	2,21E+006	1,1	5	12,8
Sample	RLMSPYETHVST	883	894	yes	100,0	92,7	890	1.516,65	44,02	5,81E+007	94,5	42	93,3
Control	RLMSPYETHVST	883	894	yes	100,0	100	890	1516,65	45,45	3,41E+006	5,5	3	6,7
Sample	RLMSPYETHVST	883	894	yes	100,0	90	890	1.500,65	45,76	1,48E+007	94,2	35	89,7
Control	RLMSPYETHVST	883	894	yes	100,0	86,3	890	1500,65	50,14	9,14E+005	5,8	4	10,3
Sample	RLMSPYETHVSTDV	883	897	yes	88,5	82,1	890	1.843,83	55,7	8,56E+007	91,8	87	89,7
Control	RLMSPYETHVSTDV	883	897	yes	100,0	85	890	1843,83	58,46	7,63E+006	8,2	10	10,3
Sample	RLMSPYETHVSTDV	883	897	yes	97,1	99	890	1.827,83	58,63	8,32E+007	98,5	70	92,1
Control	RLMSPYETHVSTDV	883	897	yes	100,0	99,9	890	1827,84	63,04	1,28E+006	1,5	6	7,9
Sample	RLMSPYETHVSTDVVGTL	883	900	yes	74,7	83,3	890	2.114,98	63,6	1,33E+008	96,0	174	88,3
Control	RLMSPYETHVSTDVVGTL	883	900	yes	95,7	99,5	890	2114,98	66,42	5,53E+006	4,0	23	11,7
Sample	RLMSPYETHVSTDVVGTL	883	900	yes	95,4	94,5	890	2.098,99	64,98	2,40E+008	88,3	87	97,8
Control	RLMSPYETHVSTDVVGTL	883	900	yes	100,0	100	890	2098,99	62,68	3,19E+007	11,7	2	2,2

Supplemental Table 3

Supplemental Table 3. Identification of two to three *in planta* phosphorylation sites (S698, S696/S698 and S886 or S893) of immunoprecipitated PSKR1-GFP by LC-ESI MS.

Peptide Properties

Sequence	Start	End	Phospho-Site Equalling	Search Engine Score [%]	phosphoRS Score [%]	Phospho-Site Position	MH+ [Da]	RT [min]	Precursor Area
RSGEVDPEIEESES MNRK	685	702	yes	100,0	99,4	698	2171,92	27,01	7,94E+006
RSGEVDPEIEESES MNRK	685	702	yes	100,0	97,7	698	2187,92	23,57	7,71E+006
SGEVDPEIEESES MNRK	686	702	yes	95,2	89,8	698	2015,82	30,13	1,55E+008
SGEVDPEIEESES MNRK	686	702	yes	73,9	81,1	698	2031,82	26,36	1,34E+008
SGEVDPEIEESES MNRKELGEIGSK	686	710	yes	81,8	99,8	698	2829,24	41,59	1,89E+008
SGEVDPEIEESES MNRKELGEIGSK	686	710	yes	82,4	85,2	698	2845,24	38,73	2,06E+008
SGEVDPEIEESES MNRKELGEIGSK	686	710	yes	100,0	100	696&698	2925,20	38,63	4,40E+007
RLMSPYETHVSTDLVGTL	883	900	yes	100,0	74,7	893	2098,99	53,63	5,06E+006
RLMSPYETHVSTDLVGTL	883	900	yes	100,0	99,4	886	2114,98	49,76	8,96E+006
LMSPYETHVSTDLVGTLGYIPPEYQQASVATYK	884	916	yes	25,0	49,4	886	3683,72	58,87	3,29E+006

Supplemental Table 4

Supplemental Table 4. Accession numbers of the AtPSKR1 orthologs identified from the Phytozome database and the respective protein accessions in NCBI. The asterisk indicates $\geq 97\%$ identity to the Phytozome sequence.

Organism	Accession Phytozome v10	Accession NCBI
<i>Physcomitrella patens</i>	Phpat.001G165500.2	-
<i>Selaginella moellendorffii</i>	121260	-
<i>Amborella trichopoda</i>	evm_27.model.AmTr_v1.0_scaffold00029.177	XP_006847965*
<i>Brachypodium distachyon</i>	Bradi3g49370.1	XP_003575411
<i>Oryza sativa</i>	LOC_Os02g41890.1	-
<i>Panicum virgatum</i>	Pavir.Ga00206.1	-
<i>Setaria italica</i>	Si016177m	XP_004953174*
<i>Sorghum bicolor</i>	Sobic.004G222100.1	XP_002454207*
<i>Zea mays</i>	GRMZM2G080537_T01	AFW72422
<i>Aquilegia coerulea</i>	Aquca_002_01421.1	-
<i>Mimulus guttatus</i>	Migut.E00603.1	EYU30259*
<i>Solanum lycopersicum</i>	Solyc01g008140.2.1	XP_004228537*
<i>Solanum tuberosum</i>	PGSC0003DMT400042178	XP_006348541*
<i>Vitis vinifera</i>	GSVIVT01014303001	CBI20272
<i>Eucalyptus grandis</i>	Eucgr.J01778.1	KCW52373
<i>Populus trichocarpa</i>	Potri.008G144700.1	XP_002312507*
<i>Linum usitatissimum</i>	Lus10005403	-
<i>Manihot esculenta</i>	cassava4.1_027914m	-
<i>Ricinus communis</i>	29801.m003229	XP_002518809*
<i>Carica papaya</i>	evm.model.supercontig_2.62	-
<i>Gossypium raimondii</i>	Gorai.005G151100.1	-
<i>Theobroma cacao</i>	Thecc1EG011306t1	XP_007045577
<i>Arabidopsis lyrata</i>	484148	XP_002876804
<i>Arabidopsis thaliana</i>	AT2G02220.1	Q9ZVR7
<i>Boechera stricta</i>	Bostr.0556s0048.1	-
<i>Brassica rapa</i>	Brara.F03427.1	-
<i>Capsella grandiflora</i>	Cagra.2767s0007.1	-
<i>Capsella rubella</i>	Carubv10019052m	XP_006292801
<i>Eutrema salsugineum</i>	Thhalv10003581m	XP_006395801
<i>Citrus sinensis</i>	orange1.1g035998m	XP_006470905*
<i>Citrus clementina</i>	Ciclev10004232m	XP_006420664
<i>Cucumis sativus</i>	Cucsa.229250.2	XP_004140449
<i>Glycine max</i>	Glyma.13G275100.1	-
<i>Malus domestica</i>	MDP0000142599	XP_008340497
<i>Medicago truncatula</i>	Medtr2g078810.1	KEH38700
<i>Phaseolus vulgaris</i>	Phvul.005G073800.1	XP_007149480*
<i>Prunus persica</i>	ppa000729m	XP_007227028

Supplemental Table 5

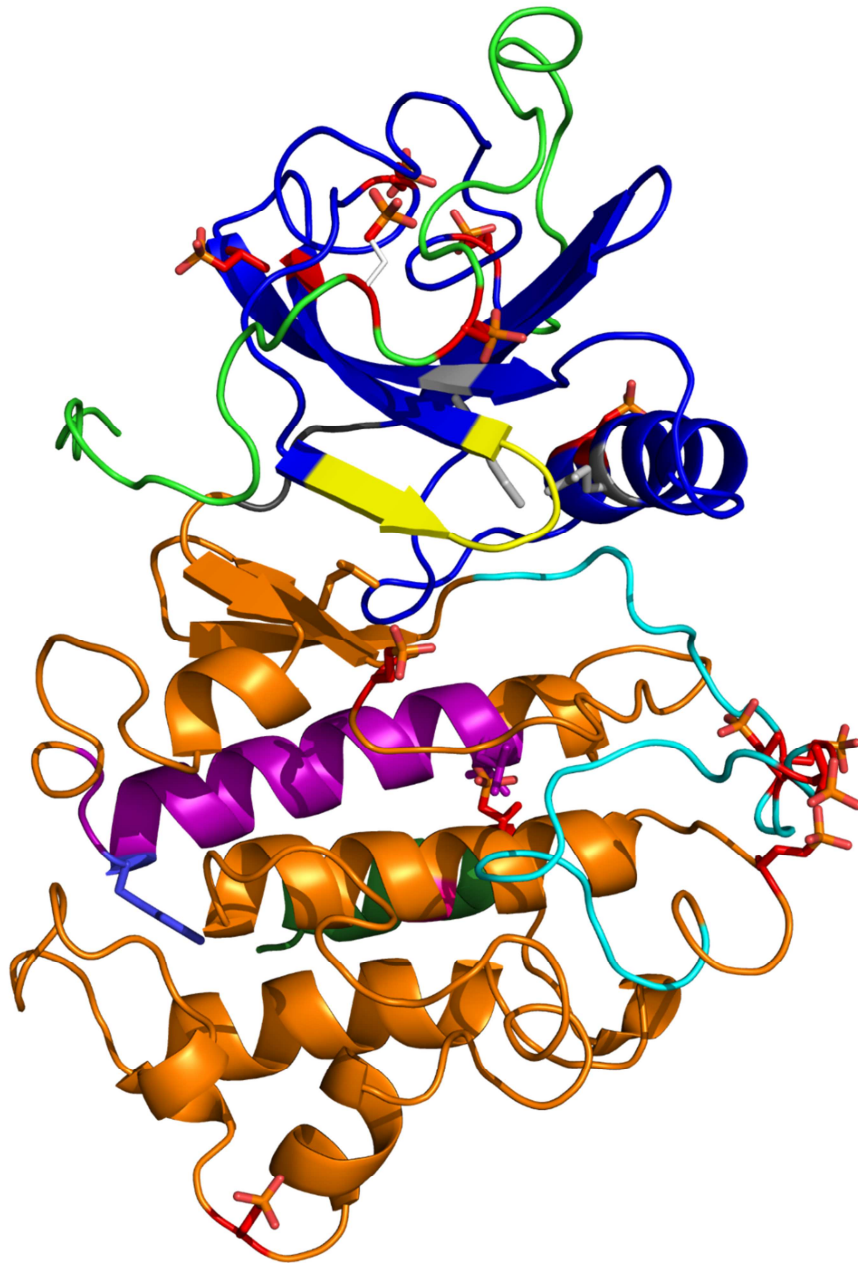
Supplemental Table54. Accession numbers of the AtPSKR2 orthologs identified from the Phytozome database and the respective protein accessions in NCBI. The asterisk indicates $\geq 97\%$ identity to the Phytozome sequence.

Organism	Accession Phytozome v10	Accession NCBI
<i>Physcomitrella patens</i>	Phpat.014G063600.1	-
<i>Selaginella moellendorffii</i>	121260	-
<i>Amborella trichopoda</i>	evm_27.model.AmTr_v1.0_scaffold00160.2	XP_006849388
<i>Brachypodium distachyon</i>	Bradi1g59360.1	XP_003561510*
<i>Oryza sativa</i>	LOC_Os04g57630.1	-
<i>Panicum virgatum</i>	Pavir.Bb00088.1	-
<i>Setaria italica</i>	Si031967m	XP_004955312*
<i>Sorghum bicolor</i>	Sobic.002G006100.1	XP_002459218*
<i>Zea mays</i>	GRMZM2G120574_T01	XP_008651929*
<i>Aquilegia coerulea</i>	Aquca_036_00102.1	-
<i>Mimulus guttatus</i>	Migut.H01950.4	EYU26371*
<i>Solanum lycopersicum</i>	Solyc07g063000.2.1	XP_004244239*
<i>Solanum tuberosum</i>	PGSC0003DMT400032398	XP_006348262*
<i>Vitis vinifera</i>	GSVIVT01014303001	-
<i>Eucalyptus grandis</i>	Eucgr.F01155.2	KCW67382*
<i>Populus trichocarpa</i>	Potri.011G116900.1	XP_002317487
<i>Linum usitatissimum</i>	Lus10009213	-
<i>Manihot esculenta</i>	cassava4.1_000747m	-
<i>Ricinus communis</i>	29668.m000312	XP_002528241*
<i>Carica papaya</i>	evm.model.supercontig_2.62	-
<i>Gossypium raimondii</i>	Gorai.002G068500.2	-
<i>Theobroma cacao</i>	Thecc1EG031592t1	XP_007021540*
<i>Arabidopsis lyrata</i>	495467	XP_002864288
<i>Arabidopsis thaliana</i>	AT5G53890.1	Q9FN37
<i>Boechera stricta</i>	Bostr.26833s0888.1	-
<i>Brassica rapa</i>	Brara.J00880.1	XP_009119929*
<i>Capsella grandiflora</i>	Cagra.2460s0051.1	-
<i>Capsella rubella</i>	Carubv10025797m	XP_006279563
<i>Eutrema salsugineum</i>	Tthhalv10012554m	XP_006401649
<i>Citrus sinensis</i>	orange1.1g001591m	XP_006464783*
<i>Citrus clementina</i>	Ciclev10007314m	XP_006451809
<i>Cucumis sativus</i>	Cucsa.032510.1	XP_004146245*
<i>Glycine max</i>	Glyma.13G275100.1	XP_006594757*
<i>Malus domestica</i>	MDP0000950533	XP_008349995*
<i>Medicago truncatula</i>	Medtr2g078810.1	-
<i>Phaseolus vulgaris</i>	Phvul.005G073800.1	-
<i>Prunus persica</i>	ppa000652m	XP_007213710

Chapter 2

Phosphorylation of the phytosulfokine peptide receptor PSKR1 controls receptor activity

Kaufmann, C., Motzkus, M., & Sauter, M. (2017).
Journal of Experimental Botany, 68(7), 1411–1423.
<https://doi.org/10.1093/jxb/erx030>





RESEARCH PAPER

Phosphorylation of the phytosulfokine peptide receptor PSKR1 controls receptor activity

Christine Kaufmann, Michael Motzkus and Margret Sauter*

Entwicklungsbiologie und Physiologie der Pflanzen, Christian-Albrechts-Universität Kiel, Am Botanischen Garten 5, 24118 Kiel, Germany

* Correspondence: msauter@bot.uni-kiel.de

Received 4 July 2016; Editorial decision 13 January 2017; Accepted 16 January 2017

Editor: Richard Napier, University of Warwick

Abstract

The phytosulfokine peptide receptor PSKR1 is modified by phosphorylation of its cytoplasmic kinase domain. We analyzed defined phosphorylation sites by site-directed mutagenesis with regard to kinase activity *in vitro* and receptor activity *in planta*. S696 and S698 in the juxtamembrane (JM) domain are phosphorylated *in planta*. The phosphomimetic S696D/S698D replacements resulted in reduced transphosphorylation activity of PSKR1 kinase *in vitro* but did not reduce autophosphorylation activity. Growth-promoting activity of the PSKR1(S696D/S698D) receptor isoform was impaired in the shoot but not in the root. The JM domain thus seems to be important for phosphorylation of a target protein required for shoot growth promotion. The phosphomimetic replacement T998D at the C-terminus (CT) abolished kinase activity *in vitro* but not receptor function *in planta*, indicating that additional levels of regulation exist *in planta*. A possible mode of receptor regulation is the interaction with regulatory proteins such as the calcium sensor calmodulin (CaM). We show that the previously reported binding of CaM2 to PSKR1 is calcium-dependent, occurs predominately to the hypophosphorylated soluble PSKR1 kinase, and does not significantly change PSKR1 kinase activity. In conclusion, our results show that peptide signaling of growth by PSKR1 is regulated by differential phosphorylation of the juxtamembrane and C-terminal domains of the intracellular receptor part and suggest that interaction of PSKR1 with CaM serves a function other than the regulation of kinase activity.

Key words: Arabidopsis, calcium, calmodulin, growth regulation, peptide signaling, phytosulfokine receptor, pull-down, receptor-like kinase, receptor phosphorylation.

Introduction

Plant peptides act as signaling molecules in developmental processes, growth regulation, and stress responses. They are of diverse nature with regard to synthesis, modification, and activities (Tavormina *et al.*, 2015), yet the known receptors that perceive peptide signals all belong to the class of leucine-rich repeat receptor-like kinases (LRR RLKs). The disulfated pentapeptide phytosulfokine (PSK) regulates growth and biotic interactions (Sauter, 2015). It is perceived by the LRR

RLKs PSKR1 (phytosulfokine receptor 1) and PSKR2 (phytosulfokine receptor 2). PSK has been shown to bind to the island domain of PSKR1 that intersects between LRR17 and LRR18 of the extracellular receptor domain (Matsubayashi *et al.*, 2002; Wang *et al.*, 2015) from where the signal is transmitted to the intracellular receptor kinase domain (PSKR1-KD).

Receptor kinases act via phosphorylation of downstream signaling or effector proteins. Protein kinases share

a conserved basic structure yet have unique properties such as substrate specificity and interactions with other proteins. It is essential for a receptor that the kinase can be maintained at an inactive state to prevent unwanted signaling. Hence regulation of kinase activity is a hallmark of receptor kinases.

Information on kinase activity can be derived from structural analysis. However, in some cases only the kinase core is amenable for crystal structure analysis, such that information on a regulatory role of N- or C-termini cannot be obtained (Taylor *et al.*, 2012), as is the case for the brassinosteroid receptor BRI1 (brassinosteroid insensitive 1) that was crystallized as an N-terminally truncated protein (Bojar *et al.*, 2014). BRI1 belongs to the same subgroup (subgroup X) of the LRR RLK family as PSKR1, PSKR2, and PSYR1 (plant peptide-containing sulfated tyrosine 1 receptor) (Shiu and Bleecker, 2001; Matsubayashi *et al.*, 2006; Amano *et al.*, 2007). For PSKR1, the extracellular LRR region with the ligand-binding

island domain, but not the intracellular receptor part, has been structurally characterized to date (Wang *et al.*, 2015).

The intracellular PSKR1-KD is structured into a juxtamembrane (JM) domain, the kinase proper with its 12 conserved subdomains, and a short C-terminus (CT) (Fig. 1) (Hartmann *et al.*, 2015). The general features of protein kinases are readily recognized in PSKR1. In general, protein kinases consist of a small N-terminal lobe (up to amino acid I806 in PSKR1) that consists mainly of β -sheets and a larger C-terminal lobe (starting with M810 in PSKR1) predominantly made up of hydrophobic α -helices (Kornev and Taylor, 2015). Sandwiched between the N- and C-lobes is the ATP binding site next to a cleft that accommodates the substrate (Taylor and Kornev, 2011).

PSKR1 belongs to the RD kinases in which the catalytic aspartate (D) in the catalytic loop in subdomain VIIb is preceded by an arginine (R) (Nolen *et al.*, 2004). In RD kinases, access to the substrate binding site is controlled by

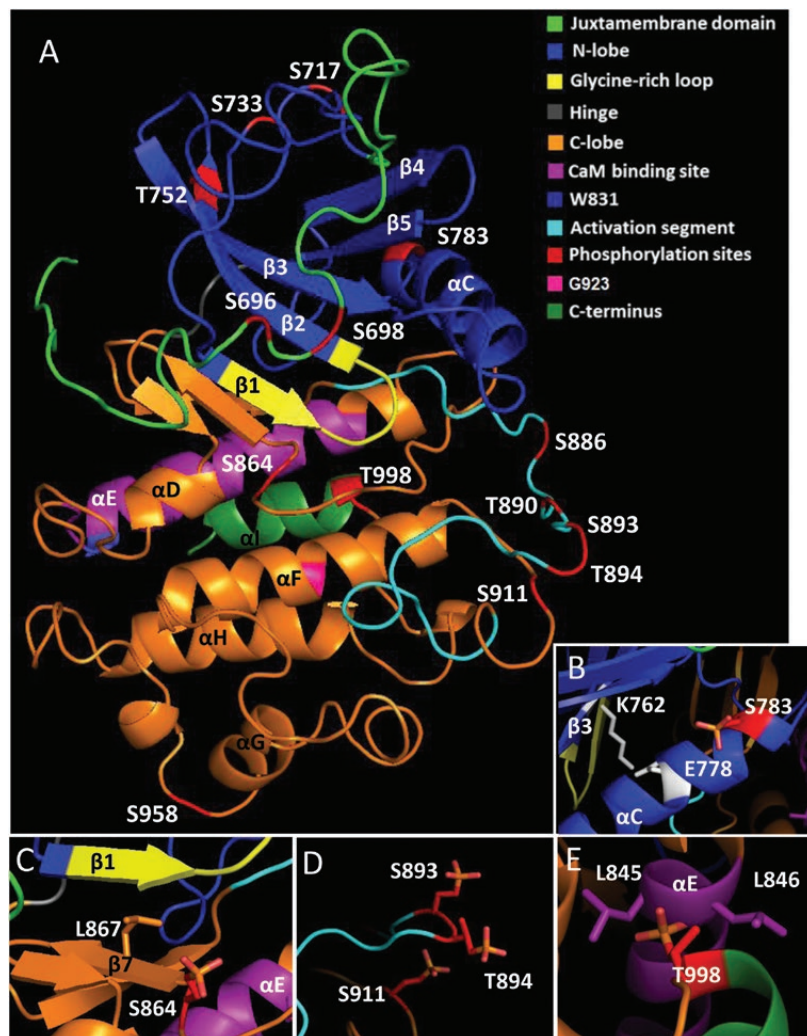


Fig. 1. Homology model of PSKR1. (A) The structure of PSKR1-KD was modeled with Phyre2 and visualized with PyMOL version 1.2. The phosphorylation sites identified by Hartmann *et al.* (2015) are highlighted in red. (B) α C harbors the phosphosite S783 and the salt bridge-forming E778. (C) The ATP binding cleft is located between the Gly-rich loop and β 7. (D) The side-chain of S911 points to the activation segment and is in close proximity to the phosphates of S893 and T894. (E) Phosphorylation of T998 interferes with α E that harbors the CaM binding site. Two leucine residues adjacent to the T998 phosphate may contribute to steric obstruction.

the activation loop (AL) (Johnson *et al.*, 1996) (Fig. 1; for a rotating homology model of PSKR1-KD see Supplementary Video S1 available at JXB online). Most RD kinases are activated via phosphorylation of their AL, as also shown recently for PSKR1 (Hartmann *et al.*, 2015). For visualization of single amino acid side-chains and phospho groups of PSKR1-KD see Supplementary Fig. S1. Phosphorylation of the AL is a conserved mode of receptor kinase regulation that results in more efficient binding of substrate and/or phosphotransfer and hence in increased kinase activity (Adams, 2003). PSKR1 homo-oligomerizes *in situ* (Ladwig *et al.*, 2015) and was shown to autophosphorylate *in vitro*, indicating a self-regulatory activation mechanism (Hartmann *et al.*, 2015). The AL of PSKR1 harbors several phosphosites. Phosphomimetic and phosphoablative site-directed point mutations of these sites showed that *in vitro* activity of the PSKR1 kinase and *in planta* activity of the PSKR1 receptor are controlled at the level of AL phosphorylation (Hartmann *et al.*, 2015).

In addition, PSKR1 is phosphorylated at sites other than the AL. Phosphosites are present both in the N-lobe and the C-lobe of the kinase, and outside of the kinase proper in the JM region and at the CT (Hartmann *et al.*, 2015) (Fig. 1A and Supplementary Fig. S2). These sites have not been characterized previously. The JM domain, CT, and the C-terminal half of the C lobe with the α G α H α I helices lie outside the catalytic kinase core. They are not directly involved in substrate phosphorylation and may mediate non-catalytic functions that nonetheless influence kinase or receptor activity, such as tethering of substrates or receptor–protein interactions (Kung and Jura, 2016). To gain better insight into the regulation of PSKR1 at the level of protein modification, we analyzed the contribution of these phosphosites with respect to the regulation of kinase and receptor activity.

A known non-catalytic function of PSKR1 is its binding to the calcium sensor calmodulin (CaM) (Hartmann *et al.*, 2014). In *Arabidopsis thaliana*, all four isoforms of CaM interact with PSKR1 via an amphipathic α -helix in subdomain VIa (Fig. 1A and Supplementary Fig. S2). Mutation of a conserved tryptophane (W831) to a serine within this α -helix impairs CaM binding and PSKR1 activity *in planta*, indicating that W831 is an essential amino acid. In this study, we set out to elucidate a possible link between PSKR1-KD phosphorylation and the PSKR1-KD/CaM interaction.

Materials and methods

Plant materials and transformation

Plants of *Arabidopsis thaliana* (L.) Heynh., ecotype Columbia-0, were grown in 2:1 potting soil/sand mixture. To avoid contamination with insect larvae, the mixture was frozen at -80°C for 2 d. For root growth measurements, seeds were sterilized in 2% (v/v) NaOCl solution for 15 min, washed five times with autoclaved water, and laid out on half-concentrated modified Murashige-Skoog medium (Duchefa) and 1.5% (w/v) sucrose, solidified with 0.4% (w/v) Gelrite (Duchefa) in square plates. Plates were placed for 2 d at 4°C in the dark for stratification. Seedlings were grown under long-day conditions (16 h, $70\ \mu\text{M}$ photons $\text{m}^{-2}\ \text{s}^{-1}$) at 22°C .

For plant transformation, the *pskr1-3 pskr2-1* (abbreviated as *r1 r2*) double knock-out mutant was used as background. The *r1 r2* line

has been described previously (Stührwohldt *et al.*, 2011; Hartmann *et al.*, 2013). Plants were transformed with *Agrobacterium tumefaciens* GV3101 using a modified floral dip method (Clough and Bent, 1998). The *Agrobacterium* was applied twice in droplets to floral organs with 1 week in between treatments. Homozygous transgenic plants were selected by spraying with $200\ \mu\text{M}$ glufosinate ammonium (Basta, AgrEvo).

Transgene expression was verified by reverse-transcription polymerase chain reaction (RT-PCR). As a control, *ACTIN2* (*ACT2*) expression was analyzed with the forward primer 5'-CAAAGACCAGCTCTCCATCG-3' and the reverse primer 5'-AGGTCCAGGAATCGTTCACAG-3', resulting in a 427-bp fragment. Primers used to amplify *PSKR1* transcripts were 5'-GTTTCGGAGTTGTGCTTCTCGAG-3' and 5'-CAAAGAGACTAACTGTTGAGTCGTTG-3', with a product size of 251 bp. In short, 1 μg of RNA was reverse-transcribed in 20 μl , of which 1 μl was used for the amplification of *ACTIN2* cDNA and 2 μl for the amplification of *PSKR1* cDNA.

Projected rosette area was determined by the rosette tracker plugin (De Vyllder, 2012) for Fiji/ImageJ open-source software (<https://imagej.net/Fiji>) using photographs of 4-week-old plants. Plants were photographed using an SMZ18 binocular microscope (Nikon). Root lengths were determined with the software NIS Elements 4.4.0 (Nikon). Plant height of 6-week-old plants was measured with a ruler.

Point mutation of PSKR1, heterologous protein expression, protein purification, and kinase assay

To introduce point mutations in *PSKR1*, an overlap extension PCR (Higuchi *et al.*, 1988) was carried out with site-specific oligonucleotides (Supplementary Table S1). For the cytoplasmic kinase domain (KD), the PCR product was ligated into pETDuet-1 (Merck) using the restriction sites *SalI* and *AvrII*, which results in an N-terminally His-tagged PSKR1 cytoplasmic domain (H_6 -PSKR1-KD). The resulting vector was transformed into *Escherichia coli* BL21 (DE3) pLys. The heterologous expression of recombinant proteins was performed in lysogeny broth (LB) Luria/Miller liquid medium with $100\ \mu\text{g}\ \text{ml}^{-1}$ ampicillin after induction with 1 mM isopropyl- β -D-thiogalactopyranoside (IPTG) for 16 h at 20°C . Cells were harvested, resuspended in extraction buffer (50 mM sodium phosphate, pH 8.0, 300 mM NaCl), incubated with $1\ \text{mg}\ \text{ml}^{-1}$ lysozyme for 20 min on ice, disrupted in a French Press (SIM-AMINCO, Spectronic Instruments), and sonicated three times for 10 s with a SONIFIER® B-12 Cell Disruptor (Branson Sonic Power Company). Crude extract was centrifuged for 30 min at $14\ 000\ g$ at 4°C . H_6 -PSKR1-KD was purified with 50 μl Talon resin in a Pierce® Spin Column (Thermo Scientific) at native conditions. To that end, the supernatant was incubated with Talon resin in a rotator for 1 h at room temperature (RT). The resin was washed three times with washing buffer (50 mM sodium phosphate, pH 8.0, 300 mM NaCl, 5 mM imidazole). Affinity-purified proteins were eluted with 50 μl of elution buffer (50 mM sodium phosphate, pH 8.0, 300 mM NaCl, 150 mM imidazole) for 5 min at RT. The protein concentration was determined by measuring the absorbance at 280 nm with a NanoDrop 2000 (Thermo Scientific). The *in vitro* kinase activities were determined in 50 mM HEPES (pH 7.4), 1 mM DTT, 10 mM MgCl_2 , 10 mM MnCl_2 , 0.2 mM unlabelled ATP, 20 μCi of [γ - ^{32}P] ATP, 0.25 μg of affinity-purified H_6 -PSKR1-KD, and 0.5 μg of myelin basic protein (MBP) as a universal substrate for 1 h at 25°C . Reactions were stopped by adding SDS loading buffer. Proteins were separated on a 15% polyacrylamide gel by SDS-PAGE and stained with Coomassie Brilliant Blue. Gels were subsequently dried and exposed to an X-ray film. The kinase and MBP bands were excised from the dried gels, mixed with scintillation liquid (Ultima Gold, PerkinElmer), and the radioactivity was determined (Tri-Carb 2910 TR instrument, PerkinElmer) in counts per minute (cpm). The background signal of the gel was subtracted and activities were calculated as $\text{cpm}\ \text{ng}^{-1}$ kinase protein for autophosphorylation and in $\text{cpm}\ \text{ng}^{-1}$ MBP for transphosphorylation activity.

To clone full-length receptor variants (FL), the Gateway™ cloning system (Life Technologies) was used. The respective point-mutated PSKR1 sequence was ligated into a modified pENTR™ 1A Dual Selection vector (Thermo Fisher Scientific) using the restricting sites *SalI* and *NotI*, which results in a PSKR1-GFP fusion protein. The fusion construct was transferred to the overexpression vector pB7WG2.0 (Karimi *et al.*, 2002) with an LR reaction to drive *PSKR1-GFP* expression under the control of the 35S Cauliflower Mosaic Virus (CaMV) promoter.

Cloning and expression of MaBP-FLAG-CaM2

The open reading frame of At2g41110 (*CaM2*) was amplified with the oligonucleotides 5'-TTTAAACCATGGCGGATCAGCTCACAGAC-3' containing an *NcoI* site and 5'-AAATTTGATATCTCACTTATCATCATCCTTATAATCGACATCAAGCTTAGCCATCATAACCTTCACAAAC-3' with an *EcoRV* site added. After restriction enzyme digestion, the product was ligated into the pMAL™-c5X vector (New England Biolabs, NEB) resulting in a *MaBP*-(maltose binding protein)-*FLAG-CaM2* fusion construct. Proper amplification was verified by sequencing prior to transformation into *E. coli* BL21(DE3) cells. Cells were grown in 30 ml LB medium, supplemented with 0.2% (w/v) glucose and 100 µg ml⁻¹ ampicillin. After induction of protein expression with 0.3 mM IPTG, cells were incubated for 2 h at 37 °C, harvested, resuspended in 4 ml extraction buffer (20 mM Tris/HCl, pH 7.5, 200 mM NaCl), disrupted in a French Press, and sonicated three times for 10 s with a SONIFIER® B-12 Cell Disruptor. After centrifugation for 30 min at 21 000 g and 4 °C, the supernatant was collected and frozen at -80 °C until use.

Pull-down assay

Equivalent amounts of H₆-PSKR1-KD and H₆-PSKR1-KD(W831S) crude extract were incubated with 20 µl MaBP-FLAG-CaM2 crude extract in 20mM Tris-HCl, pH 7.5, 200mM NaCl supplemented with 100 µM CaCl₂ or 100 µM MgCl₂ as indicated. For the analysis of autophosphorylated H₆-PSKR1-KD, cells were grown and purified as described but buffers were adjusted to pH 7.0. Eluted protein was treated with a Roti-Spin Mini-10 MWCO(KD) to adjust conditions to 50 mM HEPES/KOH, pH 7.5. Protein concentration was set to 10 µg µl⁻¹. To allow for autophosphorylation, 100 µg of purified H₆-PSKR1-KD were incubated for 1 h at 25 °C in 50 mM HEPES-KOH, pH7.5, 10 mM MnCl₂, 1 mM DTT, and 0.2 mM ATP in a total volume of 250 µl. Prior to the pull-down with MaBP-FLAG-CaM2, autophosphorylated PSKR1-KD was dialyzed to 20 mM Tris, 200 mM NaCl at pH7.5.

Interaction between H₆-PSKR1-KD and MaBP-FLAG-CaM2 was analyzed by incubating samples on a rotator for 30 min at RT, followed by another incubation step as mentioned above with washed 25 µl amylose resin (NEB) in a Pierce® Spin Column (Thermo Scientific). The amylose resin was centrifuged for 1 min at 400 g at RT, washed three times with 300 µl 20 mM Tris-HCl, pH 7.5, 200 mM NaCl with 100 µM CaCl₂ or 100 µM MgCl₂ or without any divalent cations, as indicated. To elute MaBP-FLAG-CaM2 with interacting PSKR1-KD, the amylose resin was mixed with 50 µl of 20 mM Tris-HCl, pH 7.5, 200 mM NaCl, 10 mM maltose for 5 min and centrifuged for 1 min at 400 g at RT. The protein complex was separated by SDS-PAGE using a 12.5% gel. Proteins were blotted onto a PVDF membrane. MaBP-FLAG-CaM2 was detected by monoclonal anti-FLAG M2 antibodies (Sigma) and H₆-PSKR1-KD or H₆-PSKR1-KD(W831S) by anti-His (6x-His Epitope Tag Antibody His.H8, Thermo Fisher) antibodies. As secondary antibody, a horseradish peroxidase conjugated anti-mouse antibodies (Life Technologies) was used and visualized through ECL Plus Western Blotting substrate (Pierce).

Homology modelling

A model of the cytoplasmic domain of PSKR1 was built with Phyre2 (Kelley *et al.*, 2015) by using the PDB templates 2QKW,

3TL8, 1OPL, 2FO0, 4XI2, and 4L68. A total of 93% of the sequence was modelled at >90% confidence and the first 22 amino acids of the juxtamembrane domain were modelled *ab initio*. The structure of the PSKR1 model was visualized by PyMOL version 1.2r1 (Schrödinger, LLC). Definition of domains, such as the N-lobe, was done based on the model of BRI1 generated by Bojar *et al.* (2014). Secondary structures were named according to Taylor and Kornev (2011). Phosphorylations at specific residues in the model were added using the PyMol plugin PyTMs by Warnecke *et al.* (2014).

Statistics

Statistical analysis of *in vitro* kinase activities was carried out with R (<https://CRAN.R-project.org/doc/FAQ/R-FAQ.html>). For all pairwise comparisons, a Kruskal–Wallis test with Bonferroni as *P*-value adjustment method ($\alpha=0,05$) was run. Plant growth data were analyzed with a Kruskal–Wallis comparison against a control group with Dunn's test as a *post hoc* test using a macro in Minitab (<http://www.minitab.com>).

Results

PSKR1 phosphosites regulate kinase activity in a site-specific manner

To evaluate the impact of a defined phosphorylation on PSKR1 kinase activity, we expressed soluble kinase variants with phosphosites replaced by an unphosphorylatable alanine on the one hand or by an aspartate or glutamate on the other hand to mimic a phosphorylated serine or threonine. The kinase variants were ectopically expressed in *E. coli*, affinity-purified via their N-terminal His-tag, and analyzed for *in vitro* kinase activity (Figs 2 and 3). Myelin basic protein (MBP) was added as a kinase substrate, allowing us to monitor autophosphorylation of the kinase and transphosphorylation of MBP at the same time. As controls, we included the wild-type kinase and the K762E isoform in each assay. The Lys (K762 in PSKR1) in the AxK motif of the β3-strand of the N-lobe forms a salt bridge with a Glu in the αC-helix (E778 in PSKR1) that engages in binding of the α- and β-phosphates of ATP (Huse and Kuriyan, 2002) (Fig. 1A, B). Mutating the conserved K to E abolishes kinase activity (Taylor and Kornev, 2011; Fig. 2). Kinase activities were visualized by autoradiography (Figs 2 and 3). In addition, autophosphorylated kinase and transphosphorylated MBP were quantified by liquid scintillation counting of incorporated ³²P (Figs 2 and 3).

S696 and S698 in the JM domain are phosphorylated *in planta* (Hartmann *et al.*, 2015). Regulation of kinase activity by phosphorylation at these sites was studied by generating six PSKR1 kinase variants that were mutated at either one of the two sites or at both phosphorylation sites (Fig. 2A). Mutating S696 to alanine reduced kinase activity whereas the S696D variant had wild-type activity (Fig. 2A, B). The S698 site showed an inverse impact. Since both S696 and S698 are phosphorylated *in planta*, we analyzed kinase isoforms with both sites mutated. Interestingly, the unphosphorylatable S696A/S698A variant had wild-type activity while the S696D/S698D variant had wild-type autophosphorylation activity but was impaired in transphosphorylation activity (Fig. 2A, B), suggesting that the JM residues S696 and

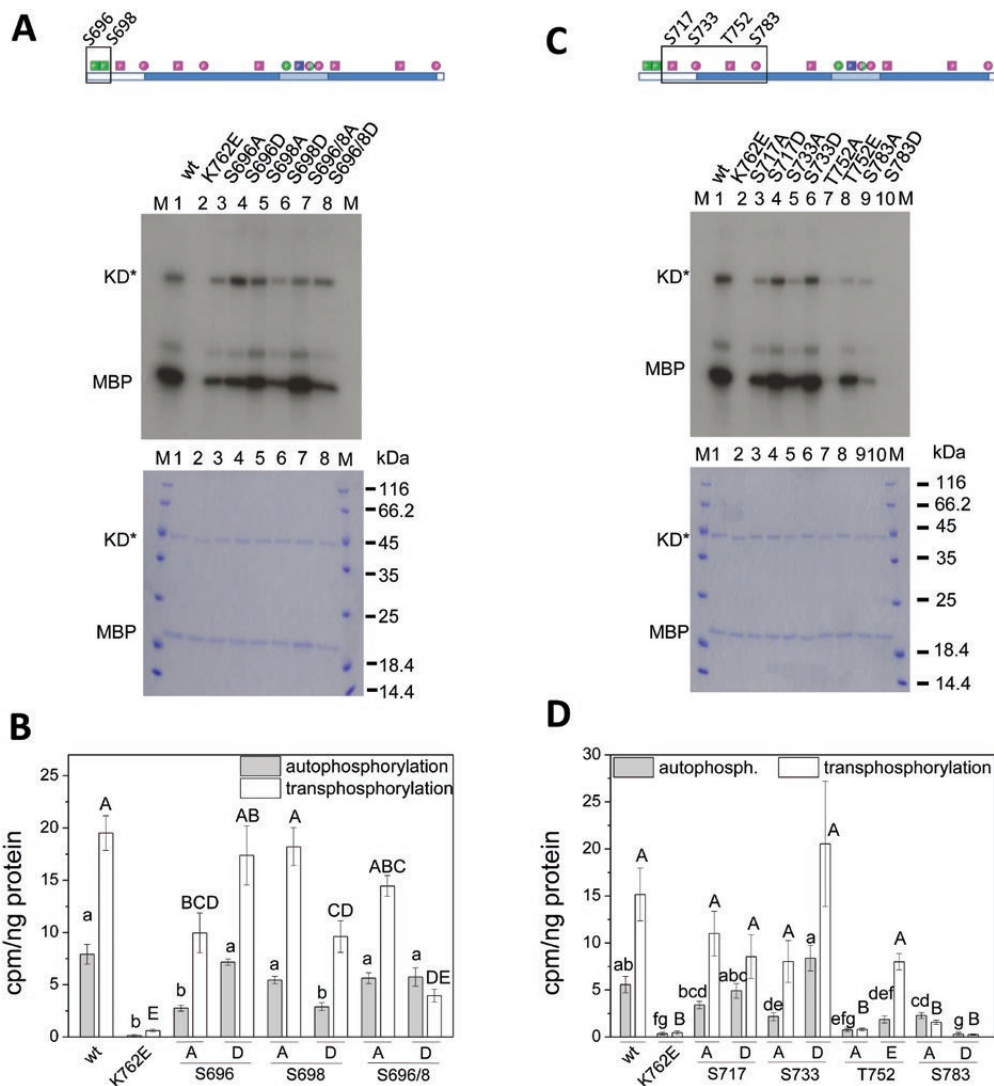


Fig. 2. Phosphosites in the JM domain and in the N-lobe differentially alter PSKR1 kinase activity. The boxed residues in the juxtamembrane domain (A) and the N-terminal lobe (C) of PSKR1-KD (shown on the top) were point-mutated to either A as phosphoablative or D as phosphomimetic mutations, and expressed as soluble PSKR1-KD (KD*) isoforms. A detailed description of the phosphosites is provided in Supplementary Fig. S2. Wild-type kinase (wt) and the inactive K762E variant were included as controls in each assay. (A, C) Kinase isoforms (0.25 μ g) were incubated with 32 P-ATP and 0.5 μ g of the substrate MBP. The autoradiograph (top) shows auto- and transphosphorylation activities. A Coomassie-stained gel (bottom) shows loading of KD* and MBP, and M indicates the size marker in kDa. (B, D) Incorporated 32 P was quantified by liquid scintillation. Auto- and transphosphorylation activities are shown as cpm ng $^{-1}$ kinase isoform or ng $^{-1}$ MBP. Results are means \pm SE from three independent experiments with two replicates each. Significantly different values are indicated by different lower case letters for autophosphorylation and with capital letters for transphosphorylation (Kruskal-Wallis, $P < 0.05$). (This figure is available in color at *JXB* online.)

S698 are involved in substrate recognition and binding or phosphotransfer to the substrate. Taken together, our data indicate that phosphorylation within the JM domain regulates PSKR1 transphosphorylation activity. By contrast, autophosphorylation activity is independent of the JM phosphorylation status.

Four phosphorylated residues were identified in the N-lobe of the PSKR1 kinase (that extends up to Y807) (Fig. 1). S717 and S733 are located within the flexible loops of the N-lobe (Fig. 1A). Mutating S717 to either A or D did not significantly alter auto- or transphosphorylation activity (Fig. 2C, D). S717 is present in PSKR1 from *Arabidopsis thaliana* but not in PSKR1 orthologs from other plants (Hartmann *et al.*, 2015) (Supplementary Fig. S2). It is hence conceivable that

this site has not acquired a detectable role in kinase regulation. S733 and T752 frame the Gly-rich loop with the GxGxxG-motif that participates in positioning of the adenine moiety and the γ P of ATP for catalysis (Kornev and Taylor, 2015). Phosphorylation of S733 favors kinase activity as the S733D variant was more active than the S733A kinase (Fig. 2C, D). T752 is located in the β 2 strand of the N-lobe (Fig. 1A), a highly conserved secondary structure of kinases. The T752A mutation abolished kinase activity, indicating that phosphorylation of this residue is crucial for receptor activation (Fig. 2C, D). Interestingly, the T752E variant was unable to autophosphorylate but did retain transphosphorylation activity.

A fourth phosphosite was identified in the ATP-binding region of the N-lobe at S783. This serine in α C is highly

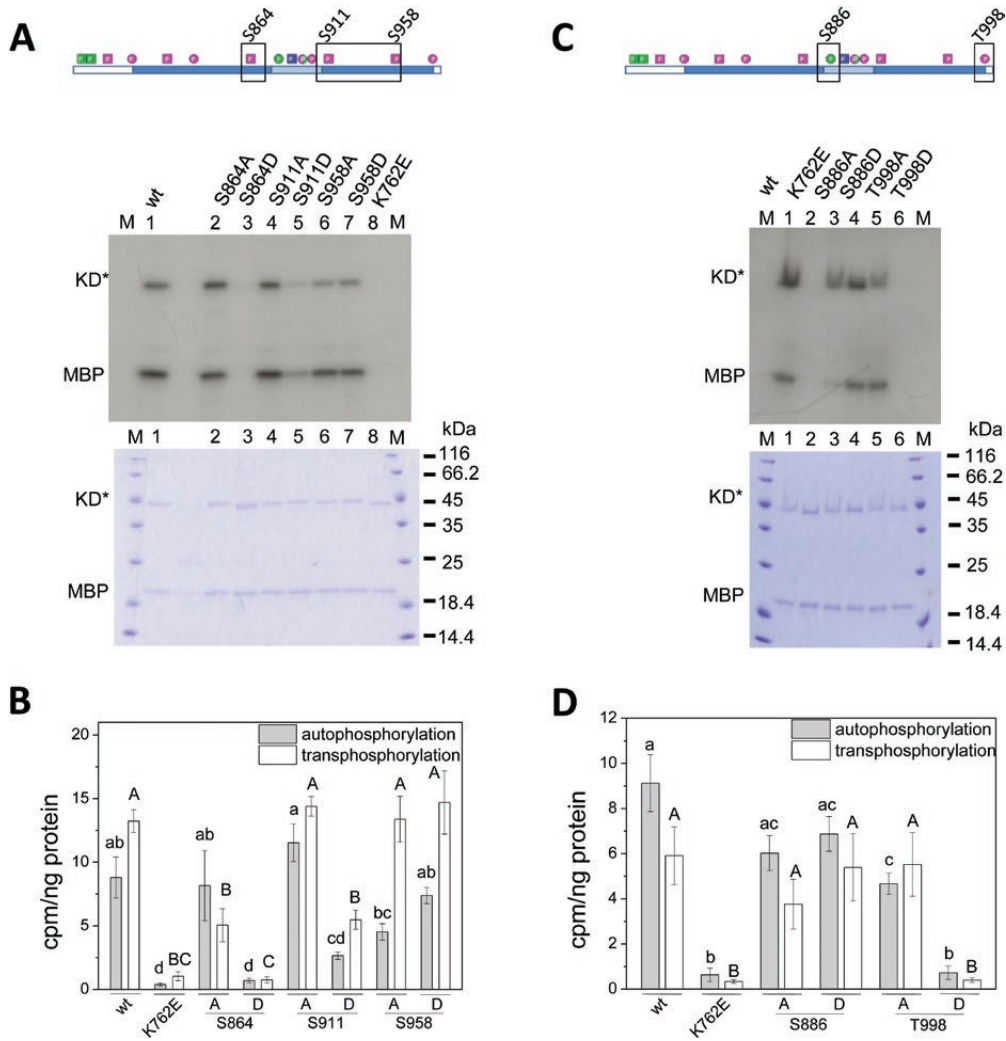


Fig. 3. Differential impact of phosphosites in the C-lobe and at the CT on PSKR1 kinase activity. The boxed residues (A, C; top) in the N-lobe of PSKR1-KD were point-mutated to either A or D, and kinase activity was compared to the wild-type and to the inactive K762E isoform. (A, C) The kinase isoforms (0.25 μ g) were incubated with 32 P-ATP and 0.5 μ g of the substrate MBP. The autoradiograph (top) shows auto- and transphosphorylation activities. A Coomassie-stained gel (bottom) shows loading of KD* and MBP, and M indicates the size marker in kDa. (B, D) 32 P incorporated in PSKR1-KD and MBP was quantified and analyzed as described in the legend for Fig.2B and 2D. Significantly different values are indicated by different lower case letters for autophosphorylation and with capital letters for transphosphorylation (Kruskal–Wallis, $P < 0.05$; B, $n = 6$; D, $n = 8$). (This figure is available in color at JXB online.)

conserved in higher plant PSKR1 orthologs (Hartmann *et al.*, 2015) (Supplementary Fig. S2). The charged residues corresponding to K762 and E778 in PSKR1 form a salt bridge that is a hallmark of an active kinase. A negative charge at S783 might interfere with the ionic interaction between K762 and E778 (Fig. 1B). However, the S783A isoform also showed strongly reduced autophosphorylation and no significant transphosphorylation activity, suggesting that S783 is a phosphorylatable residue with invariable structural characteristics.

In the C-lobe, seven phosphorylation sites were identified, of which four sites within the activation segment were characterized previously (Hartmann *et al.*, 2015). Of the three as yet uncharacterized sites, S864 is located within the catalytic loop in subdomain VIb that is N-terminal to the activation segment (Fig. 1A, C). S864 is invariant in all PSKR1 and PSKR2 orthologs (Hartmann *et al.*, 2015) (Supplementary Fig. S2), suggestive of a highly conserved function.

The phosphomimic S864D replacement abolished kinase activity, suggesting that phosphorylation of S864 is an efficient way of inactivating the receptor (Fig. 3A, B). L867 in $\beta 7$ is a functional residue of the catalytic spine and interacts with the adenine ring of ATP (Taylor and Kornev, 2011). It is conceivable that a negative charge at S864 interferes with this hydrophobic interaction (Fig. 1C). The S864A mutation did not alter autophosphorylation activity but partially impaired transphosphorylation activity, supporting a role of S864 in substrate phosphorylation.

S911 is located at the protein surface in close proximity to S893 and S894 in the activation segment (Fig. 1D). Point mutations of S911 revealed a reduced kinase activity of S911D over S911A or wild-type kinase with regard to both auto- and transphosphorylation activity, supporting the conclusion that S911 phosphorylation is a mechanism to regulate PSKR1 activity (Fig. 3A, B). By contrast, neither the S958A

nor the S958D mutation affected kinase activity significantly. S911 is highly conserved among PSKR1 orthologs whereas S958 is present only in *Arabidopsis thaliana* (Hartmann *et al.*, 2015) (Supplementary Fig. S2), arguing for a recently acquired non-functional phosphosite.

The CT of PSKR1 was found to be phosphorylated at T998 *in vitro*. This phosphosite is located in the α I helix. The T998 side-chain points to the highly conserved α E helix that harbors the CaM binding site (Fig. 1A, E). Two aliphatic leucine residues (L845 and L846) in the α E helix flank the polar T998 side-chain (Fig. 1E). Introduction of a negative charge at this site by a T998D substitution rendered the kinase completely inactive while the unphosphorylatable T998A isoform had wild-type activity. This result was confirmed in the T998E isoform where the threonine at position 998 was replaced by a glutamic acid that is more similar in size to threonine (Supplementary Fig. S3). These results demonstrated that phosphorylation of the C-terminus acts as an on/off switch for PSKR1 kinase activity.

Phosphosite mutagenesis of PSKR1 reveals organ-specific receptor regulation in planta

To study the biological function of phosphosites within the JM and CT domains we expressed mutated full-length receptor variants in the PSK receptor null background. We analyzed rosette area and plant height (Fig. 4) as well as primary root lengths of several independent lines per genotype (Figs 4 and 5). Surprisingly, the phenotypes that we observed were not consistent between root and shoot, and the kinase activities did not correlate with plant phenotypes in each case. Expression of *35S:PSKR1-GFP* in the null background was shown previously to rescue growth of both root and shoot. In both studies, transcript levels were lower than in the wild-type (Hartmann *et al.*, 2014) (Supplementary Fig. S5).

Specifically, roots expressing the PSKR1(S696A/S698A) receptor under the control of the 35S Cauliflower Mosaic Virus promoter showed an overexpression phenotype with longer roots than in the wild-type (Fig. 5A) whereas plant height and rosette areas were comparable to the wild-type (Figs 4A, B and 5B, C). These results are in agreement with wild-type kinase activity *in vitro* of the respective kinase

isoform and suggest that receptor activity is limiting in roots but not in shoots. The PSKR1(S696D/S698D) receptor isoform resulted in an overexpression phenotype in the roots (Fig. 5A) but not in the shoot where growth was reduced compared to the wild-type (Fig. 5B, C). The phosphomimic S696D/S698D kinase isoform has reduced transphosphorylation activity. Our data hence suggest that transphosphorylation activity is limiting in shoots but not in roots, pointing to organ-specific or development-dependent receptor regulation *in planta*.

The T998D as well as the T998E variants were kinase-inactive *in vitro*, indicating that phosphorylation at T998 within the CT inhibits PSKR1 kinase activity (Fig. 3C, D, Supplementary Fig. S3). *In planta*, roots of PSKR1(T998E) seedlings had wild-type length in three of four independent lines but were on average shorter than PSKR1(T998A) roots (Fig. 5A). Hence, unlike T998E kinase activity *in vitro*, PSKR1(T998E) receptor activity *in planta* was not abolished, pointing to receptor regulation beyond phosphorylation *in situ*. In contrast to roots, shoot growth of PSKR1(T998A) plants was reduced in three of four lines. PSKR1(T998E) plants had an intermediary shoot phenotype compared to the wild-type and compared to PSK receptor null plants, again indicating that this phosphorylatable threonine residue plays a different role in roots and shoots. While in roots the phosphorylation status alters receptor activity, this was not observed in the shoot. This suggests that T998 rather than its phosphorylation status is required.

In summary, *in vitro* kinase activities and *in planta* receptor activities do not correlate for each isoform analyzed, indicating additional levels of receptor regulation. Furthermore, the activity of particular receptor isoforms differs in the roots and shoot, suggesting that organ-specific or development-dependent factors influence receptor signaling. PSKR1 can hence be modified at levels other than, and possibly independent of, specific phosphorylation events.

Regulation of PSKR1 kinase by calmodulin

The kinase domains of many receptor kinases including PSKR1 are folded in their active state *in vitro*, which is in fact the basis for any *in vitro* kinase assay. If a kinase can

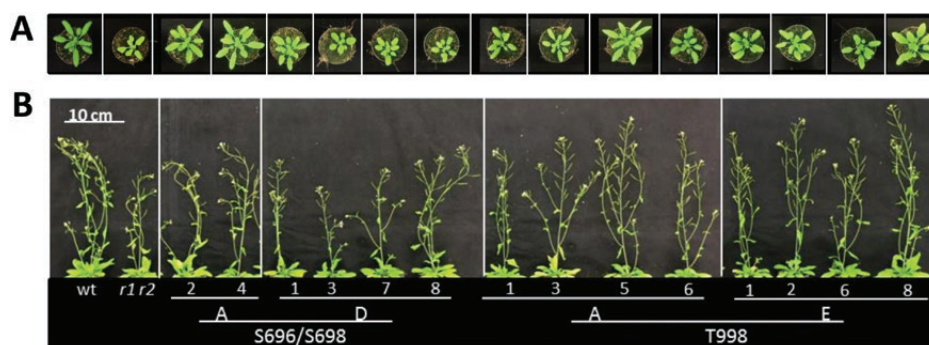


Fig. 4. Phosphorylation in the JM domain and at the CT impair shoot growth. The full-length PSKR1 receptor was mutated as indicated and introduced into the *pskr1-3 pskr2-1* receptor null background. Plants were grown on soil for (A) 4 weeks to measure rosette areas, and (B) for 6 weeks to measure plant height. The numbers indicate independently transformed lines. (This figure is available in color at JXB online.)

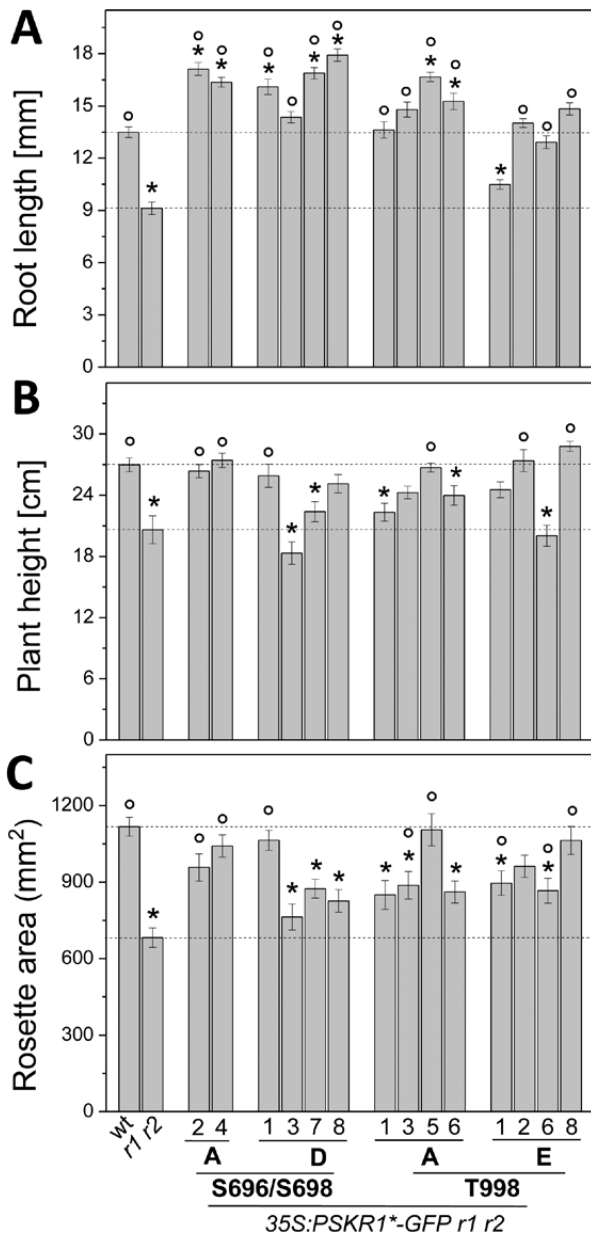


Fig. 5. Phosphorylations at the JM domain and CT differentially affect PSKR1 receptor activity in roots and shoots. Full-length PSKR1 receptor isoforms as indicated were expressed in the *pskr1-3 pskr2-1* receptor null background, with different numbers indicating independent lines. (A) Length of main root of 5-d-old seedlings grown under sterile conditions ($n=35-94$). (B) Plant height of 6-week-old soil-grown plants ($n=18-27$). (C) Projected rosette area of 4-week-old soil-grown plants ($n=19-27$). Values are means from three independent biological experiments. Significant differences compared to the wild-type (wt) are indicated by * and significant differences compared to *pskr1-3 pskr2-1* (*r1 r2*) are indicated by ° (Kruskal-Wallis with Dunn's test as *post-hoc*; $P<0.05$).

auto-activate itself not only *in vitro* but also *in planta* then mechanisms are needed to keep the kinase in check. The calcium sensor calmodulin (CaM), which has been shown previously to interact with PSKR1 (Hartmann *et al.*, 2014), might have such a regulatory function. Mutation of a conserved hydrophobic tryptophane to a hydrophilic serine (W831S) in the predicted CaM binding αE helix (Figs 1A

and 6A) abolishes CaM binding and PSKR1 receptor activity (Hartmann *et al.*, 2014). To understand the role of CaM binding for PSKR1 kinase activity we analyzed the soluble PSKR1(W831S) kinase isoform. As controls we included wild-type kinase, the inactive K762E isoform, and two kinase isoforms that were mutated at G923 within the predicted guanylyl cyclase center in αF of PSKR1 (Fig. 1A) (Kwezi *et al.*, 2011) to either a lysine (G923K) or a glutamate (G923E). The W831S point mutation abolished both auto- and transphosphorylation activity *in vitro*. This is unexpected as kinase activity was measured in the absence of CaM. It suggests that W831 is essential for kinase activity independent of CaM binding, possibly for structural reasons (Fig. 6B, C). A similar loss of activity was observed for the G923K and G923E isoforms, supporting the view that G923 is an essential amino acid irrespective of its proposed role in cGMP formation.

We next studied the impact of calcium on binding of CaM2 to PSKR1-KD using pull-down assays. CaM2/PSKR1-KD binding was stronger in the presence of Ca^{2+} than with Mg^{2+} , supporting specificity of this interaction (Fig. 7A). No interaction occurred between CaM2 and PSKR1-KD(W831S), as demonstrated previously by Bimolecular Fluorescence Complementation (Hartmann *et al.*, 2014). We next studied whether binding of CaM was influenced by phosphorylation of PSKR1-KD. Ectopically expressed PSKR1-KD is likely to be partially phosphorylated in *E. coli*, as suggested by a shift in mobility after dephosphorylation (Supplementary Fig. S4). Incubation of hypophosphorylated PSKR1-KD with ATP resulted in autophosphorylation whereas without ATP PSKR1-KD remained in its hypophosphorylated state. Subsequently, binding to CaM2 was analyzed in the absence or presence of calcium. The strongest interaction was observed between Ca^{2+} -CaM2 and hypophosphorylated PSKR1-KD (Fig. 7B) while autophosphorylation prevented binding of Ca^{2+} -CaM. In summary, the interaction of CaM2 and PSKR1 is Ca^{2+} -dependent and Ca^{2+} -CaM binds preferentially to hypophosphorylated PSKR1.

PSKR1 kinase activity is not regulated by Ca^{2+} -CaM2

To study a possible role of calmodulin in regulating PSKR1 kinase activity, we compared kinase activity of PSKR1 when pre-incubated with Ca^{2+} , CaM2, or Ca^{2+} -CaM (Fig. 8). Pre-incubation was performed under the same conditions that were used for pull-down assays (Fig. 7). Kinase activity was measured in the presence or absence of the substrate myelin basic protein (MBP) as documented in autoradiographs (Fig. 8A) and quantified by liquid scintillation counting (Fig. 8B). Unexpectedly, autophosphorylation activity was somewhat higher in the presence of MBP, possibly indicating structural rearrangements following occupation of the substrate binding site that favor autophosphorylation. Ca^{2+} -CaM2 did not significantly alter kinase activity. Our analysis further revealed that CaM2 itself is not phosphorylated by PSKR1 (Fig. 8A).

Taken together, CaM2 binds to hypophosphorylated PSKR1 in a calcium-dependent manner. Ca^{2+} -CaM2, however, does not regulate kinase activity of PSKR1-KD *in vitro*.

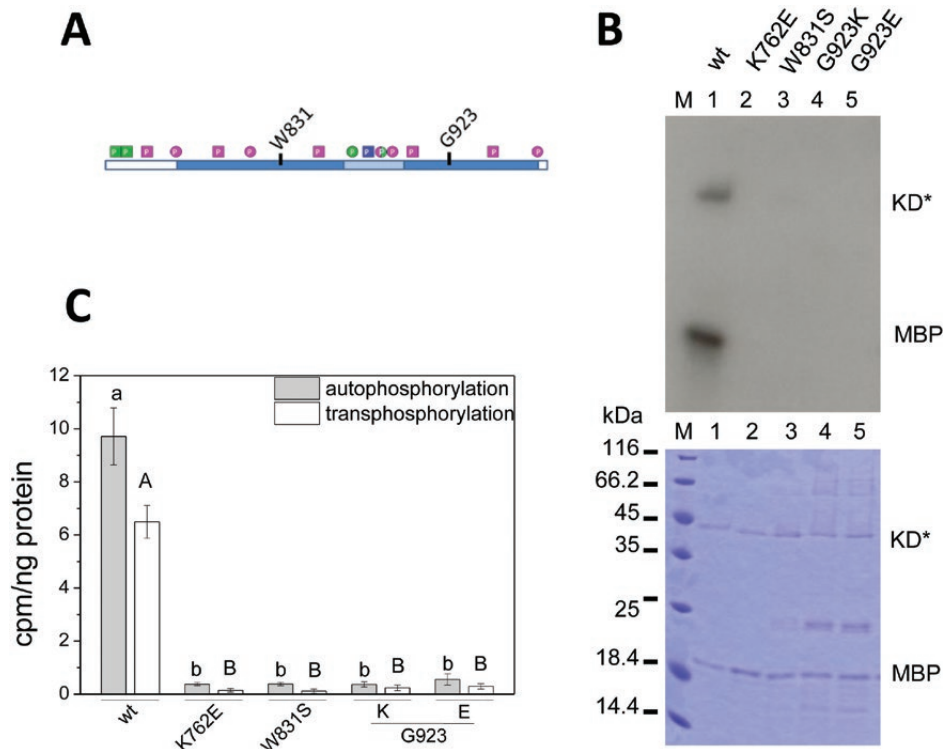


Fig. 6. Mutation of the calmodulin binding site abolishes PSKR1 kinase activity. A conserved tryptophan (W831) in the calmodulin binding site of PSKR1-KD was mutated to a serine. Included as controls were the wild-type (wt), the inactive K762E, and two isoforms in which G923 within the predicted guanylyl cyclase center was mutated to lysine or glutamate. (A) Schematic drawing of PSKR1-KD highlighting the point mutations analyzed. (B) The kinase isoforms (0.25 μ g) were incubated with 32 P-ATP and 0.5 μ g of the substrate MBP. The autoradiograph (top) visualizes auto- and transphosphorylation activities of the isoforms (KD*). The Coomassie-stained gel (bottom) shows protein loading. M indicates the size marker in kDa. (C) Incorporated 32 P was quantified by liquid scintillation. Auto- and transphosphorylation activities are shown as cpm ng $^{-1}$ kinase isoform or ng $^{-1}$ MBP. Results are means \pm SE from three independent experiments with two replicates each. Significantly different values (Kruskal–Wallis, $P < 0.05$) are indicated by different lower case letters for autophosphorylation and capital letters for transphosphorylation. (This figure is available in color at JXB online.)

Discussion

The peptide receptor PSKR1 is a highly phosphorylatable receptor kinase with phosphosites present within the kinase proper as well as in the JM and CT domains. Fourteen phosphosites were identified by our group (Hartmann *et al.*, 2015), of which six, S696, S698, S864, S886, S893, and T998, were confirmed in an independent study in which three more sites were found (Fig. 1A and Supplementary Fig. S2; Mitra *et al.*, 2015). S886, T890, S893, and S894 are located in the activation segment that includes the AL as a hallmark of RD kinases. The activation segment forms a loop across the substrate binding cleft, thereby preventing access for the substrate. Phosphorylation of activation segment residues causes a conformational change that allows substrate binding (Johnson *et al.*, 1996). Site-directed mutagenesis of single and multiple phosphosites in the activation segment of PSKR1 confirmed that this regulatory mechanism also works in PSKR1 (Hartmann *et al.*, 2015). Our observation that these phosphosites are evolutionarily highly conserved in PSKR1 orthologs supports a conserved function (summarized in Supplementary Fig. S2).

The multiple phosphosites outside of the activation segment are indicative of additional regulatory mechanisms that may target not only kinase activity. Receptor protein kinases are optimized to transmit a signal rather than for catalytic

activity. Their task is to activate downstream effectors, initiate and terminate a signal or integrate multiple signals. Differential phosphorylation of receptor kinases may hence determine substrate specificity and interactions with other proteins that serve cross-talk with other signaling pathways, as well as degradation or internalization of the receptor to terminate a signal. Analysis of *in vitro* and *in vivo* activity of PSKR1 phosphosite isoforms is a useful first step to unravel such functions.

Phosphosites in ATP binding domains are crucial for kinase activity

In PSKR1, S733 and T752 flank the glycine (G)-rich loop near the ATP binding region. The phosphomimic substitution S733D resulted in enhanced kinase activity over the S733A variant. The T752E variant was likewise more active than the unphosphorylatable T752A isoform, whereas autophosphorylation ability was impaired even in the phosphomimic isoform. In the related LRR receptor kinase BRI1 an S891D mutation within the G-rich loop resulted in severe dwarfism (Oh *et al.*, 2012), indicative of receptor inactivation. The S891A mutation of BRI1 caused hyperactivity of BRI1, resulting in seedling growth promotion. The authors concluded that S891 phosphorylation is a reversible means to deactivate BRI1. The finding that unphosphorylatable S733

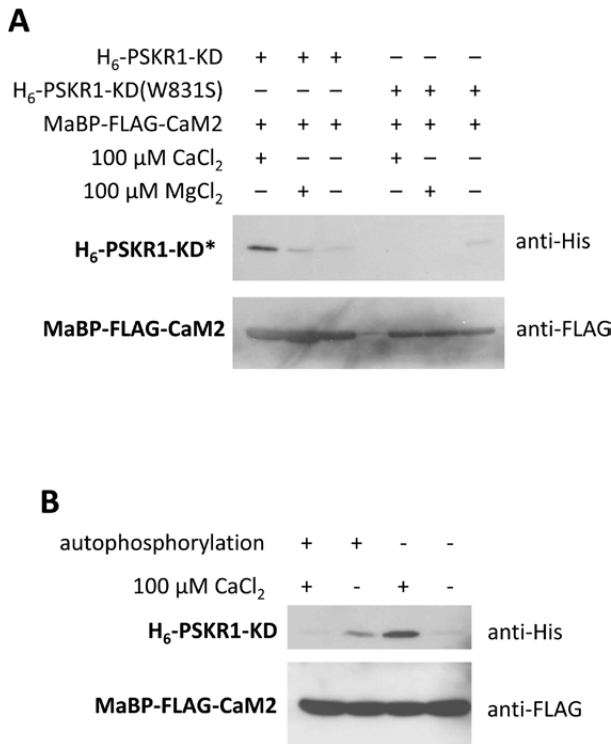


Fig. 7. Binding of CaM2 to PSKR1-KD is Ca²⁺-dependent and determined by the phosphorylation state of PSKR1-KD. (A) Western blots with His-tagged (H₆) PSKR1-KD (H₆-PSKR1-KD) or H₆-PSKR1-KD(W831S) that was bound by maltose binding protein (MaBP)-tagged and FLAG-tagged CaM2 (MaBP-FLAG-CaM2) in the presence of 100 μM CaCl₂ or 100 μM MgCl₂ or without divalent cation. (B) H₆-PSKR1-KD was incubated with ATP to allow for autophosphorylation or left unphosphorylated prior to pull-down with MBP-FLAG-CaM2 in the presence or absence of 100 μM Ca²⁺. Blots are shown in greyscale and were uniformly adjusted in contrast (-20%) and brightness (+40%). Results were confirmed in independent experiments.

and T752 reduced kinase activity suggests that the G-rich loop may be a target for receptor kinase regulation in general, with different modes acting in different receptor kinases.

A conserved Glu (E778 in PSKR1) in αC interacts with a conserved Lys (K762 in PSKR1) in β3 at the ATP binding site (Fig. 1B) (Huse and Kuriyan, 2002). When the activation segment is in its dephosphorylated state the E-K ion pair is disrupted, resulting in impaired ATP binding and lowered rates of phosphotransfer to the substrate (Huse and Kuriyan, 2002; Adams 2003). The phosphosite S783 is in αC, which is known as a dynamic regulatory element. Its position is crucial for efficient catalysis (Taylor and Kornev, 2011). S783 is a nearly invariant amino acid in PSKR1 orthologs that is close to the E-K pair (Supplementary Fig. S2) (Hartmann *et al.*, 2015). A charge at this Ser may disrupt the salt bridge, as suggested by the inactive kinase isoform S783D. However, the S783A also had strongly reduced kinase activity, arguing for an invariant residue the phosphorylation of which may act as an on/off switch.

S864 within the catalytic loop in subdomain VIb C-terminal to the RD motif (R859/D860) is an invariant amino acid in PSKR1 orthologs (Supplementary Fig. S2). The S864A

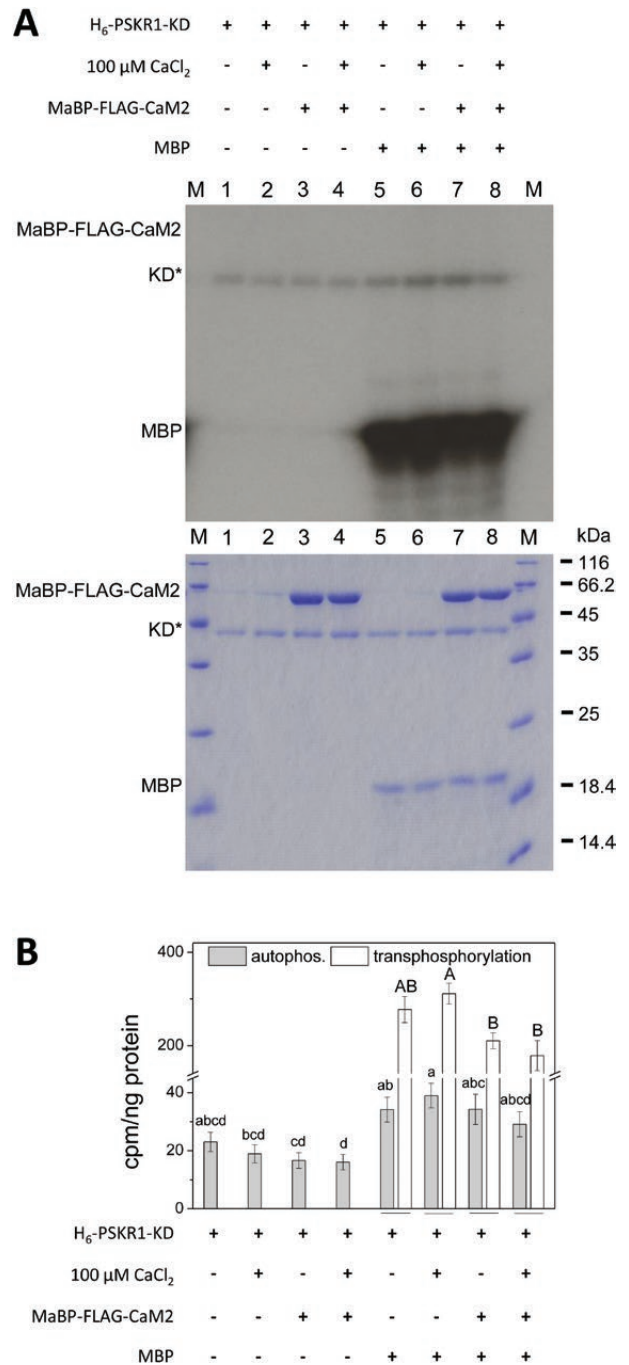


Fig. 8. PSKR1 kinase activity is not altered by binding of Ca²⁺-CaM2. (A) PSKR1-KD (0.25 μg) was incubated with MaBP-FLAG-CaM2 (1.5 μg) in the presence of 100 μM Ca²⁺ or without calcium to allow for Ca²⁺-CaM/PSKR1-KD binding, followed by a kinase assay with ³²P-ATP and 0.5 μg of the substrate MBP. The autoradiograph (top) visualizes auto- and transphosphorylation activities. The Coomassie-stained gel (bottom) shows PSKR1-KD, MaBP-FLAG-CaM2, and MBP; M indicates the size marker in kDa. (B) Incorporated ³²P was quantified by liquid scintillation. Auto- and transphosphorylation activities are shown as cpm ng⁻¹ kinase isoform or ng⁻¹ MBP. Results are means ±SE of three independent biological experiments with two technical replicates each. Significantly different values are indicated by different lower case letters for autophosphorylation and with capital letters for transphosphorylation (Kruskal-Wallis, *P*<0.05). (This figure is available in color at JXB online.)

isoform had wild-type autophosphorylation activity and reduced transphosphorylation activity. The S864D isoform was kinase-inactive, possibly indicating a role for S864 phosphorylation in regulating the catalytic cycle. Mutation of S911 suggested attenuation of kinase activity by phosphorylation. The side-chain of S911 points in the direction of the activation segment phosphosites S893 and T894, and this possibly causes a change of activation segment orientation. A similar situation was shown for BRI1 with T1039, S1042, and S1060 (Bojar *et al.*, 2014). In contrast, mutation of S958 did not significantly affect kinase activity. The S958 phosphorylation site is unique to *Arabidopsis thaliana* (Hartmann *et al.*, 2015) and is located in a flexible loop on the protein surface. It is conceivable that this phosphosite has evolved only recently and has not acquired a function with respect to kinase activity.

PSKR1 regulation by phosphorylation at the extremes

The large number of phosphosites that were identified in the cytosolic PSKR1 receptor part point to an elaborate mode of PSKR1 regulation by reversible receptor modification. Phosphosites were found not only within the kinase proper but also in the JM (S696, S698) and CT (T998) domains, which are *per se* not required for kinase function. The 3D homology model of PSKR1-KD revealed close proximity of the JM residues S696 and S698 to the ATP binding cleft (Fig. 1A, Supplementary Fig. S1). Phosphomimic modification of both residues inhibited transphosphorylation activity *in vitro*. S696 and S698 are phosphorylated *in planta* and hence are biologically functional sites. At least one of the two sites has a Ser or Thr conserved in 83% of higher plant PSKR1 orthologs, supporting the idea that these sites confer a crucial function in PSKR1 signaling. LRR RLKs function in many diverse physiological processes. Phosphorylation of JM and CT regions is one way to overcome this functional diversity and to achieve specificity. Deletion of the BRI1 JM domain abolished the signaling function of the receptor whereas phosphorylation of the JM domain activated BRI1 (Wang *et al.*, 2005, 2008). Replacing S696/S698 in PSKR1 with the negatively charged amino acid Asp reduced transphosphorylation but not autophosphorylation activity *in vitro*, pointing to regulation of substrate binding via the JM. *In planta*, the growth-impaired phenotype of PSK receptor null plants was not, or only partially, rescued by the PSKR1(S696D/S698D) variant with regard to the shoot, indicating that shoot growth may be limited by transphosphorylation activity of PSKR1. By contrast, primary root growth was promoted by both the PSKR1(S696A/S698A) and the PSKR1(S696D/S698D) isoforms, indicating that growth-promoting activity of PSKR1 in the root is independent of JM phosphorylation. These findings are in agreement with the idea that phosphorylation at the JM domain regulates defined signal outputs that can be assigned to different organs such as roots and shoot, or to different developmental stages.

The *PSKR1* gene is differentially regulated in roots and shoot, as indicated by gene expression data summarized in the eFP browser (Winter *et al.*, 2007). Expression is induced

by cold and salt stress (150 mM NaCl) in the roots but not the shoot, whereas expression increases in the shoot but not in the roots in response to osmotic stress (300 mM mannitol) (Kilian *et al.*, 2007), supporting the idea that PSKR1 activity is differentially regulated in roots and shoots in response to environmental signals. Differential phosphorylation of PSKR1 in roots and shoots may be yet another level of regulating the intensity or quality of the signal output. Different effects of distinct phosphosite mutations in roots and shoots seem plausible in light of the functional diversity of PSKR1 signaling.

While the JM seems to control the signal output by influencing substrate recognition, binding, or phosphotransfer, the CT acts as an on/off switch for kinase activity *in vitro*, with loss of activity in the T998D and T998E isoforms. A similar auto-inhibitory mechanism was observed in other receptor kinases. Deletion of the BRI1 CT domain was reported to increase kinase activity of BRI1 *in vitro* and *in planta* (Wang *et al.*, 2005), suggesting a conserved role in kinase regulation. Interestingly, plants expressing the PSKR1(T998E) isoform had reduced shoot growth but wild-type root lengths. These phenotypes are compatible with a PSKR1 receptor that is inactive in the shoot due to phosphorylations of S696/S698 at the JM domain and cannot be further inactivated via CT phosphorylation while the phosphorylation status of PSKR1 in the root may be different, allowing for inhibition by CT phosphorylation *in planta*.

Binding of CaM to PSKR1 is calcium-dependent and occurs preferentially to hypophosphorylated PSKR1

Aside from acting as kinases, receptor kinases can have non-catalytic functions such as scaffolding activity (Kung and Jura, 2016). PSKR1 was shown to interact with the co-receptor BAK1, with the proton pumps AHA1 and AHA2 (*Arabidopsis* H⁺-ATPase1 and 2) (Ladwig *et al.*, 2015), and with calmodulins (CaM) (Hartmann *et al.*, 2014). BAK1 and AHAs in turn interact with the cation channel CNGC17 (cyclic nucleotide-gated channel 17), establishing a physical link between cell wall acidification and cation uptake (Ladwig *et al.*, 2015). CNGC17 is likely to permeate mono- and divalent cations including Ca²⁺. It is hence possible that PSKR1 activity brings about a rise in intracellular calcium levels that will result in the activation of CaM and binding of Ca²⁺-CaM to hypophosphorylated PSKR1.

Similar to PSKR1, BRI1 has a CaM binding site in subdomain VIa and a similar interaction of calmodulins with BRI1 was previously reported by Oh *et al.* (2012), suggesting that CaMs may have a conserved function in LRR-RLK signaling. However, co-expression of BRI1 with CaM in *E. coli* suppressed phosphorylation of *E. coli* proteins (Oh *et al.*, 2012) whereas the *in vitro* studies described here did not reveal a significant inhibition of kinase activity by Ca²⁺-CaM. These differing results may be due to the different experimental set-ups or may reflect actual differences in the regulation of PSKR1 and BRI1. The fact that Ca²⁺-CaM preferentially binds to the hypophosphorylated BRI1 and PSKR1 receptor kinases suggests that CaM has an as yet unexplored function in PSKR1

signaling, localization, stability, recycling, or complex assembly. It will be of interest to compare the phosphorylation patterns of the hypophosphorylated Ca²⁺-CaM2 binding with that of the *in vitro* autophosphorylated PSKR1-KD. Functional analyses of these sites will help identify the crucial phosphosite(s) that engage(s) in regulating Ca²⁺-CaM2/PSKR1 interaction.

Taken together, our study showed that differential phosphorylation of the peptide receptor PSKR1 is an efficient means to control receptor activity. The multitude of phosphosites identified suggests that phosphorylation may serve in integration of other signal pathways and/or specification of signal output. Root and shoot growth is affected in a differential manner by defined phosphosite mutations, supporting this view. PSK signaling also modifies pathogen responses (Mosher *et al.*, 2013) and differentiation (Rodiuc *et al.*, 2016). It is hence conceivable that different physiological outputs are mediated by differential receptor phosphorylation. In addition, PSKR1 is subject to control by the calcium sensor CaM. CaM2 binds to hypophosphorylated PSKR1, which, however, does not alter PSKR1 kinase activity. This interaction may influence, for example, receptor turnover or complex assembly, but its biological function has yet to be clarified.

Supplementary data

Supplementary data are available at *JXB* online.

Table S1. Oligonucleotides that were used to generate point-mutated PSKR1-KD isoforms.

Video S1. Video of a rotating homology model of PSKR1-KD in *x*- and *y*-axis rolls.

Fig. S1. PyMol Session File of the homology model of PSKR1-KD with structural features marked as described in Fig. 1. This model allows the visualization of amino acid side-chains and phospho groups and the zooming-in on structures. This figure is provided as a PyMOL session file (.pse). It can be viewed with the free educational version of PyMOL that can be obtained at <http://pymol.org/edu/?q=educational/>

Fig. S2. Schematic summary of PSKR1-KD phosphosites, their evolutionary conservation, and impact on kinase activity.

Fig. S3. Kinase activity of the T998E PSKR1-KD isoform.

Fig. S4. Shift in mobility of ectopically expressed and purified PSKR1-KD after dephosphorylation.

Fig. S5. Transcript levels of *PSKR1* isoforms in the *pskr1-3 pskr2-1* background.

Acknowledgements

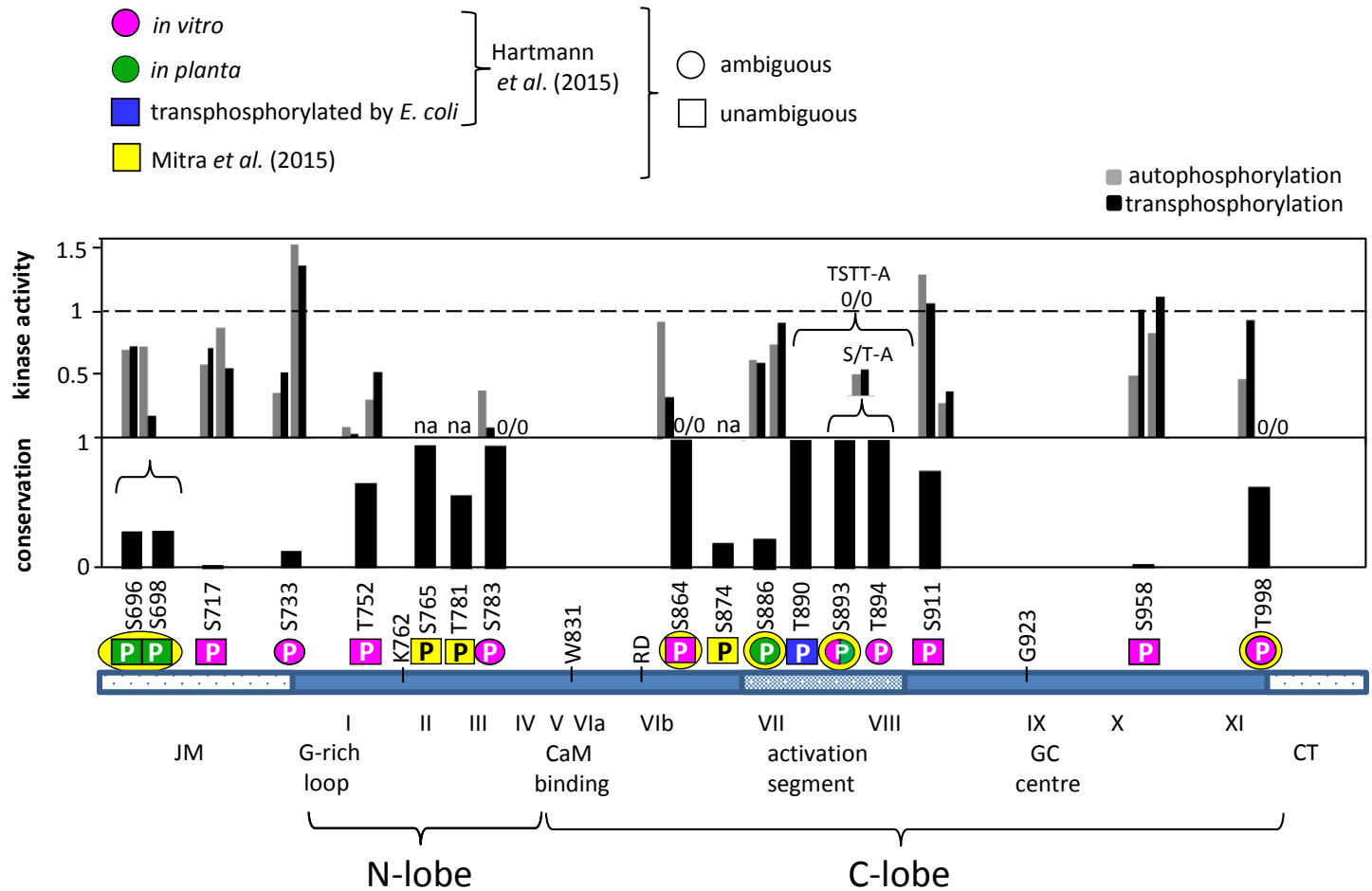
This work was funded by the Deutsche Forschungsgemeinschaft.

References

- Adams JA. 2003. Activation loop phosphorylation and catalysis in protein kinases: is there functional evidence for the autoinhibitor model? *Biochemistry* **42**, 601–607.
- Amano Y, Tsubouchi H, Shinohara H, Ogawa M, Matsubayashi Y. 2007. Tyrosine-sulfated glycopeptide involved in cellular proliferation and expansion in *Arabidopsis*. *Proceedings of the National Academy of Sciences, USA* **104**, 18333–18338.
- Bojar D, Martinez J, Santiago J, Rybin V, Bayliss R, Hothorn M. 2014. Crystal structures of the phosphorylated BRI1 kinase domain and implications for brassinosteroid signal initiation. *The Plant Journal* **78**, 31–43.
- Clough SJ, Bent AF. 1998. Floral dip: a simplified method for *Agrobacterium*-mediated transformation of *Arabidopsis thaliana*. *The Plant Journal* **16**, 735–743.
- De Vylder J, Vandenbussche F, Hu Y, Philips W, Van Der Straeten D. 2012. Rosette tracker: an open source image analysis tool for automatic quantification of genotype effects. *Plant Physiology* **160**, 1149–1159.
- Hartmann J, Fischer C, Dietrich P, Sauter M. 2014. Kinase activity and calmodulin binding are essential for growth signaling by the phytosulfokine receptor PSKR1. *The Plant Journal* **78**, 192–202.
- Hartmann J, Linke D, Bönninger C, Tholey A, Sauter M. 2015. Conserved phosphorylation sites in the activation loop of the *Arabidopsis* phytosulfokine receptor PSKR1 differentially affect kinase and receptor activity. *The Biochemical Journal* **472**, 379–391.
- Hartmann J, Stührwohldt N, Dahlke RI, Sauter M. 2013. Phytosulfokine control of growth occurs in the epidermis, is likely to be non-cell autonomous and is dependent on brassinosteroids. *The Plant Journal* **73**, 579–590.
- Higuchi R, Krummel B, Saiki RK. 1988. A general method of *in vitro* preparation and specific mutagenesis of DNA fragments: study of protein and DNA interactions. *Nucleic Acids Research* **16**, 7351–7367.
- Huse M, Kuriyan J. 2002. The conformational plasticity of protein kinases. *Cell* **109**, 275–282.
- Johnson LN, Noble ME, Owen DJ. 1996. Active and inactive protein kinases: structural basis for regulation. *Cell* **85**, 149–158.
- Karimi M, Inzé D, Depicker A. 2002. GATEWAY vectors for *Agrobacterium*-mediated plant transformation. *Trends in Plant Science* **7**, 193–195.
- Kelley LA, Mezulis S, Yates CM, Wass MN, Sternberg MJ. 2015. The Phyre2 web portal for protein modeling, prediction and analysis. *Nature Protocols* **10**, 845–858.
- Kilian J, Whitehead D, Horak J, Wanke D, Weinl S, Batistic O, D'Angelo C, Bornberg-Bauer E, Kudla J, Harter K. 2007. The AtGenExpress global stress expression data set: protocols, evaluation and model data analysis of UV-B light, drought and cold stress responses. *The Plant Journal* **50**, 347–363.
- Kornev AP, Taylor SS. 2015. Dynamics-driven allostery in protein kinases. *Trends in Biochemical Sciences* **40**, 628–647.
- Kung JE, Jura N. 2016. Structural basis for the non-catalytic functions of protein kinases. *Structure* **24**, 7–24.
- Kwezi L, Ruzvidzo O, Wheeler JI, Govender K, Iacuone S, Thompson PE, Gehring C, Irving HR. 2011. The phytosulfokine (PSK) receptor is capable of guanylate cyclase activity and enabling cyclic GMP-dependent signaling in plants. *The Journal of Biological Chemistry* **286**, 22580–22588.
- Ladwig F, Dahlke RI, Stührwohldt N, Hartmann J, Harter K, Sauter M. 2015. Phytosulfokine regulates growth in *Arabidopsis* through a response module at the plasma membrane that includes CYCLIC NUCLEOTIDE-GATED CHANNEL17, H⁺-ATPase, and BAK1. *The Plant Cell* **27**, 1718–1729.
- Matsubayashi Y, Ogawa M, Kihara H, Niwa M, Sakagami Y. 2006. Disruption and overexpression of *Arabidopsis* phytosulfokine receptor gene affects cellular longevity and potential for growth. *Plant Physiology* **142**, 45–53.
- Matsubayashi Y, Ogawa M, Morita A, Sakagami Y. 2002. An LRR receptor kinase involved in perception of a peptide plant hormone, phytosulfokine. *Science* **296**, 1470–1472.
- Mitra SK, Chen R, Dhandaydham M, Wang X, Blackburn RK, Kota U, Goshe MB, Schwartz D, Huber SC, Clouse SD. 2015. An autophosphorylation site database for leucine-rich repeat receptor-like kinases in *Arabidopsis thaliana*. *The Plant Journal* **82**, 1042–1060.
- Mosher S, Seybold H, Rodriguez P, *et al.* 2013. The tyrosine-sulfated peptide receptors PSKR1 and PSY1R modify the immunity of *Arabidopsis* to biotrophic and necrotrophic pathogens in an antagonistic manner. *The Plant Journal* **73**, 469–482.

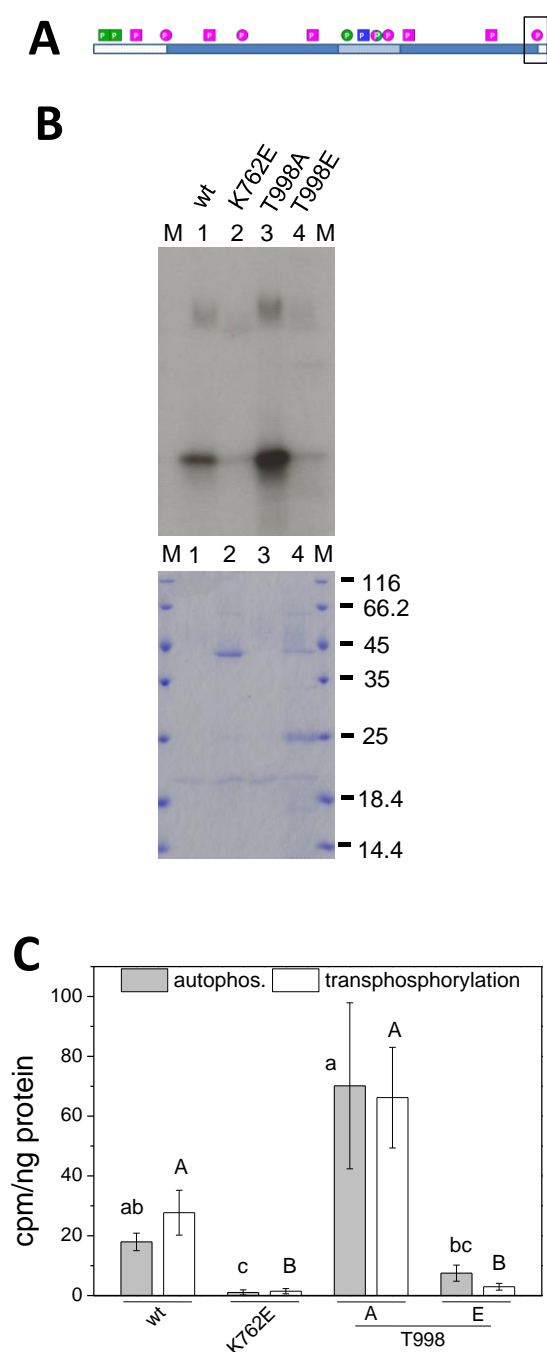
- Nolen B, Taylor S, Ghosh G.** 2004. Regulation of protein kinases; controlling activity through activation segment conformation. *Molecular Cell* **15**, 661–675.
- Oh MH, Kim HS, Wu X, Clouse SD, Zielinski RE, Huber SC.** 2012. Calcium/calmodulin inhibition of the Arabidopsis BRASSINOSTEROID-INSENSITIVE 1 receptor kinase provides a possible link between calcium and brassinosteroid signalling. *The Biochemical Journal* **443**, 515–523.
- Rodiuc N, Barlet X, Hok S, et al.** 2016. Evolutionarily distant pathogens require the Arabidopsis phytosulfokine signalling pathway to establish disease. *Plant, Cell & Environment* **39**, 1396–1407.
- Sauter M.** 2015. Phytosulfokine peptide signalling. *Journal of Experimental Botany* **66**, 5161–5169.
- Shiu SH, Bleecker AB.** 2001. Receptor-like kinases from Arabidopsis form a monophyletic gene family related to animal receptor kinases. *Proceedings of the National Academy of Sciences, USA* **98**, 10763–10768.
- Stührwohldt N, Dahlke RI, Steffens B, Johnson A, Sauter M.** 2011. Phytosulfokine- α controls hypocotyl length and cell expansion in *Arabidopsis thaliana* through phytosulfokine receptor 1. *PLoS ONE* **6**, e21054.
- Tavormina P, De Coninck B, Nikonorova N, De Smet I, Cammue BP.** 2015. The plant peptidome: an expanding repertoire of structural features and biological functions. *The Plant Cell* **27**, 2095–2118.
- Taylor SS, Keshwani MM, Steichen JM, Kornev AP.** 2012. Evolution of the eukaryotic protein kinases as dynamic molecular switches. *Philosophical Transactions of the Royal Society of London. Series B, Biological Sciences* **367**, 2517–2528.
- Taylor SS, Kornev AP.** 2011. Protein kinases: evolution of dynamic regulatory proteins. *Trends in Biochemical Sciences* **36**, 65–77.
- Wang J, Li H, Han Z, Zhang H, Wang T, Lin G, Chang J, Yang W, Chai J.** 2015. Allosteric receptor activation by the plant peptide hormone phytosulfokine. *Nature* **525**, 265–268.
- Wang X, Kota U, He K, Blackburn K, Li J, Goshe MB, Huber SC, Clouse SD.** 2008. Sequential transphosphorylation of the BRI1/BAK1 receptor kinase complex impacts early events in brassinosteroid signaling. *Developmental Cell* **15**, 220–235.
- Wang X, Li X, Meisenhelder J, Hunter T, Yoshida S, Asami T, Chory J.** 2005. Autoregulation and homodimerization are involved in the activation of the plant steroid receptor BRI1. *Developmental Cell* **8**, 855–865.
- Warnecke A, Sandalova T, Achour A, Harris RA.** 2014. PyTMs: a useful PyMOL plugin for modeling common post-translational modifications. *BMC Bioinformatics* **15**, 370.
- Winter D, Vinegar B, Nahal H, Ammar R, Wilson GV, Provart NJ.** 2007. An “Electronic Fluorescent Pictograph” browser for exploring and analyzing large-scale biological data sets. *PLoS ONE* **2**, e718.

Supplementary Figure S2



Supplementary Figure S2: Schematic overview of mapped PSKR1-KD phosphosites in *Arabidopsis thaliana* (Hartmann *et al.*, 2015; Mitra *et al.*, 2015) in relation to the 12 kinase subdomains and other functional sites referred to in the paper. The middle panel shows conservation of phosphosites in higher plant PSKR1 orthologs (taken from Hartmann *et al.*, 2015) with 1 indicating 100% conservation with S/T variations considered as conserved. The top panel shows the relative kinase activities of PSKR1-KD isoforms summarized from Figures 1, 2 and 5 and from Hartmann *et al.* (2015). At each phosphosite the two columns to the left show kinase activities of the phosphoablative A isoform; the two columns to the right show activities of the phosphomimetic D or E isoforms. 0: no activity; na: not analyzed. To allow for comparison among experiments, the kinase activities of the K762E isoform were set to zero and those of wild type were set to one in each case.

Supplementary Figure S3



Supplementary Figure S3:

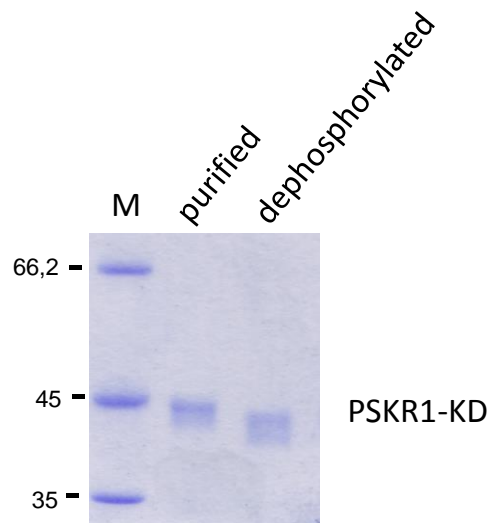
Phosphomimetic T998E mutation abolishes kinase activity. Auto- and transphosphorylation activities of the wild type PSKR1-KD (wt), the inactive PSKR1-KD(K762E) and the PSKR1-KD(T998A) and PSKR1-KD(T998E) isoforms.

(A) Schematic indicating the phosphosite analyzed.

(B) The kinase isoforms (0.25 μ g) were incubated with 32 P-ATP and the substrate MBP (0.5 μ g). The autoradiograph (top) shows auto- and transphosphorylation activities. A Coomassie-stained gel (bottom) shows loading of PSKR1-KDs and the substrate MBP; M = size marker in kDa.

(C) 32 P incorporated in PSKR1-KDs and MBP was quantified by liquid scintillation counting. Results are averages (\pm SE) from three independent experiments with two technical replicates each. Significantly different values are indicated by different lower case (autophosphorylation) or capital (transphosphorylation) letters (Kruskal-Wallis, $p < 0.05$).

Supplementary Figure S4

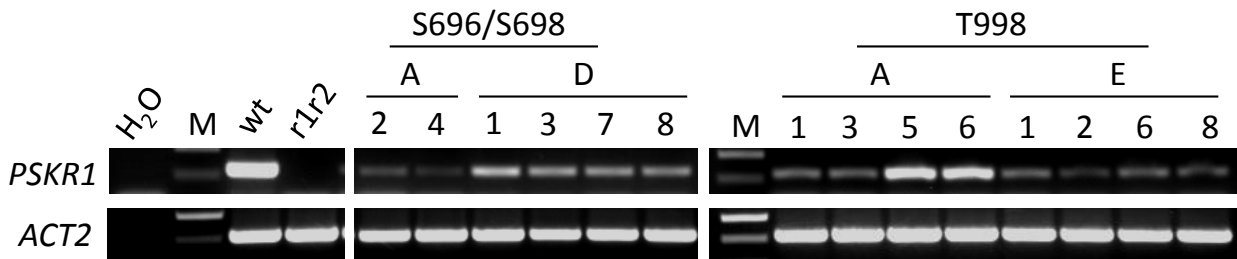


Supplementary Figure S4: Ectopically expressed, purified PSKR1-KD was treated with λ -phosphatase at room temperature for 2 h according to Muleya et al., (2016). The shift in mobility after dephosphorylation suggests that the protein is phosphorylated *in E.coli*.

REFERENCE

Muleya V, Marondedze C, Wheeler JI, Thomas L, Mok YF, Griffin MD, Manallack DT, Kwezi L, Lilley KS, Gehring C, Irving HR. 2016. Phosphorylation of the dimeric cytoplasmic domain of the phytosulfokine receptor, PSKR1. *Biochem Journal* **473**, 3081-98.

Supplementary Figure S5

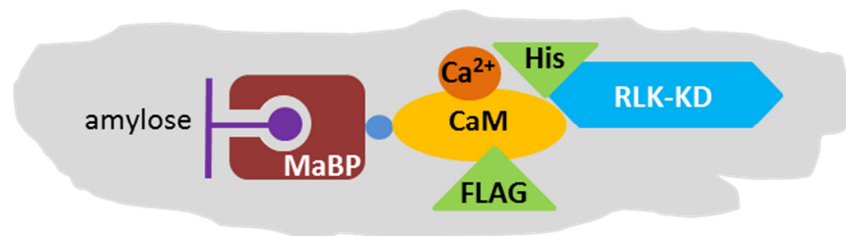


Supplementary Figure S5: *PSKR1* expression of *PSKR1* isoforms in the *pskr1-3 pskr2-1* background was analyzed by reverse transcription PCR. Numbers indicate independent T-DNA-insertion lines. M = marker, wt = wild type, *r1r2* = *pskr1-3 pskr2-1*.

Chapter 3

Pull-down Assay to Characterize Ca^{2+} /Calmodulin Binding to Plant Receptor Kinases

Kaufmann, C., & Sauter, M. (2017). In R. B. Aalen (Ed.), *Plant Receptor Kinases* (Vol. 1621, pp. 151–159). Springer Protocols. <https://doi.org/10.1007/978-1-4939-7063-6>



Pull-down Assay to Characterize Ca²⁺/Calmodulin Binding to Plant Receptor Kinases

Christine Kaufmann and Margret Sauter

Abstract

Plant receptor-like kinases (RLKs) are regulated by posttranscriptional modification and by interaction with regulatory proteins. A common modification of RLKs is (auto)phosphorylation, and a common regulatory protein is the calcium sensor calmodulin (CaM). We have developed protocols to detect the interaction of an RLK with CaM. The interaction with CaM was shown by bimolecular fluorescence complementation (BiFC) (*see* [Chapter 14](#)) and pull-down assay (this chapter). Both methods offer unique advantages. BiFC is useful in showing interaction of soluble as well as of membrane-bound proteins in planta. Pull-down assays are restricted to soluble proteins and provide *in vitro* data. The pull-down assay provides the advantage that proteins can be modified prior to binding and that experimental conditions such as the concentration of Ca²⁺ or other divalent cations can be controlled. This chapter provides a pull-down protocol to study RLK-CaM interaction with optional steps to investigate the impact of RLK phosphorylation or of Ca²⁺.

Key words Protein tagging, Calmodulin expression, Calcium, Peptide receptor kinase expression, Protein binding, Phosphorylation, Pulldown

1 Introduction

Plants possess a large number of receptor-like kinases (RLKs) with more than 600 found in *Arabidopsis thaliana* [1]. The brassinosteroid receptor brassinosteroid insensitive 1 (BRI1), the immune receptor flagellin sensing 2 (FLS2), and peptide receptors such as the phytosulfokine receptors 1 and 2 (PSKR1 and PSKR2) belong to the leucine-rich repeat (LRR) RLKs with more than 200 members in *Arabidopsis* that have an extracellular ligand-binding LRR domain [2]. The LRR is linked to an intracellular kinase by a single transmembrane helix. The intracellular receptor part of LRR RLKs can be regulated at various levels including posttranslational modification in the kinase domain, but also in the juxtamembrane region and at the C-terminus, and by binding to regulatory proteins.

For most RLKs, the regulatory mechanisms that control their activity are however not or only partly understood.

Regulation by calcium was suggested for members of subclass X of the LRR RLK family that share a conserved amphipathic α -helix (helix E) in kinase subdomain VIa that is predicted to bind the calcium sensor calmodulin (CaM) [3]. BRI1 and PSKR1 are subgroup X members [2]. For BRI1 and PSKR1, binding to CaM in vivo was demonstrated previously by the bimolecular fluorescence complementation (BiFC) method [4]. Further information and a detailed protocol of BiFC can be found in [Chapter 15](#). The methods described here and in [Chapter 15](#) should be useful to clarify if an RLK has the ability to interact with CaM and is hence likely to be regulated by calcium.

As a complementary approach to BiFC to study the RLK-CaM interaction, we developed a pull-down assay using heterologously expressed tagged CaM2 and tagged PSKR1 kinase (Fig. 1). The in vitro system allows for controlled reaction conditions such as the concentration of divalent cations. It is further possible to posttranscriptionally modify the receptor kinase prior to the interaction assay. This approach allowed us to study the impact of Ca^{2+} , of Mg^{2+} , and of kinase phosphorylation on PSKR1-CaM2 binding. An important point to consider is that this experimental setup is not suited for membrane proteins. With regard to RLKs, it is however possible to express and use the cytoplasmic receptor part (PSKR1-KD) that harbors the CaM-binding site as a soluble protein.

2 Materials for Pull-down Assay

2.1 Choice of Vectors

1. It is important that the tag does not alter protein activity. This should be considered before choosing the tags and the position of the tag. If possible, it is best to compare the activity of the tagged protein to that of the untagged protein. For PSKR1, the N-terminal 6 \times His(H_6) tag does not disturb kinase activity in vitro [5]. N-terminally H_6 -tagged fusion protein can be produced using the pETDuet vector system (*see Note 1*).
2. Calmodulin (CaM) is a regulatory protein of small size. A FLAG tag at the C-terminus can be used for detection of CaM2. Large quantities of soluble CaM2 can be obtained using the vector system pMALTM Protein Fusion and Purification System (New England Biolabs). Fusion to the maltose-binding protein (MaBP) enhances solubility and results in higher yields [6].

2.2 Materials Used to Express MaBP-CaM-FLAG

1. *Escherichia coli* strain BL21(DE3).
2. Expression medium: LB medium with 0.2% (w/v) glucose, autoclave, and add ampicillin prior to use to a final concentration of 100 $\mu\text{g}/\text{mL}$. The presence of glucose in the medium is necessary to repress expression of amylase (*see Note 2*).

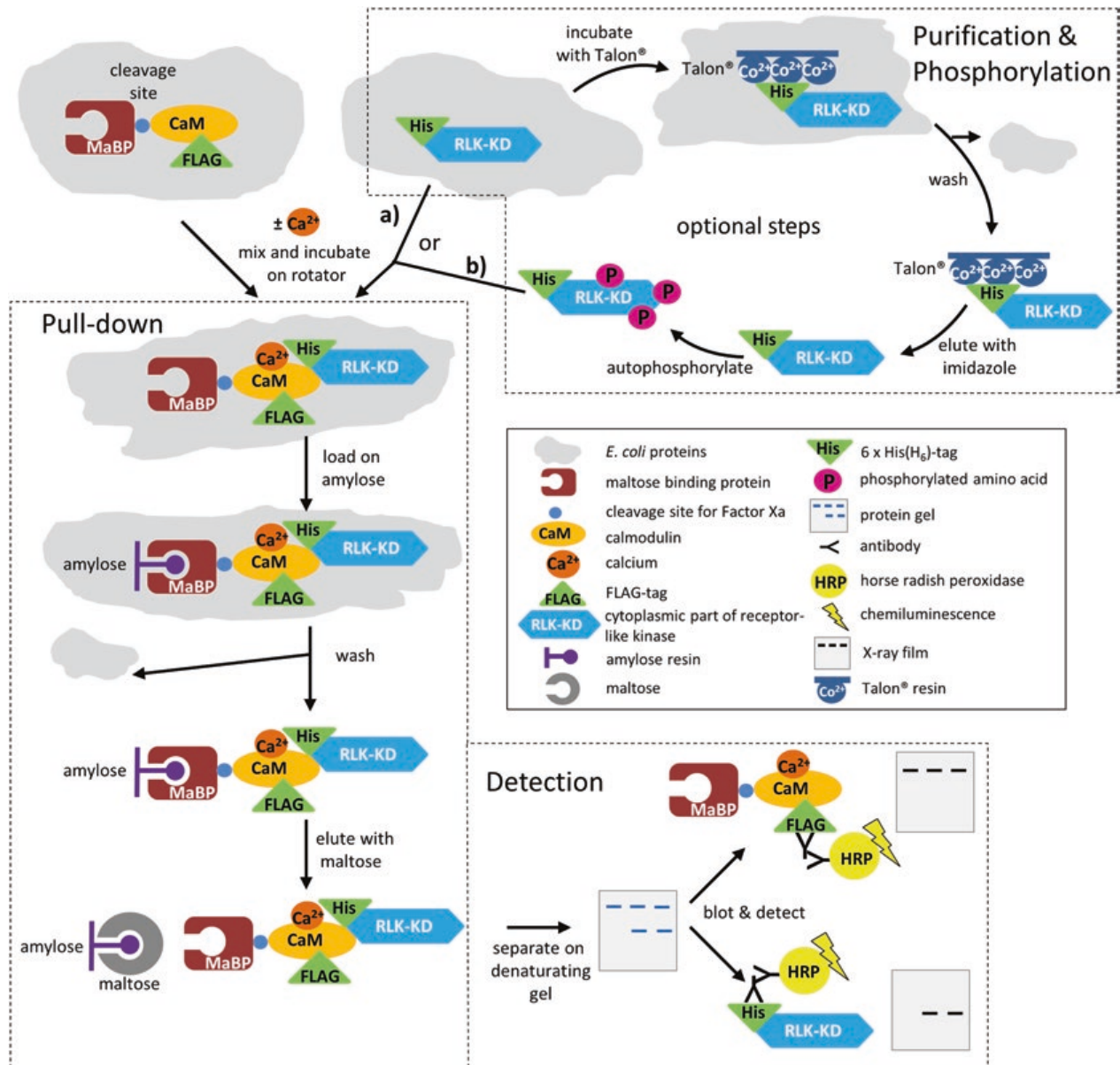


Fig. 1 Schematic overview of the pull-down assay with CaM and RLK-KD fusion proteins. **(a)** Crude *E. coli* extracts with heterologously expressed MaBP-CaM-FLAG and H₆-RLK-KD can be used directly. **(b)** To study the impact of autophosphorylation on CaM binding, H₆-RLK-KD can be affinity purified by Talon[®] using the 6×His(H₆) tag, followed by incubation with kinase buffer to allow for autophosphorylation. The purified and modified kinase is subsequently incubated with crude extract of MaBP-CaM-FLAG for binding

3. Extraction buffer: 20 mM Tris/HCl pH 7.5, 200 mM NaCl.
4. French press.
5. Cell disruptor.

2.3 Materials for the Expression of the His-Tagged Kinase Domain of a Receptor-like Kinase (H₆-RLK-KD)

1. *Escherichia coli* strain BL21(DE3).
2. Expression medium: LB medium, autoclave; add ampicillin to a final concentration of 100 µg/mL just before use.
3. Extraction buffer: 50 mM sodium phosphate pH 7.0, 300 mM NaCl.

4. French press.
5. Cell disruptor.
6. Talon[®] Metal Affinity Resin (Clontech).
7. Pierce[®] Spin Column (Thermo Scientific).
8. Washing buffer: 50 mM sodium phosphate pH 8.0, 300 mM NaCl, 5 mM imidazole.
9. Elution buffer: 50 mM sodium phosphate pH 8.0, 300 mM NaCl, 150 mM imidazole.
10. NanoDrop 2000 (Thermo Scientific).
11. Roti-Spin Mini-10 MWCO (10 kDa) (Carl Roth).
12. Kinase buffer: 50 mM HEPES/KOH pH 7.5, 10 mM MnCl₂, 1 mM dithiothreitol, 0.2 mM ATP.

2.4 Materials for Pulldown

1. Interaction buffer: 20 mM Tris/HCl pH 7.5, 200 mM NaCl. Supplement with ions (Ca²⁺ as CaCl₂, Mg²⁺ as MgCl₂), chelators (e.g., EDTA or EGTA), or other cofactors as needed.
2. Rotator.
3. Amylose resin (NEB).
4. Pierce[®] Spin Column (Thermo Scientific).
5. Elution buffer: 20 mM Tris/HCl pH 7.5, 200 mM NaCl, 10 mM maltose.

3 Pull-down Methods

3.1 Expression of MaBP-CaM-FLAG

1. Inoculate a flask with 30 mL of expression medium with cells of a verified MaBP-CaM-FLAG containing clone and incubate on a shaker at 37 °C.
2. Determine the OD₆₀₀ of the culture and proceed when culture reaches OD of 0.5.
3. Induce protein expression by adding isopropyl β-D-1-thiogalactopyranoside (IPTG) to a final concentration of 0.3 mM to the culture and shake at 37 °C for 2 h.
4. Harvest the cells by centrifugation at 4000 × *g* for 5 min at 4 °C. Discard the supernatant and resolve the pelleted cells in 4 mL extraction buffer.

3.2 Expression of H₆-RLK-KD

1. Inoculate a flask with 50 mL of expression medium with cells of a verified H₆-RLK-KD containing clone and shake at 37 °C.
2. Determine the OD₆₀₀ of each culture. At an OD₆₀₀ of 0.5 let bacteria cool down to room temperature to avoid formation of inclusion bodies (*see* **Note 3**).

3. Induce protein expression by adding IPTG to a final concentration of 1 mM to the culture and shake at room temperature for 16 h.
4. Harvest the cells by centrifugation at $4000 \times g$ for 5 min at 4 °C. Discard the supernatant and resuspend the pelleted cells in 3.5 mL extraction buffer.

3.3 Isolation of MaBP-CaM-FLAG and H₆-RLK-KD

1. Disrupt the resuspended cells in a French press with 20,000 PSIG cell pressure in a precooled cell.
2. Sonicate the solution three times for 10 s with appropriate energy amplitude setting for used microtip to destroy accumulated DNA, while having the sample kept cooled in an ice bath (*see Note 4*).
3. Centrifuge the mixture for 30 min at $21,000 \times g$ and 4 °C.
4. Collect the supernatant, discard the pellet, and freeze MaBP-CaM-FLAG at -80 °C until use or use directly for pulldown. Instead of using crude extract, MaBP-CaM-FLAG can be purified and modified prior to pulldown (*see Note 5*). For H₆-RLK-KD, use crude extract immediately or proceed with affinity purification (*see Subheading 3.4*).

3.4 Purification (See Note 6) and Auto-phosphorylation (See Note 7) of H₆-RLK-KD (Optional Steps)

1. Mix 50 µL of Talon resin with 500 µL of extraction buffer in a Pierce® Spin Column and centrifuge for 30 s at $400 \times g$ in a tabletop centrifuge at room temperature to wash out resin storage solution. Discard the flow-through.
2. Incubate the washed Talon resin with the prepared crude extract for 1 h at room temperature in a rotator.
3. Wait for a few minutes until the resin sediments to the bottom of the container by gravity or centrifuge for 1 min at $400 \times g$ at room temperature.
4. Discard the supernatant except for 500 µL. Mix the pelleted resin with the leftover 500 µL solution and load onto the Spin Column.
5. Centrifuge for 30 s at $400 \times g$ in a tabletop centrifuge at room temperature. Discard the flow-through.
6. Wash three times with 500 µL of washing buffer.
7. Elute the bound H₆-RLK-KD by adding 50 µL of elution buffer and incubate for 10 min prior to centrifugation.
8. For ultrafiltration, transfer the eluted H₆-RLK-KD to a Roti®-Spin Column (*see Note 8*), centrifuge at $12,000 \times g$ at 4 °C in a tabletop centrifuge to reduce sample volume, and discard the flow-through. Add 10× the sample volume of 50 mM HEPES/KOH pH 7.5 to the Roti®-Spin Column to adjust to the kinase buffer, centrifuge, and discard flow-through. Repeat

this procedure two to three times. Centrifuge to reduce the sample to half the volume desired. Pipette the solution from the membrane to a fresh tube. Wash residual protein from the membrane with the same volume of buffer and combine.

Determine the protein concentration with a NanoDrop by measuring the absorbance at 280 nm.

9. For kinase autophosphorylation, incubate H₆-RLK-KD for 1 h at 25 °C in kinase buffer.
10. Before using autophosphorylated kinase for pulldown, the buffer conditions need to be adjusted. To do so, ultrafiltrate and concentrate the autophosphorylated kinase protein in a Roti®-Spin Column as described above except that here the kinase buffer is replaced by interaction buffer.

3.5 Pulldown

1. Estimate the protein concentration of the proteins to be analyzed in the respective crude extracts by running an aliquot on an SDS-PAGE together with a standard, e.g., BSA, of known protein concentration (*see Note 9*).
2. Incubate equivalent amounts of H₆-RLK-KD and MaBP-CaM-FLAG crude extracts in incubation buffer in a total volume of 250 µL. We used ~50 µg protein each in our assays. Alternatively, use the purified and autophosphorylated H₆-RLK-KD. Binding of CaM may be influenced by calcium ions. To test that, add 100 µM CaCl₂ to the buffer or add 100 µM MgCl₂ as a control.
3. Place the sample(s) at room temperature for 30 min on a rotator to allow for binding.
4. Mix 25 µL of amylose resin with 300 µL of interaction buffer in a Spin Column and centrifuge for 1 min at 400 × *g* at room temperature in a tabletop centrifuge to wash out resin storage solution. Discard the flow-through. Repeat this washing procedure two times.
5. Add the washed amylose resin to the sample. Incubate for another 30 min on a rotator to allow for binding of the complex via MaBP fusion protein to amylose resin.
6. Centrifuge the mixture in a Spin Column at 400 × *g* for 1 min at room temperature. Collect the flow-through and store at 4 °C for subsequent analysis on a gel.
7. Wash three times with 300 µL interaction buffer ± ions as described above.
8. For elution, mix the amylose resin with 2× the volume of amylose resin used initially (in this case 50 µL), incubate for 5 min, and centrifuge at 400 × *g* for 1 min at room temperature.
9. Separate the protein complex on a denaturing protein gel, e.g., 12.5% SDS-gel.

10. Blot the proteins on a polyvinylidene difluoride (PVDF) membrane and detect with appropriate primary and secondary antibodies, e.g., anti-FLAG and anti-His primary antibodies and horse radish peroxidase (HRP)-conjugated anti-mouse secondary antibody. Detect proteins by exposing the membrane to an X-ray or chemiluminescence film to visualize chemiluminescence. Protein detection by Western blot analysis should be optimized prior to the pull-down experiment using crude protein extract (*see Note 10*).

4 Notes

1. In general, the Duet Vectors from Novagen have advantages if protein complexes are to be studied by coexpression. For the pull-down assay described here, any kind of vector system can be used that works properly for protein expression and purification of H₆-tagged fusion proteins.
2. Repression of amylase expression is important. Amylase degrades the amylose resin during purification and thereby leads to a lower yield of the desired fusion protein.
3. Heterologously expressed proteins can form insoluble, inaccessible and nonfunctional aggregates termed inclusion bodies. There are several ways to avoid inclusion body formation. In general, it all comes down to slow down the speed at which fusion proteins are made [7]. This can be achieved by using a low-copy number vector, by coexpression of molecular chaperones, induction with a lower IPTG concentrations (<1 mM), use of alternative media that are rich (e.g., 2YT) or less rich (e.g., LB), the duration of bacterial growth after induction, and—as described in this protocol—by lowering the temperature at which the bacteria are grown before and after induction [8].
4. Accumulated DNA increases the viscosity of the solution and blocks membranes and therefore impairs purification or interactions of proteins. Sonication of the solution leads to an increased temperature which may damage the proteins in the sample. Therefore, cooling the sample while sonicating is highly recommended. Additionally, perform sonication in three intervals to allow the mixture to cool down in between and choose a sonication energy amplitude setting as low as possible to avoid destruction of proteins.
5. As an optional step, it is possible to purify MaBP-CaM-FLAG with amylose resin followed by elution with maltose. This may be helpful if no interaction is observed after pulldown with crude extract. This result can be caused by interference by

MaBP. To exclude this scenario, MaBP can be cleaved off with Factor Xa resulting in a CaM-FLAG fusion protein. Cross-link anti-FLAG antibodies to Protein A beads, e.g., with the Pierce® Crosslink Immunoprecipitation Kit and proceed with a co-immunoprecipitation (Co-IP). The cross-link prevents release of antibodies when proteins are eluted. The heavy and light antibody chains may interfere with immunoblotting and immunodetection of the proteins of interest. In this case, a Co-IP with cross-linked anti-His antibodies can be used to confirm a specific CaM-RLK interaction.

6. If no interaction is observed, this may be due to interfering proteins in the *E. coli* crude extract. In this case, one or both interaction partners can be purified from their respective crude extracts. Pulldown with crude extracts however is preferred, because it supports the specificity of the interaction.
7. Posttranslational modifications, e.g., phosphorylation can alter the protein structure. In some cases, a conformational change is required for an interaction or may enhance or decrease the interaction. Therefore, when working with RLKs, this should be kept in mind and considered for analysis. To examine the effect of autophosphorylation of an RLK, the RLK is purified via its tag and subsequently incubated in kinase buffer to allow for autophosphorylation.
8. The Roti®-Spin Column is a commonly used centrifugal filter. You can also use alternative size exclusion filters, e.g., Centricon from Millipore. The important thing to keep in mind is to choose the appropriate size exclusion limit. This is dependent on the size of the protein to be analyzed. The sample is placed in the reservoir above the membrane. During centrifugation, proteins smaller than the specified cutoff pass the membrane pores while the protein of interest is retained in the reservoir. With a filter or membrane column, you can easily concentrate a protein sample or switch buffer conditions.
9. When working with crude extract, quantification of the expressed target protein with Bradford or other photometric methods is not possible. To determine the amount of target protein(s), an aliquot can be run on an SDS gel. To estimate protein concentration, a dilution series of a known protein, e.g., bovine serum albumin (BSA), can be included on the gel.
10. To make sure that the interacting proteins are easily detected by Western blot, optimize the 1° and 2° antibody concentrations. Begin by using the concentration suggested by the manufacturer and use higher (if no signal is detected) or lower (when the background is high) concentrations in steps of two-fold. As primary antibodies, we used a monoclonal anti-FLAG M2 (Sigma) antibody diluted 1:2500 or a 6×-His epitope tag

antibody His.H8 also diluted 1:2500 (Thermo Fisher). As secondary antibodies, horse radish peroxidase-conjugated anti-mouse antibodies diluted 1:50,000 (Life Technologies) was used. To visualize the proteins, we used the ECL Plus Western blotting substrate (Pierce).

Acknowledgment

We would like to thank the Deutsche Forschungsgemeinschaft for financial support.

References

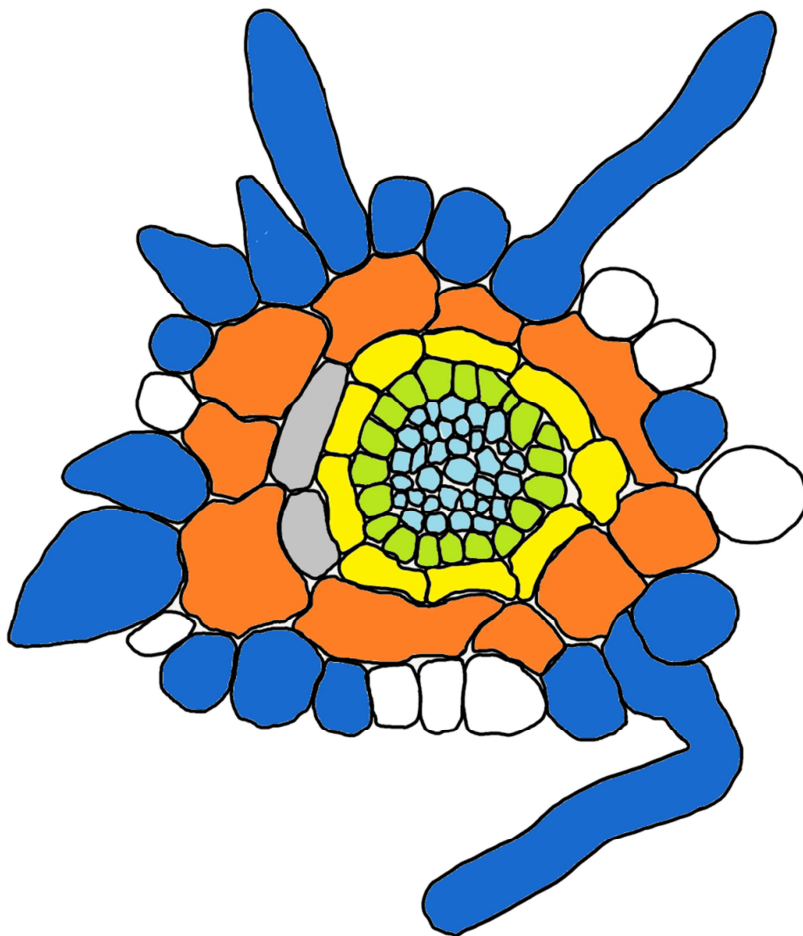
1. Shiu S, Bleecker A (2001) Receptor-like kinases from Arabidopsis form a monophyletic gene family related to animal receptor kinases. *Proc Natl Acad Sci U S A* 19:10763–10768
2. Diévert A, Clark S (2003) Using mutant alleles to determine the structure and function of leucine-rich repeat receptor-like kinases. *Curr Opin Plant Biol* 6(5):507–516
3. Oh M, Kim H, Wu X, Clouse S, Zielinski R, Huber S (2012) BRASSINOSTEROID-INSENSITIVE 1 receptor kinase provides a possible link between calcium and brassinosteroid signalling. *Biochem J* 443(2):515–523
4. Hu C-D, Chinenov Y, Kerppola TK (2002) Visualization of interactions among bzip and rel family proteins in living cells using bimolecular fluorescence complementation. *Mol Cell* 9(4):789–798
5. Hartmann J, Fischer C, Dietrich P, Sauter M (2014) Kinase activity and calmodulin binding are essential for growth signaling by the phyto-sulfonine receptor PSKR1. *Plant J* 78(2):192–202
6. New England Biolabs (2005) pMAL™ protein fusion & purification system, instruction manual. <https://www.neb.com/~media/Catalog/All-Products/FF91B67397D945E0956F3483174CF7E3/Datacards%20or%20Manuals/Manual%20E8200.pdf>
7. Fakruddin M, Mazumdar RM, Bin Mannan KS, Chowdhury A, Hossain MN (2013) Critical factors affecting the success of cloning, expression, and mass production of enzymes by recombinant *E. coli*. *ISRN Biotechnol* 2013:590587. doi:10.5402/2013/590587
8. Sanchez de Groot N, Ventura S (2006) Effect of temperature on protein quality in bacterial inclusion bodies. *FEBS Lett* 580:6471–6476

Chapter 4

Phytosulfokine receptor activity in the absence of its ligand PSK

Christine Kaufmann, Lam Dai Vu, Nils Stührwohldt, Ive de Smet and Margret Sauter

(in preparation for submission)



Phytosulfokine receptor activity in the absence of its ligand PSK

Christine Kaufmann¹, Lam Dai Vu², Nils Stührwohldt¹, Ive de Smet² and Margret Sauter^{1*}

¹ Entwicklungsbiologie und Physiologie der Pflanzen, Universität Kiel, Am Botanischen Garten 5, 24118 Kiel, Germany

² Functional Phosphoproteomics, VIB / Universiteit Gent, Technologiepark 927, 9052 Gent, Belgium

Phytosulfokine (PSK) is a disulfated pentapeptide that promotes growth, delays senescence and acts in biotic stress tolerance¹⁻⁵. Peptide hormones, including PSK, RGF1 and PSY1 are sulfated by tyrosylprotein sulfotransferase (TPST)^{6,7} a modification that is required for peptide activity⁸⁻¹⁰. The *tpst-1* knockout mutant has no detectable peptide sulfotransferase activity and displays a severe dwarf phenotype and early senescence⁶ that is partially rescued by application of PSK¹¹. PSK binds to the island domain of the leucine-rich repeat receptor-like kinase PSKR1 that interacts with the promiscuous co-receptor SERK3/BAK1^{12,13}. The dimerization model¹⁴ of LRR-RLK/SERK complex formation, states that LRR-RLK signal cascades are activated following ligand-dependent binding of receptor and co-receptor. Here we show that PSKR1 is active in the absence of its ligand PSK. Previously, it was shown that PSKR1 and BAK1 interact independent of PSK and that this interaction is stabilized by PSK¹². Here we show that PSKR1 is activated in the absence of PSK through transphosphorylation by BAK1 at conserved phosphosites in the activation segment. *In planta*, overexpression of PSKR1 in the *tpst-1* background enhances root growth. Furthermore, knock out of both PSK receptors, PSKR1 and PSKR2, in the *tpst-1* background in *tpst-1 pskr1-3 pskr2-1* results in more severe root growth retardation, and promotes lateral root density and ectopic root hair formation compared to *tpst-1*. Enhanced root hair formation is evident at

the molecular level by lowered expression of the root hair inhibitor WER. We conclude from these results that PSKR1 and BAK1 interact independent of PSK resulting in PSKR1 activation triggering PSKR1 responses. We hypothesize that basal activation of PSKR1 by BAK1 maintains a basal level of growth and development that is enhanced in the presence of ligand.

PSK signaling promotes root growth^{2,7,11}. Overexpression of PSKR1 resulted in longer roots in Arabidopsis seedlings indicating that receptor abundance limits PSK signaling of root growth^{15,16}. Surprisingly, overexpression of PSKR1 in the *tpst-1* background also resulted in root growth promotion while overexpression of PSKR2 did not, suggesting that PSKR1 signaling takes place without active PSK (Figure 1a, Supplementary Figure 1a). Seedlings of seven independent *p35S:PSKR1-GFP tpst-1* lines had significantly longer roots than *tpst-1* seedlings (Figure 1b) with a correlation between PSKR1 protein abundance and root growth promotion (Figure 1d, Supplementary Figure 2c). Treatment with 1 μ M PSK resulted in a similar final root length in *tpst-1* and in *p35S:PSKR1-GFP tpst-1* seedlings suggesting that the receptor abundance was not limiting in the presence of ligand¹⁰, and that lack of PSK can be compensated for by increased PSKR1 abundance (Supplementary Figure 2a and b). Knock out of *PSKR1* and *PSKR2* in the *tpst-1* background (Supplementary Figure 2d) conferred insensitivity to PSK and resulted in even shorter roots in *tpst-1 pskr1-3 pskr2-1* compared to *tpst-1* seedlings (Figure 1c, e and Supplementary Figure 1b, c). Also, lateral root density, root hair formation and root diameter were increased in *tpst-1 pskr1-3 pskr2-1* compared to *tpst-1* (Figure 1f, Figure 2 and Supplementary Figure 3a-c) supporting the idea that PSK receptors are active in the *tpst-1* background.

The determination of hair/non-hair cell fate is well studied in Arabidopsis. In *Brassicaceae*, hair cells are organized in interspersed cell files and epidermal cell fate is determined by position with regard to the underlying cortical cells¹⁷. *EXPANSIN7 (EXP7)* is a trichoblast-specific marker gene¹⁸. We introduced an *pEXP7:GUS* marker to distinguish non-hair forming atrichoblasts from hair-forming trichoblasts (Figure 2c-f and Supplementary Figure 4). Loss of PSK-signaling in *pskr1-3 pskr2-1* did not alter *pEXP7:GUS* expression suggesting that

trichoblast cell fate was unchanged. In contrast, in *tpst-1* seedlings, about 70% of all epidermal cells were hair cells which are about twice as many as in wild type roots that have 33% hair cells. In the triple knock out *tpst-1 pskr1-3 pskr2-1*, 80-90% of all epidermal cells had developed into root hairs. qPCR analysis confirmed elevated *EXP7* transcripts in *tpst-1* and in *tpst-1 pskr1-3 pskr2-1* roots (Supplementary Figure 5d). Since the number of cortical cells can vary e.g. due to nutrient availability^{17,19}, an increase in cortical cells would put more epidermal cells in the H-position above two neighboring cortex cells which allows them to develop into a root hair¹⁹. Indeed, *pskr1-3 pskr2-1*, *tpst-1*, and triple knock out had an increasing root diameter, whereas epidermis and cortex cell numbers remained nearly constant indicating that the increase in hair cells was not caused by an altered ratio of epidermis to cortex cells (Figure 2g, h). Analysis of root cross sections revealed that about half of the *pEXP7:GUS* expressing epidermal cells in *tpst-1* and *tpst-1 pskr1-3 pskr2-1* roots were in the N-position above a single cortex cell while this was not observed in wild type or *pskr1-3 pskr2-1* roots (Figure 2d-f and Supplementary Figure 5a-b) indicating that sulfated peptides provide positional information between cortex and epidermal cell layers that is required for proper atrichoblast/ trichoblast patterning in the epidermis. Ectopic formation of root hairs was enhanced in the triple mutant compared to *tpst-1* suggesting that PSK receptor(s) are involved in root hair cell fate signaling.

The MYB transcription factors *WEREWOLF* (*WER*) and its paralog *MYB DOMAIN PROTEIN 23* (*MYB23*) contribute to non-hair cell fate determination, with *WER* being a key repressor of hair cell fate. Loss-of-function mutants show ectopic formation of root hairs^{20,21}. Furthermore, *At1g66800*, encoding for a protein of unknown function, is expressed in atrichoblasts²² (Figure 2j). These genes were found to be down-regulated in *tpst-1* compared to wild type in a microarray study (Figure 2i). Treatment of *tpst-1* seedlings with 1 μ M PSK induced transcript levels. qPCR analysis confirmed downregulation of *WER*, *MYB23* and *At1g66800* in *tpst-1* and showed even stronger downregulation in the triple knock out (Figure 2k). While *WER*, *MYB23* and *At1g66800* were only slightly repressed in *pskr1-3 pskr2-1*, they were significantly up-regulated by PSK in *tpst-1* pointing to a role of PSK signaling in root hair formation. *WER* is repressed in trichoblasts by an unknown signal that is induced in cortical cells by the transcription factor JACKDAW (*JKD*) and that is perceived by the LRR-RLK

SCRAMBLED (SCM) at the plasma membrane of trichoblasts²³. Expression of *JKD* and *SCM* was neither significantly changed in *pskr1-3 pskr2-1*, *tpst-1* or *tpst-1 pskr1-3 pskr2-1* nor by PSK in *tpst-1* roots (Supplementary Figure 5c) possibly indicating that sulfated peptides act independent of the JKD pathway.

Analysis of the triple knock out suggested that PSK receptor signaling has a role in epidermal cell fate determination possibly in conjunction with one or more additional Tyr-sulfated peptides. *tpst-1* plants have no detectable *TPST* transcript and have lost the ability to sulfate the PSY1 precursor⁶. The genome of *Arabidopsis* does not contain genes related to *TPST* or homologs to animal-type *TPSTs*²⁴. Given that PSK is not activated by sulfation in *tpst-1* leads us to conclude that PSK receptors are activated in the absence of PSK. The cytoplasmic signal-transducing region of *PSKR1* is a functional kinase that is essential for *PSKR1* activity^{16,25-27}. The kinase gets autophosphorylated at defined Ser, Thr and Tyr residues^{25,26,28,29} the most conserved of which are in the activation loop²⁶. FLIM-FRET analysis revealed that *PSKR1* is part of a nanocluster at the plasma membrane and binds to the co-receptor *BRI1*-associated receptor kinase 1 (*BAK1*), a *SERK* family member^{12,13}. The dimerization model proposes that a receptor is activated upon heterodimerization and heterodimerization is ligand-dependent¹⁴. In fact, pathogen-related *LRR-RLK/SERK* complexes such as *FLAGELLIN SENSITIVE 2*, *EF-TU RECEPTOR* and *PEP1 RECEPTOR 1* with their respective co-receptors are only formed and activated in the presence of ligand³⁰⁻³⁵. By contrast, the *LRR-RLKs* *HAESA*, *BRASSINOSTEROID INSENSITIVE 1 (BRI1)*, *EXCESS MICROSPOROCTES 1* and *ERECTA*, involved in growth and developmental processes and likewise shown to bind to *SERK* family members, are transphosphorylated by their co-receptor in a ligand-enhanced or ligand-independent manner³⁶⁻⁴² (Supplementary Table 4). *PSKR1* was shown to bind to *BAK1* in the absence of PSK¹³, while PSK stabilized the *PSKR1/BAK1* complex. Co-expression of *PSKR1* and *BAK1* in the absence of PSK caused rapid protoplast rupture, making it impossible to investigate full-length protein interaction *in vivo*¹². To study a possible activation of PSK receptors by *BAK1* in the absence of PSK we carried out an *in vitro* transphosphorylation assay with active kinase isoforms of *PSKR1*, *PSKR2*, *BAK1* and the point-mutated, inactive isoforms *PSKR1-K762E*, *PSKR2-K782E* and *BAK1-D434N*⁴³ (Figure 3a). *PSKR1*, *PSKR2* and *BAK1* were capable of auto-

phosphorylation, whereas the point mutated isoforms were not (Figure 3a-d). Furthermore, BAK1 transphosphorylated inactive PSKR1 (Figure 3b) and PSKR2 (Figure 3c) resulting in quantitative similar radioactive signal strength as PSK receptor autophosphorylation. By contrast, PSKR1 and PSKR2 phosphorylated inactive BAK1 only to a minor degree (Figure 3d) and did not at all transphosphorylate each other (Figure 3b, c). Identification of phosphorylation sites by mass spectrometry analysis (Figure 4 and Supplementary Tables 1-3) and comparison with previously published phosphorylation site mappings of PSKR1, PSKR2 and BAK1^{26,28,37,44} revealed transphosphorylation of inactive PSKRs by BAK1 at the same positions as in active PSKR1 autophosphorylation (Figure 4a, b). PSKRs are transphosphorylated at the juxtamembrane domain (JM), the kinase domain and the C-terminus (CT) (Figure 4 a, b), suggesting full activation of PSKRs by BAK1. These sites were previously found to be phosphorylated (Figure 4a, b) and are highly conserved in PSKR1 orthologues throughout the plant kingdom^{26,28,29}. Site-directed mutagenesis of PSKR1 impaired kinase activity^{25,26}. By contrast, PSK receptors transphosphorylate BAK1 kinase only within the activation segment in accord with the low radioactive signal detected in the transphosphorylation assay (Figure 3d). Phosphorylation of the activation segment is required for most protein kinases⁴⁵, including PSKR1²⁶. However, the active state is acquired only when, in addition, the α C-helix is folded and positioned properly and the K-E salt bridge is formed^{46,47}. Recently published molecular dynamics simulation data for BRI1 and BAK1 crystal structures suggest that co-receptor binding stabilizes an unfolded disordered α C-helix which leads to the active conformation of both⁴⁸. This is in agreement with the observation that BRI1 is phosphorylated in the JM and CT domains after BAK1 binding³⁷. An *in silico* docking model of BAK1 and PSKR1 kinase with the highest cluster population shows that the α C-helix of PSKR1 is involved in their binding interface (Supplementary Figure 6), which further supports the idea of BAK1 being able to activate PSKR1. For PSKR1 activation, the crucial step is binding of PSKR1 and BAK1. The ubiquitous PLANT PHOSPHATASE 2A⁴⁹ and GLUTAREDOXIN C2⁵⁰ were shown to inhibit BAK1 kinase and could be candidates for controlling BAK1 activation of PSKR1. We conclude that PSK receptors are activated by BAK1 in the absence of ligand. We hypothesize that such a mechanism would ensure basal receptor activity and hence maintain plant growth

and ensure development at a basal level. Regulation of peptide synthesis would be a means to adjust growth rates and balance developmental processes. It will be interesting to see if such a mechanism also applies to other LRR-RLK signal pathways controlling growth and development.

Material and methods

Growth conditions and plant material

All experiments were carried out with *Arabidopsis thaliana* Col-0 (wt). The T-DNA insertion lines *tpst-1* (SALK_009847), *pskr1-3* (SALK_008585), *pskr2-1* (SALK_024464) and the double knock out line *pskr1-3 pskr2-1* were described previously^{2,6,15,51}. The triple knockout line *tpst-1 pskr1-3 pskr2-1* was generated by crossing *tpst-1* with *pskr1-3 pskr2-1*. Loss of all three transcripts was verified with RT-PCR. Seeds were surface-sterilized in 2% (v/v) NaOCl for 15 min and washed five times with autoclaved water and subsequently laid out on 0.5x modified Murashige-Skoog medium (Duchefa, Harlem, Netherlands), 1.5% (w/v) sucrose, solidified with 0.4% (w/v) Gelrite (Duchefa) and supplemented with 1 μ M PSK (Pepscan, Lelystad, Netherlands) if stated. After two days of stratification at 4°C in darkness, growth of seedlings were transferred to long-day conditions (16 h light with 70 μ M photons $m^{-2} s^{-1}$, 8 h dark) at 21°C and 60% humidity for the times indicated.

Cloning of constructs and generation of transgenic lines

For promoter analysis of *EXPANSIN7* (*At1g12560*), a 437 basepair-long region between position -386 to +48 relative to the translation initiation site was amplified using forward primer 5'-ACGCGCGGCCGCGTGTTCAATTTAACTAA-TCATTG-3' binding with a recognition site for *NotI* and reverse primer 5'-ACGCCTCGAGCTATTGAGAAGAATTTAAAGCT-3' with *XhoI* recognition site. Promoter activity of this region has previously been analyzed¹⁸. The amplified PCR product was ligated into pENTR1a DS, sequenced and recombined into pBGWFS7 by using the Gateway cloning system (Thermo Fisher Scientific). Cloning of the *p35S:PSKR1-GFP* construct into pB7WG2.0 has been described¹⁶. Plant transformation and selection occurred as described²⁵.

BAK1 and the kinase inactive BAK1-D434N isoform were provided by Benjamin Brandt (University of Geneva). The region from amino acid 250 to 615 of BAK1 encoding the kinase domain was generated as described⁵². Cloning of the PSKR1-kinase and of the PSKR1 kinase-inactive PSKR1-K762E isoform was described¹⁶. The cytoplasmic part of *PSKR2* (At5g53890) from amino acid 701 to 1036 was amplified with primers 5'-GTTATTGTCGACAGGATTTCAAGAAAAG-ATGTGG-3' and 5'-GAGTGCCCTAGGTCATTGTTGTTGAACAGACTC-3' containing *Sa*I and *Av*rII sites. An inactivating point mutation was introduced in the PSKR2 kinase domain with oligonucleotides 5'-GCAGCAGTCGAGAGGCTTTC-3' and 5'-GAAAGCCTCTCGAC-TGCTGC-3' as described²⁵ to replace Lys by Glu at position 782.

Preparation and analysis of cross sections and GUS staining

To identify hair cells, we employed *EXP7* as a marker gene. *pEXP7:GUS* seedlings were grown on plates for five days, collected and stained with GUS staining solution⁵³. Roots were separated from shoots and embedded in TechnoVit (Kulzer) as described in the manufacturer's manual. Cross sections of 10 μ m thickness were prepared with a Leica RM 2255 microtome, collected on glass slides and embedded in CV Mount solution (Leica) and analyzed with an Olympus BX41 microscope. Pictures were taken with an Infinity 3S camera using the software Infinity Analyze 6.5 (Lumenera). The number of epidermal and cortical cells were counted on pictures of cross sections. The cross section area was determined with Fiji/ImageJ open-source software (<https://imagej.net/Fiji>) from the same pictures.

RNA isolation and gene expression analyses

For microarray and qPCR analyses, roots from five-day-old seedlings that were grown on plates supplemented with or without 1 μ M PSK under sterile condition were used. Knockout or overexpression, respectively, of PSKR1 and PSKR2 was verified by RT-PCR from seedlings. Total RNA was isolated with TRI-reagent (Sigma Aldrich, St. Louis, USA) following manufacturer's instructions. The quality and quantity of RNA, dissolved in DEPC-treated H₂O, was measured with a NanoDrop spectrometer (ThermoFisher). Microarray experiments were performed with three biological replicates of three samples each, wt, *tpst-1* and *tpst-1* treated with 1 μ M PSK. AraGene-1_0-st; Affymetrix microarray slides containing

38408 transcripts were used for transcriptome analysis. Analysis of RNA quality, chip hybridization, and data processing were performed at the MicroArray Facility (Flanders Institute for Biotechnology (VIB), Leuven, Belgium). Briefly, analysis was based on the RMA expression values. To identify differentially expressed genes, the Robust Multi-Array Average (RMA) expression values at the different conditions were compared with the LIMMA package of Bioconductor (Smyth, 2004; Smyth, 2005). For each contrast of interest, it was tested if it deviated significantly from 0 with a moderated t statistic implemented in LIMMA. The resulting P values were corrected for multiple testing with Benjamini-Hochberg to control the false discovery rate (Benjamini and Hochberg (1995)). All P values given were corrected for multiple testing. A cutoff at a P value of 0.001 was used to indicate differentially expressed genes combined with a cutoff at fold change of two.

For RT-PCR and qPCR 1 μ g mRNA was digested with DNaseI and subsequently reverse-transcribed with OligodT primer. Quantitative PCR was performed with the Rotor-Gene SYBR Green PCR Kit (Qiagen, Venlo, Netherlands) according to manufacturer's instructions. The reverse transcription products were amplified using gene-specific primers as indicated in Supplementary Table 5. Reactions were performed with a Rotor Gene Q cycler (Qiagen, Venlo, Netherlands). Data (takeoff and efficiencies) was given by 'Comparative quantification analysis' from the cycler-corresponding Rotor Gene Q Series software (Qiagen). The fold change was calculated by normalization to the geometric mean of *ACT2* and *GAPC* expression. For statistical analysis \log_2 -transformed fold change values were used. At least three independent biological replicates with technical repeats each were performed.

Western blot analysis

To analyze protein abundance of PSKR1-GFP in *p35S:PSKR1-GFP tpst-1* lines, 500 mg shoot material from 22-day-old soil-grown plants were ground in liquid nitrogen with a mortar and pestle. Frozen ground powder was mixed with 1 mL cracking buffer (60 mM Tris pH 6.8, 10% (v/v) glycerol, 1% (v/v) β -mercapto ethanol, 4% (w/v) sodium dodecyl sulfate, 0.01% (w/v) bromophenol blue) for 1.5 min and shaken for 5 min at 4°C and 1100 rpm in a thermomixer. Subsequently, samples were heated for 10 min at 95°C under constant shaking

of 1100 rpm to solubilize membrane-bound PSKR1-GFP. To clear the solution, the mixture was centrifuged twice at 1.500xg for 3 min at 4°C. 800 µL of the supernatant were transferred to a new tube after the first round of centrifugation and 300 µL were transferred the second time. As a positive control, a sample with 10 ng rGFP (Roche) was included. Of each sample, 25 µL of supernatant or rGFP were separated on an SDS- 10% polyacrylamide gel and then transferred onto a PVDF membrane at 50 mA for 1.5 h. rGFP and GFP fusion proteins were detected using monoclonal anti-GFP antibodies (Roche, Cat. No. 11814460001) diluted 1:1000 and anti-mouse antibodies linked to horseradish peroxidase (Pierce #33230) at a dilution of 1:50.000. The signal was visualized using the ECL detection kit (Pierce #32132).

***In vitro* kinase assay and analysis of phosphorylation sites**

Expression and purification of active PSKR1, PSKR2, BAK1 kinases and of their inactive isoforms PSKR1-K762E, PSKR2-K782E and BAK1-D434N were performed as described⁵⁴. For transphosphorylation assays with ³²P-ATP, 1 µg of purified protein was used per each reaction as described⁵⁴. PSKR1-KD and PSKR2-KD have similar size and if incubated together and separated on a gel the protein bands overlap. In this case both proteins were excised from dried gel together and measured as one sample. For calculation of transphosphorylation on the inactive kinase the measured signal of the active kinase in the co-incubation sample was subtracted. For phosphosite analysis, 5 µg of protein was incubated without radiolabeled ATP and analyzed^{55,56}. Phosphorylation sites were marked as ambiguous when the localization probability (L.P.) was below 0.5.

***In silico* protein-protein docking**

For docking by ClusPro 2.0⁵⁷ the PSKR1 homology model²⁵ was defined as the receptor. BAK1 structure was obtained from the multimeric PDB entry 3TL8 because this has the best crystallized structure and was defined as the ligand for docking. The model with the highest cluster population size was chosen since the cluster size is proportional with its probability⁵⁷. The model of PSKR1 and BAK1 docking is visualized with PyMol 2 (Schrödinger, LLC).

Statistical analysis

Data sets were analyzed for normal distribution. In case of normal distribution for all-pairwise comparison, an ANOVA with $\alpha=0.05$ was run with Origin 8.5 software, whereas data sets that were not normally distributed were analyzed with a Kruskal–Wallis test with Bonferroni as *P*-value adjustment method ($\alpha=0.05$) by using the package “agricolae”⁵⁸ and statistics software R (<https://CRAN.R-project.org/doc/FAQ/R-FAQ.html>).

Acknowledgment

We would like to thank Benjamin Brandt for providing BAK1-expressing bacteria. This work was funded by the Deutsche Forschungsgemeinschaft (DFG) through grants SA 495/13-1 and SA 495/13-2.

Author contributions

MS conceived the project. CK and MS designed experiments. NS performed initial characterization of *tpst-1 pskr1-3 pskr2-1* and performed microarray experiment. LDV and IS performed mass spectrometry. CK performed all other experiments and analyses. CK and MS wrote manuscript.

Materials & Correspondence

Margret Sauter, msauter@bot.uni-kiel.de

Competing interests

Authors declare no competing financial interest.

References

1. Matsubayashi, Y. & Sakagami, Y. Phytosulfokine, sulfated peptides that induce the proliferation of single mesophyll cells of *Asparagus officinalis* L. *Proc. Natl. Acad. Sci. U. S. A.* **93**, 7623–7627 (1996).
2. Kutschmar, A. *et al.* PSK- α promotes root growth in Arabidopsis. *New Phytol.* **181**, 820–831 (2009).
3. Stührwohldt, N. *et al.* Phytosulfokine peptide signaling controls pollen tube growth and funicular pollen tube guidance in *Arabidopsis thaliana*. *Physiol. Plant.* **153**, 643–653 (2014).
4. Mosher, S. *et al.* The tyrosine-sulfated peptide receptors PSKR1 and PSY1R modify the immunity of Arabidopsis to biotrophic and necrotrophic pathogens in an antagonistic manner. *Plant J.* **73**, 469–482 (2013).
5. Matsubayashi, Y., Ogawa, M., Kihara, H., Niwa, M. & Sakagami, Y.

- Disruption and overexpression of Arabidopsis phytosulfokine receptor gene affects cellular longevity and potential for growth. *Plant Physiol.* **142**, 45–53 (2006).
6. Komori, R., Amano, Y., Ogawa-Ohnishi, M. & Matsubayashi, Y. Identification of tyrosylprotein sulfotransferase in Arabidopsis. *Proc. Natl. Acad. Sci. U. S. A.* **106**, 15067–15072 (2009).
 7. Sauter, M. Phytosulfokine peptide signalling. *J. Exp. Bot.* **66**, 5161–5169 (2015).
 8. Matsubayashi, Y., Hanai, H., Hara, O. & Sakagami, Y. Active fragments and analogs of the plant growth factor, phytosulfokine: Structure–activity relationships. *Biochem. Biophys. Res. Commun.* **225**, 209–214 (1996).
 9. Kwezi, L. *et al.* The phytosulfokine (PSK) receptor is capable of guanylate cyclase activity and enabling cyclic GMP-dependent signaling in plants. *J. Biol. Chem.* **286**, 22580–22588 (2011).
 10. Stührwohldt, N., Dahlke, R. I., Steffens, B., Johnson, A. & Sauter, M. Phytosulfokine- α controls hypocotyl length and cell expansion in *Arabidopsis thaliana* through phytosulfokine receptor 1. *PLOS One* **6**, e21054 (2011).
 11. Matsuzaki, Y., Ogawa-Ohnishi, M., Mori, A. & Matsubayashi, Y. Secreted peptide signals required for maintenance of root stem cell niche in Arabidopsis. *Science* **329**, 1065–1067 (2010).
 12. Wang, J. *et al.* Allosteric receptor activation by the plant peptide hormone phytosulfokine. *Nature* **525**, 265–268 (2015).
 13. Ladwig, F. *et al.* Phytosulfokine regulates growth in Arabidopsis through a response module at the plasma membrane that includes CYCLIC NUCLEOTIDE-GATED CHANNEL17, H⁺-ATPase, and BAK1. *Plant Cell* **27**, 1718–1729 (2015).
 14. Han, Z., Sun, Y. & Chai, J. Structural insight into the activation of plant receptor kinases. *Curr. Opin. Plant Biol.* **20**, 55–63 (2014).
 15. Hartmann, J., Stührwohldt, N., Dahlke, R. I. & Sauter, M. Phytosulfokine control of growth occurs in the epidermis, is likely to be non-cell autonomous and is dependent on brassinosteroids. *Plant J.* **73**, 579–90 (2013).
 16. Hartmann, J., Fischer, C., Dietrich, P. & Sauter, M. Kinase activity and calmodulin binding are essential for growth signaling by the phytosulfokine receptor PSKR1. *Plant J.* **78**, 192–202 (2014).
 17. Salazar-Henao, J. E., Vélez-Bermúdez, I. C. & Schmidt, W. The regulation and plasticity of root hair patterning and morphogenesis. *Development* **143**, 1848–1858 (2016).
 18. Cho, H.-T. & Cosgrove, D. J. Regulation of Root Hair Initiation and Expansin Gene Expression in Arabidopsis. *Plant Cell* **14**, 3237–3253 (2002).

19. Ma, Z., Bielenberg, D. G., Brown, K. M. & Lynch, J. P. Regulation of root hair density by phosphorus availability in *Arabidopsis thaliana*. *Plant, Cell Environ.* **24**, 459–467 (2001).
20. Lee, M. M. & Schiefelbein, J. WEREWOLF, a MYB-related protein in *Arabidopsis*, is a position-dependent regulator of epidermal cell patterning. *Cell* **99**, 473–483 (1999).
21. Matsui, K., Hiratsu, K., Koyama, T., Tanaka, H. & Ohme-Takagi, M. A chimeric AtMYB23 repressor induces hairy roots, elongation of leaves and stems, and inhibition of the deposition of mucilage on seed coats in *Arabidopsis*. *Plant Cell Physiol.* **46**, 147–155 (2005).
22. Deal, R. B. & Henikoff, S. A simple method for gene expression and chromatin profiling of individual cell types within a tissue. *Dev. Cell* **18**, 1030–1040 (2010).
23. Hassan, H., Scheres, B. & Blilou, I. JACKDAW controls epidermal patterning in the *Arabidopsis* root meristem through a non-cell-autonomous mechanism. *Development* **137**, 1523–1529 (2010).
24. Moore, K. L. Protein tyrosine sulfation: a critical posttranslational modification in plants and animals. *Proc. Natl. Acad. Sci. U. S. A.* **106**, 14741–14742 (2009).
25. Kaufmann, C., Motzkus, M. & Sauter, M. Phosphorylation of the phytosulfokine peptide receptor PSKR1 controls receptor activity. *J. Exp. Bot.* **68**, 1411–1423 (2017).
26. Hartmann, J., Linke, D., Bönninger, C., Tholey, A. & Sauter, M. Conserved phosphorylation sites in the activation loop of the *Arabidopsis* phytosulfokine receptor PSKR1 differentially affect kinase and receptor activity. *Biochem. J.* **472**, 379–391 (2015).
27. Irving, H. R., Kwezi, L., Wheeler, J. I. & Gehring, C. Moonlighting kinases with guanylate cyclase activity can tune regulatory signal networks. *Plant Signal. Behav.* **7**, 201–204 (2012).
28. Mitra, S. K. *et al.* An autophosphorylation site database for leucine-rich repeat receptor-like kinases in *Arabidopsis thaliana*. *Plant J.* **82**, 1042–1060 (2015).
29. Muleya, V. *et al.* Phosphorylation of the dimeric cytoplasmic domain of the phytosulfokine receptor, PSKR1. *Biochem. J.* **473**, 3081–3098 (2016).
30. Schulze, B. *et al.* Rapid heteromerization and phosphorylation of ligand-activated plant transmembrane receptors and their associated kinase BAK1. *J. Biol. Chem.* **285**, 9444–9451 (2010).
31. Sun, Y. *et al.* Structural basis for flg22-induced activation of the *Arabidopsis* FLS2-BAK1 immune complex. *Science* **342**, 624–628 (2013).
32. Koller, T. & Bent, A. F. FLS2-BAK1 extracellular domain interaction sites required for defense signaling activation. *PLOS One* **9**, e111185 (2014).

33. Roux, M. *et al.* The Arabidopsis Leucine-Rich Repeat Receptor–Like Kinases BAK1/SERK3 and BKK1/SERK4 Are Required for Innate Immunity to Hemibiotrophic and Biotrophic Pathogens. *Plant Cell* **23**, 2440–2455 (2011).
34. Tang, J. *et al.* Structural basis for recognition of an endogenous peptide by the plant receptor kinase PEPR1. *Cell Res.* **25**, 110–120 (2015).
35. Yamada, K. *et al.* Danger peptide receptor signaling in plants ensures basal immunity upon pathogen-induced depletion of BAK1. *Eur. Mol. Biol. Organ. J.* **35**, 46–61 (2016).
36. Meng, X. *et al.* Ligand-induced receptor-like kinase complex regulates floral organ abscission in Arabidopsis. *Cell Rep.* **14**, 1330–1338 (2016).
37. Wang, X. *et al.* Sequential transphosphorylation of the BRI1/BAK1 receptor kinase complex impacts early events in brassinosteroid signaling. *Dev. Cell* **15**, 220–235 (2008).
38. Bücherl, C. A. *et al.* Visualization of BRI1 and BAK1(SERK3) membrane receptor heterooligomers during brassinosteroid signaling. *Plant Physiol.* **162**, 1911–1925 (2013).
39. Hutten, S. J. *et al.* Visualization of BRI1 and SERK3/BAK1 nanoclusters in Arabidopsis roots. *PLOS One* **12**, e0169905 (2017).
40. Li, Z. *et al.* Two SERK receptor-like kinases interact with EMS1 to control anther cell fate determination. *Plant Physiol.* **173**, 326–337 (2017).
41. Meng, X. *et al.* Differential function of Arabidopsis SERK family receptor-like kinases in stomatal patterning. *Curr. Biol.* **25**, 2361–2372 (2015).
42. Jordá, L. *et al.* ERECTA and BAK1 receptor like kinases interact to regulate immune responses in Arabidopsis. *Front. Plant Sci.* **7**, 897 (2016).
43. Wang, J. *et al.* Structural insights into the negative regulation of BRI1 signaling by BRI1-interacting protein BKI1. *Cell Res.* **24**, 1328–1341 (2014).
44. Wu, X. *et al.* Transphosphorylation of *E. coli* proteins during production of recombinant protein kinases provides a robust system to characterize kinase specificity. *Front. Plant Sci.* **3**, 262 (2012).
45. Adams, J. A. Activation loop phosphorylation and catalysis in protein kinases: Is there functional evidence for the autoinhibitor model? *Biochemistry* **42**, 601–607 (2003).
46. Taylor, S. S. & Kornev, A. P. Protein kinases: Evolution of dynamic regulatory proteins. *Trends Biochem. Sci.* **36**, 65–77 (2011).
47. Endicott, J. A., Noble, M. E. M. & Johnson, L. N. The structural basis for control of eukaryotic protein kinases. *Annu. Rev. Biochem.* **81**, 587–613 (2012).
48. Moffett, A. S., Bender, K. W., Huber, S. C. & Shukla, D. Molecular

- dynamics simulations reveal the conformational dynamics of *Arabidopsis thaliana* BRI1 and BAK1 receptor-like kinases. *J. Biol. Chem.* **292**, 12643–12652 (2017).
49. Segonzac, C. *et al.* Negative control of BAK1 by protein phosphatase 2A during plant innate immunity. *EMBO J.* **33**, 1–11 (2014).
 50. Bender, K. *et al.* Glutaredoxin *AtGRXC2* catalyzes inhibitory glutathionylation of Arabidopsis BRI1-associated receptor-like kinase 1 (BAK1) in vitro. *Biochem. J.* **467**, 399–413 (2015).
 51. Amano, Y., Tsubouchi, H., Shinohara, H., Ogawa, M. & Matsubayashi, Y. Tyrosine-sulfated glycopeptide involved in cellular proliferation and expansion in Arabidopsis. *Proc. Natl. Acad. Sci. U. S. A.* **104**, 18333–18338 (2007).
 52. Bojar, D. *et al.* Crystal structures of the phosphorylated BRI1 kinase domain and implications for brassinosteroid signal initiation. *Plant J.* **78**, 31–43 (2014).
 53. Weigel, D. & Glazebrook, J. *Arabidopsis: A laboratory manual*. (Cold Spring Harbor, NY: Cold Spring Harbor Laboratory Press, 2002).
 54. Kaufmann, C. & Sauter, M. in *Plant Receptor Kinases* (ed. Aalen, R. B.) **1621**, 151–159 (Springer Protocols, 2017).
 55. Vu, L. D. *et al.* Up-to-date workflow for plant (phospho)proteomics identifies differential drought-responsive phosphorylation events in maize leaves. *J. Proteome Res.* **15**, 4304–4317 (2016).
 56. Ueda, M. *et al.* Transcriptional integration of paternal and maternal factors in the Arabidopsis zygote. *Genes Dev.* **31**, 617–627 (2017).
 57. Kozakov, D. *et al.* The ClusPro web server for protein-protein docking. *Nat. Protoc.* **12**, 255–278 (2017).
 58. de Mendiburu, F. *agricolae: Statistical Procedures for Agricultural Research*. (2016). at <<http://cran.r-project.org/package=agricolae>>

Figure legends

Figure 1: Overexpression of *PSKR1* but not *PSKR2* in *tpst-1* background leads to enhanced root growth despite absence of receptor ligand. (a-c) Mean root length (\pm SEM) of five-day-old seedlings grown under sterile conditions on plates supplemented without or with with 1 μ M PSK. Numbers indicate independent transgenic lines. (a) Short-root phenotype of *tpst-1* is partially rescued by *p35S:PSKR1-GFP* construct. Capital letters indicate significant difference (ANOVA, $P < 0.05$). ($n > 121$) (b) All independent transgenic lines with the same construct show significant longer roots than *tpst-1*. Lines respond to PSK with further elongation up to saturation of PSK-inducible elongation. Significant differences between lines and *tpst-1* as control group are indicated by an asterisk* and treated with PSK by a circle^o (Kruskal-Wallis, $P < 0.05$). ($n > 30$) (c) Triple knockout of *TPST*, *PSKR1* and *PSKR2* is insensitive for PSK and shows even decreased root length compared to *tpst-1*. Lowercase letters indicate significant differences (Kruskal-Wallis, $P < 0.05$). $n > 46$. (d) *PSKR1-GFP* appearance from lines analyzed in (a-b) investigated with anti-GFP Western Blot of 22-days-old shoot material. rGFP=recombinant GFP as positive detection control. (e) Lateral root density is affected by lack of sulfated peptides and intensified in *tpst-1 pskr1-3 pskr2-1* measured on 12-days-old seedlings grown on plates. ($n > 45$; Kruskal-Wallis, $P < 0.05$). (f) Phenotypes of three-week-old wt, *tpst-1* and *tpst-1 pskr1-3 pskr2-1* plants grown on plates under sterile conditions supplemented with or without 1 μ M PSK.

Figure 2: Absence of sulfated peptides lead to increase of root hair formation by altered position-dependent epidermal cell fate determination.

(a) Overview of root surface, autofluorescence; scale bar= 100 μ m (b) CLSM Z-stack of membrane-dye (FM4-64) stained *tpst-1* roots illustrate normal hair morphogenesis (c) Quantification of trichoblasts from crosssections; $n > 9$ (d) Representative cross sections of 5-day-old GUS-stained seedlings; scale bar=50 μ m (e-f) Cartoon showing position of trichoblasts to cortical cells (e) Trichoblasts are in H position in case of wt and *pskr1-3 pskr2-1* (f) Deregulated trichoblast/H-cell-pattern in *tpst-1* and *tpst-1 pskr1-3 pskr2-1*

(g) Increase of root thickness for *tpst-1* and *tpst-1 pskr1-3 pskr2-1* (h) Ratio of epidermal and cortical cells remains constant; $n > 9$ (i-l) Transcriptional evidence in \log_2 fold change (FC) for cell fate shift from less a- towards more trichoblasts (i) Microarray data in fold change (j) Expression location of analyzed genes shown in cartoon zoom (k) qPCR data for atrichoblast-specific genes. Significant differences are displayed between genotypes with small, capital and greek letters, whereas asterisks indicate significant differences between *tpst-1* and *tpst-1* treated with 1 μ M PSK. $n=6$ Kruskal-Wallis $p < 0.05$.

Figure 3: BAK1 transphosphorylates PSK receptors. *In vitro* kinase assay with PSKR1, PSKR2 and BAK1. Active wildtype and inactive point-mutated kinase isoforms (indicated by *) were incubated sole to test their autophosphorylation ability and in combinations of an active together with an inactive protein to test their transphosphorylation ability for offered substrate (inactive kinase). (a) autoradiograph (top) and coomassie-stained gel (bottom) (b-d) ^{32}P signal caused by kinase activity quantified by liquid scintillation counting performed from samples shown in (a). In samples with combinations the quantification of underlined component is shown. $n=6-8$; all pairwise comparison Kruskal-Wallis, $P < 0.05$.

Figure 4: Phosphosites on PSK receptors are the same when autophosphorylated or when transphosphorylated by BAK1. BAK1 transphosphorylation sites on PSKRs overlap greatly with phosphorylation sites caused by PSKRs autophosphorylation and are found all over the kinase subdomains, whereas PSKRs transphosphorylate BAK1 only in the activation segment. An overview of mapped phosphorylation sites from this study (framed bold-type) and other previous published studies for (a) PSKR1, (b) PSKR2 and (d) BAK1. Sites were identified: x=ambiguously; X=unambiguously. (c), (e) Summarizing cartoons.

Figure 1

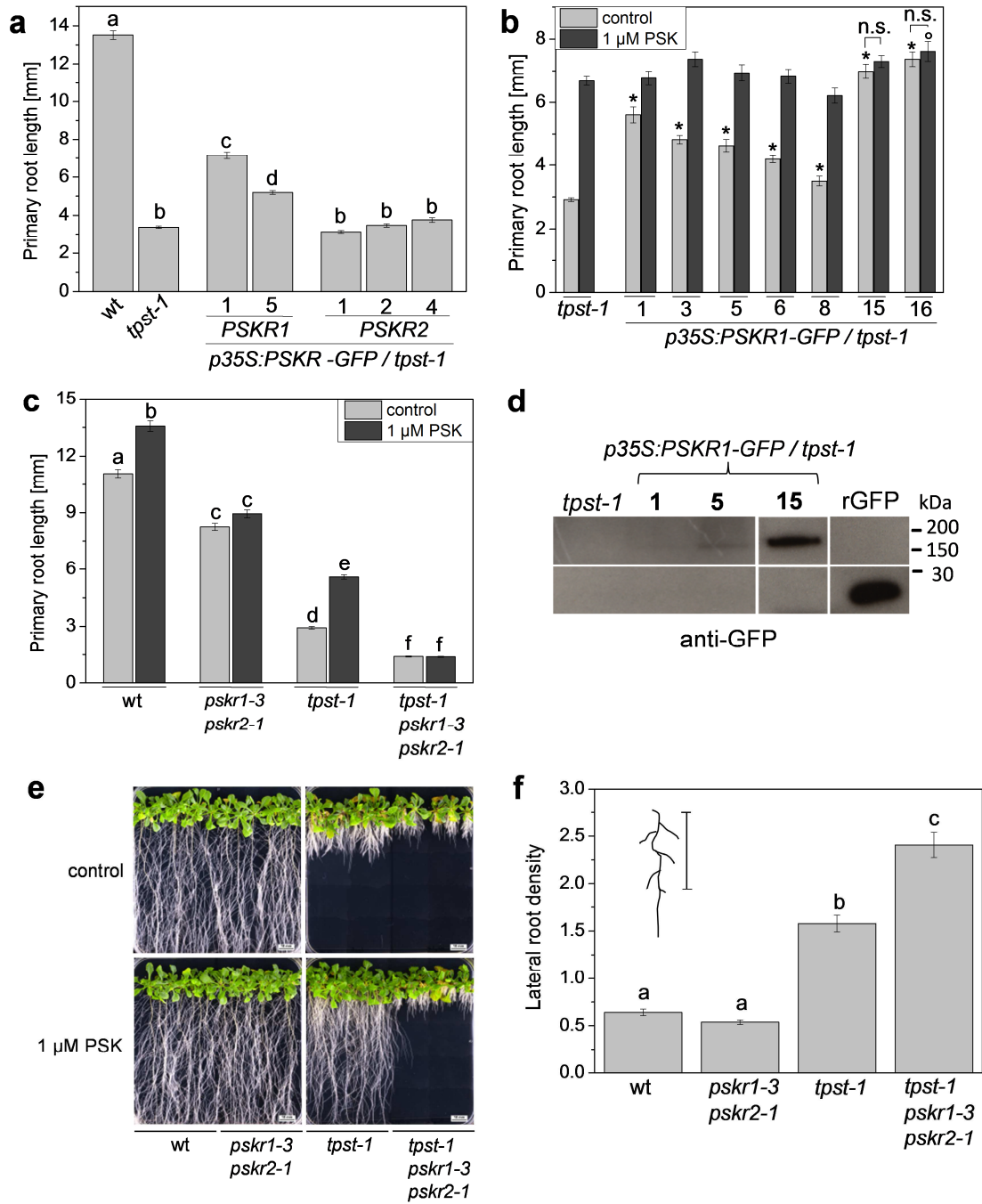


Figure 2

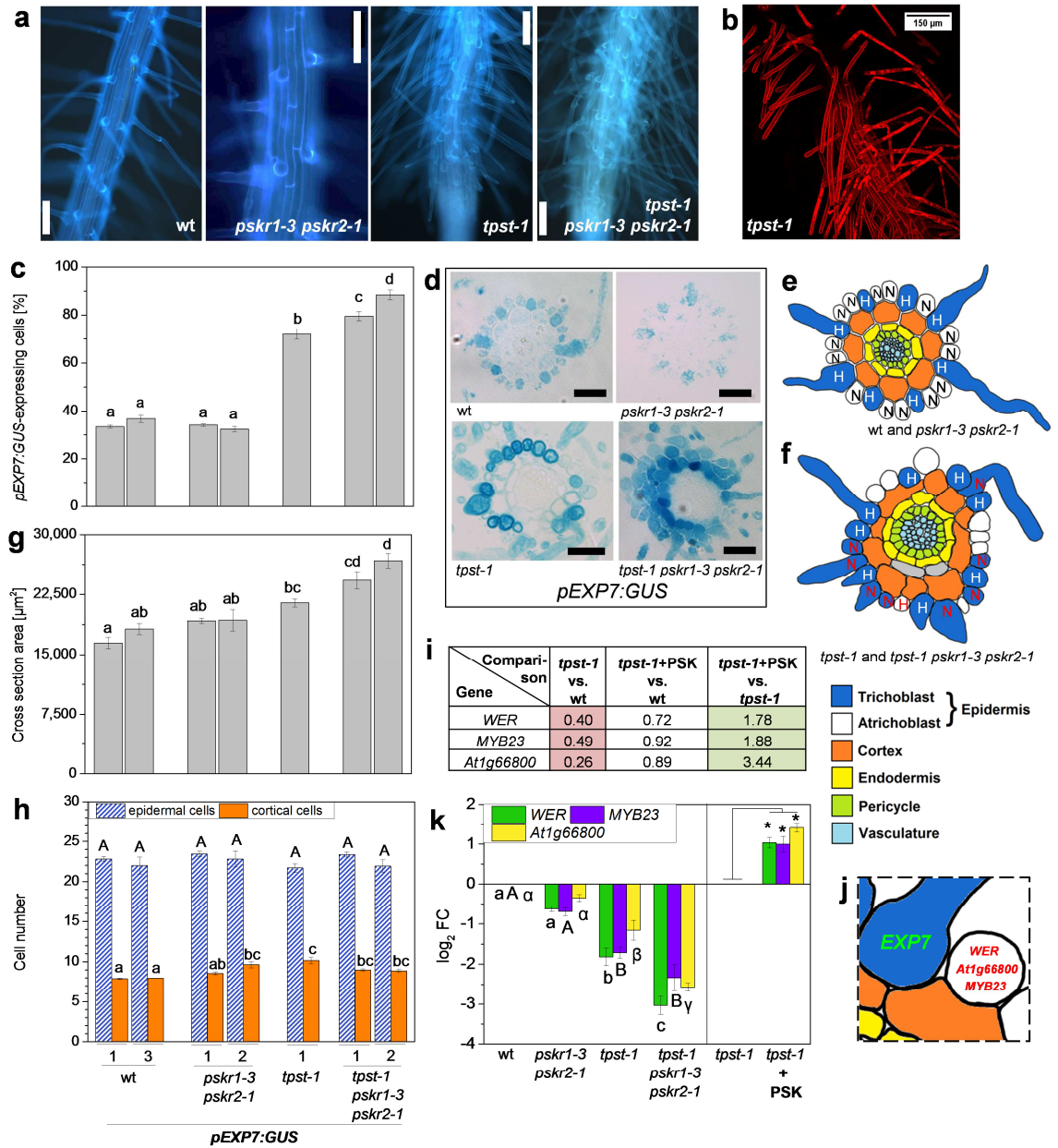


Figure 3

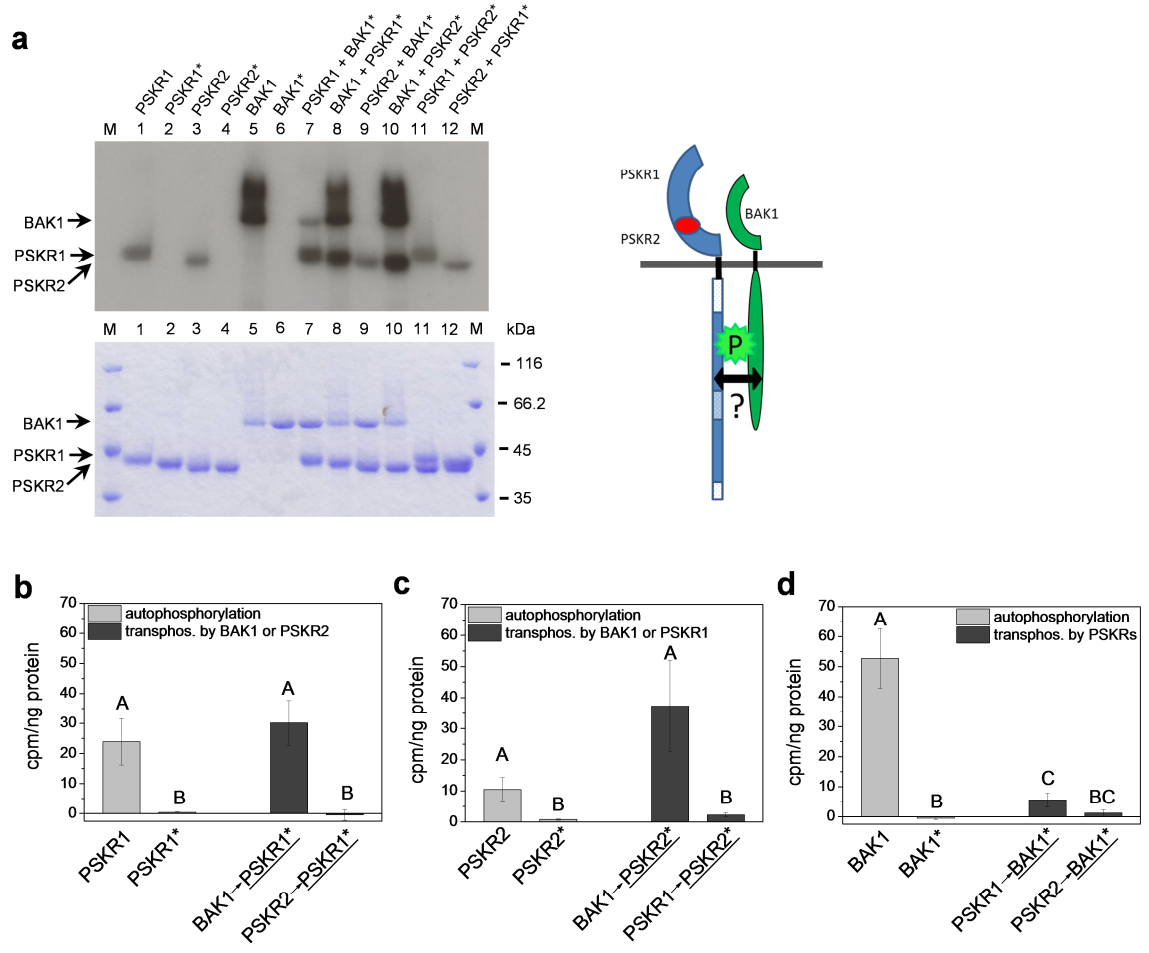
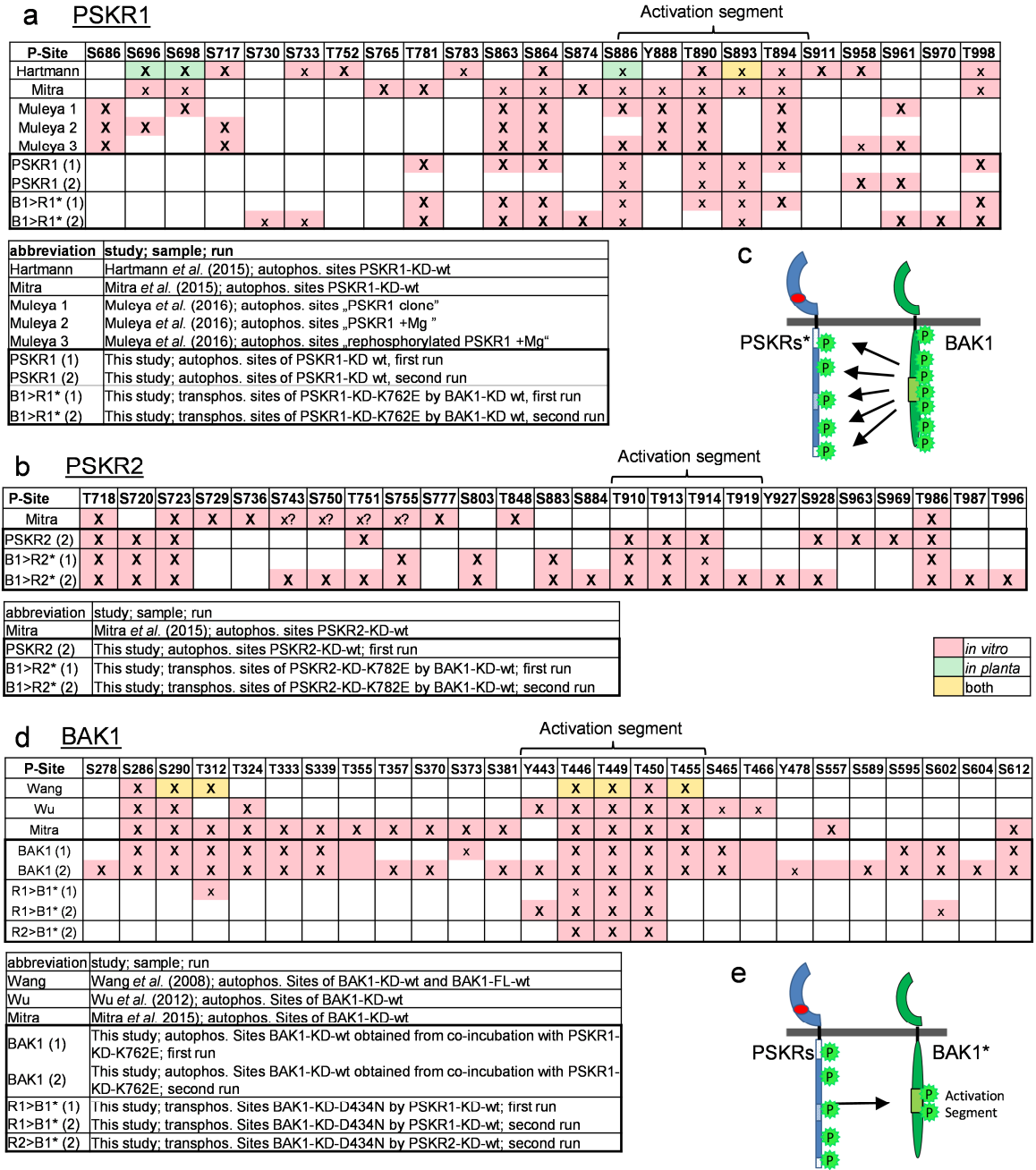
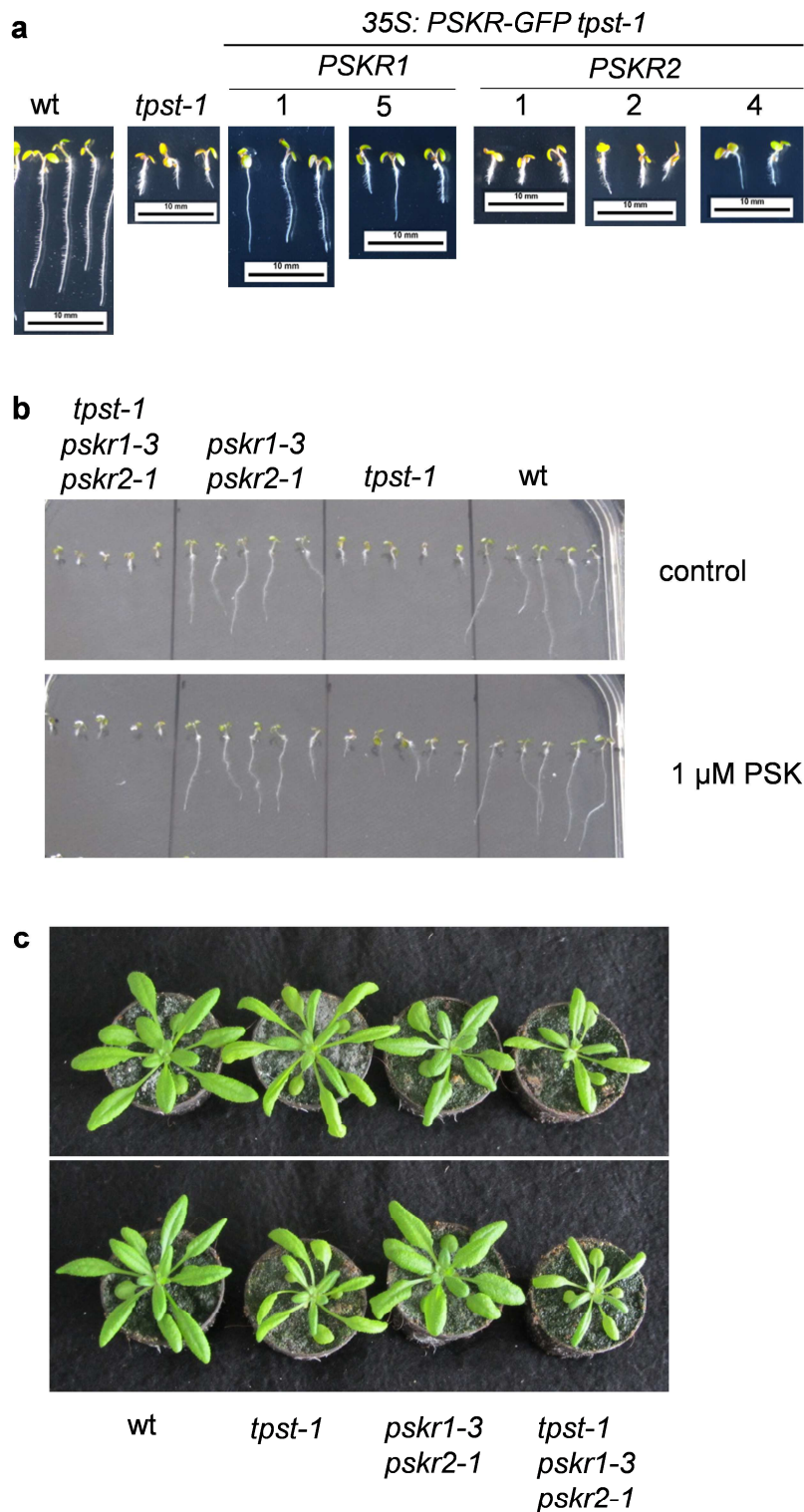


Figure 4

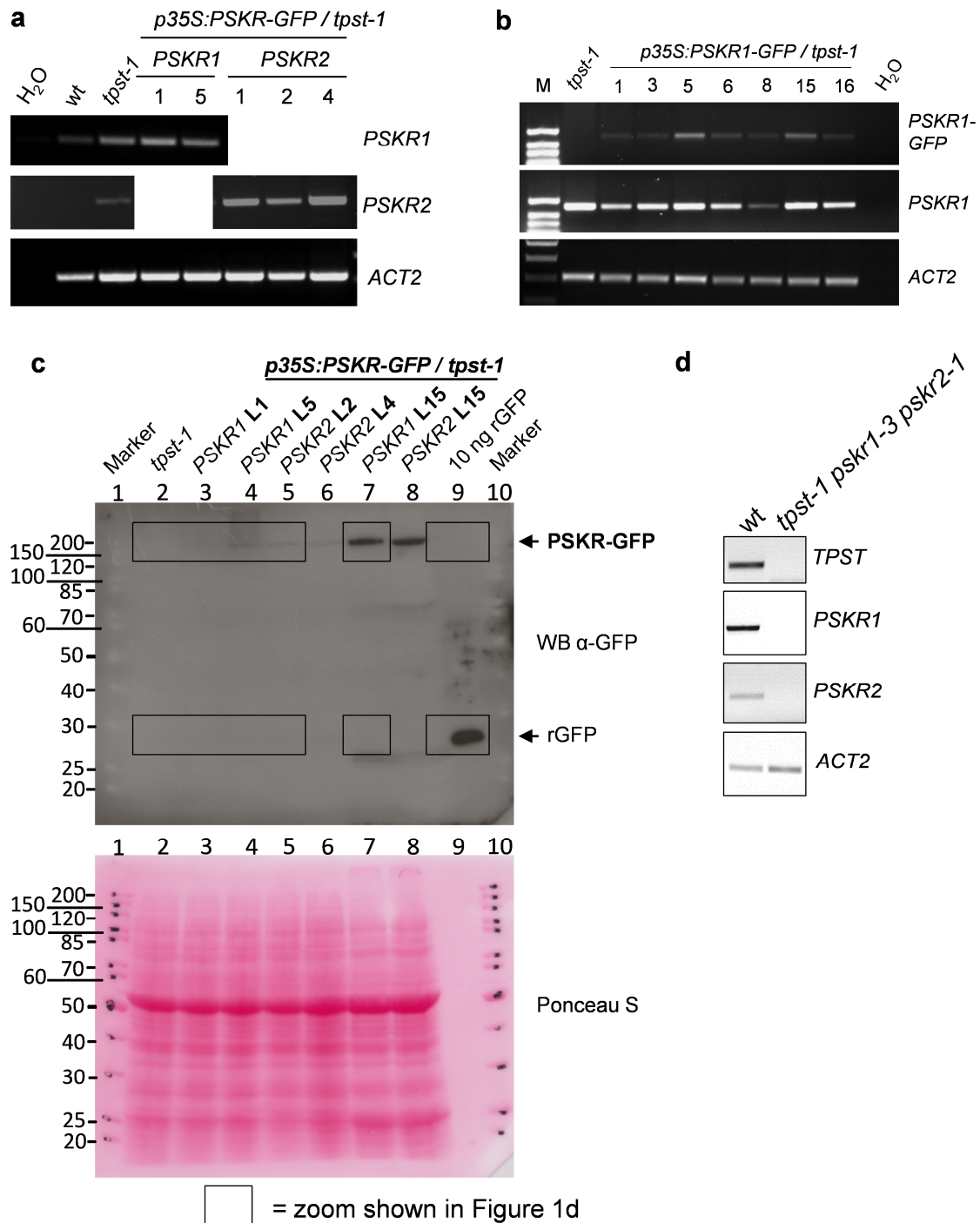


Supplementary Figure 1



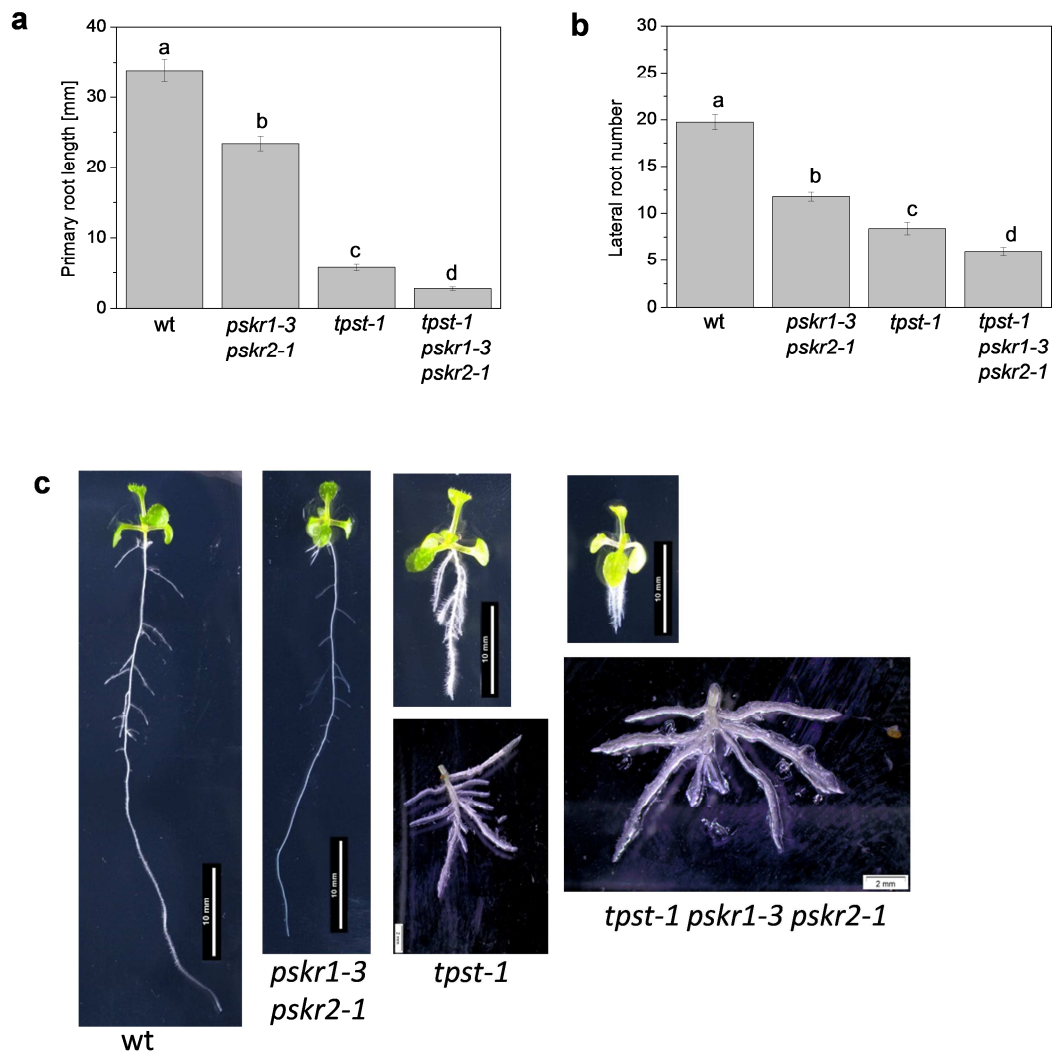
Suppl. Figure 1: Representative phenotypes from used lines. (a-b) 5-day-old seedlings grown on plates under sterile conditions. **(c)** 4-week-old soil grown plant *wt*, *tpst-1*, *pskr1-3 pskr2-1* and *tpst-1 pskr1-3 pskr2-1*.

Supplementary Figure 2



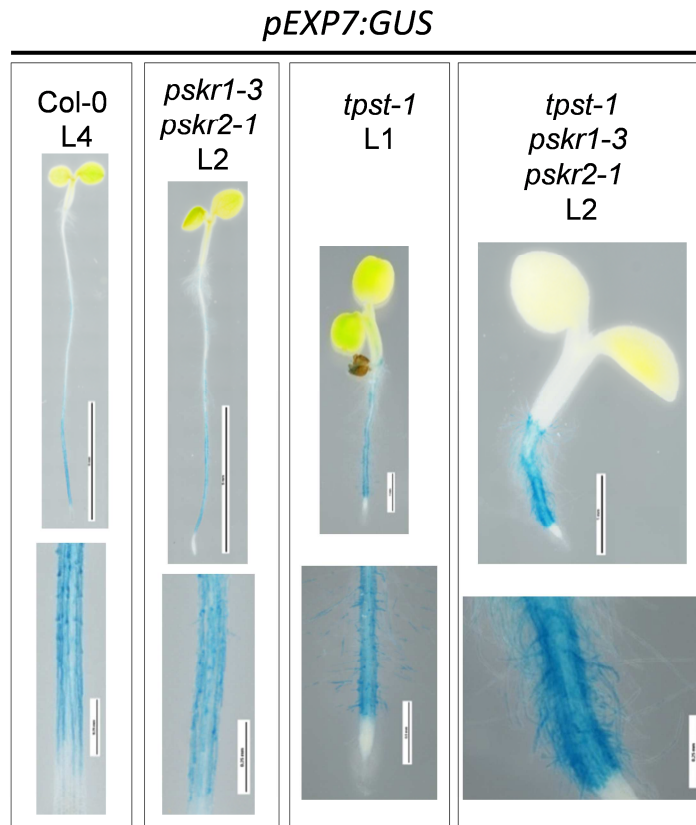
Suppl. Figure 2: Expression analyses of used lines. (a)-(c) Expression of *TPST*, *PSKR1* and *PSKR2* was analyzed by RT-PCR in 5-day-old seedlings from wild type (*wt*), *tpst-1*, *tpst-1 pskr1-3 pskr2-1* and various independent *35S:PSKR1-GFP* and *35S:PSKR2-GFP* lines in *tpst-1* background. *ACTIN2* cDNA was amplified as a control for RNA input. (d) Analysis of *PSKR-GFP* fusion protein presence in analyzed lines by GFP-tag detecting western blot.

Supplementary Figure 3



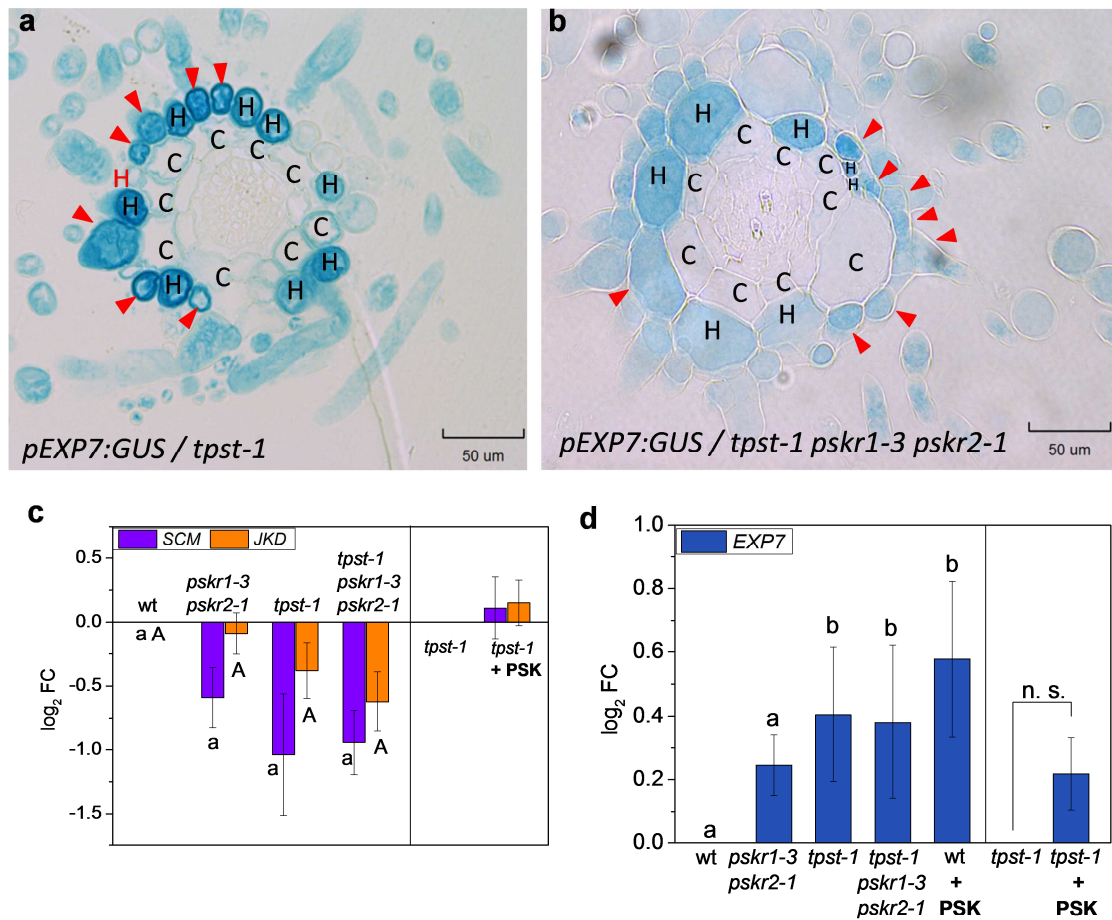
Suppl. Figure 3: Lack of sulfated peptides affects lateral root growth. (a) Mean primary root length and (b) number of lateral roots of 12-day-old seedlings grown on plates under sterile conditions. (c) Representative seedlings of lateral root density analysis. The root and shoot were separated and lateral roots were spreaded to determine initiation sites of lateral roots.

Supplementary Figure 4



Suppl. Figure 4: Overview of *EXP7* expression. These lines were used to analyze root hair cell fate change caused by absence of Tyr-sulfated peptides. *EXP7* is a marker gene for cells already determined as trichoblasts.

Supplementary Figure 5

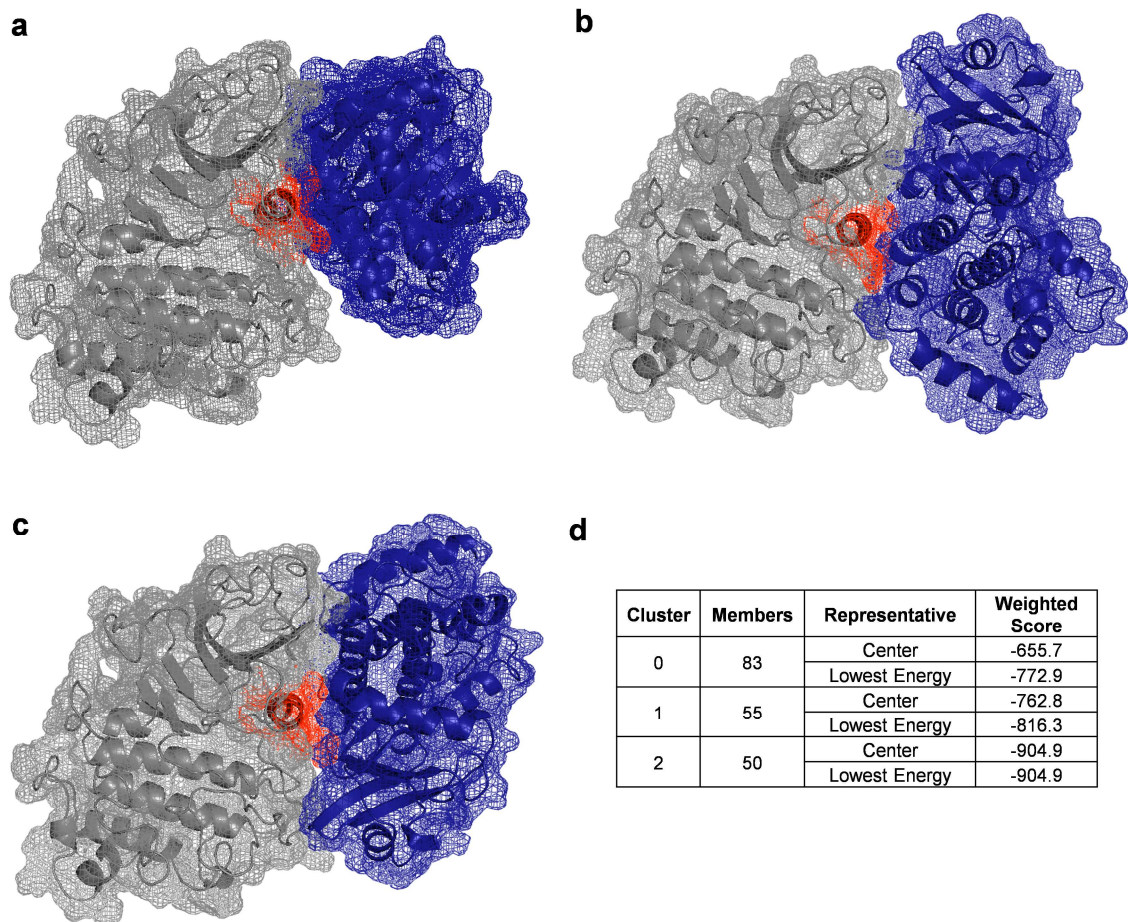


Suppl. Figure 5: The position-dependent root hair cell fate determination is changed due to lack of sulfated peptides, but expression of SCM and JKD are not significantly altered. (a-b) Cross sections of GUS-stained seedlings grown on plates for 5 days. Arrows indicate „wrongly“ *pEXP7:GUS*-expressing cells which are in the N-position. Red coloured „H“ marks a cell, which is in the H position but is not expressing *pEXP7:GUS*. **(c-d)** Quantitative transcription analysis by qPCR in 5-day-old seedlings of various genotypes and treatment of **(c)** LRR-RLK *SCRAMBLED* (SCM) and zinc-finger transcription factor *JACKDAW* (JKD). **(d)** Transcript level of *EXPANSIN7* (*EXP7*) seems to be affected by other processes than only root hair formation. PSK treatment of wild type seedlings causes root elongation and no change in root hair formation but *EXP7* transcript level is increased. *EXP7* seems to be involved in cell wall loosening for cell elongation caused by PSK. Indeed, Yu *et al.* (2016) report upregulation of several members of the Expansin protein family by overexpression of PSK4. $n=6$ Kruskal-Wallis $p<0.05$.

Reference:

Yu L, Liu Y, Liu Y, Li Q, Tang G, Luo L. 2016. Overexpression of phyto­sulfokine- α induces male sterility and cell growth by regulating cell wall development in *Arabidopsis*. Plant Cell Reports.

Supplementary Figure 6



Suppl. Figure 6: *In silico* docking results of ClusPro2.0. (a-c) The PSKR1 α C-helix (red) is involved in the PSKR1 (grey) and BAK1 (deepblue) binding interface. Protein models are shown as cartoon with the protein surface as mesh. (d) Calculated scores for ClusPro docking models shown in (a) model 0, (b) model 1 and (c) model 2 with respective cluster population member size and their weighted score by PIPER, whereby highest model probability is proportional with the biggest cluster size (model 0).

Supplementary Table 1

Suppl. Table 1: PSKR1 Phospho site evidences found by mass spectrometry.

Peptide sequence (localization probabilities of P-sites in brackets)	P-site	highest LP
PSKR1 (1) - autophosphorylation sites		
774_EFEAEVET(ph)LSR_784	T781	n.a.
860_DIKS(ph)SNILLDENFNHSLADFGLAR_883	S863	n.a.
860_DIKSS(ph)NILLDENFNHSLADFGLAR_883	S864	n.a.
884_LMS(0.234)PY(0.179)ET(0.179)HVS(0.204)T(0.204)DLVGTGLYIPPEYQQASVATYK_916	S886	0.234
884_LMS(0.297)PY(0.242)ET(0.268)HVS(0.094)T(0.094)DLVGT(0.004)LGY(0.001)IPPEYQQASVATYK_916	S886	0.297
884_LMS(0.35)PY(0.249)ET(0.295)HVS(0.049)T(0.057)DLVGTGLYIPPEYQQASVATYK_916	S886	0.35
884_LMS(0.499)PY(0.001)ET(0.499)HVSTDLVGTGLYIPPEYQQASVATYK_916	S886	0.499
884_LMS(0.079)PY(0.344)ET(0.418)HVS(0.079)T(0.079)DLVGTGLYIPPEYQQASVATYK_916	T890	0.418
884_LMS(0.072)PY(0.36)ET(0.423)HVS(0.072)T(0.072)DLVGTGLYIPPEYQQASVATYK_916	T890	0.423
884_LMS(0.041)PY(0.232)ET(0.26)HVS(0.232)T(0.232)DLVGT(0.002)LGYIPPEYQQASVATYK_916	T890	0.26
884_LMS(0.216)PY(0.315)ET(0.373)HVS(0.079)T(0.017)DLVGTGLYIPPEYQQASVATYK_916	T890	0.373
884_LMS(0.39)PY(0.333)ET(0.36)HVS(0.45)T(0.45)DLVGT(0.014)LGY(0.002)IPPEYQQASVATYK_916	S886,S893	0.39, 0.45
884_LMS(0.209)PY(0.158)ET(0.182)HVS(0.209)T(0.242)DLVGTGLYIPPEYQQASVATYK_916	T894	0.242
884_LMS(0.052)PY(0.188)ET(0.216)HVS(0.249)T(0.287)DLVGT(0.009)LGYIPPEYQQASVATYK_916	T894	0.287
994_QRPT(0.443)T(0.557)QQLVSWLDDV_1008	T998	0.557
PSKR1 (2) - autophosphorylation sites		
884_LMS(0.055)PY(0.217)ET(0.242)HVS(0.242)T(0.242)DLVGT(0.001)LGYIPPEYQQASVATYK_916	T890	0.242
884_LMS(0.361)PY(0.339)ET(0.361)HVS(0.464)T(0.464)DLVGT(0.008)LGY(0.003)IPPEYQQASVATYK_916	S886, S893	0.361, 0.464
954_MKHES(0.997)RAS(0.003)EVFDPLIYSK_971		0.997
954_MKHES(0.986)RAS(0.014)EVFDPLIYSK_971		0.986
954_MKHES(0.984)RAS(0.016)EVFDPLIYSK_971	S958	0.984
954_MKHES(0.5)RAS(0.5)EVFDPLIYSK_971		0.5
951_VVKMKHES(0.489)RAS(0.511)EVFDPLIY_969		0.511
951_VVKMKHES(0.405)RAS(0.595)EVFDPLIY_969	S961	0.595
BAK1 > PSKR1* (1) - transphosphorylation sites		
774_EFEAEVET(0.743)LS(0.257)R_784	T781	0.783
860_DIKS(0.959)S(0.041)NILLDENFNHSLADFGLAR_883	S863	0.959
860_DIKS(0.249)S(0.751)NILLDENFNHSLADFGLAR_883	S864	0.751
884_LMS(0.334)PY(0.254)ET(0.291)HVS(0.056)T(0.064)DLVGTGLYIPPEYQQASVATYK_916	S886	0.334
884_LMSPYET(ph)HVSTDLVGTGLYIPPEYQQASVATYK_916	T890	n. a.
884_LMS(0.018)PY(0.053)ET(0.063)HVS(0.187)T(0.668)DLVGT(0.01)LGYIPPEYQQASVATYK_916	T894	0.668
884_LMSPYETHVST(ph)DLVGTGLYIPPEYQQASVATYK_916	T894	n. a.
994_QRPTT(ph)QQLVSWLDDV_1008	T998	n. a.
BAK1 > PSKR1* (2) - transphosphorylation sites		
716_QSNDKELSYDDLDS(0.425)T(0.425)NS(0.151)FDQANIIGCGGF_745	S730	0.425
716_QSNDKELSYDDLDS(0.333)T(0.333)NS(0.333)FDQANIIGCGGF_745	S733	0.333
764_LSGDCGQIEREFEEAEVET(0.984)LS(0.016)R_784	T781	0.984
848_LHEGCDPHILHRDIKS(0.5)S(0.5)NILLDENFNHSLADF_879		0.5
860_DIKS(0.997)S(0.003)NILLDENFNHSLADFGLAR_883	S863	0.997
860_DIKS(0.989)S(0.011)NILLDENFNHSLADFGLAR_883		0.989
860_DIKS(0.007)S(0.993)NILLDENFNHSLADFGLAR_883	S864	0.993
863_SSNILLDENFNS(1)HLADFGLAR_883	S874	1
884_LMS(0.343)PY(0.264)ET(0.301)HVS(0.043)T(0.049)DLVGTGLYIPPEYQQASVATYK_916	S886	0.343
884_LMS(0.117)PY(0.09)ET(0.103)HVS(0.367)T(0.321)DLVGT(0.002)LGYIPPEYQQASVATYK_916	S893	0.367
951_VVKMKHES(0.405)RAS(0.595)EVFDPLIY_969	S961	0.595
960_ASEVFDPLIYS(1)KENDKEMFR_979		1
960_ASEVFDPLIYS(1)KENDKEMFR_979	S970	1
994_QRPT(0.284)T(0.716)QQLVSWLDDV_1008	T998	0.716

Supplementary Table 2

Suppl. Table 2: PSKR2 Phospho site evidences found by mass spectrometry.

Peptide sequence (localization probabilities of P-sites in brackets)	P-site	highest LP
PSKR2 (1) - autophosphorylation sites		
not analyzed		
PSKR2 (2) - autophosphorylation sites		
706_DVDDRINDVDEET(1)ISGVSK_724		1
705_KDVDDRINDVDEET(1)ISGVSK_724		1
705_KDVDDRINDVDEET(0.997)IS(0.003)GVSK_724	T718	0.997
711_INDVDEET(0.841)IS(0.152)GVS(0.007)K_724		0.841
706_DVDDRINDVDEETIS(1)GVSK_724	S720	1
711_INDVDEETISGV(1)KALGPSK_730		1
705_KDVDDRINDVDEETISGV(1)K_724		1
705_KDVDDRINDVDEETISGV(1)K_724		1
706_DVDDRINDVDEETISGV(1)KALGPSK_730		1
706_DVDDRINDVDEETISGV(1)KALGPSK_730	S723	1
706_DVDDRINDVDEETIS(0.004)GVS(0.996)K_724		0.996
706_DVDDRINDVDEETIS(0.003)GVS(0.995)KALGPS(0.001)K_730		0.995
711_INDVDEETIS(0.005)GVS(0.995)KALGPSK_730		0.995
735_HSCGCKDLSVEELLKS(0.135)T(0.802)NNFS(0.062)QANIIGCGGF_765		0.802
735_HSCGCKDLSVEELLKS(0.423)T(0.546)NNFS(0.03)QANIIGCGGF_765	T751	0.546
900_GLARLLRPY(0.003)DT(0.947)HVT(0.041)T(0.009)DLVGT(LGY)_922		0.947
904_LLRPY(0.001)DT(0.947)HVT(0.026)T(0.026)DLVGT(LGY)IPPEYSQS LIATCR_936		0.947
904_LLRPY(0.026)DT(0.727)HVT(0.12)T(0.12)DLVGT(0.007)LGYIPPEYSQS LIATCR_936	T910	0.727
904_LLRPY(0.115)DT(0.429)HVT(0.36)T(0.091)DLVGT(0.004)LGY(0.001)IPPEYSQS LIATCR_936		0.429
904_LLRPY(0.004)DT(0.356)HVT(0.307)T(0.307)DLVGT(0.012)LGY(0.011)IPPEYS(0.001)QS(0.001)LIAT(0.001)CR_936		0.356
904_LLRPY(0.041)DT(0.951)HVT(0.444)T(0.564)DLVGT(LGY)IPPEYSQS LIATCR_936	T910, T914	0.951, 0.564
904_LLRPY(0.085)DT(0.884)HVT(0.558)T(0.474)DLVGT(LGY)IPPEYSQS LIATCR_936	T910, T913	0.884, 0.558
904_LLRPYDT(0.014)HVT(0.936)T(0.05)DLVGT(LGY)IPPEYSQS LIATCR_936		0.936
904_LLRPY(0.001)DT(0.171)HVT(0.657)T(0.171)DLVGT(LGY)IPPEYSQS LIATCR_936	T913	0.657
909_DT(0.113)HVT(0.466)T(0.414)DLVGT(0.005)LGY(0.001)IPPEYSQS LIATCRGDVY_940		0.466
909_DT(0.009)HVT(0.151)T(0.839)DLVGT(0.001)LGY_922		0.839
904_LLRPYDT(0.011)HVT(0.203)T(0.779)DLVGT(0.007)LGYIPPEYSQS LIATCR_936		0.779
904_LLRPYDT(0.014)HVT(0.217)T(0.769)DLVGT(LGY)IPPEYSQS LIATCR_936	T914	0.769
904_LLRPY(0.216)DT(0.264)HVT(0.242)T(0.264)DLVGT(0.013)LGY(0.002)IPPEYSQS LIATCR_936		0.264
904_LLRPYDT(0.048)HVT(0.166)T(0.782)DLVGT(0.004)LGYIPPEY(0.007)S(0.835)QS(0.155)LIAT(0.004)CR_936	T914, S928	0.782, 0.835
904_LLRPYDTHVTTDLVGT(LGY)IPPEY(0.074)S(0.762)QS(0.16)LIAT(0.004)CR_936	S928	0.762
961_GKS(1)CRDLVSR_970	S963	1
966_DLVS(1)RVFQMK_975	S969	1
980_EAELIDT(0.998)T(0.002)IRENVNER_995		0.998
980_EAELIDT(0.845)T(0.155)IRENVNER_995	T986	0.845
BAK1 > PSKR2* (1) - transphosphorylation sites		
706_DVDDRINDVDEET(0.999)IS(0.001)GVSK_724		0.99
706_DVDDRINDVDEET(0.999)IS(0.001)GVSK_724		0.99
711_INDVDEET(1)ISGVSK_724	T718	1.00
705_KDVDDRINDVDEET(1)ISGVSK_724		1.00
706_DVDDRINDVDEETIS(1)GVSK_724		1.00
706_DVDDRINDVDEET(0.018)IS(0.938)GVS(0.044)K_724		0.93
705_KDVDDRINDVDEET(0.029)IS(0.963)GVS(0.008)K_724	S720	0.96
711_INDVDEET(0.215)IS(0.782)GVS(0.003)K_724		0.78
711_INDVDEET(0.037)IS(0.081)GVS(0.883)K_724	S723	0.83
750_S(0.308)T(0.308)NNFS(0.384)QANIIGCGGFGLVYK_770	S755	0.38
794_EFQAEVEALS(1)R_804		1.00
794_EFQAEVEALS(1)RAEHK_808	S803	1.00
880_DVKS(0.5)S(0.5)NILLDEKFEAHLADFGLAR_903	S883	0.50
904_LLRPY(0.148)DT(0.473)HVT(0.171)T(0.171)DLVGT(0.036)LGY(0.002)IPPEYSQS LIATCR_936	T910	0.47
904_LLRPY(0.005)DT(0.1)HVT(0.634)T(0.23)DLVGT(0.028)LGY(0.002)IPPEYSQS LIATCR_936	T913	0.63
904_LLRPY(0.047)DT(0.271)HVT(0.339)T(0.339)DLVGT(0.005)LGYIPPEYSQS LIATCR_936	T914	0.34
980_EAELIDT(0.996)T(0.004)IRENVNER_995		0.97
980_EAELIDT(0.845)T(0.155)IRENVNER_995	T986	0.85

Suppl. Table 2 (continued): PSKR2 Phospho site evidences found by mass spectrometry.

Peptide sequence (localization probabilities of P-sites in brackets)	P-site	highest LP
BAK1 > PSKR2* (2) - transphosphorylation sites		
	P-site	highest LP
706_DVDDRINDVDEET(1)ISGVSK_724		1
706_DVDDRINDVDEET(1)ISGVSK_724		1
711_INDVDEET(1)ISGVSK_724	T718	1
705_KDVDDRINDVDEET(1)ISGVSK_724		1
705_KDVDDRINDVDEET(0.998)IS(0.002)GVSK_724		0.998
706_DVDDRINDVDEET(0.001)IS(0.999)GVSK_724		0.999
711_INDVDEET(0.007)IS(0.935)GVS(0.058)K_724	S720	0.935
705_KDVDDRINDVDEET(0.075)IS(0.923)GVS(0.002)K_724		0.923
706_DVDDRINDVDEETISGVS(1)KALGPSK_730	S723	1
731_IVLFHSCGCKDLS(1)VEELLK_749	S743	1
735_HSCGCKDLSVEELLKS(0.685)T(0.315)NNF_754		0.685
735_HSCGCKDLSVEELLKS(0.5)T(0.5)NNF_754	S750	0.5
735_HSCGCKDLSVEELLKS(0.139)T(0.861)NNFSQANIIGCGGF_765		0.861
735_HS(0.001)CGCKDLS(0.001)VEELLKS(0.495)T(0.495)NNFS(0.008)QANIIGCGGF_765	T751	0.495
750_STNNFS(1)QANIIGCGGFGLVYK_770		1
735_HSCGCKDLSVEELLKS(0.054)T(0.054)NNFS(0.892)QANIIGCGGF_765	S755	0.892
794_EFQAEVEALS(1)RAEHKNLVSLQGYCK_818		1
794_EFQAEVEALS(1)RAEHK_808		1
794_EFQAEVEALS(1)RAEHK_808	S803	1
794_EFQAEVEALS(1)RAEHKNLVSLQGYCK_818		1
796_QAEVEALS(0.997)RAEHKNLVS(0.003)LQGY_816		0.997
880_DVKS(0.958)S(0.042)NILLDEKFEAHLADFLAR_903	S883	0.958
880_DVKS(0.032)S(0.968)NILLDEKFEAHLADFLAR_903		0.968
880_DVKS(0.034)S(0.966)NILLDEKFEAHLADFLAR_903	S884	0.966
904_LLRPYDT(0.89)HVT(0.104)T(0.006)DLVGTGLGYIPPEYSQSLIATCR_936	T910	0.89
904_LLRPY(0.061)DT(0.915)HVT(0.472)T(0.553)DLVGTGLGYIPPEYSQSLIATCR_936	T910, T914	0.915, 0.553
904_LLRPY(0.235)DT(0.701)HVT(0.357)T(0.688)DLVGT(0.019)LGYIPPEYSQSLIATCR_936		0.701, 0.688
904_LLRPYDT(0.002)HVT(0.76)T(0.193)DLVGT(0.045)LGYIPPEYSQSLIATCR_936		0.76
904_LLRPY(0.001)DT(0.022)HVT(0.488)T(0.488)DLVGTGLGYIPPEYSQSLIATCR_936	T913	0.488
904_LLRPYDT(0.019)HVT(0.16)T(0.819)DLVGT(0.001)LGYIPPEYSQSLIATCR_936		0.819
904_LLRPY(0.005)DT(0.097)HVT(0.377)T(0.52)DLVGT(0.002)LGYIPPEYSQSLIATCR_936	T914	0.52
904_LLRPY(0.001)DT(0.053)HVT(0.053)T(0.071)DLVGT(0.822)LGYIPPEYSQSLIATCR_936		0.822
904_LLRPYDTHVT(0.002)T(0.001)DLVGT(0.995)LGY(0.001)IPPEYSQSLIATCR_936	T919	0.995
904_LLRPYDTHVTTDLVGTGLGYIPPEY(0.711)S(0.204)QS(0.084)LIATCR_936	Y927	0.711
904_LLRPYDTHVTTDLVGTGLGY(0.003)IPPEY(0.155)S(0.472)QS(0.368)LIAT(0.001)CR_936	S928	0.472
980_EAELIDT(0.801)T(0.199)IRENVNER_995	T986	0.801
980_EAELIDT(0.01)T(0.99)IRENVNER_995		0.99
980_EAELIDT(0.022)T(0.978)IRENVNER_995	T987	0.978
980_EAELIDT(0.751)T(0.249)IRENVNER_995		0.751
980_EAELIDT(0.001)T(0.005)IRENVNERT(0.994)VLEMLEIACK_1006	T996	0.994

Supplementary Table 3

Suppl. Table 3: BAK1 Phospho site evidences found by mass spectrometry.

Peptide sequence (localization probabilities of P-sites in brackets)	P-site	highest LP
BAK1 (1) - autophosphorylation sites (if incubated together with PSKR1*)		
281_ELQVAS(ph)DNFS(ph)NKNILGR_297	S286, S290	n.a.
281_ELQVAS(ph)DNFS(ph)NKNILGR_297		n.a.
281_ELQVAS(0.005)DNFS(0.995)NK_292	S290	0.995
281_ELQVASDNFS(1)NKNILGR_297		1
281_ELQVASDNFS(1)NKNILGR_297		1
308_LADGT(1)LVAVKR_318	T312	1
308_LADGT(1)LVAVKR_318		1
319_LKEERT(1)QGGELQFQTEVEMISMAVHR_344	T324	1
324_T(1)QGGELQFQTEVEMISMAVHR_344		1
324_T(1)QGGELQFQT(1)EVEMISMAVHR_344	T324, T333	1, 1
324_TQGGELQFQT(1)EVEMISMAVHR_344	T333	1
324_TQGGELQFQT(1)EVEMIS(1)MAVHR_344	T333, S339	1, 1
324_TQGGELQFQTEVEMIS(1)MAVHR_344	S339	1
360_LLVYPYMANGSVAS(ph)CLR_376	S373	n.a.
440_LMDYKDT(1)HVTTAVR_453	T446	1
440_LMDYKDT(0.999)HVT(0.001)TAVR_453		0.999
440_LMDY(0.001)KDT(0.813)HVT(0.144)T(0.042)AVR_453		0.813
440_LM(ox)DYKDT(ph)HVT(ph)TAVR_453	T446, T449	n.a.
440_LMDYKDT(1)HVT(0.984)T(0.016)AVR_453	T449	0.984
440_LMDYKDT(0.997)HVT(0.864)T(0.14)AVR_453		0.864
440_LMDYKDT(0.023)HVT(0.816)T(0.161)AVR_453		0.816
440_LMDYKDTHTVT(0.733)T(0.267)AVR_453		0.733
440_LM(ox)DYKDTHTVT(ph)TAVR_453		n.a.
440_LMDYKDT(0.03)HVT(0.978)T(0.991)AVR_453	T449, T450	0.978, 0.991
440_LMDYKDTHTVT(0.148)T(0.852)AVR_453	T450	0.852
440_LMDYKDTHTVT(0.206)T(0.794)AVR_453		0.794
440_LMDYKDTHTVT(0.168)T(0.832)AVR_453		0.832
440_LMDYKDTHTVT(0.213)T(0.787)AVR_453		0.787
440_LM(ox)DYKDTHTVT(ph)TAVR_453		n.a.
454_GT(1)IGHIAPEYLSTGK_468	T455	1
454_GT(1)IGHIAPEYLSTGK_468		1
454_GTIGHIAPEYLS(0.974)T(0.026)GK_468	S465	0.974
454_GTIGHIAPEY(0.001)LS(0.777)T(0.223)GK_468		0.777
583_QDFNYPT(0.001)HHPAVS(0.999)GWIIGDSTSQIENEYPSGP_614	S595	0.999
583_QDFNYPTTHHPAVS(0.001)GWIIGDS(0.346)T(0.346)S(0.307)QIENEYPSGP_614	S602	0.346
583_QDFNYPTTHHPAVSGWIIGDS(0.888)T(0.096)S(0.016)QIENEYPS(0.999)GP_614	S602, S612	0.888, 0.999
583_QDFNYPTTHHPAVSGWIIGDSTSQIENEYPS(1)GP_614	S612	1
583_QDFNYPTTHHPAVSGWIIGDSTSQIENEYPS(1)GP_614		1
BAK1 (2) - autophosphorylation sites (if incubated together with PSKR1*)		
278_S(1)LRELQVASDNF_289	S278	1
276_RFS(1)LRELQVASDNFSNK_292		1
276_RFS(1)LRELQVASDNFSNK_292		1
278_S(1)LRELQVAS(0.001)DNFS(0.999)NKNILGRGGFGKVY_304	S278, S290	1, 0.999
278_S(1)LRELQVASDNFS(1)NKNILGRGGFGKVY_304		1, 1
281_ELQVAS(1)DNFSNK_292	S286	1
277_FSLRELQVAS(1)DNFSNKNILGR_297		1
278_SLRELQVAS(0.999)DNFS(0.001)NKNILGRGGF_300		0.999
278_SLRELQVAS(0.975)DNFS(0.025)NKNILGRGGF_300		0.975
278_S(0.008)LRELQVAS(0.993)DNFS(0.999)NKNILGRGGF_300		S286, S290
281_ELQVASDNFS(1)NKNILGR_297	S290	1
281_ELQVASDNFS(1)NKNILGR_297		1
277_FSLRELQVASDNFS(1)NKNILGR_297		1
278_SLRELQVASDNFS(1)NKNILGRGGFGKVY_304		1
290_S(1)NKNILGRGGFGKVY_304		1
278_SLRELQVAS(0.001)DNFS(0.999)NKNILGRGGFGKVY_304		0.999
306_GRLADGT(1)LVAVKR_318		T312
306_GRLADGT(1)LVAVKR_318	1	
308_LADGT(1)LVAVK_317	1	
308_LADGT(1)LVAVKR_318	1	
308_LADGT(1)LVAVKR_318	1	
308_LADGT(1)LVAVKR_318	1	

Suppl. Table 3 (continued): BAK1 Phospho site evidences found by mass spectrometry.

319_LKEERT(1)QGGELQFQTEVEMISMAVHR_343		1
319_LKEERT(0.986)QGGELQFQT(0.014)EVEMISMAVHR_343		0.986
324_T(0.904)QGGELQFQT(0.096)EVEMISMAVHR_343		0.904
319_LKEERT(1)QGGELQFQTEVEMIS(1)MAVHR_343	T324, S339	1, 1
319_LKEERT(1)QGGELQFQTEVEMIS(1)MAVHR_343		1, 1
319_LKEERT(1)QGGELQFQT(1)EVEMISMAVHR_343	T324, T333	1, 1
319_LKEERT(1)QGGELQFQT(1)EVEMISMAVHR_343		1, 1
324_TQGGELQFQT(1)EVEMISMAVHR_343	T333	1
324_TQGGELQFQT(1)EVEMIS(1)MAVHR_343		1, 1
324_TQGGELQFQT(1)EVEMIS(1)MAVHR_343	T333, S339	1, 1
324_TQGGELQFQTEVEMIS(1)MAVHR_343		1
324_TQGGELQFQTEVEMIS(1)MAVHR_343	S339	1
349_LRGFCMT(0.02)PT(0.98)ER_359		0.98
353_CMT(0.05)PT(0.95)ERLLVYPY_356	T357	0.95
360_LLVPYPMANGS(0.982)VAS(0.018)CLR_376		0.982
360_LLVPYPMANGS(0.982)VAS(0.018)CLR_376	S370	0.982
377_ERPES(1)QPPLDWPK_389	S381	1
BAK1 (2) - autophosphorylation sites (if incubated together with PSKR1*)	P-site	highest LP
440_LMDY(0.521)KDT(0.34)HVT(0.378)T(0.581)AVRGT(0.18)IGHIAPEYLSTGK_468	Y443, T450	0.521, 0.581
440_LMDY(0.606)KDT(0.34)HVT(0.215)T(0.81)AVRGT(0.028)IGHIAPEYLSTGK_468		0.606, 0.81
440_LMDYKDT(0.996)HVT(0.004)T(0.001)AVR_453	T446	0.996
440_LMDY(0.001)KDT(0.997)HVT(0.002)TAVR_453		0.997
440_LMDYKDT(1)HVTTAVR_453		1
440_LMDYKDT(0.998)HVT(0.002)TAVR_453		0.998
440_LMDYKDT(0.715)T(0.285)AVR_453		0.715
440_LMDYKDT(0.889)T(0.11)AVR_453		0.889
440_LMDYKDT(0.005)HVT(0.857)T(0.138)AVR_453		0.857
440_LMDY(0.001)KDT(0.998)HVT(0.001)TAVR_453		0.998
440_LMDYKDT(0.117)HVT(0.383)T(0.383)AVRGT(0.117)IGHIAPEYLSTGK_468	T449	0.383
440_LMDYKDT(0.189)HVT(0.527)T(0.142)AVRGT(0.142)IGHIAPEYLSTGK_468		0.528
440_LMDYKDT(0.01)HVT(0.921)T(0.055)AVRGT(0.014)IGHIAPEYLSTGK_468		0.921
445_DT(0.026)HVT(0.944)T(0.03)AVR_453		0.994
454_DTHVT(0.026)T(0.972)AVRGT(0.002)IGHIAPEYLSTGK_468		0.972
440_LMDYKDT(0.335)T(0.665)AVR_453		0.665
440_LMDYKDT(0.002)HVT(0.118)T(0.511)AVRGT(0.37)IGHIAPEYLSTGK_468	T450	0.511
440_LMDYKDT(0.003)T(0.941)AVRGT(0.056)IGHIAPEYLSTGK_468		0.941
440_LMDYKDT(0.004)HVT(0.138)T(0.858)AVRGTIGHIAPEYLSTGK_468		0.858
440_LMDYKDT(0.046)T(0.046)AVRGT(0.907)IGHIAPEYLSTGK_468		0.907
436_GLAKLMDY(0.051)KDT(0.226)HVT(0.226)T(0.226)AVRGT(0.271)IGHIAPEYLSTGKSSEKTDVF_476	T455	0.271

Suppl. Table 3 (continued): BAK1 Phospho site evidences found by mass spectrometry.

440_LMDY(0.176)KDT(0.824)HVT(0.915)T(0.085)AVR_453		0.824, 0.915
440_LMDYKDT(1)HVT(0.953)T(0.047)AVR_453		1, 0.953
440_LMDY(0.01)KDT(0.989)HVT(0.89)T(0.112)AVR_453		0.989, 0.89
440_LMDYKDT(1)HVT(0.988)T(0.012)AVR_453		1, 0.988
440_LMDYKDT(1)HVT(0.872)T(0.128)AVR_453		1, 0.872
440_LMDYKDT(0.999)HVT(0.816)T(0.185)AVR_453	T446, T449	0.999, 0.816
440_LMDYKDT(1)HVT(0.925)T(0.061)AVRGT(0.014)IGHIAPEYLSTGK_468		1, 0.925
440_LMDY(0.012)KDT(0.975)HVT(0.807)T(0.103)AVRGT(0.103)IGHIAPEYLSTGK_468		0.975, 0.807
440_LMDY(0.007)KDT(0.991)HVT(0.548)T(0.454)AVRGTIGHIAPEYLSTGK_468		0.991, 0.548
LMDY(0.242)KDT(0.755)HVT(0.725)T(0.278)AVR_453		0.755, 0.725
440_LMDY(0.074)KDT(0.866)HVT(0.184)T(0.358)AVRGT(0.517)IGHIAPEYLSTGK_468	T446, T455	0.866, 0.517
440_LMDYKDT(0.016)HVT(0.93)T(0.797)AVRGT(0.257)IGHIAPEYLSTGK_468		0.93, 0.797
440_LMDYKDT(0.056)HVT(0.947)T(0.997)AVRGTIGHIAPEYLSTGK_468		0.947, 0.997
440_LMDYKDT(0.004)HVT(0.998)T(0.999)AVR_453	T449, T450	0.998, 0.999
440_LMDYKDT(0.09)HVT(0.914)T(0.995)AVR_453		0.914, 0.995
440_LMDYKDT(0.066)HVT(0.82)T(0.557)AVRGT(0.557)IGHIAPEYLSTGK_468		0.82, 0.557
440_LMDYKDT(0.008)HVT(0.939)T(0.056)AVRGT(0.997)IGHIAPEYLSTGK_468	T449, T455	0.939, 0.997
440_LMDY(0.233)KDT(0.606)HVT(0.71)T(0.763)AVRGT(0.688)IGHIAPEYLSTGK_468	T449, T450, T455	0.71, 0.763, 0.688
440_LMDY(0.017)KDT(0.07)HVT(0.923)T(0.993)AVRGT(0.998)IGHIAPEYLSTGK_468	T449, T450, T455	0.923, 0.993, 0.998
440_LMDYKDT(0.025)HVT(0.978)T(0.997)AVRGT(1)IGHIAPEYLSTGK_468		0.978, 0.997, 1
440_LMDY(0.075)KDT(0.935)HVT(0.86)T(0.67)AVRGT(0.459)IGHIAPEYLSTGK_468		0.935, 0.86, 0.67
440_LMDY(0.298)KDT(0.76)HVT(0.882)T(0.927)AVRGT(0.133)IGHIAPEYLSTGK_468	T446, T449, T450	0.76, 0.882, 0.927
440_LMDY(0.001)KDT(0.999)HVT(0.993)T(0.979)AVRGT(0.028)IGHIAPEYLSTGK_468		0.999, 0.993, 0.979
454_GTIGHIAPEYLS(0.889)T(0.111)GK_468		0.889
454_GTIGHIAPEYLS(0.473)T(0.473)GKS(0.018)S(0.018)EKT(0.018)DVFGYGVMLL ELITGQR_490	S465	0.473
454_GTIGHIAPEYLS(0.359)T(0.359)GKS(0.137)S(0.137)EKT(0.007)DVFGYGVMLL ELITGQR_490		0.359
469_S(0.244)S(0.244)EKT(0.244)DVFGY(0.267)GVMLLELITGQR_490	Y478	0.267
582_RQDFNYPT(1)HHPAVSGW_597		1
582_RQDFNYPT(1)HHPAVSGW_597	T589	1
598_IIGDS(0.333)T(0.333)S(0.333)QIENEY(0.001)PSGP_614		0.333
598_IIGDS(0.961)T(0.039)SQIENEYPSGP_614	S602	0.961
583_QDFNYPTHHPAVSGWIIGDS(0.959)T(0.036)S(0.006)QIENEYPSGP_614		0.959
598_IIGDS(0.001)T(0.405)S(0.595)QIENEYPSGP_614	S604	0.595
583_QDFNYPTHHPAVSGWIIGDS(0.679)T(0.21)S(0.111)QIENEYPS(1)GP_614	S602, S612	0.679, 1
583_QDFNYPT(0.004)HHPAVS(0.994)GWIIGDS(0.003)T(0.002)S(0.005)QIENEYPS(0.993)GP_614	S595, S612	0.994, 0.993
583_QDFNYPTHHPAVSGWIIGDS(0.102)T(0.102)S(0.007)QIENEY(0.374)PS(0.416)GP_614		0.416
598_IIGDSTSQIENEYPS(1)GP_614	S612	1
598_IIGDSTSQIENEYPS(1)GP_614		1
PSKR1 > BAK1* (1) - transphosphorylation sites	P-site	highest LP
308_LADGT(ph)LVAVKR_318	T312	n.a.
440_LMDYKDT(ph)HVTTAVR_453	T446	n.a.
440_LMDYKDT(0.001)HVT(0.939)T(0.06)AVR_453		0.939
440_LMDYKDT(0.5)T(0.5)AVR_453	T449	0.5
440_LMDYKDT(0.5)T(0.5)AVR_453		n.a.
440_LMDYKDT(0.065)T(0.935)AVR_453		0.935
440_LMDYKDT(0.15)T(0.85)AVR_453		0.85
440_LMDYKDT(0.155)T(0.845)AVR_453	T450	0.845
440_LMDYKDT(0.155)T(0.845)AVR_453		n.a.

Suppl. Table 3 (continued): BAK1 Phospho site evidences found by mass spectrometry.

PSKR1 > BAK1* (2) - transphosphorylation sites	P-site	highest LP	
440_LMDY(0.989)KDT(0.011)HVT(AVR_453)	Y443	0.989	
440_LMDY(0.161)KDT(0.754)HVT(0.079)T(0.006)AVR_453	T446	0.754	
DTHVT(0.95)T(0.05)AVR_453	T449	0.95	
440_LMDYKDT(0.002)HVT(0.892)T(0.106)AVR_453		0.892	
440_LMDYKDT(0.068)HVT(0.884)T(0.048)AVR_453		0.884	
440_LMDYKDT(0.004)HVT(0.819)T(0.177)AVR_453		0.819	
440_LMDYKDT(0.038)HVT(0.685)T(0.138)AVRGT(0.138)IGHIAPEYLSTGK_468		0.685	
440_LMDYKDT(0.096)HVT(0.682)T(0.199)AVRGT(0.023)IGHIAPEYLSTGK_468		0.682	
DTHVT(0.004)T(0.996)AVR_453	T450	0.996	
440_LMDYKDTHVT(0.056)T(0.944)AVR_453		0.944	
440_LMDYKDTHVT(0.077)T(0.923)AVR_453		0.923	
440_LMDYKDT(0.002)HVT(0.174)T(0.823)AVRGTIGHIAPEYLSTGK_468		0.823	
440_LMDYKDT(0.001)HVT(0.196)T(0.803)AVR_453		0.803	
440_LMDYKDT(0.221)HVT(0.221)T(0.483)AVRGT(0.074)IGHIAPEYLSTGK_468		0.483	
598_IIGDS(0.333)T(0.333)S(0.333)QIENEYPSGP_614	S602	0.333	
PSKR2 > BAK1* (1) - transphosphorylation sites			
not analyzed in first run			
PSKR2 > BAK1* (2) - transphosphorylation sites			
	P-site	highest LP	
436_GLAKLMDYKDT(0.401)HVT(0.383)T(0.108)AVRGT(0.108)IGHIAPEYLSTGKSSEKTDV F_476	T446	0.383	
440_LMDYKDT(0.999)HVT(0.001)T(AVR_453)	T449	0.999	
440_LMDYKDT(0.006)HVT(0.974)T(0.02)AVR_453		0.974	
440_LMDYKDT(0.009)HVT(0.966)T(0.025)AVR_453		0.966	
440_LMDYKDT(0.01)HVT(0.958)T(0.031)AVRGTIGHIAPEYLSTGK_468		0.958	
440_LMDYKDT(0.001)HVT(0.943)T(0.056)AVR_453		0.943	
440_LMDYKDT(0.015)HVT(0.755)T(0.23)AVR_453		0.755	
444_KDT(0.015)HVT(0.655)T(0.165)AVRGT(0.165)IGHIAPEYLSTGKSSEKTDV F_476		0.655	
436_GLAKLMDYKDT(0.529)HVT(0.373)T(0.095)AVRGT(0.003)IGHIAPEYLSTGKSSEKTDV F_476		0.529	
440_LMDYKDT(0.247)HVT(0.512)T(0.131)AVRGT(0.109)IGHIAPEYLSTGK_468		0.512	
440_LMDY(0.001)KDT(0.007)HVT(0.502)T(0.364)AVRGT(0.126)IGHIAPEYLSTGK_468		0.502	
436_GLAKLMDYKDT(0.124)HVT(0.433)T(0.433)AVRGT(0.011)IGHIAPEYLSTGKSSEKTDV F_476		0.433	
440_LMDY(0.027)KDT(0.257)HVT(0.543)T(0.7)AVRGT(0.473)IGHIAPEYLSTGK_468		T449, T450	0.543, 0.7
445_DTHVT(0.028)T(0.972)AVR_453		T450	0.972
445_DTHVT(0.029)T(0.97)AVRGT(0.002)IGHIAPEYLSTGK_468	0.97		
440_LMDYKDTHVT(0.028)T(0.972)AVR_453	0.972		
440_LMDYKDT(0.009)HVT(0.087)T(0.837)AVRGT(0.067)IGHIAPEYLSTGK_468	0.837		
440_LMDYKDTHVT(0.178)T(0.822)AVR_453	0.822		
440_LMDYKDT(0.012)HVT(0.184)T(0.804)AVR_453	0.804		
440_LMDYKDT(0.002)HVT(0.047)T(0.762)AVRGT(0.189)IGHIAPEYLSTGK_468	0.762		
440_LMDYKDTHVT(0.25)T(0.75)AVRGTIGHIAPEYLSTGK_468	0.75		

Supplementary Table 4

Suppl. Table 4: Comparison of LRR-RLK and SERK interactions. In pathways involved in growth and developmental processes (light yellow) their LRR-RLK/SERK interactions are mostly ligand-enhanced or ligand-independent (green) and only shown to be ligand-dependent (red) if analyzed in vitro. Pathogen-defense related interactions are marked with light blue.

LRR-RLK	SERK	Ligand	function	Interaction		phosphorylation		LRR sub	Ref.
				ligand-dependency	shown by	direction	shown by		
PSKR1	SERK1 SERK2 BAK1	PSK	growth, development	ligand-enhanced	in vivo, IP; transiently expressing Arabidopsis protoplasts (was only able to perform after deletion of KD of PSKR1, because protoplasts ruptured)	n.a.		X	Wang et al. (2015)
	n.a.			In planta; FRET-FLIM	n.a.		Ladwig et al. (2015)		
	n.a.			transphosphorylate each other	in vitro; KDs only	this study			
BRI1	BAK1	BL	growth, development	ligand-enhanced	in planta; IP with transgenic lines	transphosphorylate each other	in vitro; kinase assay with KDs	X	Wang et al. (2008)
				ligand-independent	in planta; VAEM and SSO-FLIM	n.a.			Hutten et al. (2017)
				ligand-enhanced	in planta; FRET-FLIM	n.a.			Bücherl et al. (2013)
	ligand-dependent			in vitro; size exclusion chromatography	n.a.		Santiago et al. (2013)		
SERK1									
PSY1R	SERK1 SERK2 BAK1 SERK5	PSY1	growth	n.a.	in planta; BiFC (tobacco)	transphosphorylate each other	in vitro; KDs only	X	Oehlschlaeger et al. (2017)
EMS1	SERK1	TPD1	cell diff. Anther development	ligand-independent	in vivo; BiFC, FRET (Arabidopsis protoplasts); in planta Co-IP	transphosphorylate each other	in vitro; kinase assay with KDs	X	Li et al. (2017)
	n.a.			n.a.	only EMS1 phosphorylation analyzed	in vivo; size shift by phosphatase-treatment	Jia et al. (2008)		
HAE/ HSL2	SERK1 SERK2 BAK1 SERK4	IDA	floral organ abscission	ligand-enhanced	in planta; BiFC; in vivo; IP; transfected Arabidopsis protoplasts; in vitro pull down assay with heterologously expressed KDs	transphosphorylate each other	in vitro; kinase assay with KDs	XI	Meng et al. (2016)
HAE	BAK1			ligand-dependent	in vitro; size exclusion chromatography	transphosphorylate each other	in vitro; kinase assay with KDs		Santiago et al. (2016)
ER	SERK1 SERK2 BAK1 SERK4	EPF2	stomatal patterning	ligand-enhanced	in vivo; IP; transiently transformed A.th. Protoplasts	transphosphorylate each other	in vitro; KDs only	XIII	Meng et al. (2015)
	BAK1	PcBMM spores		ligand-independent	in vivo; IP; transiently transformed tobacco Leafs	n.a.			Jorda et al. (2016)
ERL1	SERK1 SERK2 BAK1 SERK4	EPF1		ligand-enhanced	in vivo; IP; transiently transformed A.th. Protoplasts	transphosphorylate each other	in vitro; kinase assay with KDs	XIII	Meng et al. (2015)
PEPR1	SERK1 SERK2 BAK1 SERK4	PEP2 (DAMP)	pathogen-defense	ligand-dependent	in vivo; IP; transiently transformed tobacco Leafs	n.a.		XI	Yamada et al. (2016)
	BAK1	PEP1 (DAMP)		ligand-dependent	in vitro; IP heterologously expressed purified proteins	n.a.			Tang et al. (2015)
EFR	SERK1 SERK2 BAK1 SERK4	elf18 (PAMP)		Ligand-dependent	in vivo; IP; transiently transformed tobacco Leafs	n.a.		XII	Roux et al (2011)
				Ligand-dependent	in vivo; IP; transiently transformed tobacco Leafs	n.a.			Koller & Bent (2014)
FLS2	BAK1	flg22 (PAMP)		Ligand-dependent	in vivo & in vitro; IP; Arabidopsis cells; microsomal fraction	both	in vivo; Arabidopsis cells; microsomal fraction	XII	Schulze (2010)
				ligand-dependent	in vivo; IP transiently transformed tobacco Leafs	n.a.			Koller & Bent (2014)
				ligand-dependent	in vivo IP; transfected Arabidopsis mesophyll cells; in vitro; Pull down with heterologously expressed proteins	both	in vivo; IP; transfected Arabidopsis mesophyll cells		Sun et al. (2013)

References (of Suppl. Table 4)

Santiago J, Brandt B, Wildhagen M, Hohmann U, Hothorn LA, Butenko MA, Hothorn M. 2016. Mechanistic insight into a peptide hormone signaling complex mediating floral organ abscission. *eLife* **5**, e15075.

Jia G, Liu X, Owen HA, Zhao D. 2008. Signaling of cell fate determination by the TPD1 small protein and EMS1 receptor kinase. *Proceedings of the National Academy of Sciences* **105**, 2220–2225.

Oehlenschläger CB, Gersby LBA, Ahsan N, Pedersen JT, Kristensen A, Solakova T V., Thelen JJ, Fuglsang AT. 2017. Activation of the LRR Receptor-Like Kinase PSY1R Requires Transphosphorylation of Residues in the Activation Loop. *Frontiers in Plant Science* **8**, 1–12.

Santiago J, Henzler C, Hothorn M. 2013. Molecular mechanism for plant steroid receptor activation by somatic embryogenesis co-receptor kinases. *Science* **341**, 889–892.

Supplementary Table 5

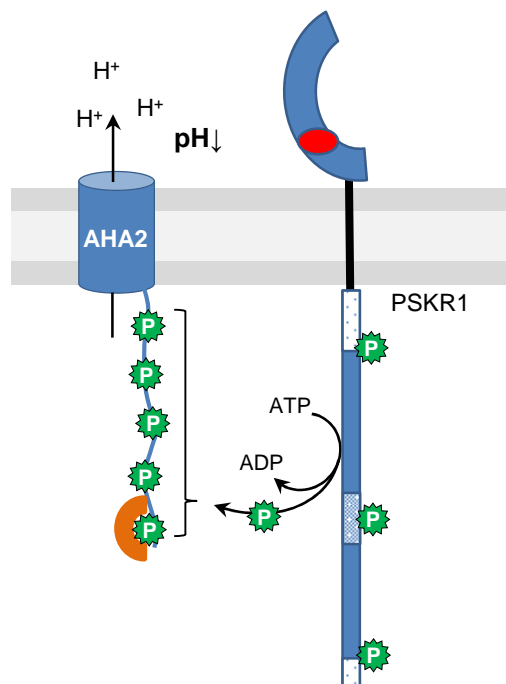
Suppl. Table 5: Oligonucleotides used for qPCR and RT-PCR analyses

locus	name/function	abbrev	primer sequence (5' to 3')	analysis
At3g04120	<i>GLYCERALDEHYDE-3-PHOSPHATE DEHYDROGENASE C SUBUNIT 1</i>	<i>GAPC1</i>	GATTCTACAATGGCTGACAAGAAGA	qPCR
			ATGAAGGGGTCGTTGACAGC	qPCR
At3g18780	<i>ACTIN2</i>	<i>ACT2</i>	ACATTCCAGCAGATGTGGATCTC	qPCR
			GATCCCATTTCATAAAACCCAGC	qPCR
At5g14750	<i>WEREWOLF</i>	<i>WER</i>	TCGTATTGCCAAAAAGACTGGTTTA	qPCR
			TGATAAGATCCTCTTCTTGCTCGG	qPCR
At5g40330	<i>MYB23</i>	<i>MYB23</i>	CTCCTCGGCAACAGATGGTC	qPCR
			GGCTTTGACGGCAGTTGAAT	qPCR
At1g11130	<i>SCRAMBLED</i>	<i>SCM</i>	AATCGGGGAAGGGTCGATTG	qPCR
			TTGAGGAATTCGCCGTCCT	qPCR
At1g66800	enriched in non-root hair cells		GCGATGAAGGCATGGTATGG	qPCR
			GCAAACTGGTCCGATCACG	qPCR
At5g03150	<i>JACKDAW</i>	<i>JKD</i>	ATGCGCAAGGTCTATCCGAG	qPCR
			AGGGTTTGTGGAAGTCATTGGA	qPCR
At1g12560	<i>EXPANSIN7</i>	<i>EXP7</i>	TGCATACCGAAGAGTGCCAT	qPCR
			AACGGCCATGCTCTTGATGT	qPCR
At3g18780	<i>ACTIN2</i>	<i>ACT2</i>	CAAAGACCAGCTCTCCATCG	RT-PCR
			AGGTCCAGGAATCGTTCACAG	RT-PCR
At1g08030	<i>TYROSYLPROTEIN SULFOTRANSFERASE</i>	<i>TPST</i>	GGCTCTTTTGCGGAACCTTGA	RT-PCR
			CTTCAATTTTCGTGCATCTCG	RT-PCR
At2g02220	<i>PHYTOSULFOKINE RECEPTOR 1</i>	<i>PSKR1</i>	GTTTCGGAGTTGTGCTTCTCGAG	RT-PCR
			CCAAGAGACTAACTGTTGAGTCGTTG	RT-PCR
At2g02220-GFP	<i>Fusion of PSKR1-GFP</i>	<i>PSKR1-GFP</i>	AGATGTTTTCGGGTTCTGAGATTG	RT-PCR
			CAGATGAACTTCAGGGTCAG	RT-PCR
At5g53890	<i>PHYTOSULFOKINE RECEPTOR 2</i>	<i>PSKR2</i>	CACCGAGGAGACTATCAGCGGGG	RT-PCR
			GGCCTAAGCAACCTCGCTAA	RT-PCR

Chapter 5

Phytosulfokine signaling activates proton pumps

Christine Kaufmann, Dennis Linke, Andreas Tholey, Lana Shabala, Nana Su, Sergey Shabala and Margret Sauter



Phytosulfokine signaling activates proton pumps

Christine Kaufmann¹, Dennis Linke², Andreas Tholey², Lana Shabala³, Nana Su³, Sergey Shabala³ and Margret Sauter¹

¹ Entwicklungsbiologie und Physiologie der Pflanzen, Christian-Albrechts-University at Kiel, Am Botanischen Garten 5, 24118 Kiel, Germany

² Systematische Proteomics und Bioanalytik, Christian-Albrechts-University at Kiel, Niemannsweg 11, 24105 Kiel, Germany

³ School of Land and Food, University of Tasmania, Hobart, Tasmania 7001, Australia

Abstract

Phytosulfokine (PSK) is a posttranslationally modified pentapeptide that promotes cell expansion. PSK receptor 1 (PSKR1) interacts with the proton pump H⁺-ATPase 2 (AHA2) at the plasma membrane. Here we report that the PSKR1 kinase phosphorylates AHA2 at the autoinhibitory C-terminus *in vitro* at positions Thr881, Ser904, Thr924 and possibly at the penultimate Thr947. The most frequently phosphorylated amino acid was Thr924, a phosphosite that has not been mapped before. *In vivo* measurements on *Arabidopsis thaliana* seedling roots indicated that PSK promotes proton efflux mainly in the elongation zone. These results suggest that cell expansion is initiated by activating phosphorylation of AHAs by PSKR1.

Introduction

Cell expansion is a cellular process important for plant growth in general and developmental processes like root hair formation, pollen tube growth and abscission of floral organs (Patterson, 2001; Hepler *et al.*, 2013; Grierson *et al.*, 2014). Cell shape and cell size are determined by the surrounding cell wall. According to the acid growth theory hydrogen bonds between cellulose and hemicellulose loosen after acidification of the apoplast, which is performed by proton-extruding pumps.

Subsequently, activation of cell-wall-loosening enzymes, a cation influx and water uptake occurs, which then ultimately increases the cell size (Hager, 2003). Throughout the life cycle of plants, cell expansion is highly regulated depending on tissues and developmental stages by different phytohormones. In addition to the non-proteinaceous phytohormones, small secreted peptides were recently found to have a hormonal activity (reviewed in Matsubayashi, 2014; Tavormina *et al.*, 2015). One of them, phytosulfokine (PSK), is a disulfated pentapeptide localized in the apoplast that promotes root growth, differentially alters the susceptibility to pathogens and promotes pollen germination as well as pollen tube elongation (reviewed in Sauter, 2015). PSK-driven root growth promotion is caused by cell expansion in the root elongation zone (Kutschmar *et al.*, 2009). Perception of PSK occurs by binding to the island domain of the extracellular part of a plasma membrane-bound leucine-rich repeat receptor-like kinase (LRR-RLKs) (Matsubayashi *et al.*, 2006; Wang *et al.*, 2015). *Arabidopsis thaliana* has two PSK receptors termed PSKR1 and PSKR2. PSK receptors are conserved throughout the plant kingdom including mosses (Hartmann *et al.*, 2015) indicating that they evolved early during land plant evolution and that they have a conserved function in regulating plant growth. PSK-enhanced growth and protoplast expansion are to a large part conveyed by PSKR1 (Amano *et al.*, 2007; Stührwohldt *et al.*, 2011), whereas the function of PSKR2 is less clear. Knocking out both PSK receptors in *pskr1-3 pskr2-1* leads to insensitivity to exogenously applied PSK and displays retarded shoot and root growth (Hartmann *et al.*, 2013). The signal transducing cytosolic part of PSKR1 possesses a functional kinase domain, a calmodulin (CaM) binding site and guanylate cyclase (GC) activity (Kwezi *et al.*, 2011; Hartmann *et al.*, 2014). PSKR1 kinase activity is essential for PSK signaling *in planta* (Hartmann *et al.*, 2014), whereas the impact of CaM binding and GC activity for PSK signal transduction is unclear. Point mutations in the intracellular part of PSKR1 that were generated to inhibit CaM binding or GC activity lead to kinase inactivation at the same time. It has therefore not been possible so far to assess the effect of GC activity and CaM binding on PSKR1 activity *in planta* (Kaufmann *et al.*, 2017). The molecular mechanism by which PSK promotes cell expansion is not known, but protein interaction studies including a yeast split-ubiquitin assay and FRET-FLIM analysis revealed that PSKR1 is part of a nanocluster that consists of PSKR1, its co-receptor LRR-RLK BRI1-ASSOCIATED RECEPTOR KINASE 1 (BAK1), a channel likely permissive for cations, CYCLIC

NUCLEOTIDE-GATED CHANNEL 17 (CNGC17) and Arabidopsis H⁺-ATPases 1 and 2 (AHA1/2) (Ladwig *et al.*, 2015). The aquaporine PLASMA MEMBRANE INTRINSIC PROTEIN 2;1 (PIP2;1) and AHA2 were found by immunoprecipitation to interact with PSKR1 *in vivo* (unpublished data). These membrane proteins may together be able to drive the cell expansion in response to PSK. AHA1 and AHA2 are plasma membrane-bound P-type_{3A} autoinhibited H⁺-ATPases (Baxter *et al.*, 2003). These enzymes translocate protons into the apoplast, thereby acidifying the cell wall which induces cell expansion (Hager, 2003). The activity of AHAs is regulated at the protein level by phosphorylation (Haruta *et al.*, 2015). The cytosolic autoinhibitory C-terminus is a target of regulatory kinases and gets phosphorylated on serine, threonine or tyrosine residues with differing effects on AHA activity (Rudashevskaya *et al.*, 2012). Auxin signaling activates AHAs by phosphorylation of the penultimate threonine (Thr947 in AHA2) (Caesar *et al.*, 2011; Witthöft *et al.*, 2011; Takahashi *et al.*, 2012). This creates a binding site for regulatory 14-3-3 proteins, with activation of the proton pump as a consequence (Olsson *et al.*, 1998; Fuglsang *et al.*, 1999). However, not every phosphorylation of the C-terminus leads to an activation of the proton pump. The Ser/Thr kinase PROTEIN KINASE SOS2-LIKE 5 (PKS5) negatively regulates AHA2 activity by phosphorylating Ser931 (Fuglsang *et al.*, 2007). Since PSKR1 was shown to interact with the two most important and abundant proton pumps in Arabidopsis, AHA1 and AHA2, we investigated the possibility that proton pumps are a target of phosphorylation by PSKR1.

Results

PSKR1 phosphorylates AHA2 predominately on activating positions

To test whether the regulatory C-terminus of AHA2 (AHA2-CT) was a substrate for PSKR1 kinase (PSKR1-KD), AHA2-CT and PSKR1-KD were heterologously expressed for use in an *in vitro* kinase assay (Figure 1). PSKR1-KD showed autophosphorylation activity as described previously (Hartmann *et al.*, 2014). In addition, PSKR1-KD phosphorylated FLAG-tagged AHA2-CT. The calculated molecular mass of the 117 amino acid peptide AHA2-CT-FLAG is 13.6 kDa. The sequence of AHA2-CT-FLAG was confirmed by mass spectrometry (Table 1). However, the N-terminal 32 amino acids were not detected (Table 1). An unexpected cleavage site of protease factor Xa might be the reason for the shortened peptide.

Nonetheless, phosphorylation sites (P-sites) were identified and listed with their confidence level in Table 1. Phosphorylation of Thr881, Ser904 and Thr924 were most often introduced by PSKR1 with high confidence. Three phosphopeptides provided evidence that Ser931 was phosphorylated with medium confidence. The P-site(s) in the tryptic peptide from Glu930 to Val948 could not be assigned. This peptide was found four times, once also as triply phosphorylated. However, in all cases the confidence level was below the threshold of 0.05 based on the *q*-value, are therefore rejected and localization probabilities were low. Due to sequence length with a high number of phosphorylatable amino acids within the sequence P-site(s) could not be identified unambiguously. It is possible that Ser944, Tyr946 and/or the penultimate Thr947 are phosphorylated by PSKR1. Residues in AHA2-CT that are phosphorylated by PSKR1 *in vitro* are schematically shown in Figure 2. Previously published data that are also summarized in Figure 2 indicate that PSKR1 activity can promote or suppress AHA2 activity and can alter 14-3-3 protein binding.

PSK promotes proton efflux

To elucidate the effect of PSK on proton pumping activity *in vivo*, measurements were performed with the non-invasive MIFE technique. Wild-type seedlings showed a strong and immediate response in the elongation zone following PSK application, with net H⁺ flux shifting towards efflux by ~ 40 nmol·m⁻²·s⁻¹ (Figure 3a) which indicates an increased proton trans-location into the apoplast. This stimulation was more attenuated in the mature root zone (a shift in net H⁺ flux of 20 nmol·m⁻²·s⁻¹; Figure 3b). In the mature zone, the initial net proton flux was restored after 10 min whereas enhanced proton pumping in the elongation zone remained stable for the entire measurement period of 20 min (Figure 3a). Seedlings of the double receptor knockout line *pskr1-3 pskr2-1* showed no effect on net proton flux (Figure 3c) indicating that the activation of AHAs was mediated by the PSK receptor signaling. The tyrosylprotein sulfotransferase (TPST) catalyzes the sulfation of PSK. PSK-deficient *tpst-1* seedlings displayed increased proton efflux following PSK application (Figure 3d).

Discussion

PSK signaling promotes plant growth driven by cell expansion mainly through PSKR1 activity (Kutschmar *et al.*, 2009; Hartmann *et al.*, 2014). Protoplast expansion experiments showed that the PSK-promoted cell expansion (1) is observable already after 5 min after PSK application, (2) depends on PSKR1 but not PSKR2, (3) is dependent on its co-receptor BAK1, (4) is promoted by potassium availability in the medium, (5) is negatively affected by knockout of the cation channel CNGC17 and (6) is independent of *de novo* protein synthesis (Stührwohldt *et al.*, 2011; Ladwig *et al.*, 2015). These findings led to the hypothesis that PSK-induced cell expansion is initiated on the protein level by activation of AHAs by PSKR1. In recent years, regulation of AHA1/2 activity by small secreted peptides, hormones and bacterial elicitors was reported including PLANT PEPTIDE CONTAINING SULFATED TYROSINE 1 (PSY1), RAPID ALKALINIZATION FACTOR (RALF), brassinolide and flagellin fragment flg22 mediated by their receptor-like kinases PSY1 RECEPTOR (PSY1R), FERONIA (FER), BRASSINOSTEROID INSENSITIVE 1 (BRI1) and FLAGELLIN-SENSITIVE 2 (FLS2) (Nühse *et al.*, 2007; Caesar *et al.*, 2011; Fuglsang *et al.*, 2014; Haruta *et al.*, 2015). We tested if PSK signaling activates proton pumps (AHAs) to initiate cell expansion according to the acid growth theory (Hager, 2003) by phosphorylation of the autoinhibitory C-terminal domain (Takahashi *et al.*, 2012; Haruta *et al.*, 2015). We showed that the PSKR1 kinase phosphorylates the C-terminus of AHA2 *in vitro* at positions Thr881, Ser904, Thr924, Ser931 and possibly at Thr947, where phosphorylation at Thr881 and Thr924 were most abundant. The position of phosphorylation differentially affects AHA activity as investigated by *pma1* yeast complementation assays and 14-3-3 binding overlay assays with phosphoablative and phosphomimic point mutated AHA2 isoforms (Palmgren, 2001; Fuglsang *et al.*, 2003, 2007, 2014; Rudashevskaya *et al.*, 2012). Phosphorylation at Thr881 and Ser904 activates AHA2. Fuglsang *et al.* (2014) showed that PSY1R phosphorylates Thr881 *in planta* and *in vivo* measurements confirmed that PSY1 application activates AHAs indicated by enhanced proton efflux. Surprisingly, the phosphorylation of Thr924 that was introduced by PSKR1 has not previously been found in AHA1/2 phosphorylation site analyses. Substitution of Thr924 by either Ala or Asp impairs AHA function by rendering the proton pump inactive. T924A impairs binding to 14-3-3 protein and fusicoccin, an AHA-activating fungal toxin (Fuglsang *et al.*, 2003; Rudashevskaya *et al.*, 2012). These results were interpreted in the way

that the amino acid residue threonine at this position is essential to form a 14-3-3/AHA-complex independent of its phosphorylation state. Interestingly, the same result is observed for Thr947 and its phosphorylation is known to create a binding site for 14-3-3 proteins and to be essential for AHA1/2 activity (Olsson *et al.*, 1998; Fuglsang *et al.*, 1999). Phosphorylation doesn't lead to activation in all cases. The flg22-binding FLS2 as well as RALF-binding FER are involved in immune responses. FLS2 and FER introduce a phosphate group at Ser899, which inactivates AHA2 and leads to alkalinization of the apoplast (Felix *et al.*, 1999; Nühse *et al.*, 2007; Haruta *et al.*, 2014). The cytosolic kinase PKS5 phosphorylates specifically Ser931 and thereby inactivates AHA2 (Fuglsang *et al.*, 2007). Ser931 was also phosphorylated by PSKR1 with medium confidence. Most phosphorylation sites introduced by PSKR1 at AHA2-CT were shown by single substitution analyses to activate the proton pump. Sites introduced *in planta* by PSKR1 haven't been mapped so far. It has yet to be analyzed how the combination of phosphosites that were found *in vitro* affect AHA activity. We did however show that PSK application lead to enhanced AHA activity and this response is mediated by PSK receptors. Taken together, the results suggest PSK signaling mediated by PSKR1 activates the proton pump AHA2 by phosphorylation at its autoinhibitory C-terminus.

Methods

Cloning of constructs, heterologous protein expression and purification

Cloning of the cytoplasmic part (amino acid position 686 to 1008) of PSKR1 (At2g02220) into pETDuet-1 (Novagen), and expression and purification of His-tagged H₆-PSKR1-KD-wt were described previously (Hartmann *et al.*, 2014; Kaufmann *et al.*, 2017). The C-terminal domain (amino acid position 842-948) of AHA2 (At4g30190) was amplified with oligonucleotides 5'-TTTAAACCATGGTTCGATACATCTTGAGCG-3' and 5'-AAATTTGATATCTCACTTATCATCATCCTTATAATCCACAGTGTAGTACTGGGAG-3' containing *Nco*I and *Eco*RV restriction sites. The product was digested and subsequently ligated into the pMAL-c5x vector (New England Biolabs). Expression of the resulting MaBP-(Maltose-Binding-Protein)-AHA2-CT-FLAG fusion protein was performed as described (Kaufmann *et al.*, 2017). The fusion of AHA2-CT to MaBP facilitates soluble expression and purification. The

crude extract with protein in 20 mM Tris/HCl pH 7.4, 200 mM NaCl, 1 mM EDTA was loaded onto amylose resin (New England Biolabs, Cat Nr. E8021S) and washed with 20 volumes washing buffer 20 mM Tris/HCl pH 7.4, 200 mM NaCl, 1 mM EDTA. MaBP-AHA2-CT-FLAG was eluted with 2 volumes elution buffer (washing buffer with 10 mM maltose). To avoid that MaBP interferes with the interaction of PSKR1 with AHA2 it was cleaved off by digestion with factor Xa protease (New England Biolabs, Cat. Nr. P8010S) with 0.2 µg protease/1 µg fusion protein incubated at 4°C over night. For ultrafiltration the sample was transferred to a centrifugal filter (Roti-Spin Mini-3 MWCO) and centrifuged at 12.000 x g at 4°C. Subsequently, the protein was washed with 10 volumes 20 mM Tris/HCl pH 8, 25 mM NaCl. The residual protein on the Roti-Spin column was resuspended in washing buffer. To separate AHA2-CT-FLAG from MaBP and the protease factor Xa, ion exchange chromatography was performed. The sample was transferred onto a Q-Hyper D-10 column (Beckmann) in a System Gold HPLC (Beckmann) and a gradient elution with buffer A (20 mM Tris/HCl pH 8, 25 mM NaCl) and buffer B (20 mM Tris/HCl pH 8, 500 mM NaCl) was run. The elution fractions were loaded onto a protein gel to determine the fraction with the highest protein content of AHA2-CT-FLAG, which was then used for subsequent analyses.

***In vitro* kinase assay**

Transphosphorylation of the C-terminus of AHA2 by PSKR1 kinase was analyzed in a kinase assay with radiolabeled [γ - ^{32}P]ATP. Approximately 2 µg freshly expressed and purified PSKR1 kinase was incubated with approximately 0.75 µg AHA2-CT-FLAG in 50 mM HEPES, pH 7.4, 1 mM DTT, 10 mM MgCl₂, 10 mM MnCl₂, 0.2 mM unlabeled ATP and 30 µCi [γ - ^{32}P] ATP for 1 h at 25°C. SDS loading buffer was added to stop reactions. The samples were heated for 5 min at 95°C. Proteins were separated on a 15% polyacrylamide gel by SDS-PAGE and subsequently stained with Coomassie Brilliant Blue. To visualize incorporation of ^{32}P the gel was dried and an X-ray film was exposed to the dried gel.

Phosphorylation site mapping

To verify transphosphorylation of AHA2-CT by PSKR1 and to determine specific sites at which phosphorylation occurred, a mapping by mass spectrometry analysis was performed. AHA2-CT was phosphorylated without [γ - ^{32}P]ATP as described above.

The protein band below the 14.4 kDa marker band was excised from the Coomassie-stained but not dried gel. In-gel digestion with the four enzymes elastase, GluC, trypsin and chymotrypsin, phosphopeptide enrichment, mass spectrometry and data evaluation were performed as described (Hartmann *et al.*, 2015). Level of confidence for identified sites were determined with a validation threshold of 0.01 for high confidence and of 0.05 for medium confidence based on the *q*-value.

Ion flux measurements

Arabidopsis thaliana ecotype Col-0 (wild-type) and T-DNA insertion lines *tpst-1* (SALK_009847) and *pskr1-3 pskr2-1* (SALK_008585 and SALK_024464) were used in experiments. Their phenotypes were previously described (Komori *et al.*, 2009; Hartmann *et al.*, 2013). Plants were grown in half strength MS media in Petri dishes for six days with a 16 h light/8 h dark photoperiod. Before measurements, an intact plant was transferred to a liquid basic salt media (BSM) containing 0.5 mM KCl and 0.1 mM CaCl₂, pH 5.8. Plants were immobilized on a plastic block using a parafilm strip and placed into a small Petri dish, used as a measuring chamber, to which 1 mL of BSM was added. Plants were left for 40 min adaptation.

Net fluxes of H⁺ were measured using the non-invasive microelectrode ion flux measuring (MIFE) technique. The theory of non-invasive MIFE measurements and all specific details of microelectrode fabrication and calibration are available in prior publications (Shabala *et al.*, 2006). Briefly, microelectrodes with an external tip diameter of ~2 μm were pulled, salinized and filled with H⁺- selective cocktail (H⁺ 95297, Sigma). Electrodes were mounted on a 3D-micromanipulator (MMT-5, Narishige, Toyko, Japan) and calibrated in a set of three pH standards. A measuring chamber with the immobilized plant containing 1 ml BSM was placed into a Faraday cage. H⁺- selective micro-electrode was positioned 20 μm away from the measuring site. During measurements, a computer-controlled stepper motor moved micro-electrodes in a slow 6s/6s square-wave cycle between the two positions, close to (20 μm) and away from (70 μm) the root surface. The potential difference between two positions was recorded by the MIFE CHART software (Shabala *et al.*, 1997) and converted into an electrochemical potential difference using the calibrated Nernst slopes of the electrodes. Net ion fluxes were calculated using the MIFEFLUX software for cylindrical diffusion geometry.

Net fluxes of H⁺ were measured from the elongation (~500-700 μm from the root tip) and mature *Arabidopsis* root zones in response to PSK application to the bath. Ion flux measurements were conducted for 5 min in BSM, to ensure steadiness of fluxes. Then PSK stock was added to the measuring chamber to a final concentration of 1 μM, and the measurements conducted for a further 20 min. At least five individual plants were measured in each treatment. The sign convention is “efflux-negative”.

References

- Amano Y, Tsubouchi H, Shinohara H, Ogawa M, Matsubayashi Y.** 2007. Tyrosine-sulfated glycopeptide involved in cellular proliferation and expansion in *Arabidopsis*. Proceedings of the National Academy of Sciences of the United States of America **104**, 18333–18338.
- Baxter I, Tchieu J, Sussman MR, Boutry M, Palmgren MG, Gribskov M, Harper JF, Axelsen KB.** 2003. Genomic comparison of P-type ATPase ion pumps in *Arabidopsis* and rice. Plant Physiology **132**, 618–628.
- Caesar K, Elgass K, Chen Z, Huppenberger P, Witthöft J, Schleifenbaum F, Blatt MR, Oecking C, Harter K.** 2011. A fast brassinolide-regulated response pathway in the plasma membrane of *Arabidopsis thaliana*. Plant Journal **66**, 528–540.
- Felix G, Duran JD, Volko S, Boller T.** 1999. Plants have a sensitive perception system for the most conserved domain of bacterial flagellin. The Plant Journal **18**, 265–276.
- Fuglsang AT, Borch J, Bych K, Jahn TP, Roepstorff P, Palmgren MG.** 2003. The binding site for regulatory 14-3-3 protein in plant plasma membrane H⁺-ATPase: Involvement of a region promoting phosphorylation-independent interaction in addition to the phosphorylation-dependent C-terminal end. Journal of Biological Chemistry **278**, 42266–42272.
- Fuglsang AT, Guo Y, Cuin TA, et al.** 2007. *Arabidopsis* protein kinase PKS5 inhibits the plasma membrane H⁺-ATPase by preventing interaction with 14-3-3 protein. The Plant Cell **19**, 1617–1634.
- Fuglsang AT, Kristensen A, Cuin TA, et al.** 2014. Receptor kinase-mediated control of primary active proton pumping at the plasma membrane. The Plant Journal **80**, 951–964.
- Fuglsang AT, Visconti S, Drumm K, Jahn T, Stensballe A, Mattei B, Jensen ON, Aducci P, Palmgren MG.** 1999. Binding of 14-3-3 protein to the plasma membrane H⁺-ATPase AHA2 involves the three C-terminal residues Tyr⁹⁴⁶-Thr-Val and requires phosphorylation of Thr⁹⁴⁷. The Journal of Biological Chemistry **274**, 36774–36780.
- Grierson C, Nielsen E, Ketelaar T, Schiefelbein J.** 2014. Root Hairs. The *Arabidopsis* Book **12**.1–25.

- Hager A.** 2003. Role of the plasma membrane H⁺-ATPase in auxin-induced elongation growth: historical and new aspects. *Journal of Plant Research* **116**, 483–505.
- Hartmann J, Fischer C, Dietrich P, Sauter M.** 2014. Kinase activity and calmodulin binding are essential for growth signaling by the phyto-sulfokine receptor PSKR1. *The Plant Journal* **78**, 192–202.
- Hartmann J, Linke D, Bönninger C, Tholey A, Sauter M.** 2015. Conserved phosphorylation sites in the activation loop of the Arabidopsis phyto-sulfokine receptor PSKR1 differentially affect kinase and receptor activity. *Biochemical Journal* **472**, 379–391.
- Hartmann J, Stührwohldt N, Dahlke RI, Sauter M.** 2013. Phyto-sulfokine control of growth occurs in the epidermis, is likely to be non-cell autonomous and is dependent on brassinosteroids. *The Plant Journal* **73**, 579–90.
- Haruta M, Gray WM, Sussman MR.** 2015. Regulation of the plasma membrane proton pump (H⁺-ATPase) by phosphorylation. *Current Opinion in Plant Biology* **28**, 68–75.
- Haruta M, Sabat G, Stecker K, Minkoff BB, Sussman MR.** 2014. A peptide hormone and its receptor kinase regulate plant cell expansion. *Science* **343**, 408–411.
- Hepler PK, Rounds CM, Winship LJ.** 2013. Control of cell wall extensibility during pollen tube growth. *Molecular Plant* **6**, 998–1017.
- Kaufmann C, Motzkus M, Sauter M.** 2017. Phosphorylation of the phyto-sulfokine peptide receptor PSKR1 controls receptor activity. *Journal of Experimental Botany* **68**, 1411–1423.
- Komori R, Amano Y, Ogawa-Ohnishi M, Matsubayashi Y.** 2009. Identification of tyrosylprotein sulfotransferase in Arabidopsis. *Proceedings of the National Academy of Sciences of the United States of America* **106**, 15067–15072.
- Kutschmar A, Rzewuski G, Stührwohldt N, Beemster GTS, Inzé D, Sauter M.** 2009. PSK- α promotes root growth in Arabidopsis. *The New Phytologist* **181**, 820–831.
- Kwezi L, Ruzvidzo O, Wheeler JI, Govender K, Iacuone S, Thompson PE, Gehring C, Irving HR.** 2011. The phyto-sulfokine (PSK) receptor is capable of guanylate cyclase activity and enabling cyclic GMP-dependent signaling in plants. *The Journal of Biological Chemistry* **286**, 22580–22588.
- Ladwig F, Dahlke RI, Stührwohldt N, Hartmann J, Harter K, Sauter M.** 2015. Phyto-sulfokine regulates growth in Arabidopsis through a response module at the plasma membrane that includes CYCLIC NUCLEOTIDE-GATED CHANNEL17, H⁺-ATPase, and BAK1. *The Plant Cell* **27**, 1718–1729.
- Matsubayashi Y.** 2014. Posttranslationally modified small-peptide signals in plants. *Annual Review of Plant Biology* **65**, 385–413.
- Matsubayashi Y, Ogawa M, Kihara H, Niwa M, Sakagami Y.** 2006. Disruption and overexpression of Arabidopsis phyto-sulfokine receptor gene affects cellular longevity

and potential for growth. *Plant physiology* **142**, 45–53.

Nühse TS, Bottrill AR, Jones AME, Peck SC. 2007. Quantitative phosphoproteomic analysis of plasma membrane proteins reveals regulatory mechanisms of plant innate immune responses. *The Plant Journal* **51**, 931–940.

Olsson A, Svennelid F, Ek B, Sommarin M, Larsson C. 1998. A phosphothreonine residue at the C-terminal end of the plasma membrane H⁺-ATPase is protected by fusicoccin-induced 14-3-3 binding. *Plant Physiology* **118**, 551–555.

Palmgren MG. 2001. Plant plasma membrane H⁺-ATPases: Powerhouses for nutrient uptake. *Annual Review of Plant Physiology and Plant Molecular Biology* **52**, 817–845.

Patterson SE. 2001. Cutting loose. Abscission and dehiscence in *Arabidopsis*. *Plant Physiology* **126**, 494–500.

Rudashevskaya EL, Ye J, Jensen ON, Fuglsang AT, Palmgren MG. 2012. Phosphosite mapping of P-type plasma membrane H⁺-ATPase in homologous and heterologous environments. *The Journal of Biological Chemistry* **287**, 4904–4913.

Sauter M. 2015. Phytosulfokine peptide signalling. *Journal of Experimental Botany* **66**, 5161–5169.

Shabala SN, Newman IA, Morris J. 1997. Oscillations in H⁺ and Ca²⁺ ion fluxes around the elongation region of corn roots and effects of external pH. *Plant Physiology* **113**, 111–118.

Shabala L, Ross T, McMeekin T, Shabala S. 2006. Non-invasive microelectrode ion flux measurements to study adaptive responses of microorganisms to the environment. *FEMS Microbiology Reviews* **30**, 472–486.

Stührwohldt N, Dahlke RI, Steffens B, Johnson A, Sauter M. 2011. Phytosulfokine- α controls hypocotyl length and cell expansion in *Arabidopsis thaliana* through phytosulfokine receptor 1. *PloS one* **6**, e21054.

Takahashi K, Hayashi K, Kinoshita T. 2012. Auxin activates the plasma membrane H⁺-ATPase by phosphorylation during hypocotyl elongation in *Arabidopsis*. *Plant Physiology* **159**, 632–641.

Tavormina P, De Coninck B, Nikonorova N, De Smet I, Cammue BPA. 2015. The plant peptidome: An expanding repertoire of structural features and biological functions. *The Plant Cell* **27**, 2095–2118.

Wang J, Li H, Han Z, Zhang H, Wang T, Lin G, Chang J, Yang W, Chai J. 2015. Allosteric receptor activation by the plant peptide hormone phytosulfokine. *Nature* **525**, 265–268.

Witthöft J, Caesar K, Elgass K, Huppenberger P, Kilian J, Schleifenbaum F, Oecking C, Harter K. 2011. The activation of the *Arabidopsis* P-ATPase 1 by the brassinosteroid receptor BRI1 is independent of threonine 948 phosphorylation. *Plant Signaling & Behavior* **6**, 1063–1066.

Figure legends

Figure 1: PSKR1 phosphorylates the autoinhibitory C-terminus of AHA2 *in vitro*. A kinase assay was carried out with N-terminally His-tagged PSKR1 kinase domain and the heterologously expressed purified C-terminus of AHA2 in the presence of radiolabeled [γ - 32 P]ATP. The autoradiograph (top) shows autophosphorylation of PSKR1-KD and transphosphorylation of the C-terminus of AHA2 (AHA-CT). The corresponding Coomassie-stained gel (bottom) shows protein loading. The sizes of the marker proteins are indicated in kDa.

Figure 2: PSKR1 phosphorylates AHA2-CT at Ser and Thr residues. Schematic structure of AHA2 with ten helical transmembrane regions (M1-10), N-terminal domain, catalytic domain and autoinhibitory C-terminus. Numbers indicate amino acid residues phosphorylated by PSKR1. The phosphosite at Thr947 was found four times with low confidence and is therefore shown in grey. Activity *in vitro*¹ indicates AHA proton pumping activity tested in a *pma1* yeast complementation assay whereas *in planta* activity² is tested by proton flux measurements. 14-3-3 binding³ refers to binding of AHA2 to 14-3-3 proteins tested by overlay assay (Olsson *et al.*, 1998, Fuglsang *et al.*, 2003, 2007, 2014, Rudashevskaya *et al.*, 2012). n.t.= not tested.

Figure 3: PSK induces proton efflux from Arabidopsis root cells. Net proton fluxes [$\text{nmol}\cdot\text{m}^{-2}\cdot\text{s}^{-1}$] were measured using the MIFE technique from the root elongation (a, c, d) and mature (b) zones. Six-day-old seedlings were grown in Petri dishes containing $\frac{1}{2}$ MS media and the measurements conducted in BSM (0.1 mM CaCl_2 , 0.5 mM KCl, pH 5.8). Arrows indicate the time of PSK application to a final concentration of 1 μM . Mean \pm SEM (n=5). Dotted lines indicate steady flux levels before treatment.

Table legend

Table 1: Mass spectrometric analysis of amino acids in AHA2-CT phosphorylated by PSKR1. Ectopically expressed FLAG-tagged C-terminus of AHA was phosphorylated by PSKR1-KD *in vitro* and phosphosites were subsequently identified by mass spectrometry. Underlined sequences indicate the FLAG-tag. The shaded background indicates a triply phosphorylated tryptic peptide. The sequence below the table shows the C-terminus of AHA2 with the FLAG-tag attached. Only the sequence shown in bold was identified by mass spectrometry. Validation threshold for confidence high was 0.01 and for confidence medium 0.05 based on the *q*-value.

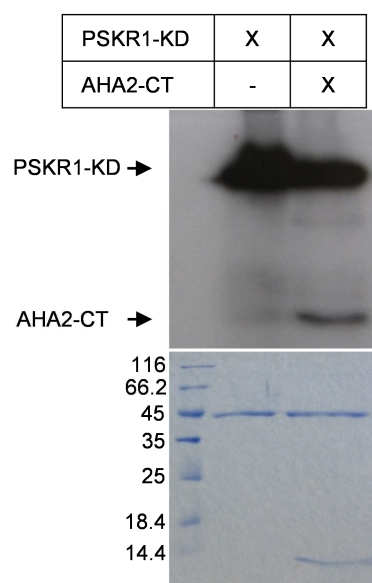
Figure 1

Figure 2

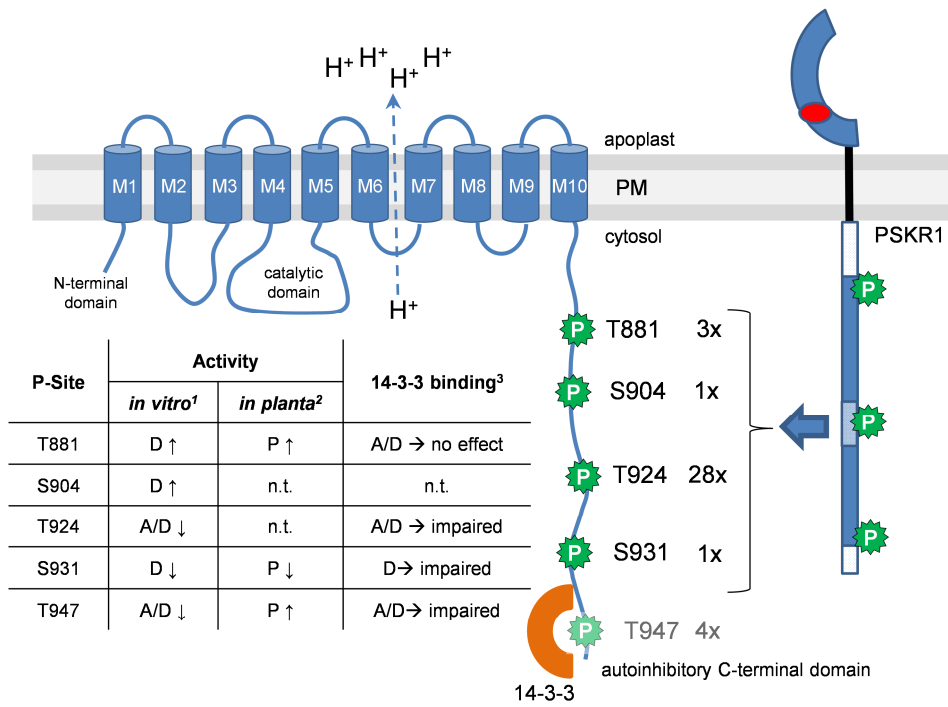


Figure 3

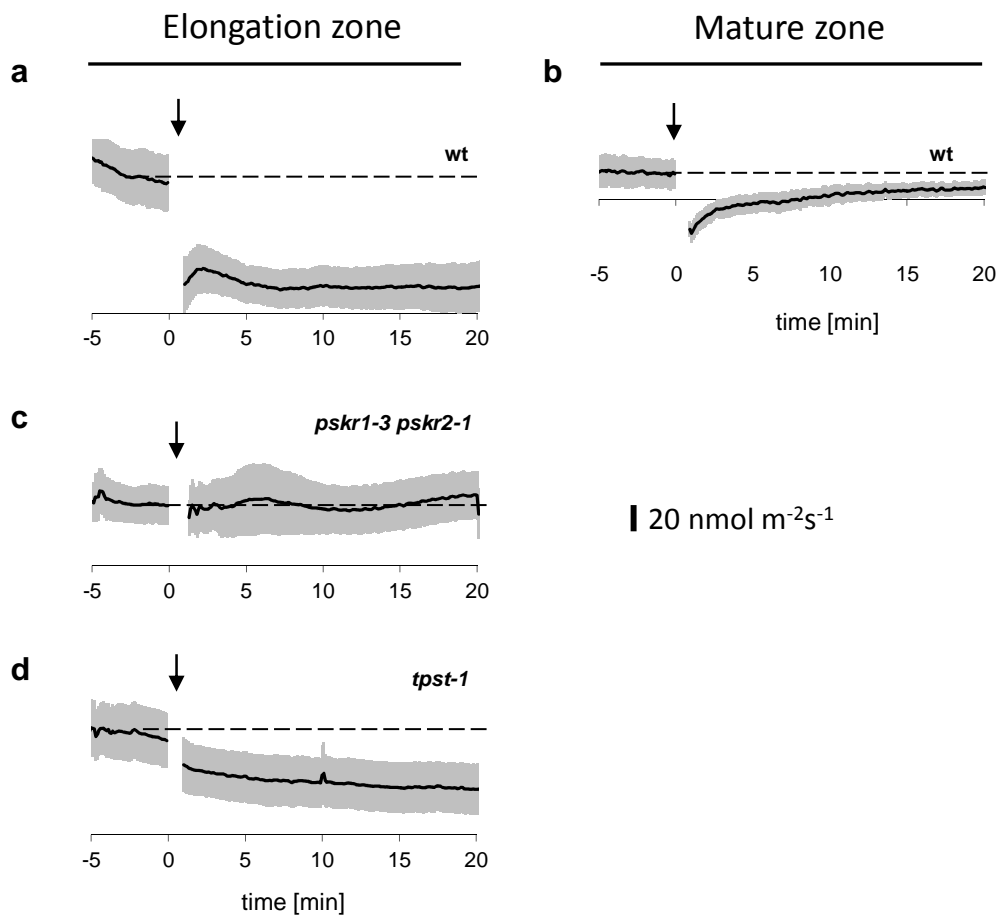


Table 1

Peptide sequence (localization probabilities/phosphoRS in brackets)	P-site	Confidence	Peptide Score
881_T(1)LHGLQPK_888	T881	high	1.44, 1.26
881_T(1)LHGLQPKEAVNIFPEKG_898		medium	1.28
902_ELS(1)EIAEQAKR_912	S904	high	1.04
889_EAVNIFPEKGS(0.33)Y(0.33)RELS(0.33)EIAEQAKR_912		rejected	1.53
921_ELHT(1)LKGHVESVVK_934	T924	high	0.81, 2.83, 1.75, 2.94, 3.00, 0.94
919_LRELHT(1)LKGHVESVVK_934		high	4.95, 2.77, 4.36, 3.79, 3.38, 1.57, 1.81, 2.02, 2.11, 2.40, 2.09, 2.23, 2.11
921_ELHT(1)LKGHVESVVK_934		high	2.83, 2.94, 3.00
922_LHT(1)LKGHVE_930		high	1.54
919_LRELHT(1)LKGHVESVVK_934		high	4.95, 2.77, 4.36, 2.40
919_LRELHT(1)LK		medium	1.35
924_T(1)LKGHVES(1)VVK_934		T924, S931	rejected
929_VES(1)VVKLK_935	S931	medium	0.75
927_GHVES(1)VVKLK_935		rejected	1.54
931_S(0.2)VVKLKGLDIET(0.2)PS(0.2)HY(0.2)T(0.2)V_948_DYKDDDDK	?S944, Y946, T947?	rejected	0.75
939_DIET(0.25)PS(0.25)HY(0.25)T(0.25)V_948_D_YKDDDDK		rejected	0.92
939_DIET(0.25)PS(0.25)HY(0.25)T(0.25)V_948_D_YKDDDDK		rejected	0.92
930_ES(0.6)VVKLKGLDIET(0.6)PS(0.6)HY(0.6)T(0.6)V_948_DYKDDDDK		rejected	0.92

Protein coverage:

MVRYILSGKA WLNLFENKTA FTMKKDYGKE EREAQWALAQ RTLHGLQPKE AVNIFPEKGS
YRELSEIAEQ AKRRAEIARL RELHTLKGHV ESVVKLKGLD IETPSHYTVD_YKDDDDK

Conclusive discussion and perspectives

PSKR1 kinase structure and intramolecular activation mechanism is conserved

PSK regulates plant growth, development and immunity (Sauter, 2015). The PSK responses described to date are mainly conveyed by the PSK receptor PSKR1 (Igarashi *et al.*, 2012; Hartmann *et al.*, 2013), which was analyzed in detail in this study. The plasma membrane-bound PSKR1 receptor has a functional kinase domain able to auto- and transphosphorylate. PSK signaling is dependent on kinase activity of PSKR1 (Hartmann *et al.*, 2014). Sequence analysis of PSKR1 showed that the kinase belongs to the class of arginine/aspartate (RD) kinases with conserved subdomains I to XI (Hartmann *et al.*, 2015). A homology model of PSKR1 revealed that the subdomains fold into a bilobal structure typical of eukaryotic protein kinases that is observed as well in BRI1 (Taylor and Kornev, 2011; Bojar *et al.*, 2014; Kaufmann *et al.*, 2017). The smaller N-terminal N-lobe contains a β -sheet and a highly conserved α C-helix. The C-lobe is mainly α -helical and includes the activation loop in the activation segment. Phosphorylation of kinases at specific residues leads to a conformational change and thereby regulates protein activity and/or its affinity to other proteins (Huse and Kuriyan, 2002). A combined *in vitro* and *in planta* phosphosite mapping of PSKR1 identified phosphosites within several kinase subdomains, mainly in the activation segment, as well as in the JM and CT domains (Hartmann *et al.*, 2015). Multiple phosphorylation events and overrepresented occurrence of phosphosites in these regions are common for RD-type LRR-RLKs (Mitra *et al.*, 2015). For kinase activation of RD-type kinases, phosphorylation at positions within the activation segment is necessary (Adams, 2003) and alters its conformation (Nolen *et al.*, 2004). The crystal structure of BRI1 shows that the phosphosites that were identified in the activation loop are required to form a catalytically competent activation loop (Bojar *et al.*, 2014). The altered conformation of the activation segment leads to a properly arranged ATP binding site, enables substrate binding and enhances phosphotransfer (Hubbard, 1997; Adams, 2003). A combination of phosphoablative point mutations at mapped activation segment phosphosites in BRI1 and PSKR1 impaired kinase activity *in vitro* and receptor

activity *in planta* (Wang *et al.*, 2005a; Hartmann *et al.*, 2015). An alignment of PSKR1 orthologues from higher plant species revealed a high degree of conservation of phosphosites in the activation segment and beyond (Hartmann *et al.*, 2015). As described for other animal and plant RD-type kinases, phosphorylation in the activation segment is an essential and conserved mode for activation of PSKR1. However, additional conditions have to be met in eukaryotic protein kinases to acquire an active state. These include the formation of the catalytic and regulatory spines. The regulatory spine is dependent on a correctly folded and proximally positioned α C-helix, an outward-positioned phenylalanine in the DFG motif and a salt bridge between a lysine (Lys762 in PSKR1) in the β 4-strand of the N-lobe with a glutamate (Glu778 in PSKR1) in the α C-helix (Taylor and Kornev, 2011; Endicott *et al.*, 2012). In accord with these requirements, mutation of Lys762 or the Ser783 in the α C-helix of PSKR1 which likely prevent the Lys-Glu salt bridge and correct α C-helix conformation, respectively, inactivate the PSKR1 kinase (Hartmann *et al.*, 2014; Kaufmann *et al.*, 2017).

Phosphorylation of the JM domain regulates PSKR1 activity

The N-terminal JM and the C-terminal CT domains that flank the kinase core are less conserved between LRR-RLKs, and they are not essential for kinase activity. Rather, these variable regions are involved in regulation (Endicott *et al.*, 2012). *In vitro* and *in vivo* analysis of truncated isoforms of BRI1 showed that the JM promotes BRI1 kinase activity, whereas the CT domain inhibits it (Wang *et al.*, 2005b; Oh *et al.*, 2009). Moreover, phosphosite substitutions to alanine in the JM domain of BRI1 don't affect autophosphorylation but revealed that these phosphosites are required for substrate phosphorylation (Wang *et al.*, 2005a). Phosphosites can hence influence signal transduction by creating substrate docking sites (Pawson, 2004) or by controlling receptor trafficking (Robatzek *et al.*, 2006). In PSKR1, phosphorylation of the JM modulates substrate phosphorylation (Muleya *et al.*, 2016; Kaufmann *et al.*, 2017). While PSKR1 autophosphorylation is not altered when the phosphosites are mutated, the phosphomimic isoform showed reduced substrate phosphorylation and PSK signaling *in planta* (Kaufmann *et al.*, 2017). S686, identified by Muleya *et al.* (2016) as a phosphosite in the JM of PSKR1, seems to invert this regulation. The

S686D/S696S/S698D triple phosphomimic PSKR1 isoform shows increased substrate phosphorylation (Muleya *et al.*, 2016). The function of phosphosites is in many cases analyzed *in vitro* using site-mutated kinase isoforms (Hartmann *et al.*, 2015). PSK signaling *in planta* can vary depending on the phosphorylation status, on co-factors, substrates, scaffolders and interacting proteins. Some kinases, such as CDK2, are active only after binding to a regulatory subunit. Cyclin A binding to CDK2 shifts the conformation of the α 1-helix, corresponding to α C in PSKR1, thereby promoting the formation of the K-E salt bridge which results in an active CDK2 conformation (Jeffrey *et al.*, 1995).

Finally, receptor activity can be controlled at the level of subcellular localization. Mutation of Thr967 in the JM of FLS2 delays and strongly reduces endocytosis of FLS2 after activation by flg22 (Robatzek *et al.*, 2006). Internalization of PSKR1 after PSK application was shown (Rodiuc *et al.*, 2015), but a possible role of specific phosphosites in this process has not been examined.

Contradictory to the dimerization model: PSKR1 is active in the absence of PSK

PSK binding to the extracellular island domain of PSKR1 induces heterodimerization with its co-receptor (Wang *et al.*, 2015). Receptor complex formation was shown for several LRR-RLKs and co-receptors of the SERK family (Ma *et al.*, 2016). The dimerization model proposes that the co-receptor is required for receptor activation and dimerization as well as activation are only accomplished in the presence of the respective ligand (Hohmann *et al.*, 2017). Indeed, it was shown that PSKR1 and BAK1 interact *in planta*. Furthermore, PSK-promoted protoplast expansion is dependent on BAK1 (Ladwig *et al.*, 2015). Increased root hair and lateral root formation observed in *tpst-1 pskr1-3 pskr2-1* seedlings compared to the *tpst-1* seedlings, that are devoid of PSK, and enhanced root growth by overexpression of PSKR1 in the *tpst-1* background support the conclusion that PSKR1 signaling can occur in the absence of PSK. This further suggests that ligand binding is not required for receptor/co-receptor dimerization as an on/off switch. Heterodimerization is seen as the crucial step for receptor activation via bidirectional transphosphorylation of the receptor and co-receptor kinases as shown here for PSKR1 and BAK1 (Chapter 4).

Phosphosite mapping revealed that BAK1 can activate PSKR1 and BAK1 could alter the PSKR1 kinase conformation to promote the active state in a similar way as shown for human CDK2 and cyclinA (Jeffrey *et al.*, 1995). Molecular dynamics simulation based on crystal structures suggests that heterodimerization of BRI1 and BAK1 promotes the active state by stabilizing the α C-helix (Moffett *et al.*, 2017). The model with the highest cluster population calculated by *in silico* docking of the BAK1 kinase crystal structure and the PSKR1 kinase homology model supports the same mode as their binding interface includes the PSKR1 α C-helix.

The comparison of LRR-RLK/SERK interactions showed that only PAMP- and DAMP-binding receptors such as PEPR1 (Tang *et al.*, 2015; Yamada *et al.*, 2016), EFR (Roux *et al.*, 2011; Koller and Bent, 2014) and FLS2 (Schulze *et al.*, 2010; Sun *et al.*, 2013; Koller and Bent, 2014) interactions with their co-receptors are ligand-dependent. Interactions of BRI1 (Wang *et al.*, 2008; Bücherl *et al.*, 2013; Hutten *et al.*, 2017), HAESA and HSL2 (Meng *et al.*, 2016), EMS1 (Li *et al.*, 2017), ER and ERL1 (Meng *et al.*, 2015; Jordá *et al.*, 2016), which are mainly involved in regulating growth and developmental processes, are enhanced by their respective ligand or occur ligand-independent. The interaction of PSKR1 with its co-receptor is stabilized by PSK but can occur without PSK. Overexpression of PSKR1 and its co-receptor in protoplasts results in rapid protoplast rupture indicating that PSKR1 is highly active without ligand (Wang *et al.*, 2015). A subpopulation of BRI1 and BAK1 form heterodimers as so-called preformed complexes independently of its ligand brassinolide (Bücherl *et al.*, 2013), whereas the nanocluster signal strength decreases after brassinolide treatment, indicating endocytosis after ligand-binding to the BRI1/BAK1-complex (Hutten *et al.*, 2017). It has not been analyzed however if the preformed BRI1/BAK1 complexes fulfill a biological role.

If BAK1 can activate PSKR1 in the absence of PSK, the question arises if receptor activation *in planta* is regulated e.g. at the level of BAK1 activity (Figure 3). In fact, two *Arabidopsis* proteins and two proteins from *P. syringae* were shown to inhibit BAK1 kinase. In a study focused on the complex FLS2-BAK1, it was shown that BAK1 constitutively associates with the Ser/Thr phosphatase type 2A (PP2A). PP2A negatively regulates the BAK1 phosphorylation status (Segonzac *et al.*, 2014). The PP2A regulatory subunit PP2AA3 was found to co-immunoprecipitate with PSKR1 (Sauter *et al.*, unpublished data) pointing to a similar regulatory mechanism. Treatment with the plant phosphatase inhibitor cantharidin elicited ROS production to

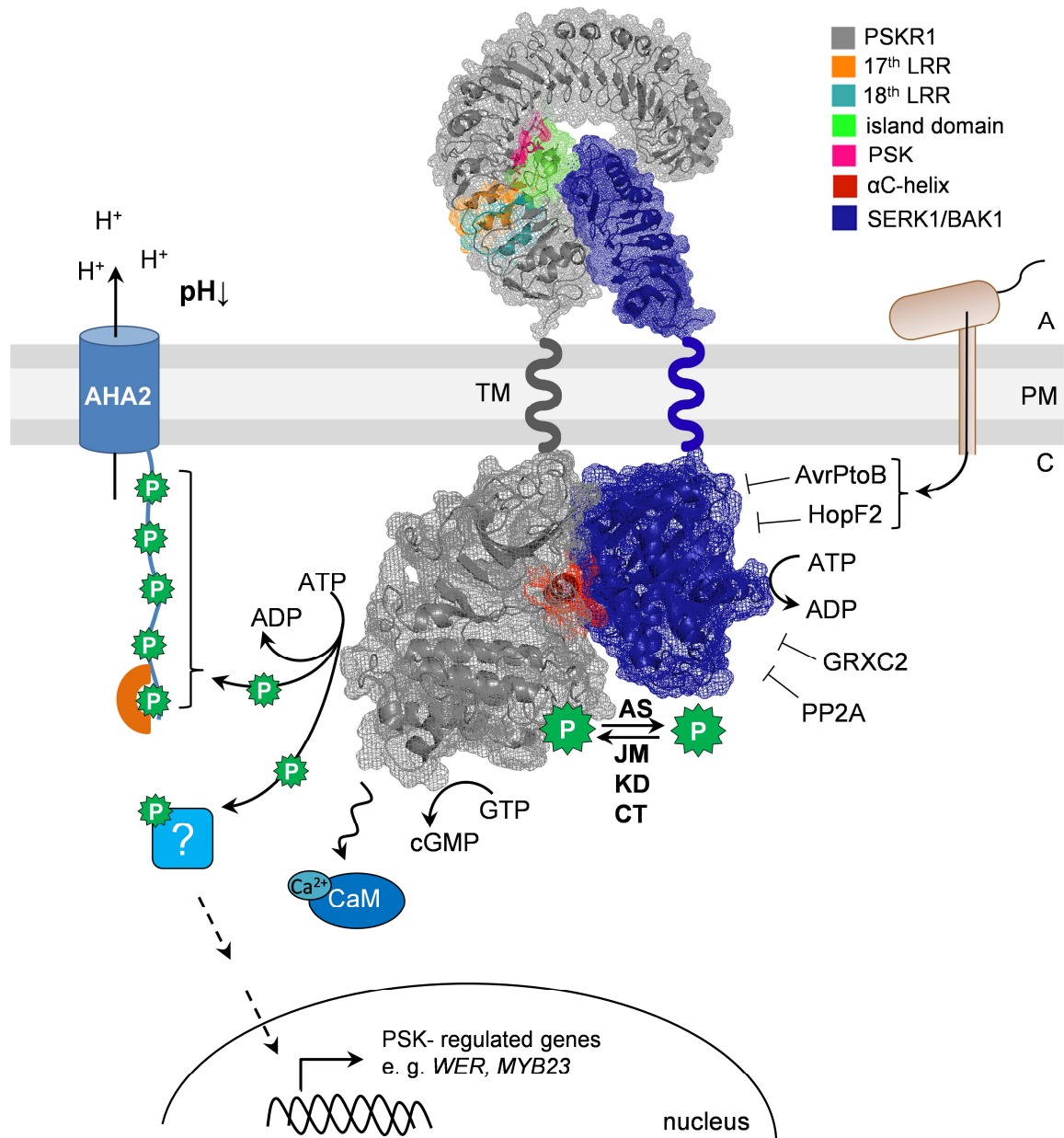


Figure 3: Regulation and activities of PSKR1. BAK1 phosphorylates (dark green star) PSKR1 in the juxtamembrane (JM), kinase domain (KD) and C-terminus (CT), whereas PSKR1 phosphorylates BAK1 only in the activation segment (AS). Their binding interface involves the PSKR1 α C-helix (red), which likely promotes active kinase conformation. Activation of PSKR1 leads to cGMP formation. Ca^{2+} -calmodulin (CaM) is released from PSKR1 after autophosphorylation. PSK promotes cell expansion by enhanced proton efflux. The autoinhibitory CT of Arabidopsis H^+ -ATPase 2 (AHA2) is a phosphorylation target of PSKR1. A 14-3-3 protein (orange) binds on the phosphorylated CT and activates AHA2. Further phosphorylation targets, which possibly transduce the signal to the nucleus have not been identified yet. PSKR1 and BAK1 can heterodimerize in the absence of PSK and induce basal PSK signaling that is enhanced by PSK, possibly, by stabilizing the interaction with BAK1. BAK1 is inhibited by *Pseudomonas syringae* (brown) type III effectors, by Arabidopsis phosphatase PP2A and glutaredoxin GRXC2. TM: helical transmembrane domain, A: apoplast, PM: plasma membrane, C: cytosol.

the same degree as flg22 or elf18 did, further supporting regulation by phosphatases. Additionally, BAK1 kinase is a target of glutathionylation by GLUTAREDOXIN C2, which destabilizes the active conformation of the BAK1 kinase (Bender *et al.*, 2015).

AvrPtoB and HopF2, which are type III effectors from *P. syringae*, bind to the BAK1 kinase, block its activity and thereby suppress flg22-induced signaling (Shan *et al.*, 2008; Cheng *et al.*, 2011; Zhou *et al.*, 2014). Furthermore, overexpression of AvrPtoB results in a dwarf stature, which is not observed when pattern recognition receptors were knocked out in *fls2-0/fls2-24*, *efr-1* or *pepr1/pepr2* (Gómez-Gómez and Boller, 2000; Zipfel *et al.*, 2006; Krol *et al.*, 2010). Some defects are shown to arise from suppressed brassinolide signaling, which cannot be complemented by treatment with the pathway activating ligand brassinolide (Shan *et al.*, 2008), further pointing to a regulation of several LRR-RLK pathways by BAK1.

Taken together, PSK binding increases the PSKR activity, but unlike predicted by the dimerization model, PSK does not act as an on/off-switch. PSK receptor activity is determined independent of PSK by the abundance of receptor, co-receptor and possibly regulation of BAK1 activity. It will be of interest to learn if this applies to more SERK/BAK1-dependent receptors.

The proton pump AHA2 is a target of the PSKR1 kinase while CaM is not

It was shown that CaM2, CaM4, CaM6, and CaM7 but not CaM-like proteins bind to PSKR1 but the role of CaM in PSK signaling remains unsolved. It was reported that binding of CaM is essential for PSKR1 activity, because a point mutation in the CaM binding site of PSKR1 impaired growth (Hartmann *et al.*, 2014). However the point mutation also abolishes PSKR1 kinase activity so that the role of CaM in PSK signaling remains unresolved (Kaufmann *et al.*, 2017). Unlike in animals (Benaim and Villalobo, 2002), CaM is not a phosphorylation target of PSKR1 (Kaufmann *et al.*, 2017). Co-expression of BRI1 and CaM7 inhibited BRI1 autophosphorylation (Oh *et al.*, 2012), suggesting a regulatory role of CaM. PSKR1 kinase activity is neither promoted nor inhibited by Ca²⁺ and/or CaM. Rather, Ca²⁺ promotes CaM binding whereas phosphorylation of PSKR1 inhibits it (Kaufmann *et al.*, 2017). This suggests that upon activation of PSKR1 Ca²⁺/CaM is released from PSKR1. It is conceivable

that CaM-binding to PSKR1 affects recycling of the receptor, substrate binding or GC activity.

PSK-enhanced growth is mainly driven by cell expansion e. g. of cells in the root elongation zone (Kutschmar *et al.*, 2009). The molecular mechanism how PSK signaling induces cell expansion was described as being independent of apoplastic pH regulation (Stührwohldt *et al.*, 2011). Using a more sensitive method, data presented in Chapter 5 show that PSK signaling enhances proton efflux into the apoplast. According to the acid-growth theory, acidification of the cell wall by enhanced activity of H⁺-ATPases, AHAs in Arabidopsis, at the plasma membrane is required for cell expansion (Hager, 2003). The receptor kinases PSY1R, FERONIA and FLS2 were shown to phosphorylate the autoinhibitory C-terminus of the AHAs leading to an active or inactive pump depending on the phosphorylation sites (Nühse *et al.*, 2007; Fuglsang *et al.*, 2014; Haruta *et al.*, 2014). AHA1 and AHA2 are the most abundant proton pumps in Arabidopsis that interact directly with PSKR1 *in planta* (Ladwig *et al.*, 2015) and the C-terminus of AHA2 is phosphorylated by PSKR1 *in vitro* at sites that enhance AHA activity and at a site that has not been functionally characterized yet (Olsson *et al.*, 1998; Fuglsang *et al.*, 1999, 2003, 2007, 2014; Rudashevskaya *et al.*, 2012). These results suggest that PSKR1-promoted cell expansion occurs through activation of AHAs by PSKR1 at the protein level.

In conclusion, this study shows that PSKR1 activity is differentially regulated by phosphorylation. On one hand, activation of the PSKR1 kinase occurs by autophosphorylation at defined positions or is accomplished by transphosphorylation by its co-receptor BAK1 at the same activating positions. On the other hand, phosphorylation of the JM domain determines substrate transphosphorylation and thereby regulates PSK signaling. The calcium sensor CaM binds to PSKR1 dependent on calcium and preferentially to the hypophosphorylated state of PSKR1. Ca²⁺/CaM does not regulate PSKR1 kinase activity but may influence e.g. receptor turnover, GC activity or substrate binding affinities, which needs to be clarified. The plasma membrane-localized proton pump AHA2, that was previously shown to bind to PSKR1, was identified here as a substrate of PSKR1 kinase by *in vitro* PSKR1 transphosphorylation of the autoinhibitory C-terminus of AHA2 at activating phosphosites. Furthermore, PSK signaling *in planta* leads to acidification of the apoplast supporting the conclusion that cell expansion is induced by PSKR1 via AHA2-dependent cell wall acidification. Finally, the PSK signal pathway is active at a

basal level even in the absence of PSK, and hence does not function as an on/off switch. Phenotypical defects caused by loss of sulfated peptides including PSK are ameliorated by overexpression of PSKR1 and are enhanced by knockout of PSKRs indicating that the abundance of PSKRs limits PSK signaling in the absence of the ligand.

Declaration of author contributions

Author abbreviations (alphabetical order): **AT** Andreas Tholey, **CK** Christine Kaufmann, **DL** Dennis Linke, **IS** Ive de Smet, **JH** Jens Hartmann, **LDV** Lam Dai Vu, **LS** Lana Shabala, **MM** Michael Motzkus, **MS** Margret Sauter, **NS** Nana Su, **NSt** Nils Stührwohldt, **SS** Sergey Shabala

Chapter 1:

JH, DL, AT and MS designed experiments. JH, DL and CK performed the research. All authors analyzed the data. MS wrote the paper.

Chapter 2:

CK and MS conceived the project and designed the experiments. CK and MM performed the research. CK and MS analyzed the data and wrote the paper.

Chapter 3:

CK and MS wrote the book chapter.

Chapter 4:

MS conceived the project. CK and MS designed the experiments. NSt performed initial characterization of *tpst-1 pskr1-3 pskr2-1* and performed microarray experiment. LDV and IS performed mass spectrometry. CK performed all other experiments and analyses. CK and MS wrote manuscript.

Chapter 5:

CK and MS conceived the project and designed the experiments. CK, LS and DL performed the research. CK, NS, SS and MS analyzed the data and wrote the chapter.

References

- Adams JA.** 2003. Activation loop phosphorylation and catalysis in protein kinases: Is there functional evidence for the autoinhibitor model? *Biochemistry* **42**, 601–607.
- Amano Y, Tsubouchi H, Shinohara H, Ogawa M, Matsubayashi Y.** 2007. Tyrosine-sulfated glycopeptide involved in cellular proliferation and expansion in *Arabidopsis*. *Proceedings of the National Academy of Sciences of the United States of America* **104**, 18333–18338.
- Bahryrcz A, Matsubayashi Y, Ogawa M, Sakagami Y, Konopińska D.** 2004. Plant peptide hormone phytosulfokine (PSK- α): Synthesis of new analogues and their biological evaluation. *Journal of Peptide Science* **10**, 462–469.
- Bahryrcz A, Matsubayashi Y, Ogawa M, Sakagami Y, Konopińska D.** 2005. Further analogues of plant peptide hormone phytosulfokine- α (PSK- α) and their biological evaluation. *Journal of Peptide Science* **11**, 589–592.
- Balagué C, Lin B, Alcon C, Flottes G, Malmström S, Köhler C, Neuhaus G, Pelletier G, Gaymard F, Roby D.** 2003. HLM1, an essential signaling component in the hypersensitive response, is a member of the cyclic nucleotide-gated channel ion channel family. *The Plant Cell* **15**, 365–379.
- Batistič O, Kudla J.** 2012. Analysis of calcium signaling pathways in plants. *Biochimica et Biophysica Acta* **1820**, 1283–1293.
- Benaim G, Villalobo A.** 2002. Phosphorylation of calmodulin: Functional implications. *European Journal of Biochemistry* **269**, 3619–3631.
- Bender K, Wang X, Cheng G, Kim H, Zielinski R, Huber S.** 2015. Glutaredoxin AtGRXC2 catalyzes inhibitory glutathionylation of *Arabidopsis* BR11-associated receptor-like kinase 1 (BAK1) *in vitro*. *Biochemical Journal* **467**, 399–413.
- Blatt MR.** 2000. Ca²⁺ signalling and control of guard-cell volume in stomatal movements. *Current Opinion in Plant Biology* **3**, 196–204.
- Bojar D, Martinez J, Santiago J, Rybin V, Bayliss R, Hothorn M.** 2014. Crystal structures of the phosphorylated BR11 kinase domain and implications for brassinosteroid signal initiation. *Plant Journal* **78**, 31–43.
- Brady SM, Orlando DA, Lee J-Y, Wang JY, Koch J, Dinneny JR, Mace D, Ohler U, Benfey PN.** 2007. A high-resolution root spatiotemporal map reveals dominant expression patterns. *Science* **318**, 801–806.
- Bücherl CA, van Esse GW, Kruis A, Luchtenberg J, Westphal AH, Aker J, van Hoek A, Albrecht C, Borst JW, de Vries SC.** 2013. Visualization of BR11 and BAK1(SERK3) membrane receptor heterooligomers during brassinosteroid signaling. *Plant Physiology* **162**, 1911–1925.
- Caesar K, Elgass K, Chen Z, Huppenberger P, Witthöft J, Schleifenbaum F, Blatt MR, Oecking C, Harter K.** 2011. A fast brassinolide-regulated response pathway in the plasma membrane of *Arabidopsis thaliana*. *Plant Journal* **66**, 528–540.

- Chen Y, Matsubayashi Y, Sakagami Y.** 2000. Peptide growth factor phytosulfokine- α contributes to the pollen population effect. *Planta* **211**, 752–755.
- Cheng C-Y, Krishnakumar V, Chan AP, Thibaud-Nissen F, Schobel S, Town CD.** 2017. Araport11: a complete reannotation of the *Arabidopsis thaliana* reference genome. *The Plant Journal* **89**, 789–804.
- Cheng W, Munkvold KR, Gao H, Mathieu J, Schwizer S, Wang S, Yan Y, Wang J, Martin GB, Chai J.** 2011. Structural analysis of *Pseudomonas syringae* AvrPtoB bound to host BAK1 reveals two similar kinase-interacting domains in a type III effector. *Cell Host and Microbe* **10**, 616–626.
- Chinchilla D, Shan L, He P, de Vries S, Kemmerling B.** 2009. One for all: the receptor-associated kinase BAK1. *Trends in Plant Science* **14**, 535–541.
- Czyzewicz N, Yue K, Beeckman T, De Smet I.** 2013. Message in a bottle: Small signalling peptide outputs during growth and development. *Journal of Experimental Botany* **64**, 5281–5296.
- Diévert A, Clark SE.** 2003. Using mutant alleles to determine the structure and function of leucine-rich repeat receptor-like kinases. *Current Opinion in Plant Biology* **6**, 507–516.
- Donaldson L, Ludidi N, Knight MR, Gehring C, Denby K.** 2004. Salt and osmotic stress cause rapid increases in *Arabidopsis thaliana* cGMP levels. *FEBS Letters* **569**, 317–320.
- Durner J, Wendehenne D, Klessig DF.** 1998. Defense gene induction in tobacco by nitric oxide, cyclic GMP, and cyclic ADP-ribose. *Proceedings of the National Academy of Sciences of the United States of America* **95**, 10328–10333.
- Ehrhardt DW, Wais R, Long SR.** 1996. Calcium spiking in plant root hairs responding to rhizobium modulation signals. *Cell* **85**, 673–681.
- Endicott JA, Noble MEM, Johnson LN.** 2012. The structural basis for control of eukaryotic protein kinases. *Annual Review of Biochemistry* **81**, 587–613.
- Franklin-Tong VE, Ride JP, Read ND, Trewavas AJ, Franklin FCH.** 1993. The self-incompatibility response in *Papaver rhoeas* is mediated by cytosolic free calcium. *The Plant Journal* **4**, 163–177.
- Fuglsang AT, Borch J, Bych K, Jahn TP, Roepstorff P, Palmgren MG.** 2003. The binding site for regulatory 14-3-3 protein in plant plasma membrane H⁺-ATPase: Involvement of a region promoting phosphorylation-independent interaction in addition to the phosphorylation-dependent C-terminal end. *Journal of Biological Chemistry* **278**, 42266–42272.
- Fuglsang AT, Guo Y, Cuin TA, et al.** 2007. Arabidopsis protein kinase PKS5 inhibits the plasma membrane H⁺-ATPase by preventing interaction with 14-3-3 protein. *The Plant Cell* **19**, 1617–1634.
- Fuglsang AT, Kristensen A, Cuin TA, et al.** 2014. Receptor kinase-mediated control of primary active proton pumping at the plasma membrane. *The Plant Journal* **80**, 951–964.

- Fuglsang AT, Visconti S, Drumm K, Jahn T, Stensballe A, Mattei B, Jensen ON, Aducci P, Palmgren MG.** 1999. Binding of 14-3-3 protein to the plasma membrane H⁺-ATPase AHA2 involves the three C-terminal residues Tyr⁹⁴⁶-Thr-Val and requires phosphorylation of Thr⁹⁴⁷. *The Journal of Biological Chemistry* **274**, 36774–36780.
- Gómez-Gómez L, Boller T.** 2000. FLS2: An LRR receptor-like kinase involved in the perception of the bacterial elicitor flagellin in Arabidopsis. *Molecular Cell* **5**, 1003–1011.
- Gou X, He K, Yang H, Yuan T, Lin H, Clouse SD, Li J.** 2010. Genome-wide cloning and sequence analysis of leucine-rich repeat receptor-like protein kinase genes in *Arabidopsis thaliana*. *BMC genomics* **11**, 19.
- Hager A.** 2003. Role of the plasma membrane H⁺-ATPase in auxin-induced elongation growth: historical and new aspects. *Journal of Plant Research* **116**, 483–505.
- Hanai H, Nakayama D, Yang H, Matsubayashi Y, Hirota Y, Sakagami Y.** 2000. Existence of a plant tyrosylprotein sulfotransferase: Novel plant enzyme catalyzing tyrosine O-sulfation of prephytytosulfokine variants *in vitro*. *FEBS Letters* **470**, 97–101.
- Han Z, Sun Y, Chai J.** 2014a. Structural insight into the activation of plant receptor kinases. *Current Opinion in Plant Biology* **20**, 55–63.
- Han J, Tan J, Tu L, Zhang X.** 2014b. A peptide hormone gene, *GhPSK* promotes fibre elongation and contributes to longer and finer cotton fibre. *Plant Biotechnology Journal* **12**, 861–871.
- Hartmann J, Fischer C, Dietrich P, Sauter M.** 2014. Kinase activity and calmodulin binding are essential for growth signaling by the phytosulfokine receptor PSKR1. *The Plant Journal* **78**, 192–202.
- Hartmann J, Linke D, Bönninger C, Tholey A, Sauter M.** 2015. Conserved phosphorylation sites in the activation loop of the Arabidopsis phytosulfokine receptor PSKR1 differentially affect kinase and receptor activity. *Biochemical Journal* **472**, 379–391.
- Hartmann J, Stührwohldt N, Dahlke RI, Sauter M.** 2013. Phytosulfokine control of growth occurs in the epidermis, is likely to be non-cell autonomous and is dependent on brassinosteroids. *The Plant Journal* **73**, 579–90.
- Haruta M, Burch HL, Nelson RB, Barrett-Wilt G, Kline KG, Mohsin SB, Young JC, Otegui MS, Sussman MR.** 2010. Molecular characterization of mutant Arabidopsis plants with reduced plasma membrane proton pump activity. *Journal of Biological Chemistry* **285**, 17918–17929.
- Haruta M, Gray WM, Sussman MR.** 2015. Regulation of the plasma membrane proton pump (H⁺-ATPase) by phosphorylation. *Current Opinion in Plant Biology* **28**, 68–75.
- Haruta M, Sabat G, Stecker K, Minkoff BB, Sussman MR.** 2014. A peptide hormone and its receptor kinase regulate plant cell expansion. *Science* **343**, 408–411.

- Hecht V, Vielle-Calzada JP, Hartog M V, Schmidt ED, Boutilier K, Grossniklaus U, de Vries SC.** 2001. The *Arabidopsis* SOMATIC EMBRYOGENESIS RECEPTOR KINASE 1 gene is expressed in developing ovules and embryos and enhances embryogenic competence in culture. *Plant Physiology* **127**, 803–816.
- Hepler PK, Vidali L, Cheung AY.** 2001. Polarized cell growth in higher plants. *Annual Review of Cell and Developmental Biology* **17**, 159–187.
- Hohmann U, Lau K, Hothorn M.** 2017. The structural basis of ligand perception and signal activation by receptor kinases. *Annual Review of Plant Biology* **68**, 109–137.
- Hua BG, Mercier RW, Zielinski RE, Berkowitz GA.** 2003. Functional interaction of calmodulin with a plant cyclic nucleotide gated cation channel. *Plant Physiology and Biochemistry* **41**, 945–954.
- Hubbard SR.** 1997. Crystal structure of the activated insulin receptor tyrosine kinase in complex with peptide substrate and ATP analog. *EMBO Journal* **16**, 5572–5581.
- Huse M, Kuriyan J.** 2002. The conformational plasticity of protein kinases. *Cell* **109**, 275–282.
- Hussain J, Chen J, Locato V, et al.** 2016. Constitutive cyclic GMP accumulation in *Arabidopsis thaliana* compromises systemic acquired resistance induced by an avirulent pathogen by modulating local signals. *Scientific Reports* **6**, 1–18.
- Hutten SJ, Hamers DS, Den Toorn MA, Van Esse W, Nolles A, Bücherl CA, De Vries SC, Hohlbein J, Borst JW.** 2017. Visualization of BRI1 and SERK3/BAK1 nanoclusters in *Arabidopsis* roots. *PLOS ONE* **12**, e0169905.
- Igarashi D, Tsuda K, Katagiri F.** 2012. The peptide growth factor, phytosulfokine, attenuates pattern-triggered immunity. *Plant Journal* **71**, 194–204.
- Igasaki T, Akashi N, Ujino-Ihara T, Matsubayashi Y, Sakagami Y, Shinohara K.** 2003. Phytosulfokine stimulates somatic embryogenesis in *Cryptomeria japonica*. *Plant Cell Physiology* **44**, 1412–1416.
- Jeffrey PD, Russo AA, Polyak K, Gibbs E, Hurwitz J, Massagué J, Pavletich NP.** 1995. Mechanism of CDK activation revealed by the structure of a cyclinA-CDK2 complex. *Nature* **376**, 313–320.
- Jordá L, Sopena-Torres S, Escudero V, Nuñez-Corcuera B, Delgado-Cerezo M, Torii KU, Molina A.** 2016. ERECTA and BAK1 receptor like kinases interact to regulate immune responses in *Arabidopsis*. *Frontiers in Plant Science* **7**, 897.
- Kaufmann C, Motzkus M, Sauter M.** 2017. Phosphorylation of the phytosulfokine peptide receptor PSKR1 controls receptor activity. *Journal of Experimental Botany* **68**, 1411–1423.
- Kobayashi T, Eun C-H, Hanai H, Matsubayashi Y, Sakagami Y, Kamada H.** 1999. Phytosulphokine- α , a peptidyl plant growth factor, stimulates somatic embryogenesis in carrot. *Journal of Experimental Botany* **50**, 1123–1128.
- Köhler C, Merkle T, Neuhaus G.** 1999. Characterisation of a novel gene family of putative cyclic nucleotide- and calmodulin-regulated ion channels in *Arabidopsis thaliana*. *The Plant Journal* **18**, 97–104.

- Koller T, Bent AF.** 2014. FLS2-BAK1 extracellular domain interaction sites required for defense signaling activation. *PLOS ONE* **9**, e111185.
- Komori R, Amano Y, Ogawa-Ohnishi M, Matsubayashi Y.** 2009. Identification of tyrosylprotein sulfotransferase in Arabidopsis. *Proceedings of the National Academy of Sciences of the United States of America* **106**, 15067–15072.
- Krol E, Mentzel T, Chinchilla D, et al.** 2010. Perception of the Arabidopsis danger signal peptide 1 involves the pattern recognition receptor AtPEPR1 and its close homologue AtPEPR2. *Journal of Biological Chemistry* **285**, 13471–13479.
- Kutschmar A, Rzewuski G, Stührwohldt N, Beemster GTS, Inzé D, Sauter M.** 2009. PSK- α promotes root growth in Arabidopsis. *The New Phytologist* **181**, 820–831.
- Kwezi L, Ruzvidzo O, Wheeler JI, Govender K, Iacuone S, Thompson PE, Gehring C, Irving HR.** 2011. The phytosulfokine (PSK) receptor is capable of guanylate cyclase activity and enabling cyclic GMP-dependent signaling in plants. *The Journal of Biological Chemistry* **286**, 22580–22588.
- Ladwig F, Dahlke RI, Stührwohldt N, Hartmann J, Harter K, Sauter M.** 2015. Phytosulfokine regulates growth in Arabidopsis through a response module at the plasma membrane that includes CYCLIC NUCLEOTIDE-GATED CHANNEL17, H⁺-ATPase, and BAK1. *The Plant Cell* **27**, 1718–1729.
- Leng Q.** 1999. Cloning and first functional characterization of a plant cyclic nucleotide-gated cation channel. *Plant Physiology* **121**, 753–761.
- Leng Q, Mercier RW, Hua B-G, Fromm H, Berkowitz GA.** 2002. Electrophysiological analysis of cloned cyclic nucleotide-gated ion channels. *Plant physiology* **128**, 400–410.
- Li Z, Wang Y, Huang J, Ahsan N, Biener G, Paprocki J, Thelen JJ, Raicu V, Zhao D.** 2017. Two SERK receptor-like kinases interact with EMS1 to control anther cell fate determination. *Plant Physiology* **173**, 326–337.
- Li J, Wen J, Lease KA, Doke JT, Tax FE, Walker JC.** 2002. BAK1, an Arabidopsis LRR receptor-like protein kinase, interacts with BRI1 and modulates brassinosteroid signaling. *Cell* **110**, 213–222.
- Loivamäki M, Stührwohldt N, Deeken R, Steffens B, Roitsch T, Hedrich R, Sauter M.** 2010. A role for PSK signaling in wounding and microbial interactions in Arabidopsis. *Physiologia Plantarum* **139**, 348–357.
- Lorbiecke R, Sauter M.** 2002. Comparative analysis of PSK peptide growth factor precursor homologs. *Plant Science* **163**, 321–332.
- Luan S, Kudla JJ, Rodriguez-concepcion M, et al.** 2002. Calmodulins and calcineurin B-like proteins: calcium sensors for specific signal response coupling in plants. *The Plant Cell* **14**, S389–S400.
- Ma W, Berkowitz GA.** 2007. The grateful dead: Calcium and cell death in plant innate immunity. *Cellular Microbiology* **9**, 2571–2585.
- Maathuis FJ, Sanders D.** 2001. Sodium uptake in Arabidopsis roots is regulated by

cyclic nucleotides. *Plant physiology* **127**, 1617–1625.

Ma X, Xu G, He P, Shan L. 2016. SERKING coreceptors for receptors. *Trends in Plant Science* **21**, 1017–1033.

Matsubayashi Y, Hanai H, Hara O, Sakagami Y. 1996. Active fragments and analogs of the plant growth factor, phytosulfokine: Structure–activity relationships. *Biochemical and Biophysical Research Communications* **225**, 209–214.

Matsubayashi Y, Ogawa M, Kihara H, Niwa M, Sakagami Y. 2006. Disruption and overexpression of *Arabidopsis* phytosulfokine receptor gene affects cellular longevity and potential for growth. *Plant physiology* **142**, 45–53.

Matsubayashi Y, Ogawa M, Morita A, Sakagami Y. 2002. An LRR receptor kinase involved in perception of a peptide plant hormone, phytosulfokine. *Science* **296**, 1470–1472.

Matsubayashi Y, Sakagami Y. 1996. Phytosulfokine, sulfated peptides that induce the proliferation of single mesophyll cells of *Asparagus officinalis* L. *Proceedings of the National Academy of Sciences of the United States of America* **93**, 7623–7627.

Matsubayashi Y, Takagi L, Omura N, Morita A, Sakagami Y. 1999. The endogenous sulfated pentapeptide phytosulfokine- α stimulates tracheary element differentiation of isolated mesophyll cells of *Zinnia*. *Plant Physiology* **120**, 1043–1048.

Matsuzaki Y, Ogawa-Ohnishi M, Mori A, Matsubayashi Y. 2010. Secreted peptide signals required for maintenance of root stem cell niche in *Arabidopsis*. *Science* **329**, 1065–1067.

McAinsh MR, Pittman JK. 2009. Shaping the calcium signature. *New Phytologist* **181**, 275–294.

Meng X, Chen X, Mang H, Liu C, Yu X, Gao X, Torii KU, He P, Shan L. 2015. Differential function of *Arabidopsis* SERK family receptor-like kinases in stomatal patterning. *Current Biology* **25**, 2361–2372.

Meng X, Zhou J, Tang J, Li B, Oliveira MVV de, Chai J, He P, Shan L. 2016. Ligand-induced receptor-like kinase complex regulates floral organ abscission in *Arabidopsis*. *Cell Reports* **14**, 1330–1338.

Mitra SK, Chen R, Dhandaydham M, Wang X, Kevin Blackburn R, Kota U, Goshe MB, Schwartz D, Huber SC, Clouse SD. 2015. An autophosphorylation site database for leucine-rich repeat receptor-like kinases in *Arabidopsis thaliana*. *The Plant Journal* **82**, 1042–1060.

Moffett AS, Bender KW, Huber SC, Shukla D. 2017. Molecular dynamics simulations reveal the conformational dynamics of *Arabidopsis thaliana* BRI1 and BAK1 receptor-like kinases. *Journal of Biological Chemistry* **292**, 12643–12652.

Moore KL. 2003. The biology and enzymology of protein tyrosine O-sulfation. *The Journal of Biological Chemistry* **278**, 24243–24246.

Moore KL. 2009. Protein tyrosine sulfation: a critical posttranslation modification in plants and animals. *Proceedings of the National Academy of Sciences of the United States of America* **106**, 14741–14742.

- Morillo SA, Tax FE.** 2006. Functional analysis of receptor-like kinases in monocots and dicots. *Current Opinion in Plant Biology* **9**, 460–469.
- Mosher S, Seybold H, Rodriguez P, et al.** 2013. The tyrosine-sulfated peptide receptors PSKR1 and PSY1R modify the immunity of Arabidopsis to biotrophic and necrotrophic pathogens in an antagonistic manner. *The Plant Journal* **73**, 469–482.
- Motose H, Iwamoto K, Endo S, Demura T, Sakagami Y, Matsubayashi Y, Moore KL, Fukuda H.** 2009. Involvement of phytosulfokine in the attenuation of stress response during the transdifferentiation of Zinnia mesophyll cells into tracheary elements. *Plant Physiology* **150**, 437–447.
- Muleya V, Marondedze C, Wheeler JI, et al.** 2016. Phosphorylation of the dimeric cytoplasmic domain of the phytosulfokine receptor, PSKR1. *Biochemical journal* **473**, 3081–3098.
- Nam KH, Li J.** 2002. BRI1/BAK1, a receptor kinase pair mediating brassinosteroid signaling. *Cell* **110**, 203–212.
- Nolen B, Taylor S, Ghosh G.** 2004. Regulation of protein kinases: Controlling activity through activation segment conformation. *Molecular Cell* **15**, 661–675.
- Nühse TS, Bottrill AR, Jones AME, Peck SC.** 2007. Quantitative phosphoproteomic analysis of plasma membrane proteins reveals regulatory mechanisms of plant innate immune responses. *The Plant Journal* **51**, 931–940.
- Oh M, Kim HS, Wu X, Clouse SD, Zielinski RE, Huber SC.** 2012. BRASSINOSTEROID-INSENSITIVE 1 receptor kinase provides a possible link between calcium and brassinosteroid signalling. *Biochemical Journal* **443**, 515–523.
- Oh M-H, Wang X, Kota U, Goshe MB, Clouse SD, Huber SC.** 2009. Tyrosine phosphorylation of the BRI1 receptor kinase emerges as a component of brassinosteroid signaling in Arabidopsis. *Proceedings of the National Academy of Sciences of the United States of America* **106**, 658–663.
- Oldroyd GED, Downie JA.** 2008. Coordinating nodule morphogenesis with rhizobial infection in legumes. *Annual Review of Plant Biology* **59**, 519–546.
- Olsson A, Svanellid F, Ek B, Sommarin M, Larsson C.** 1998. A phosphothreonine residue at the C-terminal end of the plasma membrane H⁺-ATPase is protected by fusicoccin-induced 14-3-3 binding. *Plant Physiology* **118**, 551–555.
- Pawson T.** 2004. Specificity in signal transduction : from phosphotyrosine-SH2 domain interactions to complex cellular systems. *Cell* **116**, 191–203.
- Robatzek S, Chinchilla D, Boller T.** 2006. Ligand-induced endocytosis of the pattern recognition receptor FLS2 in Arabidopsis. *Genes and Development* **20**, 537–542.
- Rodiuc N, Barlet X, Hok S, et al.** 2015. Evolutionarily distant pathogens require the Arabidopsis phytosulfokine signalling pathway to establish disease. *Plant, Cell and Environment* **39**, 1396–1407.
- Roux M, Schwessinger B, Albrecht C, Chinchilla D, Jones A, Holton N, Malinovsky FG, Tör M, de Vries S, Zipfel C.** 2011. The Arabidopsis leucine-rich

repeat receptor-like kinases BAK1/SERK3 and BKK1/SERK4 are required for innate immunity to hemibiotrophic and biotrophic pathogens. *The Plant Cell* **23**, 2440–2455.

Rudashevskaya EL, Ye J, Jensen ON, Fuglsang AT, Palmgren MG. 2012. Phosphosite mapping of P-type plasma membrane H⁺-ATPase in homologous and heterologous environments. *The Journal of Biological Chemistry* **287**, 4904–4913.

Santiago J, Brandt B, Wildhagen M, Hohmann U, Hothorn LA, Butenko MA, Hothorn M. 2016. Mechanistic insight into a peptide hormone signaling complex mediating floral organ abscission. *eLife* **5**, 1–19.

Santiago J, Henzler C, Hothorn M. 2013. Molecular mechanism for plant steroid receptor activation by somatic embryogenesis co-receptor kinases. *Science* **341**, 889–892.

Santner A, Calderon-Villalobos LIA, Estelle M. 2009. Plant hormones are versatile chemical regulators of plant growth. *Nature Chemical Biology* **5**, 301–307.

Sauter M. 2015. Phytosulfokine peptide signalling. *Journal of Experimental Botany* **66**, 5161–5169.

Schmidt ED, Guzzo F, Toonen M a, de Vries SC. 1997. A leucine-rich repeat containing receptor-like kinase marks somatic plant cells competent to form embryos. *Development* **124**, 2049–2062.

Schulze B, Mentzel T, Jehle AK, Mueller K, Beeler S, Boller T, Felix G, Chinchilla D. 2010. Rapid heteromerization and phosphorylation of ligand-activated plant transmembrane receptors and their associated kinase BAK1. *Journal of Biological Chemistry* **285**, 9444–9451.

Segonzac C, Macho AP, Sanmartín M, Ntoukakis V, Sánchez-Serrano JJ, Zipfel C. 2014. Negative control of BAK1 by protein phosphatase 2A during plant innate immunity. *The EMBO journal* **33**, 1–11.

Seidah NG, Prat A. 2012. The biology and therapeutic targeting of the proprotein convertases. *Nature Reviews Drug Discovery* **11**, 367–383.

Shan L, He P, Li J, Heese A, Peck SC, Nürnberger T, Martin GB, Sheen J. 2008. Bacterial effectors target the common signaling partner BAK1 to disrupt multiple MAMP receptor-signaling complexes and impede plant immunity. *Cell Host and Microbe* **4**, 17–27.

Shinohara H, Ogawa M, Sakagami Y, Matsubayashi Y. 2007. Identification of ligand binding site of phytosulfokine receptor by on-column photoaffinity labeling. *The Journal of Biological Chemistry* **282**, 124–131.

Srivastava R, Liu J-X, Howell SH. 2008. Proteolytic processing of a precursor protein for a growth-promoting peptide by a subtilisin serine protease in *Arabidopsis*. *The Plant Journal* **56**, 219–227.

Stührwohldt N, Dahlke RI, Kutschmar A, Peng X, Sun MX, Sauter M. 2014. Phytosulfokine peptide signaling controls pollen tube growth and funicular pollen tube guidance in *Arabidopsis thaliana*. *Physiologia Plantarum* **153**, 643–653.

Stührwohldt N, Dahlke RI, Steffens B, Johnson A, Sauter M. 2011.

Phytosulfokine- α controls hypocotyl length and cell expansion in *Arabidopsis thaliana* through phytosulfokine receptor 1. *PLOS ONE* **6**, e21054.

Sun Y, Li L, Macho AP, Han Z, Hu Z, Zipfel C, Zhou J-M, Chai J. 2013. Structural basis for flg22-induced activation of the Arabidopsis FLS2-BAK1 immune complex. *Science* **342**, 624–628.

Talke IN, Blaudez D, Maathuis FJM, Sanders D. 2003. CNGCs: Prime targets of plant cyclic nucleotide signalling? *Trends in Plant Science* **8**, 286–293.

Tang J, Han Z, Sun Y, Zhang H, Gong X, Chai J. 2015. Structural basis for recognition of an endogenous peptide by the plant receptor kinase PEPR1. *Cell Research* **25**, 110–120.

Tavormina P, De Coninck B, Nikonorova N, De Smet I, Cammue BPA. 2015. The plant peptidome: An expanding repertoire of structural features and biological functions. *The Plant Cell* **27**, 2095–2118.

Taylor SS, Kornev AP. 2011. Protein kinases: Evolution of dynamic regulatory proteins. *Trends in Biochemical Sciences* **36**, 65–77.

Urquhart W, Gunawardena AHLAN, Moeder W, Ali R, Berkowitz GA, Yoshioka K. 2007. The chimeric cyclic nucleotide-gated ion channel ATCNGC11/12 constitutively induces programmed cell death in a Ca^{2+} dependent manner. *Plant Molecular Biology* **65**, 747–761.

Volotovski ID, Sokolovsky SG, Molchan OV, Knight MR. 1998. Second messengers mediate increases in cytosolic calcium in tobacco protoplasts. *Plant Physiology* **117**, 1023–1030.

Wang X, Goshe MB, Soderblom EJ, Phinney BS, Kuchar JA, Li J, Asami T, Yoshida S, Huber SC, Clouse SD. 2005a. Identification and functional analysis of *in vivo* phosphorylation sites of the Arabidopsis BRASSINOSTEROID-INSENSITIVE1 receptor kinase. *The Plant cell* **17**, 1685–1703.

Wang X, Kota U, He K, Blackburn K, Li J, Goshe MB, Huber SC, Clouse SD. 2008. Sequential transphosphorylation of the BRI1/BAK1 receptor kinase complex impacts early events in brassinosteroid signaling. *Developmental Cell* **15**, 220–235.

Wang J, Li H, Han Z, Zhang H, Wang T, Lin G, Chang J, Yang W, Chai J. 2015. Allosteric receptor activation by the plant peptide hormone phytosulfokine. *Nature* **525**, 265–268.

Wang X, Li X, Meisenhelder J, Hunter T, Yoshida S, Asami T, Chory J. 2005b. Autoregulation and homodimerization are involved in the activation of the plant steroid receptor BRI1. *Developmental Cell* **8**, 855–865.

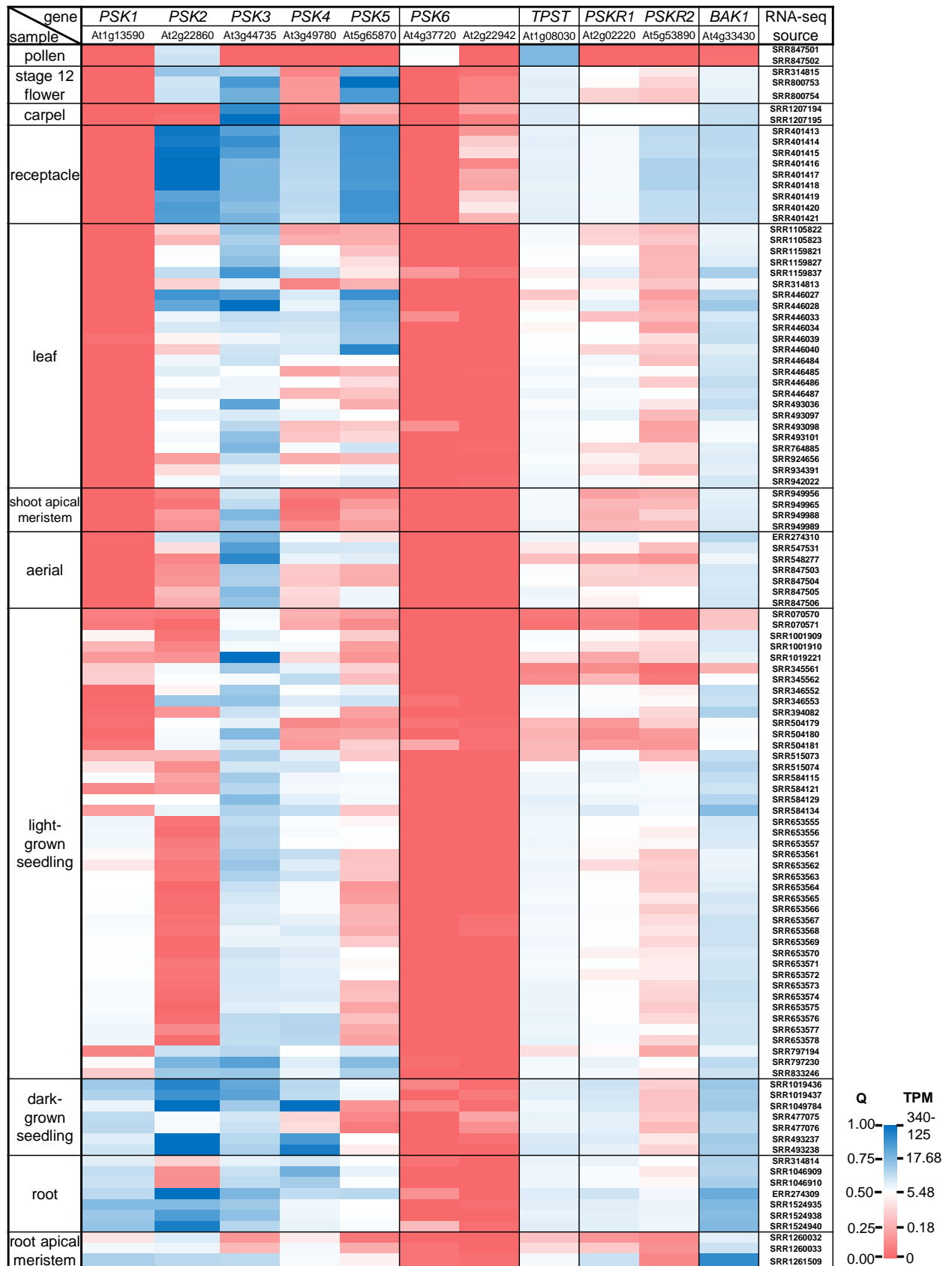
Wheeler JI, Irving HR. 2010. Evolutionary advantages of secreted peptide signalling molecules in plants. *Functional Plant Biology* **37**, 382–394.

Wu Y, Xun Q, Guo Y, Zhang J, Cheng K, Shi T, He K, Hou S, Gou X, Li J. 2016. Genome-wide expression pattern analyses of the Arabidopsis leucine-rich repeat receptor-like kinases. *Molecular Plant* **9**, 289–300.

Yamada K, Yamashita-Yamada M, Hirase T, Fujiwara T, Tsuda K, Hiruma K,

- Saijo Y.** 2016. Danger peptide receptor signaling in plants ensures basal immunity upon pathogen-induced depletion of BAK1. *The European Molecular Biology Organization Journal* **35**, 46–61.
- Yamakawa S, Sakuta C, Matsubayashi Y, Sakagami Y, Kamada H, Satoh S.** 1998. The promotive effects of a peptidyl plant growth factor, phytosulfokine- α , on the formation of adventitious roots and expression of a gene for a root-specific cystatin in cucumber hypocotyls. *Journal of Plant Research* **111**, 453–458.
- Zhou W, Wei L, Xu J, et al.** 2010. Arabidopsis tyrosylprotein sulfotransferase acts in the auxin/PLETHORA pathway in regulating postembryonic maintenance of the root stem cell niche. *The Plant Cell* **22**, 3692–3709.
- Zhou J, Wu S, Chen X, Liu C, Sheen J, Shan L, He P.** 2014. The *Pseudomonas syringae* effector HopF2 suppresses Arabidopsis immunity by targeting BAK1. *Plant Journal* **77**, 235–245.
- Zielinski RE.** 1998. Calmodulin and calmodulin-binding proteins in plants. *Annual Review of Plant Physiology and Plant Molecular Biology* **49**, 697–725.
- Zipfel C, Kunze G, Chinchilla D, Caniard A, Jones JDG, Boller T, Felix G.** 2006. Perception of the bacterial PAMP EF-Tu by the receptor EFR restricts *Agrobacterium*-mediated transformation. *Cell* **125**, 749–760.

Supplemental



Supplementary Figure 1: Expression heatmap for genes encoding PSK precursors, TPST, PSKR1, PSKR2 and BAK1 of *Arabidopsis thaliana*. (111 RNA-seqs; source: Araport11) Q=quantile; TPM = transcript per million.

Danksagung

Ich möchte mich ganz herzlich bei meiner Doktormutter Frau Prof. Dr. Margret Sauter für die gute Zusammenarbeit und Betreuung bedanken. Durch konstruktive Kritik und durch die Bereitschaft zu engagierter, fachlicher Diskussion hat sie meinen sportlichen Ehrgeiz angesprochen und damit meine wissenschaftliche Entwicklung sehr gefördert.

Ich bedanke mich bei meiner gesamten Arbeitsgruppe für eine tolle gemeinsame Zeit, mentale Unterstützung und Diskussionsbereitschaft. Insbesondere möchte ich Emese, Martina, Tanja, Ulli, Timo und Michael einen Dank aussprechen. Mit euch im Team zu arbeiten hat mir großen Spaß bereitet.

Ich danke allen Kooperationspartnern für die gute Zusammenarbeit und die nette Kommunikation.

Die Zeit einer Doktorarbeit kann nervenaufreibend sein – gespickt mit Erfolgen und Tiefschlägen. Meine Eltern, meine Geschwister und insbesondere mein Mann haben alle Momente mit mir erlebt, mitgefeiert, mitgefiebert. Ich danke ihnen für ihre volle Unterstützung zu jeder Zeit.

Lebenslauf

Christine Kaufmann

Persönliche Daten:

Geburtsname: Bönninger
Geburtstag: 10.04.1987
Geburtsort: Sassenberg
Staatsangehörigkeit: deutsch
Familienstand: verheiratet

Schulbildung:

06/2006 Abitur; Integrierte Gesamtschule Friedrichsort in Kiel

Hochschulbildung:

09/2007-11/2010/ Biologiestudium; Christian-Albrechts-Universität zu Kiel
Abschluss Bachelor of Science (B. Sc.)

09/2010-08/2013 Biologiestudium; Christian-Albrechts-Universität zu Kiel
Abschluss Master of Science (M. Sc.)

Promotion:

seit 3/2014 Promotionsstudium; Christian-Albrechts-Universität zu Kiel

Erklärung

Hiermit erkläre ich, dass die vorliegende Arbeit „Regulation and activities of phytosulfokine receptor PSKR1 in *Arabidopsis thaliana*“, abgesehen von der Beratung durch meine Betreuerin Frau Prof. Dr. Margret Sauter, nach Inhalt und Form meine eigene Arbeit ist. Die vorliegende Arbeit hat zu keinem Teil bereits in einem anderen Prüfungsverfahren vorgelegen und wurde weder ganz noch zum Teil veröffentlicht oder zur Veröffentlichung eingereicht. Die vorliegende Arbeit ist unter Einhaltung der Regeln guter wissenschaftlicher Praxis der Deutschen Forschungsgemeinschaft entstanden.

Teile der Arbeit sind in folgenden Publikationen enthalten:

Hartmann J, Linke D, Bönninger C, Tholey A, Sauter M. 2015.

Conserved phosphorylation sites in the activation loop of the Arabidopsis phytosulfokine receptor PSKR1 differentially affect kinase and receptor activity. *Biochemical Journal* **472**, 379–391.

Kaufmann C, Motzkus M, Sauter M. 2017.

Phosphorylation of the phytosulfokine peptide receptor PSKR1 controls receptor activity. *Journal of Experimental Botany* **68**, 1411–1423.

Kaufmann C, Sauter M. 2017.

Pull-down assay to characterize Ca²⁺/Calmodulin binding to plant receptor kinases. In: Aalen RB, ed. *Plant Receptor Kinases*. Springer Protocols, 151–159.

Kiel, den

Christine Kaufmann